AD_____

GRANT NUMBER: DAMD17-94-J-4436

TITLE: Genetic Immunization for Lentiviral Immunodeficiency Virus Infection and Disease

PRINCIPAL INVESTIGATOR: Murray B. Gardner, M.D.

CONTRACTING ORGANIZATION: University of California
Davis, CA 95616-8671

REPORT DATE: October 1996

TYPE OF REPORT: Annual

PREPARED FOR: Commander
U.S. Army Medical Research and Materiel Command
Fort Detrick, Frederick, MD 21702-5012

# DISCLAIMER NOTICE


**THIS DOCUMENT IS BEST QUALITY AVAILABLE. THE COPY FURNISHED TO DTIC CONTAINED A SIGNIFICANT NUMBER OF PAGES WHICH DO NOT REPRODUCE LEGIBLY.**

# REPORT DOCUMENTATION PAGE

*Form Approved*
*OMB No. 0704-0188*



| 1. AGENCY USE ONLY *(Leave blank)* | 2. REPORT DATE | 3. REPORT TYPE AND DATES COVERED |
|---|---|---|
| | October 1996 | Annual (30 Sep 95 - 29 Sep 96) |

**4. TITLE AND SUBTITLE**
Genetic Immunization for Lentiviral Immunodeficiency Virus Infection and Disease

**5. FUNDING NUMBERS**
DAMD17-94-J-4436

**6. AUTHOR(S)**
Murray B. Gardner, M.D.

**7. PERFORMING ORGANIZATION NAME(S) AND ADDRESS(ES)**
University of California
Davis, CA 95616-8671

**8. PERFORMING ORGANIZATION REPORT NUMBER**

**9. SPONSORING/MONITORING AGENCY NAME(S) AND ADDRESS(ES)**
Commander
U.S. Army Medical Research and Materiel Command
Fort Detrick, MD 21702-5012

**10. SPONSORING/MONITORING AGENCY REPORT NUMBER**

**11. SUPPLEMENTARY NOTES**

**12a. DISTRIBUTION / AVAILABILITY STATEMENT**
Approved for public release; distribution unlimited

**12b. DISTRIBUTION CODE**

**13. ABSTRACT** *(Maximum 200*

In year two of this project we have developed and characterized four novel SIV envelope expression vectors and one vector expressing both envelope and core components for genetic immunization of rhesus monkeys. Experiments using test antigens to determine optimum DNA vaccine parameters are near completion. Beginning in January 1997 we will test one or more of these SIV DNA vaccines for protection against SIV challenge infection via systemic (IV) and mucosal (vaginal) routes of administration. As a potential secondary challenge, should the vaccinated monkeys be protected against homologous SIV, we have developed a pathogenic SIV/HIV (SHIV) envelope recombinant. Cytokine profiles of acutely infected monkeys have been characterized and a large number of rhesus cytokine, B-chemokine and chemokine receptor genes have been cloned, sequenced and recombinant molecules prepared for possible use as immune modulators or adjuvants.

| 14. SUBJECT TERMS | 15. NUMBER OF PAGES |
|---|---|
| HIV, SIV, Immunodeficiency, Vaccines, DNA | 187 |
| | 16. PRICE CODE |

| 17. SECURITY CLASSIFICATION OF REPORT | 18. SECURITY CLASSIFICATION OF THIS PAGE | 19. SECURITY CLASSIFICATION OF ABSTRACT | 20. LIMITATION OF ABSTRACT |
|---|---|---|---|
| Unclassified | Unclassified | Unclassified | Unlimited |

FOREWORD

Opinions, interpretations, conclusions and recommendations are those of the author and are not necessarily endorsed by the U.S. Army.

N/A Where copyrighted material is quoted, permission has been obtained to use such material.

N/A Where material from documents designated for limited distribution is quoted, permission has been obtained to use the material.

X Citations of commercial organizations and trade names in this report do not constitute an official Department of Army endorsement or approval of the products or services of these organizations.

X In conducting research using animals, the investigator(s) adhered to the "Guide for the Care and Use of Laboratory Animals," prepared by the Committee on Care and use of Laboratory Animals of the Institute of Laboratory Resources, national Research Council (NIH Publication No. 86-23, Revised 1985).

N/A For the protection of human subjects, the investigator(s) adhered to policies of applicable Federal Law 45 CFR 46.

N/A In conducting research utilizing recombinant DNA technology, the investigator(s) adhered to current guidelines promulgated by the National Institutes of Health.

N/A In the conduct of research utilizing recombinant DNA, the investigator(s) adhered to the NIH Guidelines for Research Involving Recombinant DNA Molecules.

N/A In the conduct of research involving hazardous organisms, the investigator(s) adhered to the CDC-NIH Guide for Biosafety in Microbiological and Biomedical Laboratories.

Murray B. Gardner 10/29/96

PI - Signature Date

TABLE OF CONTENTS

**Grant # DAMD17-94-J-4436**
**"Genetic Immunization for Lentiviral Immunodeficiency Virus Infection and Disease"**

## Genetic Immunization for Lentiviral Immunodeficiency Virus Infection and Disease

Introduction

The purpose of this contract, now finishing the second year, has been to test the feasibility and effectiveness of DNA vaccination [1] and cytokine augmentation [2,3] in eliciting protective immunity for simian immunodeficiency virus (SIV) induced infection and disease in rhesus macaques. In recent years, so called "genetic immunization", using antigen expressing plasmid DNAs, has proven able to elicit long lasting cellular and humoral immunity [4] and protection against certain pathogens, e.g. influenza virus [6,7], herpes simplex virus [8], rabies virus [9]. Efforts to raise protective immunity by DNA vaccination against lentiviruses, such as SIV and its human relative, the human immunodeficiency virus, strains 1 and 2 (HIV-1, HIV-2), have just got underway in the last 2-3 years. In mice, HIV-1 envelope (env) DNA has induced both neutralization antibody and cytotoxic T lymphocyte (CTL) responses [10-14], and, in macaques HIV-1 env DNA has raised env-specific antibody and SIV specific CTLs and conferred some reduction in viral load after challenge with a SIV/HIV-1 env recombinant virus (SHIVenv) [15-17]. Following a boost with rgp 160 and saporin high neutralizing antibody and CTL anamnestic responses were generated in macaques who had been primed by SIV gp 120 DNA and two of two such animals were protected against intravenous (IV) challenge with a low dose (24TCID/50) of nonpathogenic SHIV env-3B [17]. In the only study reported so far in which a SIV DNA vaccine has been tested in macaques against a virulent $SIV_{mac251}$ challenge given IV, protection against infection or disease was not achieved although the vaccine may have provided some attenuation of the acute phase of infection [18]. Because this vaccine consisted of five DNA plasmids expressing different combinations and forms of SIVmac proteins and was given by multiple inoculations, it was not possible to evaluate the role of individual SIV antigens or rule out the possibility of induced immune tolerance; therefore, the field remains wide open and our task is to build on this previous experience and our own experimental observations to develop and test the most optimum SIV DNA vaccine construct(s), cytokine adjuvant(s) and protocol(s).

During the past year we have progressed toward this goal by concentrating on preparing four SIV envelope expression vectors, optimizing and verifying their expression and purifying them in large quantity. Because of plasmid stability problems, this work has progressed more slowly than we anticipated so we are about nine months behind schedule in testing the immunogenicity and extent of protection against SIV challenge conferred by these plasmids in rhesus monkeys. At this time, we are using these vectors expressing influenza and *E. coli* B-galactosidaes genes to optimize the amount of DNA, volume of injection and route of inoculation in rhesus monkeys. This evaluation will include CTL as well as antibody assays. Immunization of rhesus macaques with the SIVenv DNA plasmid is scheduled to start in January 1997 to be followed by SIV challenge probably in March. Because of the delay in making and growing up the SIVenv plasmids we will carry forward the money allocated for this purpose until year three, and in order to follow the results of challenge for at least six months, we will probably request a no-cost extension to complete the vaccine study.

While waiting to carry out the definitive DNA vaccine experiment in macaques, we have moved ahead in other areas related to the broad goal of genetic immunization in the SIV macaque model. Dr. Malone has compared different gene delivery methods to express antigens within tissues of mice that result in systemic humoral and cellular immune responses. Most recently, he has explored mucosal immune responses to test antigen DNA in mice using a replication defective recombinant Semliki Forest virus (SFV) preparation, and found that intranasal inoculation uniquely resulted in the production of antigen specific mucosal immune responses [19]. Dr. McChesney has shown the presence of MHC-restricted antiviral CTLs in the vaginal mucosa of SIV infected macaques [16]. (See Paper in Appendix.) He is also adapting a new virus neutralization test based on blocking infectivity of

Paper in Appendix.) He is also adapting a new virus neutralization test based on blocking infectivity of rhesus PBMCs by primary rather than T-cell line adapted SIV (R. Desrosiers, pers. com.). SIV vaccine studies in macaques have recently shown that protective immune responses are associated with the presence of SIV-specific serum antibodies that have a high titer to native envelope, that are high avidity, and that neutralize primary SIV *isolates in vitro* [21].

Together these observations suggest that we might also try to induce genital mucosal immunity to SIV in macaques by intranasal DNA vaccination using cationic lipid mediated transfection of SIV envelope plasmids or recombinant defective SFV vectors expressing the same env sequences. To first test the feasibility of exploiting the "common mucosal immune system" in order to obtain protection against SIV vaginal infection, we will test rhesus vaginal fluids for specific IgA antibodies after intranasal inoculation of the B-gal plasmid DNA. No group has yet tested HIV or SIV DNA mucosal vaccines for protection against genital mucosal transmission which, of course, represents the major route of HIV transmission around the world. The California Research Primate Center has pioneered this genital mucosal transmission model for SIV [22-24].

As an alternate SIV genetic vaccine candidate, Dr. Torres has constructed a plasmid containing a 1.6 lb. deletion encompassing the coding regions for the integrase, vif, vpx, and vpr proteins, a genetic lesion that was initially found by collaborators in Puerto Rico in a defective SIVsm provirus stably integrated into the CEMX179 cell line [25]. This defective provirus makes noninfectious virus-like particles, which induce partial protective immunity vs virulent SIVsm challenge in macaques. The plasma containing this DNA is immunogenic in rabbits.

As another potential genetic vaccine-challenge system targeting HIV-1 env in macaques, Dr. Luciw and colleagues have developed a pathogenic SHIV bearing the env of HIV-1 SF33 (Subgroup B), a T-cell tropic, syncytial-inducing variant [26]. Acute disease with dramatic loss of CD4 T-cells has been induced in juvenile and newborn rhesus with this SHIV [27]. In addition he has prepared and tested *in vitro* a SHIV bearing the envelope of HIV-1 subgroup E strain from Thailand [28]. (See Preprint in Appendix.) The pathogenic $SHIV_{SF33}$ could be used to cross challenge monkeys that will have already been immunized against the homologous SIVmac should they be protected against the homologous virus. The subgroup E SHIV may also be useful for testing future vaccines developed for use in Thailand. Dr. Luciw has also shown that a SIV IL2 recombinant is pathogenic for newborn but apparently not in older macaques [29]. This result is relevant to the safety issue of using such cytokines as immune adjuvants in HIV-1 infected humans or as genetic vaccine components.

Dr. Ansari and Villinger at Emory University have continued their cytokine analyses on PBMC and lymph node samples for acutely SIV infected macaques. Significant changes are found in the relative RNA levels of cytokines in PBMCs and lymph node cells of rhesus macaques after SIV infection and the pattern of changes appears related to the tempo of disease. PBMCs show changes distinct from lymph nodes collected at the same time from the same animal. A T-helper 2 cytokine pattern seems to be favored in the more rapid progressors. Over the 24-week course of infection an increased constitutive expression of TNFa, IL6 and IL10 mRNA occurs in PBMCs and increased expression of TNFa occurs, in lymph nodes of the rapid progressors. Similar results have been reported by others using this model [30-32]. Cytokine mRNA levels in PBMC of monkeys immunized with varying doses of the test plasmids used for optimizing the vaccine protocol and SIVenv DNA vaccines administered by various routes will be done in an attempt to correlate cytokine patterns with the quality and quantity of the immune response. Many rhesus macaque cytokines, chemokines and chemokine receptors have been cloned and sequenced and recombinant molecules prepared for possible immune modulation [33-35]

Finally Dr. Lee at the Naval Medical Research Institute, Bethesda, MD and colleagues have shown that the same B7-B28 costimulatory pathway is involved in DNA vaccination as in protein immunization [36] (See Preprint in Appendix). Therefore, the B7 plasmid might be another useful immune adjuvant to use with genetic vaccination.

Cytokine Profiles: Drs. Ansari/Villinger, Emory University

1. Methods

a. Samples analyzed: PBMC's and lymph node cells were analyzed from each of 4 SIV mac251 infected rhesus macaques, and for purposes of control in parallel 2 uninfected rhesus macaques, for relative levels of cytokine mRNA. For PBMC's both constitutive (ex-vivo) and mitogen induced (cells incubated in media containing 10 ug/ml of PHA-P for 24 hrs before RNA harvest) relative quantitation of cytokine mRNA was performed, whereas only constitutive mRNA levels were analyzed for lymph node samples. For the purposes of this report only the data for the constitutive levels of mRNA coding for the cytokines analyzed from PBMC and lymph node samples is presented. Mitogen induced changes were reported during our previous year's report.

b. Sampling times: PBMC samples were obtained at 6, 5 and 3 weeks prior to SIV infection (baseline samples), a sample on the day of SIV infection (day 0), and one at 8 weeks post infection. The lymph node samples represented nodes that were excised from each animal 6 weeks prior to SIV infection, on the day of SIV infection (day0), 2 weeks post SIV infection and those collected at necropsy(4.5 months p.i. for monkey # 26161 and 5.5 months p.i. for the remaining 3 SIV infected monkeys in the study). The necropsy lymph node samples included nodes excised from 5 different anatomic locations in efforts to determine whether changes (if any) were uniform for all lymph nodes or whether there the changes were only observed in select lymph nodes etc. The different anatomic locations included axillary, iliac, inguinal, mesenteric and obturator nodes.

c. Cytokine mRNA quantitation: Standard semi-quantitative RT-PCR procedures as standardized by our laboratory (1-3) were utilized for the relative quantitation of mRNA levels of IL-1b, IL-2, IL-4, IL-6, IL-10, IFN-g, TNF-a, and the chemokine MIP-1 a. Briefly, total RNA was isolated from fresh frozen PBMC's and lymph node cells using guanidium isothiocyanate. A fixed amount of RNA was reverse transcribed using random hexamers and MULV. After verification of the quality of the cDNA, as defined by the amplification of the household keeping GAPDH gene in the cDNA, aliquots of the various cDNA samples (representing 0.5 ug/sample of the original total RNA extracted from the cell sample) were subjected to amplification with primer pairs specific for IL-1 b, IL-2, IL-4, IL-6, IL-10, IFN-g, TNF-a, and the chemokine MIP-1 a, in parallel with varying dilutions of known concentrations of DNA coding for the various cytokine genes being analyzed. All PBMC samples and lymph node samples were amplified in one reaction for each cytokine using a 96 well cycler format in efforts to minimize relative quantitative errors due to potential inter-assay variabilities during the amplification procedure. After gel electrophoresis, blotting and hybridization to a digoxigenin labelled internal probe, the relative signal intensities obtained with the unknown samples were compared with the signal intensities of the various dilution standards of the

same cytokine that was run in parallel and the data was expressed as copy equivalents per 0.5 ug of total RNA.

d. Intracellular detection and quantitation of the cytokine protein: While the procedure described above under © concerns mRNA quantitation, it was reasoned that quantitation of the cytokine in question at the protein level in addition to the single cell level with the possibility of identifying the precise cell surface phenotype that expresses the cytokine of interest would be important to establish. Thus, mRNA levels may not reflect the quantitative levels of the bioactive molecules present in the fluids of interest and, in addition, rapid re-utilization of the cytokine by the cells would make it difficult if not impossible to define precise quantitation of cytokine proteins in biological fluids. We utilized the protocols described by Schauer et al [37] , Jung et al [38] and Elson et al [39] which involved first permeabilizing and fixing cells in a single cell suspension. This is followed by staining aliquots of such cell suspensions with fluorescent tagged monoclonal antibodies against the cytokine to be studied. While the technique appears straightforward, in practice however the reagents and assays had to be standardized for the detection of non-human primate cytokines. With support from this grant our laboratory utilized the knowledge we had previously acquired on those monoclonal antibodies that are against human cytokines that do in fact cross react with corresponding rhesus macaque cytokines as well as data from other colleagues [33-35,40]. In addition, we defined the optimum time intervals post mitogen activation when each individual cytokine could easily be detected intra-cellularly and developed a panel of CHO- DG44 cell lines that are individually stably transfected with a number of rhesus macaque cytokine expressing genes. These cell lines, analyzed in parallel with the unknown sample allow for both positive control and the parent vector (in this case pED6) transfected CHO cell line (negative control) and in addition allow for relative quantitation between different runs with each panel of unknowns.The procedure for permeabilizing and fixing rhesus macaque lymphoid cells is essentially similar to that described elsewhere [37-39]. We have been successful in establishing techniques for detection and quantitation (both by intensity of staining and by comparison with CHO cell staining) of rhesus macaque IL-2, IL-4, IL-6, and IFN-g. See Results below.

e. Preparation of rhesus macaque cytokine/cytokine expression constructs as adjuvants/adjuncts to genetic immunization: The role of select cytokines as adjuvants to be used for immunization with a variety of antigens continues to be exploited in a variety of rodent models. It has been reasoned that those cytokines that promote an effective cell mediated immune response would be the ideal cytokines to utilize especially for responses against intracellular parasites including viruses. Several cytokines and molecules that promote either antigen presentation or T cell response or both have been identified in mice and man. While considerable homology exists between non human primate cytokine genes and the corresponding human cytokine genes, most of these genes differ just enough to

result in coding for proteins that when introduced in the discordant host induce potent, but more importantly, neutralizing immune responses obviating their in vivo utilization in the discordant host. These lines of evidence have prompted our laboratory to clone, sequence and prepare non human cytokine genes. In addition our laboratory has also cloned and sequenced a number of non human primate growth factors, chemokines and a number of cell surface molecules known to play an important role in the regulation and orchestration of immune responses. This list includes but is not limited to IL-1 a, IL-1b, IL-2, IL-4, IL-5, IL-6, IL-8, IL-10, IL-12 a, IL-12 b, IL-15, IL-16, IL-18, IFN-a, IFN-b, IFN-g, TNF-a, TNF-b, GM-CSF, SCF, MIP-1 a, MIP-1 b, RANTES, fusin, CC-C-C-CKR5, CD28, B7.1, B7.2, CTLA-4 and V-CAM etc. A number of these have been prepared in recombinant form primarily for purposes of in vivo use. This includes macaque IL-2, IFN-g, IL-15, IL-12, GM-CSF, IL-16, MIP-1 a, MIP-1 b and RANTES.

Results and Discussion

1. CYTOKINE PROFILE OF PBMC'S AND LYMPH NODE CELLS OF RHESUS MACAQUES FOLLOWING SIV INFECTION:

Our experience so far has taught us that there is considerable variability in the disease course of rhesus macaques experimentally infected with SIVmac251. Thus the tempo of immunological changes such as cytokine synthesis etc vary from animal to animal and from one tissue sample to another within the same animal . Differences in the kinetics of the disease among rhesus macaques of similar age and sex given the same dose of virus may be due to a number of factors. These include the immune status of the individual monkey at the time of virus infection, presence of other often asymptomatic infections that are undetectable, genetic heterogeneity, variable response to stress and as yet unknown factors. This knowledge has prompted our laboratory to analyze data of individual monkeys in the study with the bias that the data obtained during the baseline studies of individual monkeys serve as a reference point to changes if any that can be quantified. Data on cytokine changes can thus be evaluated with reference to baseline values and correlations can be made with pathological changes, virus load, CD4 count and extent of disease. Issues relevant to our interpretation of the cytokine studies are highlighted below.

This study involved analysis of cytokine data obtained on PBMC and lymph node samples of 4 rhesus macaques that were experimentally infected with SIV mac 251 and for purposes of control similar samples obtained at the same time intervals from 2 uninfected rhesus macaques. Out of the 4 rhesus macaques, 2 (Animal nos. 26161 and 26470) failed to develop detectable levels of anti-SIV reactive antibodies and progressed relatively rapidly towards clinical disease. As a consequence, monkey # 26161 had to be euthanized at 4.5 month p.i. while the other SIV infected monkeys were euthanized at 5.5 months p.i., at the termination of the experiment. Pathological evaluation of the tissues at autopsy showed that, based on lymphoid cell depletion and evidence of encephalitis and pneumonitis etc, the monkeys 26161 and 26470 were the most severely affected. Monkey

#26320 was still asymptomatic but clearly had significant lymphoid cell depletion and monkey # 26474 was the least affected and had striking lymphoid follicular hyperplasia (B cell hyperactivity). The pathological evaluation of aliquots of the excised lymph nodes (source for the cytokine studies reported herein) obtained during the course of the infection confirm the final pathological evaluation obtained at autopsy described above. The findings therefore suggested progressive development of the lesions as found and confirmed the autopsy findings. For purposes of discussion below (recognizing the pitfalls inherent in our bias) we would like to consider monkey 26161 as most severely ill with a rapid decease course and followed in order of decreasing severity of disease with monkey # 26470 and then 26320 and lastly monkey #26474 being the least ill.

a. Cytokine profile of PBMC samples: A summary of the relative levels of mRNA coding for IL-1 b, IL-4, IL-6, IL-10, IFN-g and TNF-a constitutively expressed by PBMC samples from each of the 4 SIV infected rhesus macaques is shown in Fig.1 (see appendix).

(i) IL-1 b: As seen in Fig.1a, there is no significant difference in the level of IL-1 b (the decrease seen in some of the samples from PBMC's obtained 4 weeks prior to and on day 0 of SIV infection is difficult to understand at present and could reflect exposure as yet unknown insult or the extent of variability inherent with the techniques being employed) seen in samples prior to and those post SIV infection. There also does not appear to be any difference noted between severity of disease and changes in IL-1 b mRNA levels.

(ii) IL-4: There was no detectable constitutive level of IL-4 mRNA in any of the PBMC samples examined (see Fig. 1a). Some of the samples obtained prior to SIV infection showed mitogen induced increase in the relative level of IL-4 mRNA levels. However, this ability to synthesize IL-4 upon mitogen stimulation was lost following SIV infection (data not shown).

(iii) IL-6: When one examines the relative levels of IL-6 mRNA, there appears to be a marked increase in the constitutive levels of this cytokine in samples following 8 weeks post SIV infection (see Fig. 1a, also please note scale) from at least 3 of the 4 monkeys. Again, there did not appear to be any correlation with levels of IL-6 mRNA constitutively expressed and the level of disease severity while a general increase was noted.

(iv) IL-10: As seen in Fig. 1b, (except for sample obtained from monkey #26320 on 4 weeks prior to SIV infection), in general there was approximately 500 to 2500 copies of IL-10 mRNA being constitutively synthesized by the various PBMC samples obtained at 6, 5, and 3 weeks and at the time of SIV infection. However, at 8 weeks post SIV infection there was a dramatic increase in the constitutive levels of IL-10 mRNA in

only the severely ill animals (animal #26161 and #26470) but not the other 2 animals.

(v) IFN-g: There was no significant constitutive IFN-g mRNA level that could be detected in any of the PBMC sample examined. This was not due to the failure of the technique since the positive controls showed significant mRNA level for IFN-g.

(vi) TNF-a: As seen in Fig. 1b, the profile for TNF-a is similar to that seen for IL-10. Thus, constitutive levels of approximately 5000 copies or less per 0.5 ug of RNA was noted in PBMC samples prior to SIV infection. However, post SIV infection, there was a dramatic increase (>7 fold) in the constitutive levels of TNF-a mRNA synthesized by the PBMC of at least 3 of the 4 SIV infected animals. No clear correlation, however could be made between severity of disease and constitutive levels of TNF-a mRNA.

b. Cytokine profile of lymph node samples : As mentioned above and due to obvious limitations on the number of lymph node biopsies that can be performed, lymph node samples from each of the 4 SIV infected monkeys and for purposes of control the 2 uninfected monkeys were analyzed for constitutive levels of cytokine mRNA. The results of these analyses are depicted in summary form in Fig. 2.

(i) IFN-g: (Fig. 2a) There was generally relatively low levels of IFN-g mRNA synthesized by the lymph node cell samples at 2 weeks post infection, the values being similar to those from the samples from the same animals prior to SIV infection and from the uninfected control animals. There appeared to be an increase in the relative levels of IFN-g mRNA levels from select lymph node samples obtained at autopsy . This increase was more marked in monkey 26474 that showed lymphoid hyperplasia instead of depletion seen in the other three animals.

(ii) IL-1 b: (Fig. 2b) Significant constitutive levels of IL-1 b are synthesized by lymph node cells of each of the monkeys prior to SIV infection ( 90 to 170 copies of mRNA per 0.5 ug). Increase in the levels of mRNA was noted at 2 weeks post SIV infection in 2 of the 4 monkeys (see Fig.2). Variable levels of IL-1 b mRNA increases from baseline values were noted in the lymph node samples from various anatomic locations of the 4 SIV infected monkeys. The reason for this variability in the various lymph nodes of individual animals is not clear at present, It may represent differential sites in which the virus may be replicating or may be artifactual.

(iii) IL - 2: As seen in Fig.2c, lymph node samples from the 2 monkeys that were the most severely ill (monkey # 26161 and 26470) showed a relative increase in the mRNA copy number for IL-2 at necropsy (4.5 months p.i.) in select lymph nodes for the former and at 2 weeks for the latter compared

to their own individual baseline levels and to values obtained for lymph node specimens from normal uninfected macaques. Lymph node samples from the other 2 monkeys did not show any appreciable change that could be detected with very low baseline values that continued to be low following SIV infection. It should be noted that while the values for IL-2 copy numbers are low, our laboratory has consistently found low values for IL-2 both at the protein and mRNA level in mitogen activated T cells from rhesus macaques [33,35]. The reason for this is not clear at present but may account for the general lack of several laboratories including ours in our inability to clone and maintain $CD^{+}T$ cell lines from rhesus macaques.

(iv) IL - 4: (Fig. 2d) There was very little if any detectable constitutive levels of IL -4 being synthesized by lymph node cells from multiple samples of the 2 control uninfected animals and the 4 SIV infected animals at any of the sampling times pre and post SIV infection.

(v) IL - 6: The relative levels of IL-6 mRNA, while variable (from <10 to 60 copies of mRNA / 0.5 ug) in lymph node samples from the 4 SIV infected animals pre- and post-infection, were not different from those seen in multiple samples of lymph node specimens from control uninfected animals (see Fig.2e). However, there did appear to be a marked increase in the relative levels of IL-6 mRNA copy number/0.5 ug in the majority (11/15) of the lymph node samples from 3 of the 4 SIV infected animals at autopsy (from 80 to 330 copies of mRNA/0.5 ug). These data support the view that SIV infection does increase IL-6 mRNA synthesis in lymph nodes and PBMC's of infected animals.

(vi) IL - 10: As seen in Fig. 2f, it appears that lymph node samples from the 2 SIV infected monkeys that were severely ill (monkeys 26161 and 26470) contained higher (constitutive) relative levels of IL-10 mRNA copy numbers per 0.5 ug at 2 weeks p.i. as compared to values of lymph node samples from the same respective monkeys prior to and on day 0 of SIV infection. In contrast the other 2 SIV infected monkeys that were relatively less ill had high relative baseline mRNA copy numbers for IL-10 prior to and on day 0 of SIV infection. The values for lymph node samples from these 2 monkeys at 2 weeks p.i. decreased. The lymph node samples at autopsy from these 4 SIV infected animals gave variable results and are therefore hard to interpret. It should be kept in mind that lymph nodes from uninfected normal monkeys give approx. 265+/-88 copies of IL-10 mRNA (values representing mean+/S.D. of 7 samples assayed). (Fig. 2i)

(vii) TNF-a: (Fig. 2g) Constitutive levels of TNF-a mRNA appeared to be relatively high for 3 of the 4 monkeys prior to SIV infection (2500, 8000 and 3000 mRNA copy number/0.5 ug). These values markedly decreased in lymph node samples from these same monkeys at 2 weeks post SIV

infection (850, 650 and 100 mRNA copy number/0.5 ug , respectively). Normal constitutive levels of TNF-a levels in lymph nodes from healthy animals also run high with an average value of 2891 +/- 778 mRNA copy number/ 0.5 ug (value represents mean +/- S.D. of 8 samples analyzed). Analysis of lymph node samples from these 3 animals at autopsy on the other hand showed that some of the nodes gave values higher than the respective baseline values providing suggestive evidence that there may be a transient decrease of TNF-a mRNA synthesis perhaps during the acute infection period, but that these values either return to baseline or show an increase . It is of interest to examine the data from the animal which showed the highest index of illness (animal #26161). Most, if not all values from this monkey showed markedly reduced TNF-a mRNA levels in lymph nodes. This supports our hypothesis that certain monkeys in the colonies have either a chronic non-detectable infection or are immune activated such that experimental infection of these animals may lead to a disease course distinct from the other monkeys in the colony.

(ix) MIP -1 a: As seen in Fig.2h, the data for this cytokine is the most dramatic. In all 4 SIV infected monkeys the values for the relative mRNA copy number increased dramatically in lymph node samples obtained at 2 weeks post infection as compared to values obtained on lymph node samples from these same monkeys prior to SIV infection (values of >10,000, >10,000, >10,000 and 1600 mRNA copy number / 0.5 ug seen on the week 2 p.i. samples as compared with 830,5, 100 and 40 mRNA copy number / 0.5 ug sample prior to SIV infection, respectively). Interestingly, all these high values at 2 weeks p.i. returned back to either baseline or lower values on lymph node samples from these same monkeys at autopsy. It is interesting to speculate that the marked increase in MIP-1 a during the acute phase of SIV infection (2 weeks p.i.) may be induced as a natural response to block and/ or reduce viral replication but disease is marked by a rapid decrease of MIP-1 a synthesis.

2. ESTABLISHMENT OF TECHNIQUES TO DETECT INTRACELLULAR CYTOKINES:

As described above in the methods section, this technique has some clear advantages over other techniques designed to detect and quantitate cytokine levels. The rationale is detailed in the methods section also. As seen in Fig. 3, aliquots of PBMC's from rhesus macaques stimulated in vitro with con-A for 48 hrs and then permeabilized and fixed readily demonstrate intracellular levels of IFN-g (Fig. 3B), IL-2 (Fig. 3C) IL-4 (Fig. 3D) and IL-6 (Fig. 3E) . The specificity of this staining was documented with the use of the CHO-DG44 cell lines that are stably and permanently transfected with constructs expressing monkey cytokines developed in our laboratory ( Villinger, F. et al, In preparation). Thus , CHO cells transfected with an empty pED vector do not stain with a cocktail of the anti-IL-2/anti IL-4 mAb's (see Fig.3 F). In contrast Fig.3 G and H show

the staining profile of CHO cells transfected stably and expressing rhesus macaque recombinant IL-2 and IL-4 , respectively stained with the respective mAb's. We are in the process of preparing similar CHO cell lines expressing a variety of other nonhuman primate cytokine genes. It should be noted that these CHO cell lines provide 2 important tools. Firstly, they can obviously be utilized as positive controls for the detection of non human primate cytokines. But, more importantly, the relative intensity of staining (mean channel ratio) obtained with each of these cell lines (with known copy number for the cytokine gene) when optimally stained will allow for deriving some comparative data which can be utilized to control for intra-assay variability.

3. PREPARATION OF CYTOKINE/CYTOKINE EXPRESSION CONSTRUCTS FOR POTENTIAL USE AS ADJUVANTS AND/OR MODIFIERS FOR GENETIC IMMUNIZATION PROTOCOLS:

The role of select cytokines to serve as adjuvants and or modifiers when incorporated within genetic immunization protocols remains to be elucidated in models other than rodents. It is reasoned that cytokines and in some cases growth factors that promote and/or facilitate cell mediated immune responses would be desirable for intracellular parasites such as viruses. A growing list of cytokines have been identified, some of which enhance antigen processing and presentation, others that influence the quality of the immune response, and others that induce increases in precursor cell pools etc. for both rodent and man. While a high degree of homology has been documented between sequences coding for the human and the nonhuman primate equivalent cytokines and other immunologically and hematologically important molecules, there are sufficient differences between the species that lead to a) non-reactivity of anti-human reagents to react with equivalent molecules from the non-human primate species and , b) Immunogenicity of the molecules in the discordant species. These thoughts have been summarized by our laboratory [33-35]. In efforts to address this issue our laboratory has cloned and sequenced genes coding for a number of non-human primate a) Cytokines, b) Growth factors, c) Chemokines, and d) Immunologically important molecules that orchestrate and/or regulate immune responses.

These so far include :

IL-1 a/b, IL-2, IL-4, IL-5, IL-6, IL-8, IL-10, IL-12 a/b, IL-15, IL-16, IL-18, IFN-a/b/g, TNF a/b, GM-CSF, SCF, MIP-1 a/b, RANTES, FUSIN, CC-CKR5, CD 28, B 7.1, B 7.2, CTLA-4 and VCAM-1. Of particular relevance to this proposal are the cytokines IL-12, IL-18, the growth factor GM-CSF and the immunologically important molecules B 7.1 and B 7.2. Efforts are currently underway to prepare SIV and SHIV constructs that include the entire coding regions for select cytokines.A number of these cytokines, growth factors and chemokines have been prepared in recombinant form to facilitate their use for in vivo studies. These so far include rhesus macaque IL-2, IL-4, IL-12 heterodimer, IL-15, IL-16, IL-18, GM-CSF . The strategy utilized to prepare such recombinants and comparative sequence analyses of some of these molecules from non human primates has been published by our laboratory [33-35]. One of these recombinant proteins, IL -12 has

been difficult to prepare occupying a considerable amount of effort by our laboratory, but the effort is justified as this cytokine may be one of the most important candidates for in vivo use. To provide an appreciation for this effort, a brief description is herein provided. We utilized the pGL3 enhancer vector backbone (Promega) and replaced the luciferase reporter gene with the macaque IL-12 a gene under the the control of the SV40 promoter and enhancer using NcoI and XbaI. The NcoI cloning site created an ATG codon upstream of the IL-12 a ATG site. Thus this site was destroyed by BAL31 digestion after linearization with NcoI and religation of blunted ends. After verification of the sequence, the vector was electroporated into COS cells and shown to synthesize IL-12 a. The macaque IL-12 b chain had to be first subcloned in the TA3 vector (Invitrogen) under the control of the CMV promoter. The promoter and insert were then excised using Pvu1 and SmaI from the pTA3-macIL-12 b construct and introduced into the pGL3 mac-IL-12 a following digestion with PvuI and SspI, thus placing the pCMV-IL-12 b site just downstream from the pGL3 synthetic polyA signal, resulting in a 6263bp construct. After verification of the orientation and insertion sites by DNA sequencing, this construct was electoporated into COS 7 cells and the production of the IL-12 heterodimer and the IL-12a homodimers is currently being evaluated.

Figure 1: Comparative analyses of cytokine mRNA levels in unmanipulated (ex vivo) PBMC samples from 4 SIV infected macaques collected at 6 weeks, 5 weeks, 3 weeks prior to infection, on the day of infection (day 0) and 8 weeks post infection. The data are reported in copy equivalents (CE)/ 0.5 ug of total RNA as measured by RT-PCR. The cytokine mRNA analyzed were IL-1b , IL-4, IL-6, IL-10, IFN-g and TNF-a`.

Figure 2: Comparative analyses of cytokine mRNA levels in lymph node biopsies (ex vivo) from 4 SIV infected macaques collected at 6 weeks prior infection, on day of infection (day 0), 2 weeks post infection and at necropsy (5 lymphnodes). The data are reported in copy equivalents (CE)/ 0.5 ug of total RNA as measured by RT-PCR. The cytokine mRNA analyzed were IL-1b, IL-2, IL-4, IL-6, IL-10, IFN-g , TNF-a` and MIP-1a`.

Figure 3: Detection of intracellular cytokine synthesis by flow cytometry in PBMC samples from rhesus macaques and in CHO cells expressing recombinant macaque IL-2 and IL-4. The panels represent macaque PBMC stained with isotype control antibodies (A), anti-IFN-g (B), anti-IL-2 (C), anti-IL-4 (D), anti-IL-6 (E) antibodies or CHO/pED6 control cells stained with anti-IL-2, anti-IL-4 antibodies (F) or CHO cells expressing rmacIL-2 stained with anti-IL-2 antibodies (G) and CHO cells expressing rmacIL-4 stained with anti-IL-4 antibodies (H).

Figure 1a

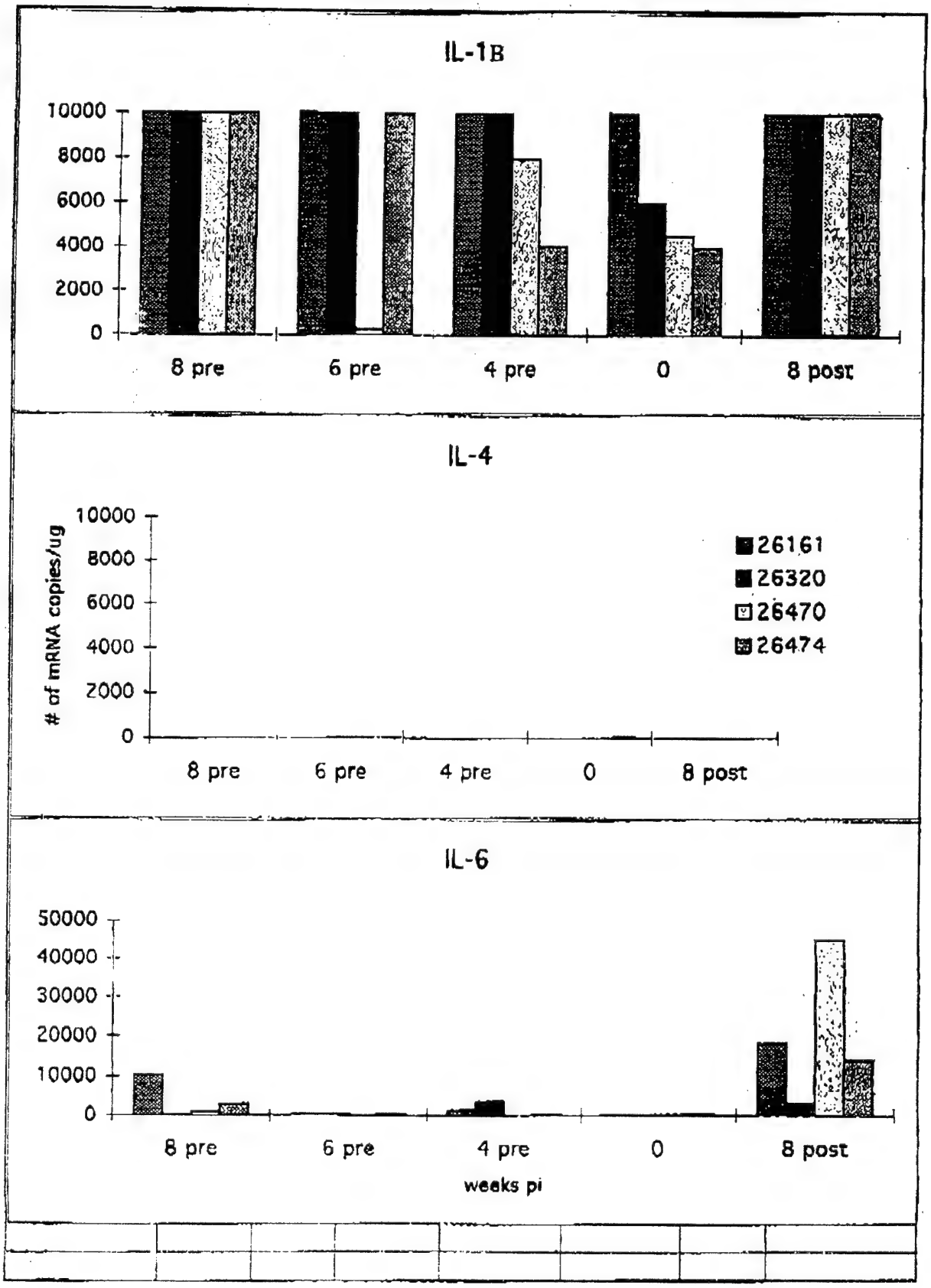
IL-1B
10000
8000
6000
4000
2000
0
8 pre
6 pre
4 pre
0
8 post
IL-4
# of mRNA copies/ug
10000
8000
6000
4000
2000
0
26161
26320
26470
26474
8 pre
6 pre
4 pre
0
8 post
IL-6
50000
40000
30000
20000
10000
0
8 pre
6 pre
4 pre
0
8 post
weeks pi

Figure 1b

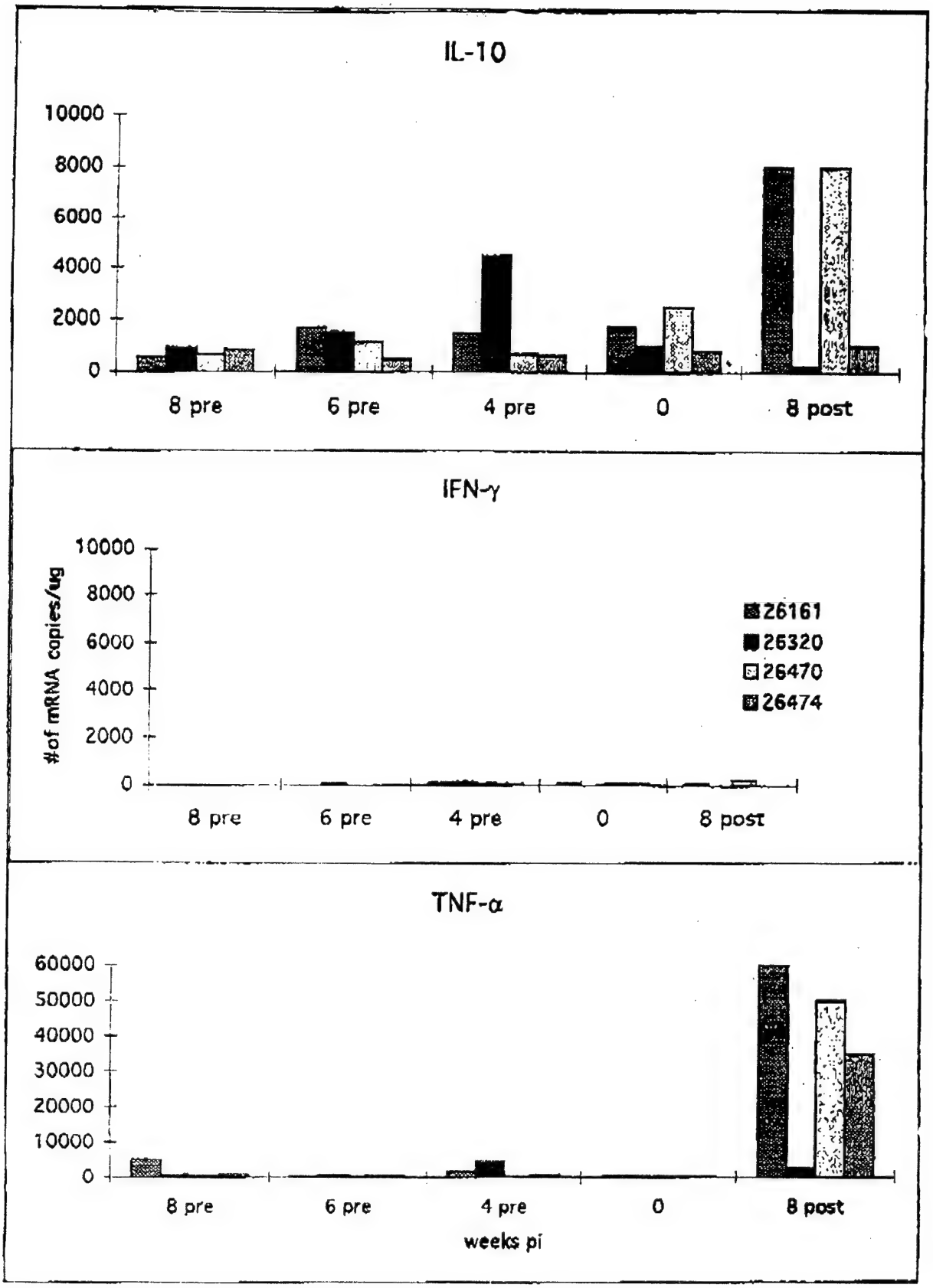
IL-10
10000
8000
6000
4000
2000
0
8 pre
6 pre
4 pre
0
8 post
IFN-γ
#of mRNA copies/ug
10000
8000
6000
4000
2000
0
26161
26320
26470
26474
8 pre
6 pre
4 pre
0
8 post
TNF-α
60000
50000
40000
30000
20000
10000
0
8 pre
6 pre
4 pre
0
8 post
weeks pi

Figure 2a

IFN-γ

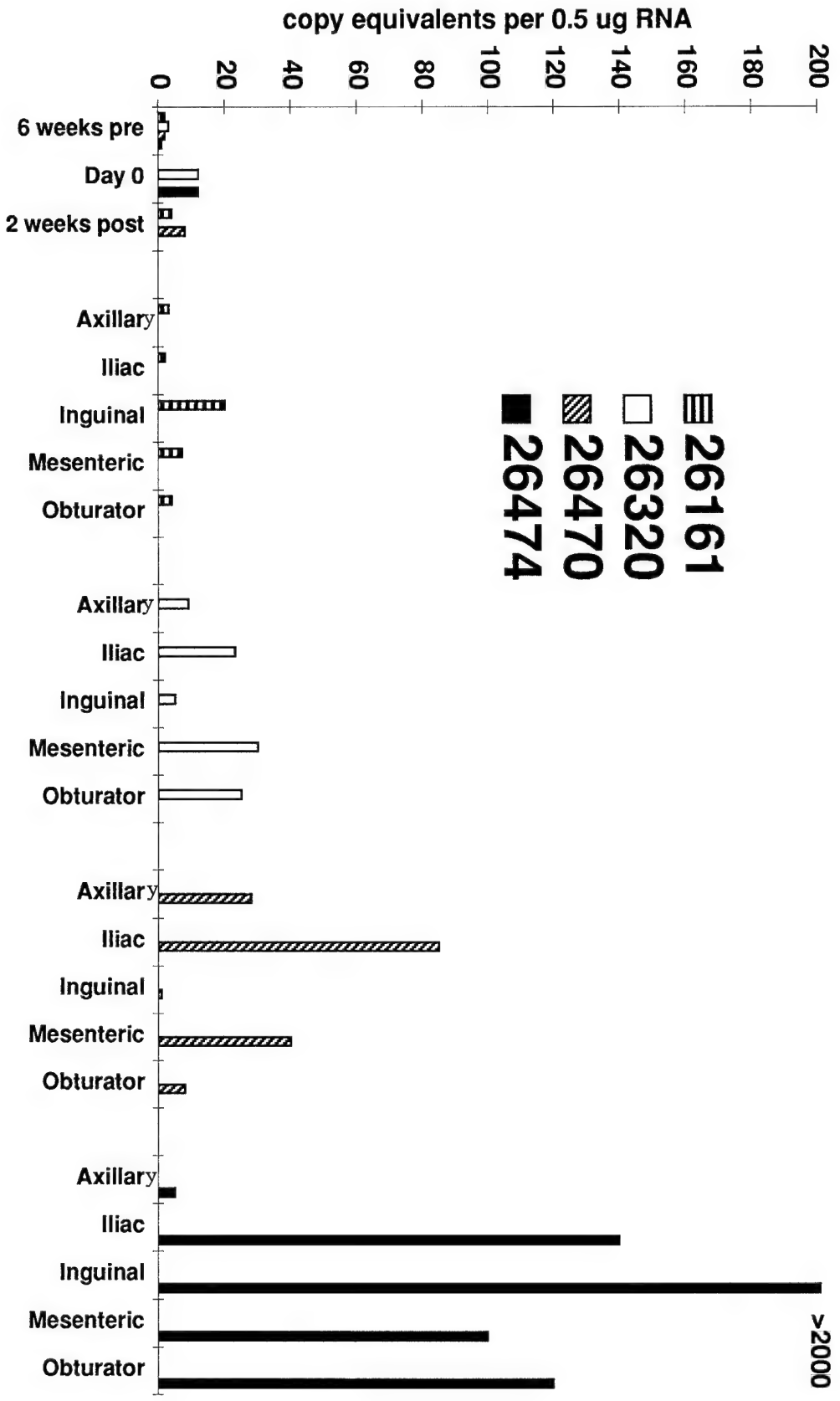

Figure 2b

IL-1β

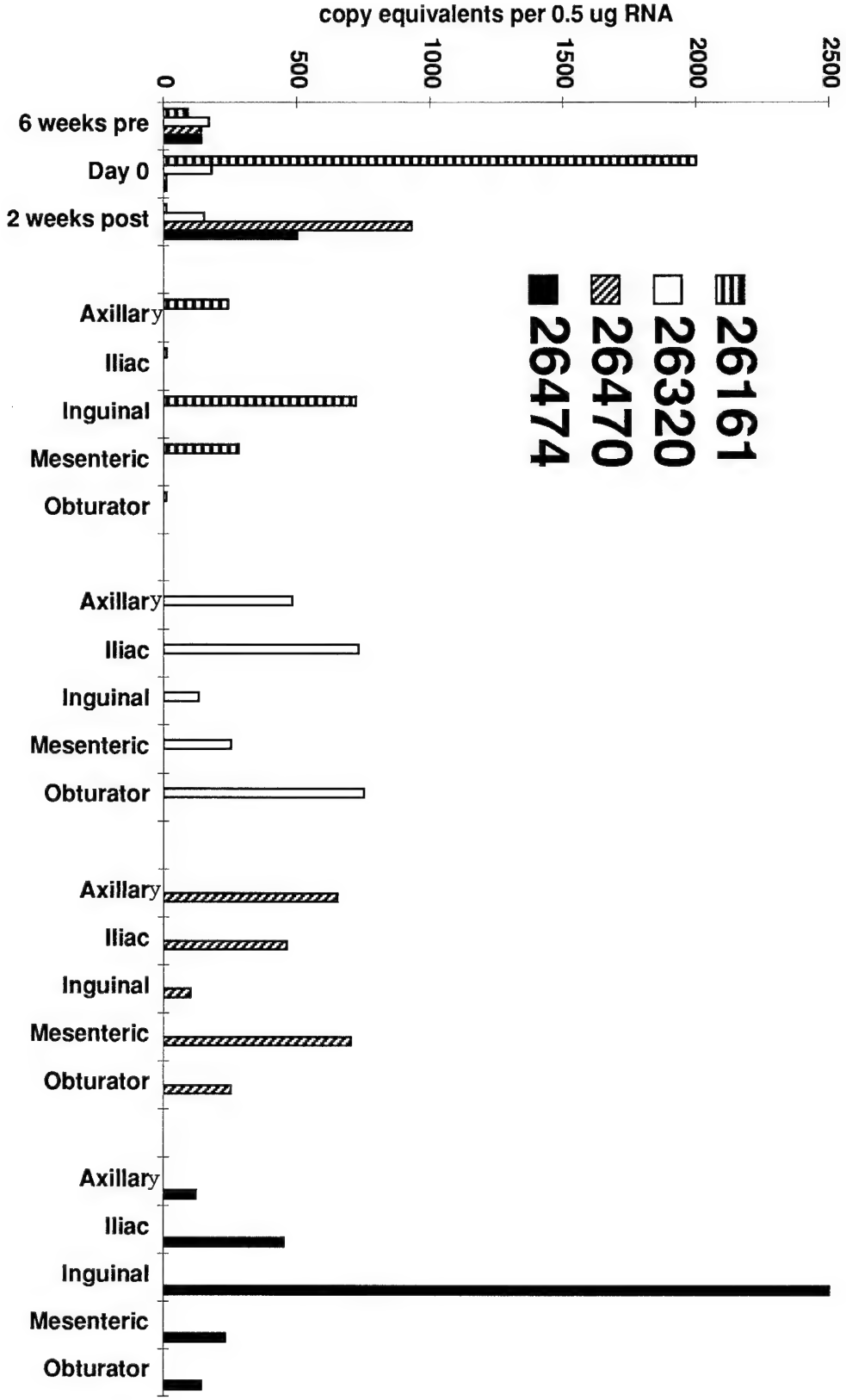

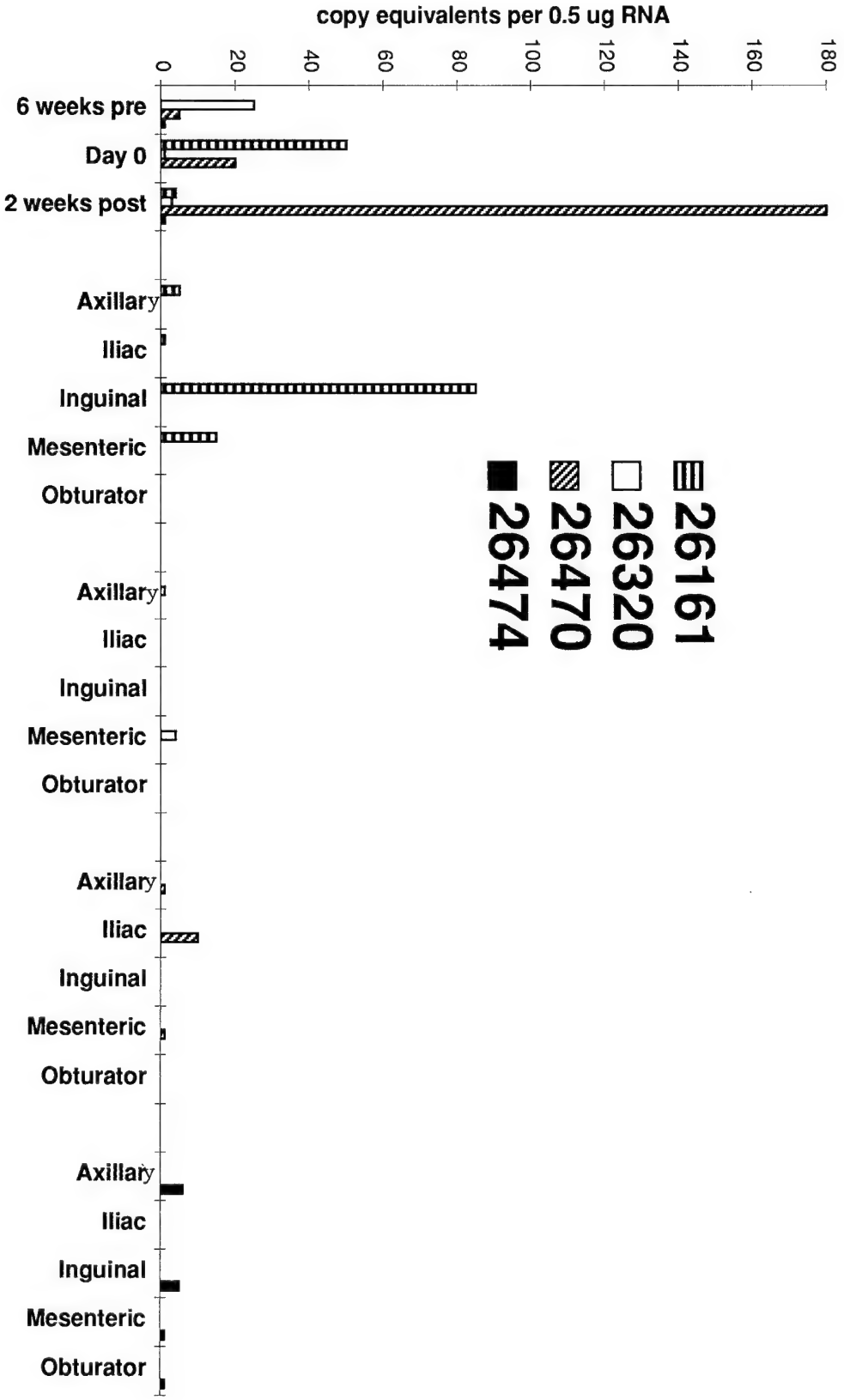


Figure 2c

IL-2

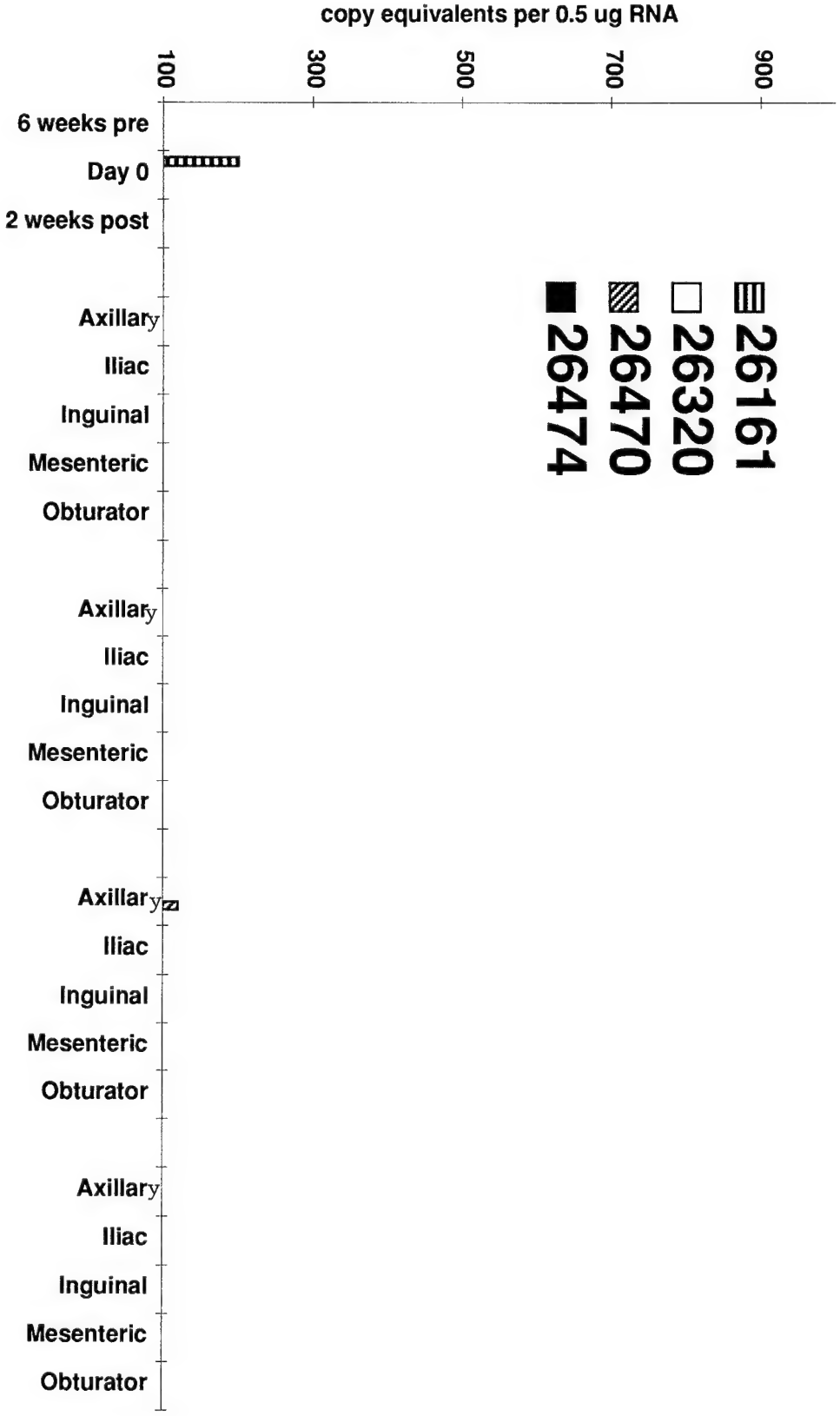


Figure 2d

IL-4

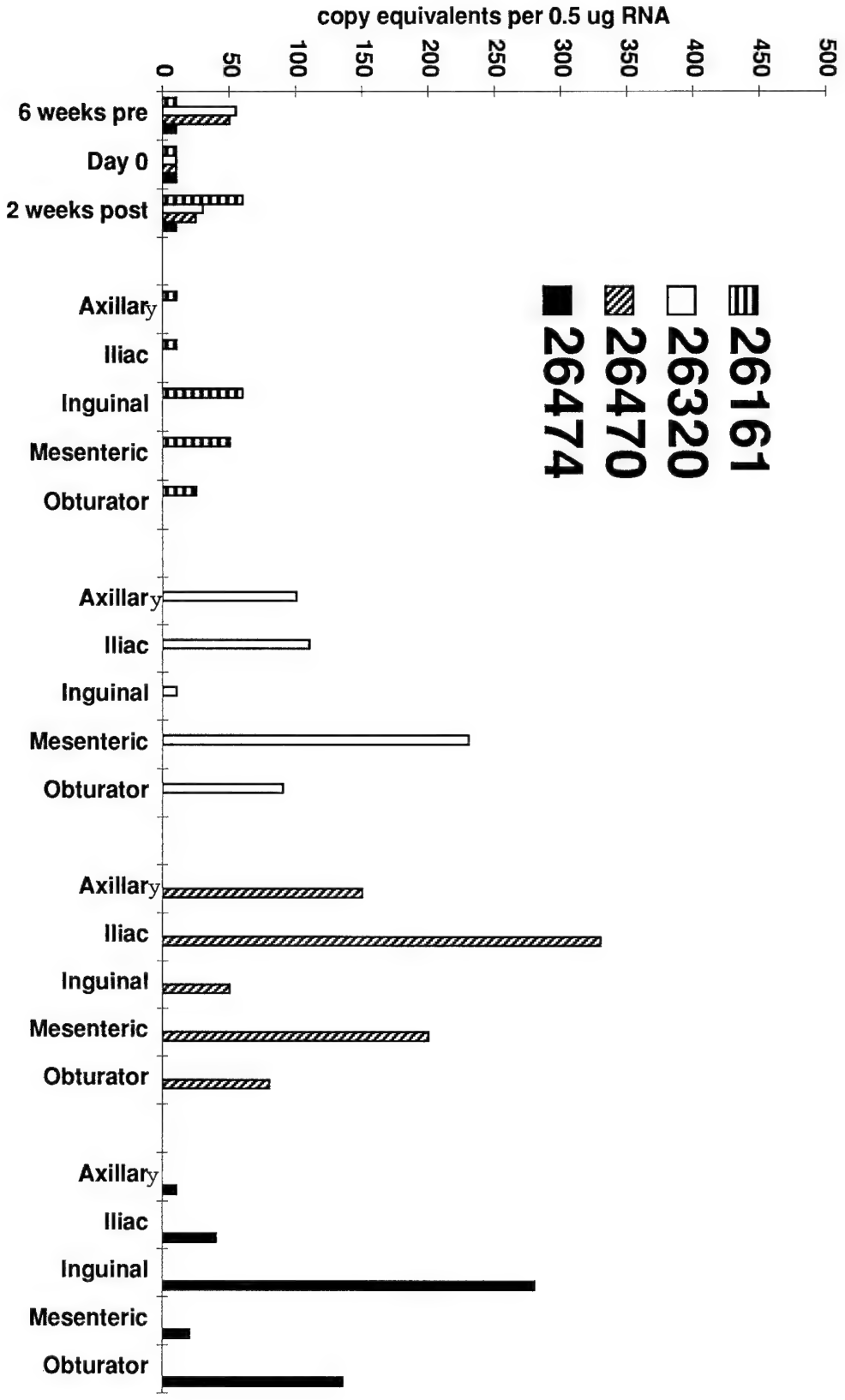


Figure 2e

IL-6

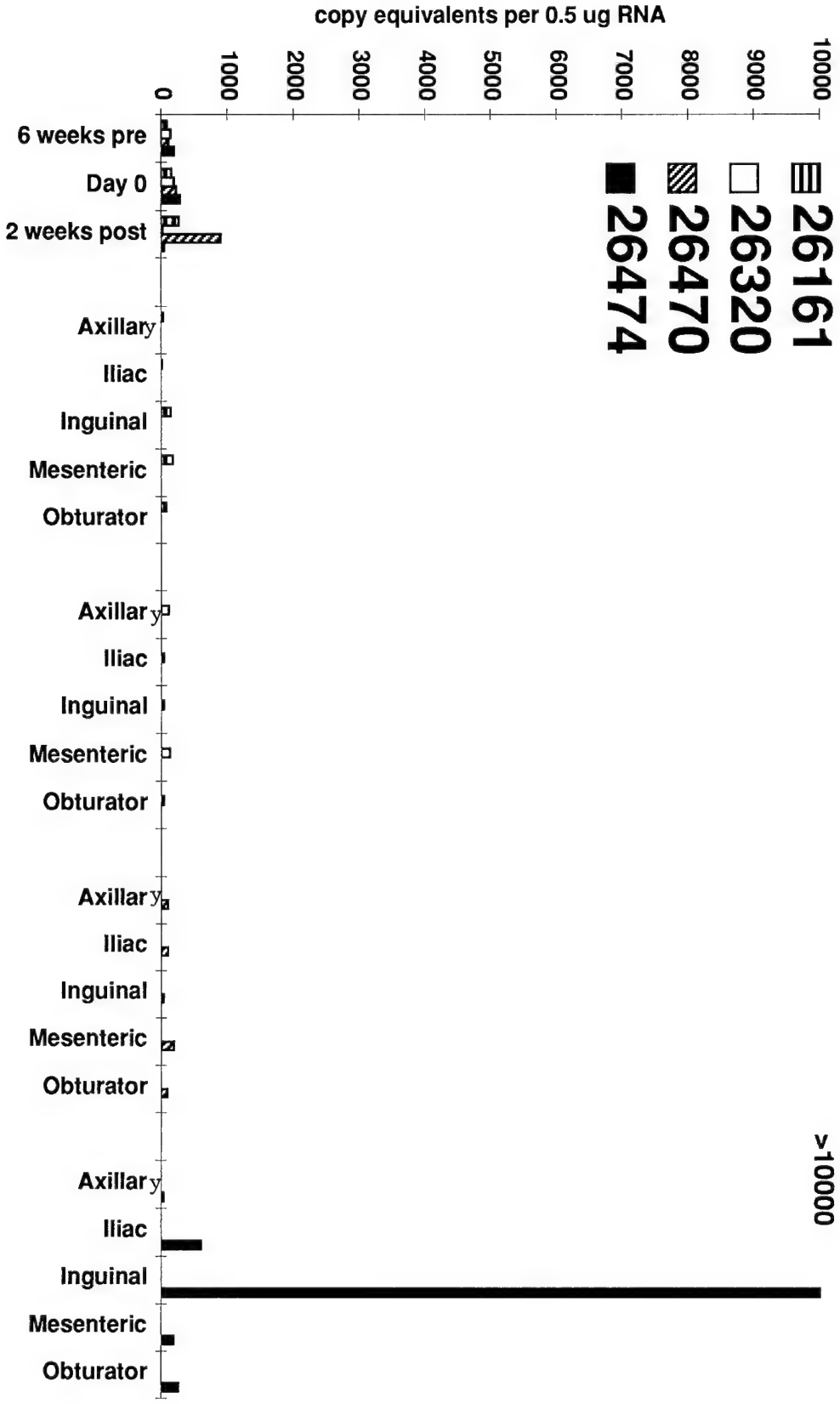


Figure 2f

IL-10

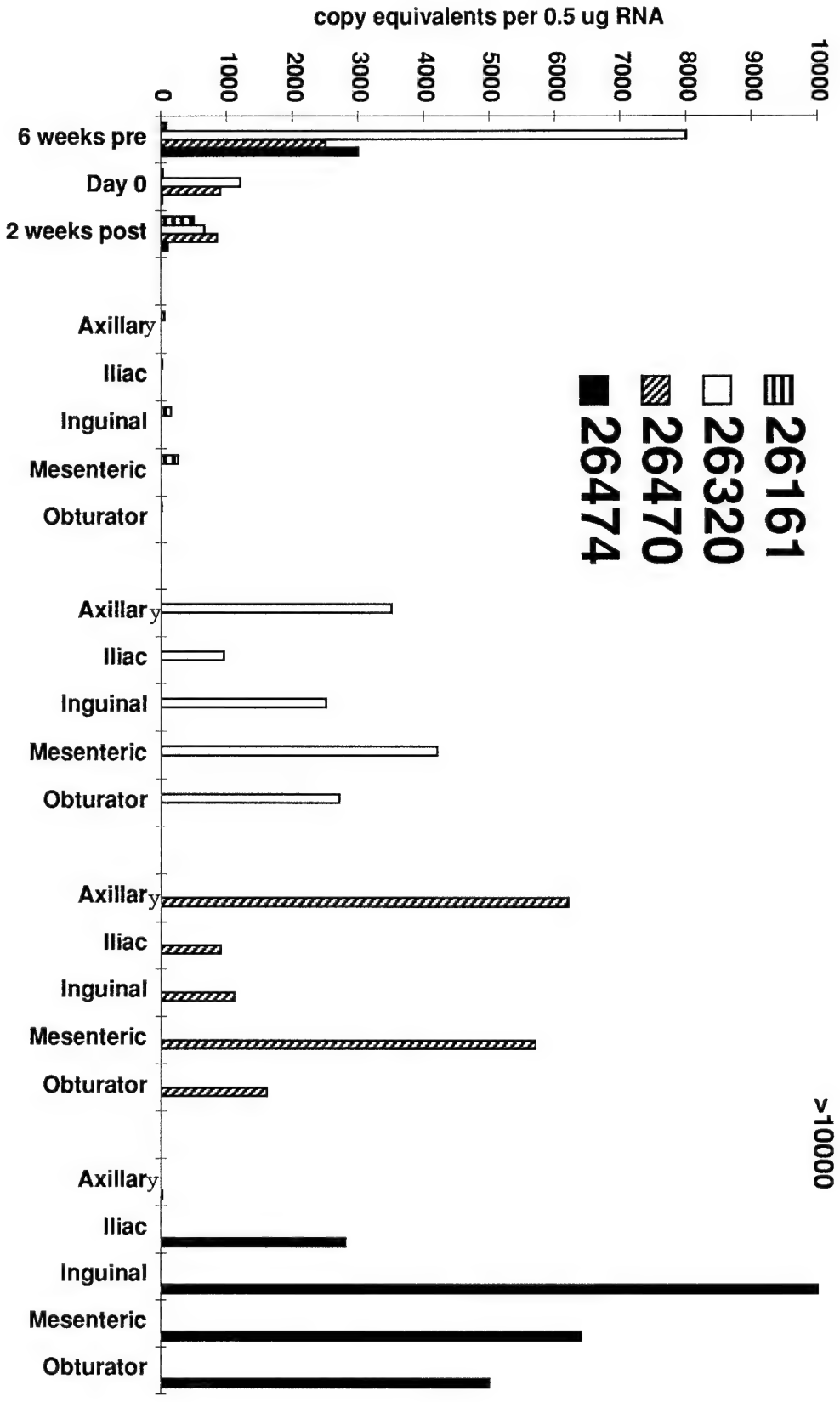


Figure 2g

TNF-α

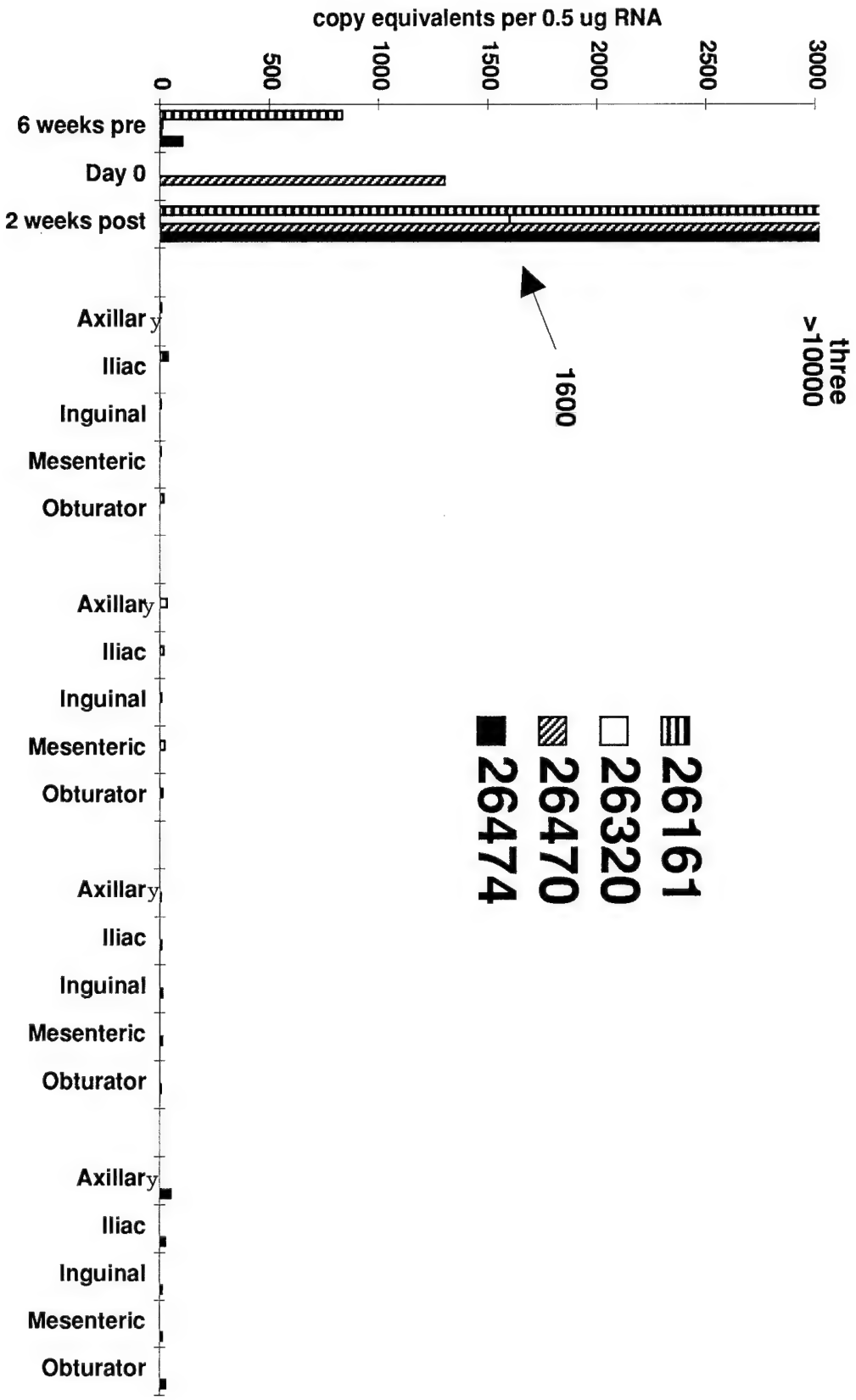


Figure 2h

MIP-1α

Figure 2i

# Control Monkeys

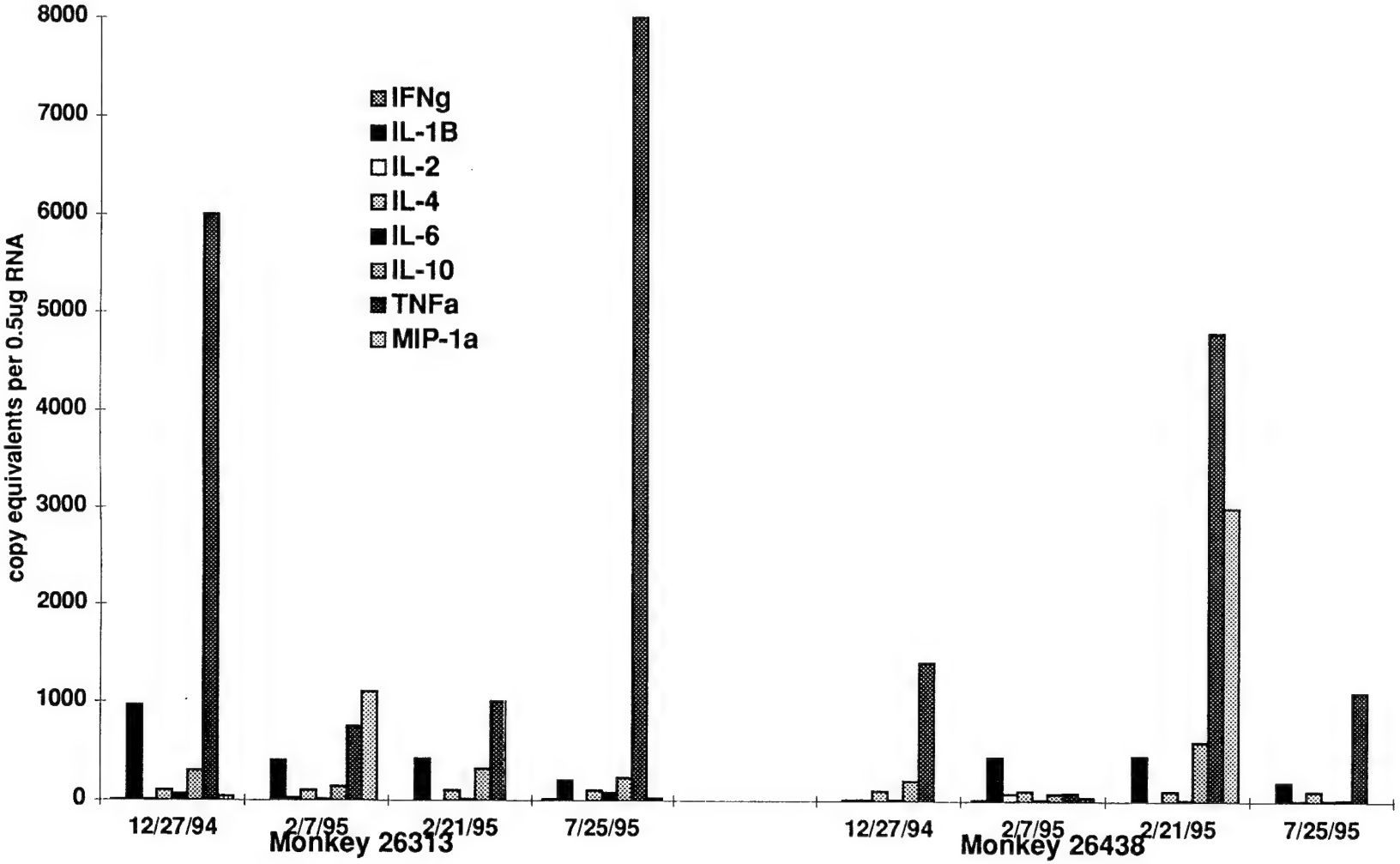

Macaque PBMC Figure 3

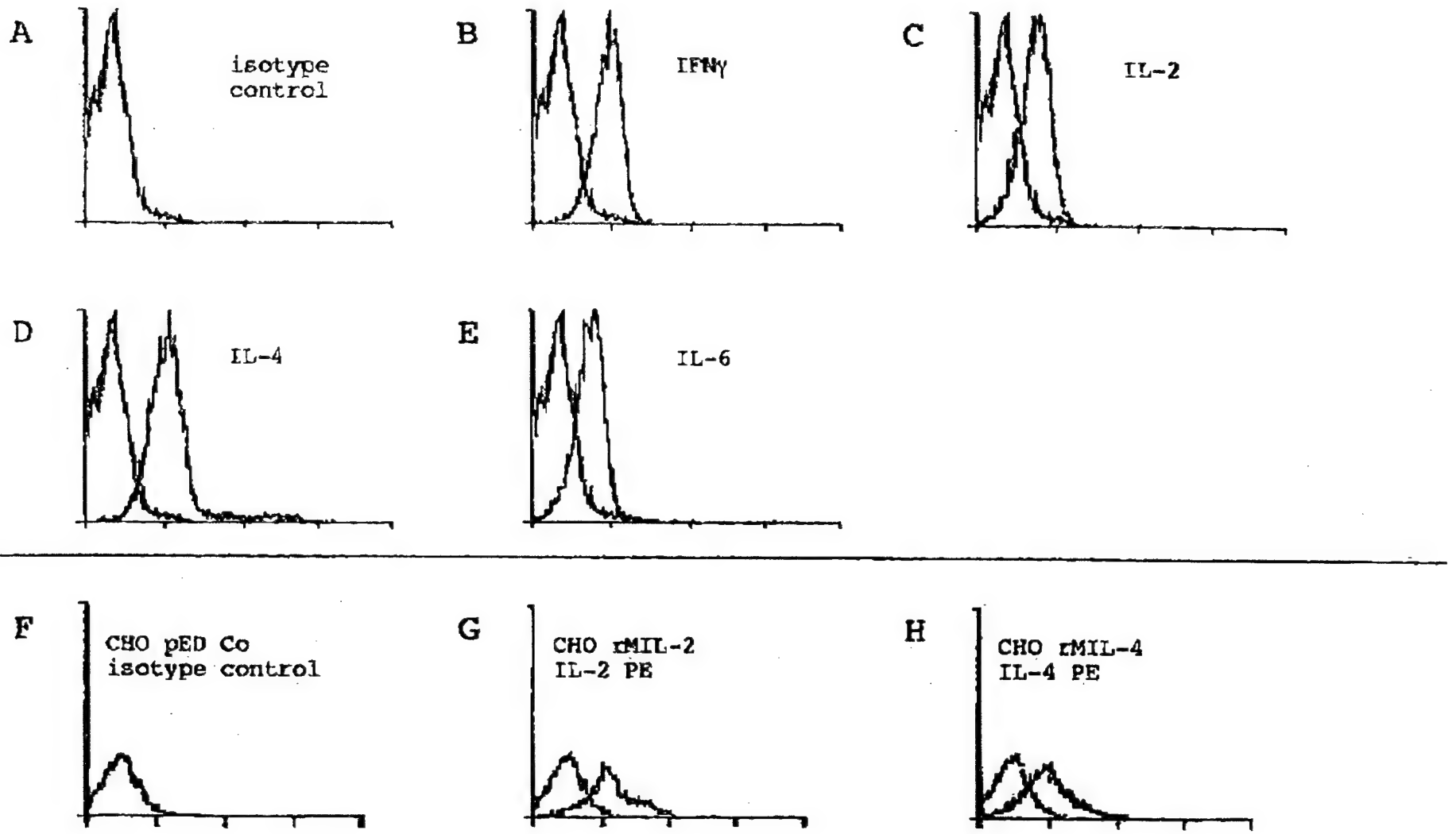

Vaccination of Primates, Dr. Gary Rhodes

The project is divided into two parts. The first consists of injecting animals with test antigens in order to optimize the injection procedures in primates. The second part of the experiment is to construct, and ultimately vaccinate animals with a series of plasmids which have C-terminal truncations in the *env* gene.

I. Optimization of Vaccination in primates.

A. Background: Nucleic acid vaccination has been extensively studied in mice. One of its most attractive properties in the rodent system is that a single injection of the antigen gene gives an immune response which lasts for the lifetime of the animal [41]. This long lasting immunity is seen with antigen genes from bacteria (an example is shown in Table 1 below), for influenza proteins (also shown in Table 1) and for the HIV gp120 gene (G. Rhodes, unpublished data, R. Malone, unpublished data). The data obtained in mice contrasts sharply to that seen in experiments reported in primates where a weak, transient response is found after gene injection and repeated injections appear to be required for a sustained response [5,11]. Two possible explanations can be proposed to account for the differences between species in the immune responses. One could argue that the HIV and SIV antigens that have been tested in primates are inherently weakly immunogenic and thus are unable to induce robust immunity [5]. We consider this explanation unlikely. As mentioned above, the HIV gp120 gene does generate a long lasting immunity in mice. Also, strong immune responses have to HIV and SIV gp120 have been induced by protein immunization in primates. Nevertheless, our initial experiments will study the response to highly immunogenic influenza and *E. coli* genes for which there is no evidence of transient immunity.

A more likely explanation for the weak immunity generated in primates is because DNA injections conditions have not been optimized for the larger animals. Some support for this idea has been obtained by studying expression of reporter genes in mice and rats. Intramuscular injection of 50 μg of plasmid DNA in 50 μl of saline gives about 10 times higher expression in mice than it does in rats. However, injection of the same amount of DNA in 500 ul gives the same expression in rats as optimal injection in mice (G. Rhodes, unpublished). This result is understandable if one considers that one is injecting a substantial fraction of the muscle volume during the normal mouse injections. Thus, we expect injection volume to scale with the size of the animal. No experiments have been reported to date in which this has been studied in larger animals. Thus, our first experimental study will be to find injection conditions in primates which optimize the immune response to test antigens.

We will use vectors expressing influenza nucleoprotein (NP), influenza hemagluttinin (HA) and *E. coli* ß-galactosidase (ßgal) genes. Experiments are designed to optimize the dose of DNA injected per animal, the injection volumes, and the route of injection (intradermal or intramuscular). In order to minimize the number of animals used in this experiment, each animal will be injected with three antigens, each antigen testing a different injection procedure.

B. Results: The plasmids pND-NP, pND-HA and pND-ßgal have been constructed and tested for their ability to generate and immune response in mice. Examples of such experiments are shown in Table 1 in which mice were immunized with a single injection of 50 μg of the plasmid DNA and tested for antibody response at 3 and 6 weeks after injection. There are three conclusions to these

experiments. First, the plasmids are active and able to generated immunity in mice. Secondly, a single DNA injection is sufficient to produce immunity. Thirdly, there is no evidence of a fall off in the immune response at least for the 6 weeks in which the animals were monitored.

Table 1
Immune Response in Mice to pND-ßgal and pND-NP

| Animal | Plasmid | Route | Week 0 | Week 3 | Week 6 |
|---|---|---|---|---|---|
| A | pND-ßgal | im | 0.085 | 0.641 | 0.601 |
| B | pND-ßgal | im | nd | 1.116 | 2.500 |
| C | pND-NP | im | 0.095 | 1.197 | 1.056 |
| D | pND-NP | id | 0.107 | 0.644 | 1.174 |

Animals were injected with 50 µg of the plasmid DNA and were bled at the times shown. Serum was diluted 1/320 and antibodies were measured in an ELISA using purified antigen to coat plates. The numbers shown are the absorbance obtained at 405 nm after 1 hour reaction with substrate. Abbreviations: nd -- not determined, im -- intramuscular injection, id -- intradermal injection.

C. Protocol for Primate Injection: We will utilize 9 animals in these studies which will be divided into three groups of three animals. The NP antigen will be used to test dose of DNA required for intramuscular injection, ß-galactosidase to test the volume of injection and HA to test the amount of DNA to use in intradermal injections (Table 2).

Table 2
Injection Protocol for Optimization in Primates

| Group | NP DNA (intramuscular) | ß-gal DNA (intramuscular) | HA DNA (intradermal) |
|---|---|---|---|
| A | 50 µg DNA<br>500 µl volume | 200 µg DNA<br>100 µl volume | 20 µg DNA<br>200 µl volume |
| B | 200 µg DNA<br>500 µl volume | 200 µg DNA<br>500 µl volume | 80 µg DNA<br>200 µl volume |
| C | 1000 µg DNA<br>500 µl volume | 200 µg DNA<br>2500 µl volume | 320 µg DNA<br>200 µl volume |

The DNA for all injection will be dissolved in sterile normal saline. Intramuscular injection will be into the triceps muscle group. The NP DNA will be injected into the left triceps and the ß-gal DNA into the right muscle. Intradermal injection will be given as two 100 µl injections at separate sites on a shaved area on the under side of the forearm. Animals will be bled three weeks before vaccination, at the time of vaccination and at two week intervals for two months. Animals may be reinjected at 4 or 6 weeks if the observed immune responses are weak. Blood will be heparinized

during collection with sample size ranging for 20 to 50 ml depending on the size of the animal (see Table 3 below). Plasma samples will be assayed for antibodies to each antigen. PBL, collected at the same time points, will be isolated tested for CTL. PBL will also be restimulated with antigen protein *in vitro* for 3 days and then assayed for proliferation (at Davis), and for the production of $Th_1$ and $Th_2$ cytokines (at Emory, see the cytokine section for protocols).

Animals for these experiments have been chosen and are shown in Table 3. The amount of blood obtained per bleed depends on the size of the animals and is shown in the table also. The number of cellular assays which will be performed will depend on the blood volume and the priority will be CTL then cytokines and then proliferation.

Table 3
Assignment of animals to groups and bleed volume

| | | | |
|---|---|---|---|
| Group A | MMU24877 (20 ml) | MMU26787 (20 ml) | MMU26267 (30 ml) |
| Group B | MMU26728 (40 ml) | MMU26214 (40 ml) | MMU26024 (40 ml) |
| Group C | MMU26159 (40 ml) | MMU25456 (50 ml) | MMU21049 (50 ml) |

C. Status: Plasmid DNA (5 to 15 mg of each plasmid) has been purified by double CsCl banding and tested in mice (Table 1). Animals have been selected and assigned to groups (Table 2 and Table 3). A prebleed has been obtained and B cells have been transformed with *H. papio* virus. Animals will be injected as soon as the transformed cell lines are confirmed as Foamy Virus free and are frozen which is expected this week.

II. Preparation and analysis of SIV env expressing plasmids.

A. *Env* plasmids to be tested. As discussed in last year's report, we plan to test four envelope expression vectors which contain the full length gp160 (pNDc-G4) and envelope proteins containing increasing sizes of C-terminal deletions (pNDc-G3 to pNDc-G1). These are illustrated in Fig. 1. All vectors but pNDc-G1 produce recombinant antigens which dimerize. Dimers of envelope protein have been proposed to be important for the generation of neutralization antibodies [42].

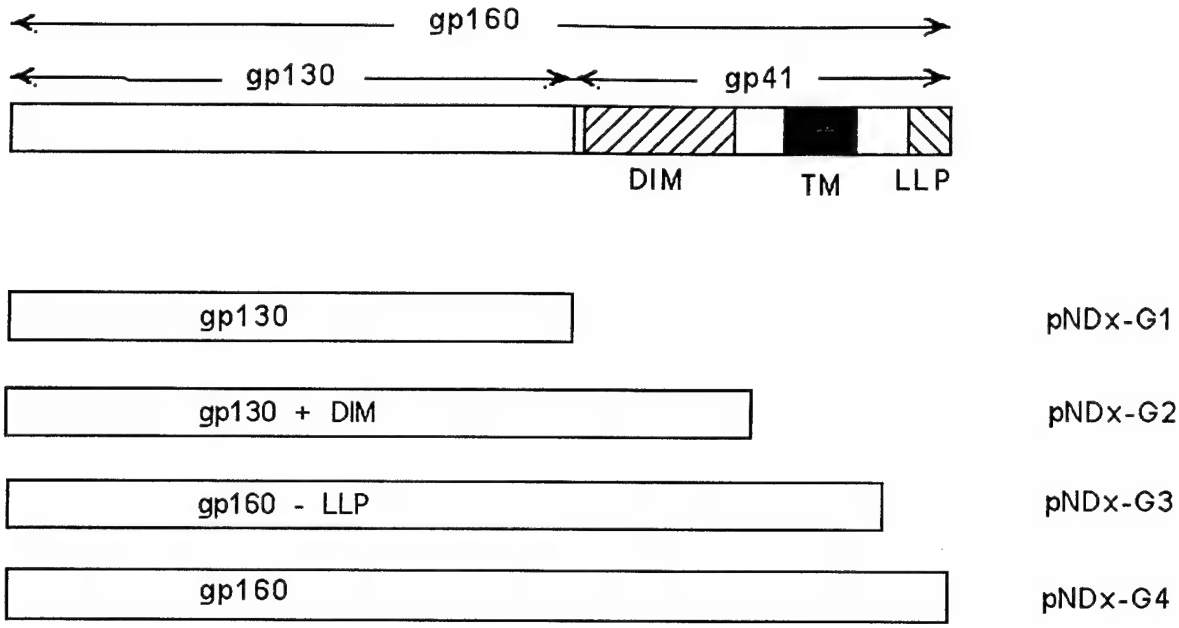


Fig. 1. Diagram of expression vectors containing portions of the *env* gene. DIM indicates the dimerization domain of gp41 and LLP indicates a region which is toxic to cells and which binds calmodulin. TM indicates the transmembrane domain.

1. **pNDc-G1** contains the gp130 region of the envelope gene.
2. **pNDc-G2** contains all of the gp130 region plus additional sequences in the N-terminal portion of gp41 which codes for a dimerization domain of the gp160 molecule. This construct should secrete env dimers.
3. **pNDc-G3** contains all of gp160 except the C-terminal 42 amino acids. This plasmid should give membrane bound env dimers.
4. **pNDc-G4** contains the full length gp160.

B. Results: The expression vectors pNDc-G1 to pNDc-G4 have all been made. Restriction digest to confirm the constructions are shown in Fig. 2. Both the ApaL I and Afl III enzymes give the expected pattern showing an increasing size of one of the intermediate bands with increasing size of the plasmid.

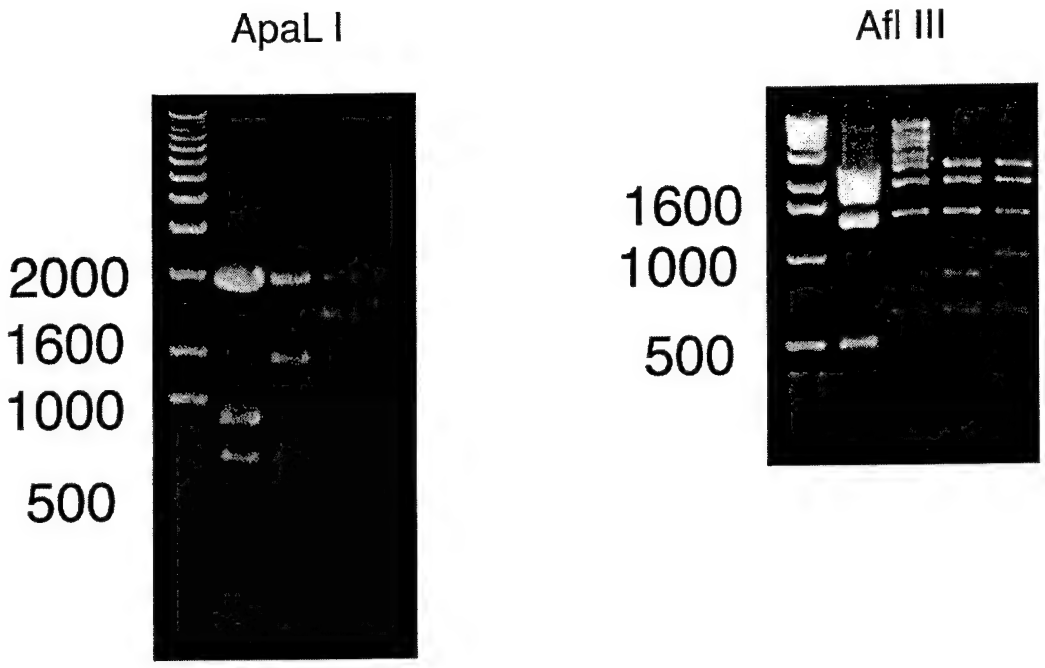


Fig. 2. Restriction digest of the pNDc-Gx plasmids. Each vector was digested with the enzyme ApaL I (left hand side) and Afl III (right hand panel). The lanes from left to right are 1, markers; 2, pNDc-G1; 3. pNDc-G2;, 4, pNDc-G3; 5, pNDc-G4. The expected size for the ApaL I digestion are: G1: 2964+1478+**1246**+497, G2: 2964+**1970**+1246+497, G3: 2964+**2435**+1246+497, G4: 2964+**2577**+1246+497. The expected sizes for the Afl III digestion are: G1:2368+1935+1389+**493**, G2:2368+1935+1389+622+**363**, G3: 2368+1935+1389+**828**+622, G4: 2368+1935+1389+**970**+622. Expected differences are shown in bold type. The marker sizes are shown.

Western blots have been performed to confirm expression of plasmids pNDc-G1, -G2 and -G4. An example is shown in Fig. 3 where a blot of cells transfected with pNDc-G4 was probed from sera from an acutely infected animal. The extract has a band which runs identically with recombinant gp160. Transfection experiments are continuing with constructs from the new vector, pND4 (see below). We are also characterizing the RNA found in transfected cells in order to confirm the efficient *rev* gene independent transport from nucleus to cytoplasm [43].

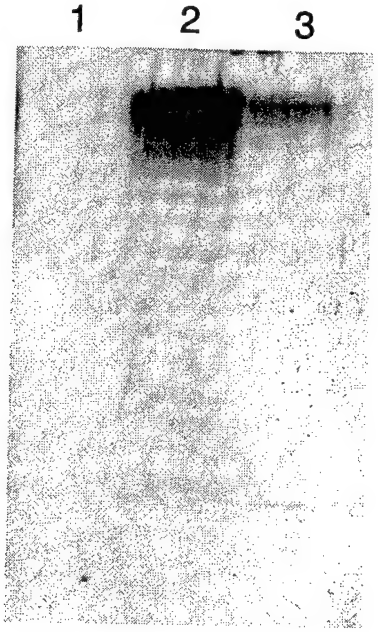


Fig. 3. Western blots of cells transfected with plasmid pNDc-G4. BHK cells were transfected with CsCl purified plasmid DNA and cell extracts were run on a 7.5% acrylamide gel and transferred to polyvinylidene filters. The filter was probed with a 1/250 dilution of serum from an acutely infected animal, washed and probed with alkaline phosphatase labeled antibody to human IgG. Lane 1 contains extract from untransfected controls, lane 2 contains extract from cells transfected with pNDc-G4 and lane 3 contains a recombinant gp160 protein produced in CHO cells and kindly provided by Dr. C. Walker from the Primate Center at the University of California at Davis.

As discussed above, all pNDc derived plasmids have been made. Five to ten milligrams of plasmids pNDc-G1, -G2 and -G4 have been grown and purified by double CsCl banding. A large scale preparation of plasmid pNDc-G3 has not been made yet because of stability problems. I am currently working on two solutions to this problem. The first is to find growth conditions (vary temperature, bacterial strain, selection conditions) will allow large scale growth in liquid media. The second approach involves construction of a new vector system, pND4, which reverses the orientation of the $amp^r$ gene relative to the inserted env sequence (see maps in Fig. 4 below). Our hypothesis is the read-through transcription form the amp promotor produces expression of a toxic *env* derived product in bacteria. The pND4 vector has been made as has the pND4-G1 plasmid. The new plasmids appear to be more stable. I am currently testing pND4-G1 for expression as well as adding the other envelope sequences to this vector.

Mice have been injected with pNDc-G1, pNDc-G2 and pNDc-G4 and serum samples have been obtained at 3 and 6 weeks post injection. The serum will be assayed for antibodies to gp160 next week. They will also be assayed for neutralizing antibodies in order to help select the vectors which will be tested in primates. Finally, CTL assays will be performed on the vaccinated mice 10 weeks post injection.

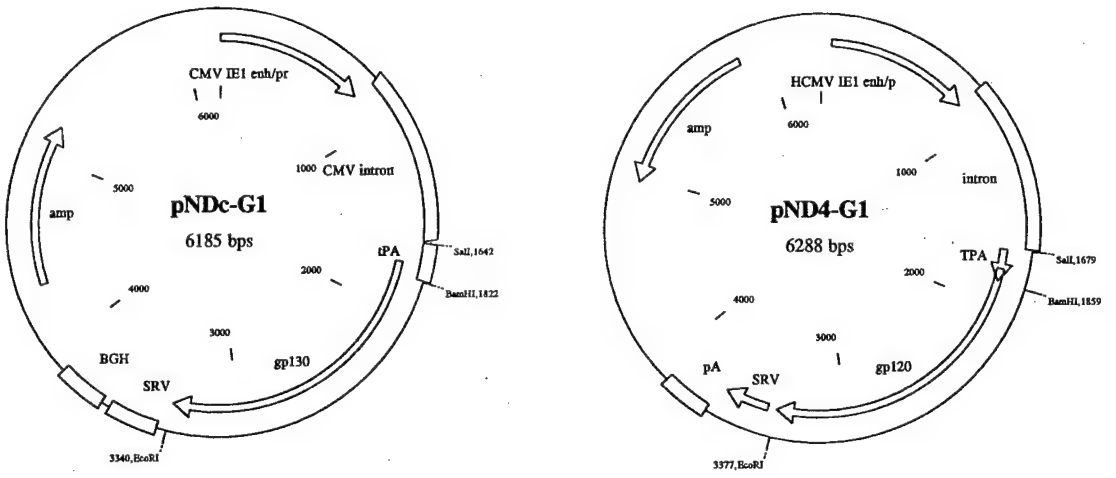


Fig. 4. Map of the expression vectors pNDc-G1 and pND4-G1. Note that the orientation of the bacterial backbone of the plasmid has been reversed relative to the inserted eukaryotic and viral sequence.

C. Primate Challenge Experiment. We have budgeted 12 animals for the challenge experiment which is enough for 4 groups of 3 animals or 3 groups of 4 animals. This means that we will be unable to test all of the plasmid vectors that we have constructed. Vaccine candidates will be chosen based on the immunological parameters measured in the mouse experiment. Specifically we will chose those candidate vectors which produce the highest neutralizing antibodies and give a vigorous CTL response.

Expression Vector Development Part B, Dr. Torres

Our laboratory is currently characterizing a mutant SIV provirus that is stably integrated as a single copy into the $CD4^+$ CEMx174 cell line. The mutant, SIV B7, was obtained by limiting dilution of cells infected with pathogenic SIVsmH3 and subsequent expansion of a single cell clone. Initial characterization has shown that purified B7 defective virus particles do not infect HUT-78, MT4, MolT-4 and CEMx174 cell lines, or rhesus and human PBL and macrophages. Sequencing of PCR products from the B7 provirus in our laboratory has revealed that a 1.6 kb deletion exists encompassing the coding regions for the integrase, vif, vpx, and vpr proteins **(table 1, figure 1)**. Mutations in integrase alone do not halt virus production , but the multiple lesions in B7 appear to be sufficient to render the virus non-pathogenic *in vivo* . The *vif* gene product is important in early stages of infection, and loss of this gene alone in HIV-1 can result in the loss of infectivity in primary lymphocytes and macrophages . It has been shown that *vpx/vpr* double mutants of SIV replicate poorly *in vitro* and do not produce disease. Inefficient proteolytic cleavage of gag and gag-pol polyproteins by mutation, deletion, or inhibition of the viral protease can also lead to production of non-infectious virus. The multiple lesions in our mutant results in a highly attenuated virus, but one that will elicit a strong immune response. We have constructed a plasmid in which the genetic lesions found in SIV B7 have been introduced into the molecular clone of the parental SIV smH3. In addition to the deletion we have substituted the CMV promoter/enhancer in place of the U3 region of the 5= LTR **(figure 2)**. We hypothesize that when injected into rabbits and monkeys using a needleless $CO_2$ injection system (Biojector) the construct will express viral proteins endogenously, thereby promoting a cellular immune response, and have the possibility of producing defective viral particles, (that have already been shown to be non-pathogenic in Rhesus macaques), to promote a humoral response. Since the most effective vaccine developed against SIV so far involves a low level infection with a live attenuated virus, we feel that our approach is promising.

Three female New Zealand white rabbits were injected with 200:g of plasmid in 500:l of sterile PBS in two sites in the hip. The rabbits were boosted at 14 weeks with the same dosage. The humoral response was evaluated by ELISA **(table 2)**. ( Fig. 3).

**Table 1** Sequence data of SIV smB7 provirus.

| Region | Nucleotides sequenced | Base changes from SIV smH4 |
|---|---|---|
| p8 | 2091-2602 | NONE |
| protease | 2437-3108 | 2883 (AYG) 2901 (AYG) |
| pol / env | 3086-6634 | 4362 (GYA) 4431 (TYC)<br>4467 (CYA) 4522 (AYG) |

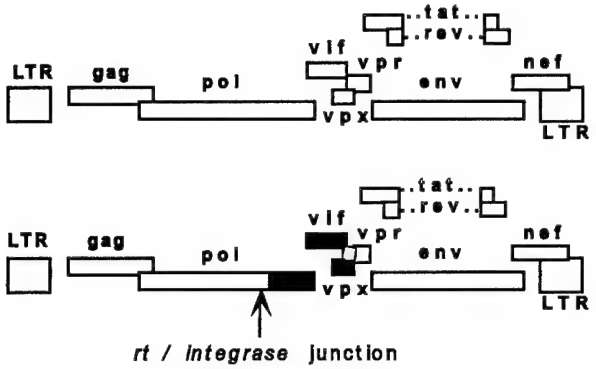


**Figure 1** Partial sequence comparison of SIV smH4 (top) to SIV smB7 (bottom). Shaded areas are deleted in SIV smB7 provirus. All sequences were determined from a minimum of three different PCR-derived subclones per region.

**Table 2** Antibody response of rabbits injected with pCMV-B7

| Animal | 6379 | | 6398 | | | | 6400 | | | |
|---|---|---|---|---|---|---|---|---|---|---|
| Antigen | B7 [1] | | B7 | | gp130 [2] | | B7 | | gp130 | |
| week | 1:20 [3] | 1:80 | 1:20 | 1:80 | 1:20 | 1:80 | 1:20 | 1:80 | 1:20 | 1:80 |
| 2 | 0.84 | 0.97 | 1.62 | 1.74 | 1.50 | 1.38 | 0.82 | 1.03 | 1.41 | 1.25 |
| 4 | 0.78 | 0.90 | 1.52 | 1.50 | 1.14 | 1.20 | 1.01 | 1.02 | 1.75 | 2.18 |
| 6 | 1.06 | 1.21 | 1.70 | 1.74 | 1.71 | 1.46 | 1.19 | 1.34 | 2.33 | 1.96 |
| 8 | 0.98 | 1.42 | 1.80 | 1.97 | 1.83 | 1.65 | 1.40 | 1.53 | 2.08 | 2.14 |
| 10 | 1.63 | 1.86 | 1.11 | 1.30 | 1.03 | 0.97 | 1.42 | 2.00 | 1.76 | 1.61 |
| 13 | 1.71 | 1.91 | 1.29 | 1.36 | 1.15 | 1.15 | 1.37 | 1.77 | 2.39 | 2.93 |
| 16 | 1.72 | 2.19 | 1.19 | 1.08 | 0.84 | 1.04 | 1.24 | 1.42 | 2.11 | 2.52 |
| 18 | 1.66 | 2.00 | 1.40 | 1.48 | 1.67 | 1.54 | 1.34 | 1.49 | 2.00 | 2.41 |
| 21 | 1.50 | 1.83 | 1.26 | 1.44 | 1.32 | 1.27 | 1.57 | 1.84 | - | - |

1 Wells were coated with 500ng of disrupted SIV-B7 defective virus particles
2 Recombinant gp130 was plated at a concentration of 500ng/well
3 Plasma was diluted 1:20 and 1:80
4 Values are calculated as the experimental OD/prebleed OD

**Figure 2** Plasmid map of pCMV-B7.

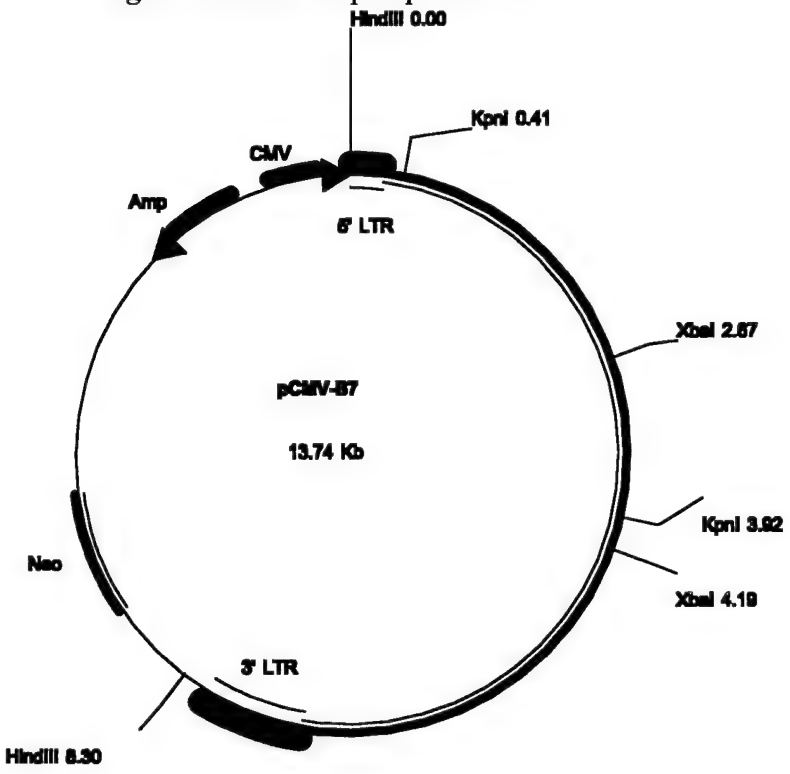


## Conclusions and future plans

The pCMV-B7 plasmid elicits a humoral immune response in rabbits to recombinant gp130 and disrupted SIV. The response to gp130 suggests that the viral message is being spliced and translated similar to the wild type message. Western blot analysis is currently under way to qualify the antibody response. The highest titer that gives a significant response (E/P ratio of 1.5 or greater) has not been determined. The cellular response is being evaluated by T-cell proliferation to SIV gag and envelope peptides.

FIGURE 3

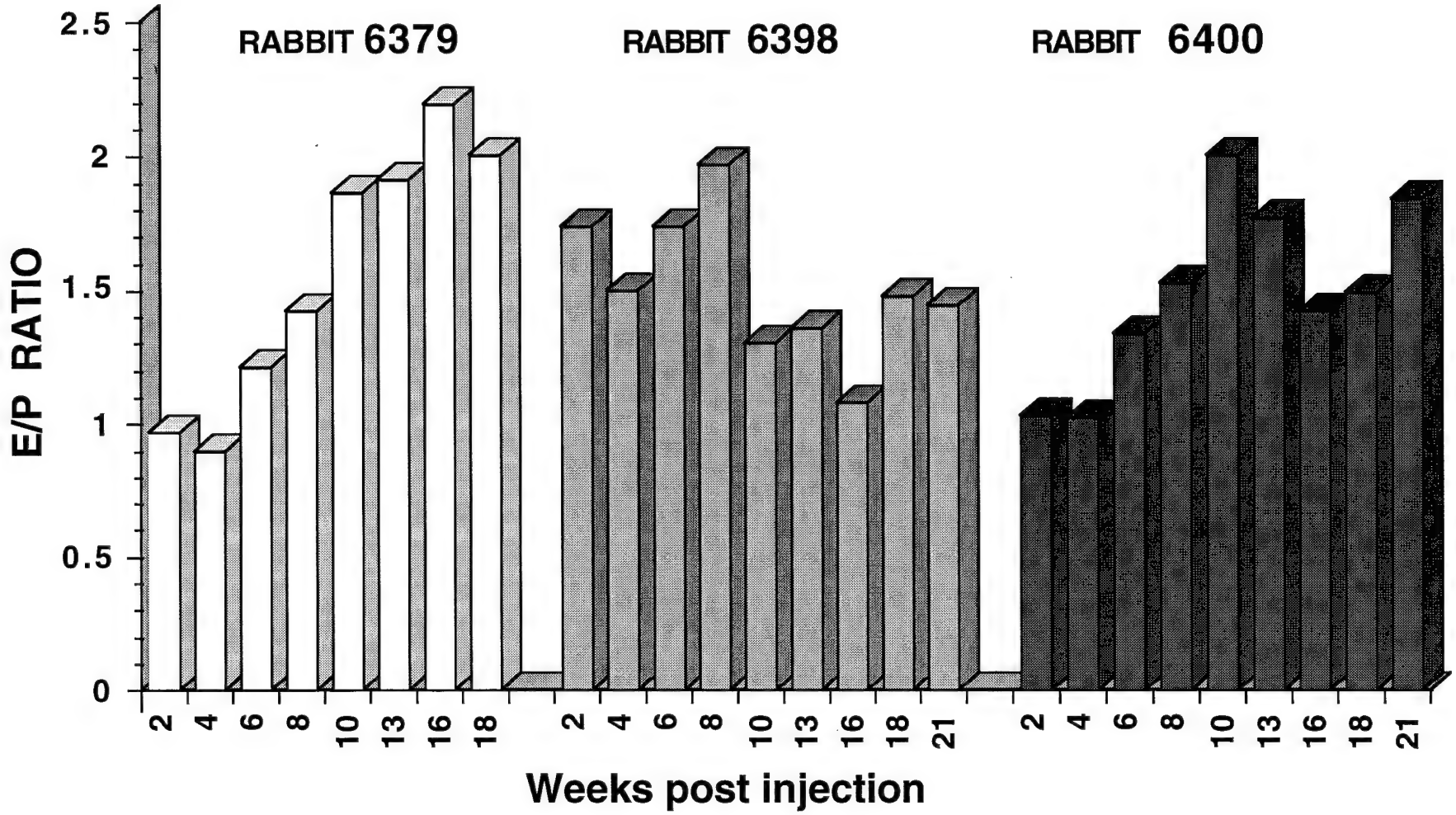


**Antibody response of New Zealand white rabbits to disrupted SIV-B7 defective virus particles in an ELISA format at a 1:80 serum dilution. Values are experimental OD/ prebleed OD. Animals were injected with 200μg of pCMV-B7 in500μl of sterile PBS and boosted with the same dosage at 14 weeks.**

Fatal Immunopathogenesis by SIV/HIV-1 (SHIV) in Juvenile and Newborn Rhesus Macaques, Dr. Paul A. Luciw

**Synopsis**

Selected SIV/HIV-1 (SHIV) chimeric clones, constructed by substituting portions of the pathogenic clone SIVmac239 with counterpart portions from HIV-1 clones, establish persistent infection in juvenile and adult rhesus macaques [26]. Our studies have focused on $SHIV_{SF33}$ which contains the *tat*, *rev*, and *env* genes of the cytopathic, T-cell line tropic clone $HIV\text{-}1_{SF33}$ (subtype-B). At about 16 months post-infection, one of four $SHIV_{SF33}$ infected juvenile macaques exhibited depletion of CD4+ T-cells in peripheral blood and lymph nodes and other symptoms of simian AIDS (SAIDS) (Table 1, Fig. 1 and 2). Virus recovered from this macaque in the symptomatic stage was designated $SHIV_{SF33A}$ (A, adapted); this virus displayed several amino acid sequence changes throughout the HIV-1 *env* gene compared to the input $SHIV_{SF33}$ clone (Fig. 3). Additionally, a mutation in $SHIV_{SF33A}$ restored the open reading frame for the *vpu* gene. *In vitro* evaluations in tissue culture systems revealed that $SHIV_{SF33A}$ was more highly cytopathic that $SHIV_{SF33}$ (data not shown). Transfusion of blood from the macaque harboring $SHIV_{SF33A}$ into two healthy uninfected juvenile macaques caused rapid decline of CD4+ T-cells and resulted in SAIDS in one recipient at 6 months post-transfusion (Table 2, Fig. 4). In two newborn rhesus macaques, a cell-free preparation of $SHIV_{SF33A}$ produced high virus load and rapid depletion of CD4+ T-cells; one of these neonates developed severe and fatal neurological disease at 4 weeks post-infection (Table 3, Fig. 6). The precipitous and sustained decline in CD4+ T-cells early after infection with $SHIV_{SF33A}$ contrasts strikingly with the minimal and transient decrease in CD4+ T-cells in the acute stage of infection of macaques with pathogenic strains of SIVmac. Taken together, these experiments on pathogenic SHIV establish the basis for further investigations on the role of the HIV-1 *env* gene in virus adaptation and the mechanism(s) of immunodeficiency in primates.

**Table 1. Virus load in juvenile rhesus macaques inoculated with $SHIV_{SF33}$.** Four macaques were inoculated with 500 $TCID_{50}$ cell-free $SHIV_{SF33}$ by the intravenous route. PBMC were recovered at various time intervals, and serial 1/10 dilutions of these PBMC were co-cultured with CEMX174 cells. Four wells in a microtiter plate were used for each sample. Supernatants from these co-cultures were assayed for SIV p27 gag antigen by ELISA to monitor virus replication. Viorus load was calculated by the Reed-Meunch formula and is expressed as $TCID_{50}$ per $10^6$ cells. Data for SIVmac239 infected animals is also included. All SHIV-infected macaques contained substantial amounts of cell-associated virus in the acute stage; virus load declined after about 4 weeks. Only macaque 25814 showed an increase in virus at 72 weeks post-infection in PBMC. At this time, this animal exhibited early signs of SAIDS (i.e., persistent lymphadenopathy, weight loss, lymphopenia, CD4 decline).

**Table 2. Virus load in the serial recipient juvenile macaques.** Cell-associated virus load in PBMC was measured as described in Table 1. Virus load data are also presented for juvenile macaques infected with the attenuated virus SIVmac239-delta nef and the pathogenic virus SIVmac239 nef-open. Macaque 27843 exhibited weight loss, lymphadenopathy, and pneumonia and was euthanized at 32 weeks post-transfusion; analysis at necropsy revealed lymphoid depletion. Infection with *Pneumocystis* is suspected; confirmation is pending. Macaque 27823 remains relatively healthy, although this animal is lymphopenic with low numbers of CD4-positive lymphocytes (Fig. 5).

**Table 3. Virus load in newborn macaques inoculated with $SHIV_{SF33A}$.** Cell-associated virus load in PBMC was measured as described in Table 1. Newborn macaque 29801 exhibit acute signs of disease (primarily neurological symptoms) and was euthanized at 4 weeks post-infection. Necropsy revealed lymphoid depletion. Analysis of the brain showed severe pathology characteristic of progressive multifocal leukoencephalopathy. The opportunistic agent SV40 is suspected; confirmation is pending.

**Figure 1. CD4 lymphocyte numbers after $SHIV_{SF33}$ infection of macaque 25814.** The number of CD4 lymphocytes was measured by flow cytometry at various timepoints after infection of macaque 25814 with $SHIV_{SF33}$. The decline in CD4 cells became evident at about 72 weeks post-infection, at which time virus load showed an increase (Table 1). The total lymphocyte number, measured by complete differential blood count (CBC), also declined at 72 weeks. At about 90 weeks, the total lymphocyte number was about 200 cells per ul with less than 50 CD4-positive cells per ul.

**Figure 2. Disease symptoms in macaque 25814.** Several signs of SAIDS were evident in macaques 25814 in the late stages of SHIVSF33 infection. Findings at necropsy confirmed that this animal had developed SAIDS. The main opportunistic pathogen was *Pneumocystis*.

**Figure 3. Sequence changes in the env gene of SHIVSF33 *in vivo*.** Virus was recovered from PBMC from macaque 25814 at 52, 72, and 96 weeks post-infection, and the env gene was amplified by PCR, cloned, and sequenced. Shown are amino acid changes in the V3 loop. Interestingly, virus recovered at late timepoints shows a new potential glycosylation site in V3. Sequencing revealed about 20 changes in gp120; these changes were largely in variable regions.

**Figure 4. CD4 lymphocyte numbers after serial passage of $SHIV_{SF33}$ in juvenile macaques.** Two macaques (27823 and 27843) were inoculated by blood transfusion from macaque 25814 at 96 weeks post-infection. Flow cytometry analysis of peripheral blood of macaques 27823 and 27843 showed a rapid and dramatic decline in CD4-positive cells; both animals also exhibited a decline in total lymphocyte numbers.

**Figure 5. CD4 lymphocyte numbers in newborn macaques inoculated with $SHIV_{SF33A}$.** Two newborn animals (29800 and 29801), at 2 days of age, were inoculated with 200 $TCID_{50}$ of a cell-free preparation of $SHIV_{SF33A}$. $SHIV_{SF33A}$ is the virus recovered from PBMC of macaque 25814 at 104 weeks post-infection. Both newborn macaques showed rapid decline in CD4-positive lymphocytes; total lymphocytes also declined. Newborn macaque was euthanized at 4 weeks of age because of severe disease signs (see Table 3).

Table 1. Virus load in juvenile rhesus macaques inoculated with SHIV-SF33.

| | weeks post-infection | | | | | | | |
|---|---|---|---|---|---|---|---|---|
| | 2 | 4 | 8 | 32 | 53 | 72 | 91 | 106 |
| **SHIV-SF33** | | | | | | | | |
| 25814 | 10,000 | 470 | 100 | 10 | 1 | 47 | 4,700 | 100 |
| 26074 | 4,700 | 47 | 22 | 3 | + | + | - | 3 |
| 26131 | 22,000 | 47 | 3 | + | + | + | - | - |
| 26240 | 4,700 | 32 | 10 | 2 | + | - | - | - |
| **SIVmac239** | | | | | | | | |
| 26084 | 47,000 | 32,000 | 2,200 | 10,000 | 3,200 ← SAIDS | | | |
| 27098 | 22,000 | 470 | 10,000 | 2,200 | 10,000 | | | |

Table 2. Virus load in the serial passage juvenile macaques.

| | weeks after infection | | | | | |
|---|---|---|---|---|---|---|
| | 2 | 4 | 8 | 16 | 24 | 32 |
| SHIV-SF33A | | | | | | |
| 27823 | 154 | 22 | 10 | 464 | 1,000 | 17 ← SAIDS |
| 27843 | 2,700 | na | 464 | 47 | 32 | 47 |
| SIVmac Δnef | | | | | | |
| 26873 | 3,160 | 100 | 100 | <1 | <1 | <1 |
| 26939 | 100K | 3,160 | 4 | 100 | 5 | <1 |
| SIVmac239 | | | | | | |
| 26084 | 47,000 | 31,600 | 2,200 | 31,600 | 10,000 | 3,160 |
| 27098 | 22,000 | na | 100K | 1,000 | 4,700 | 10,000 |

Table 3. Virus load in newborn macaques inoculated with SHIV-SF33A.

| | weeks after infection | | | |
|---|---|---|---|---|
| | 1 | 2 | 4 | 8 |
| neonate | | | | |
| 29800 | 100,000 | 320 | 1,000 | in progress |
| 29801 | 215,000 | 10,000 | 32 ← SAIDS | |

Figure 1. CD4+ lymphocyte number in juvenile macaque 25814 inoculated with SHIV-SF33.

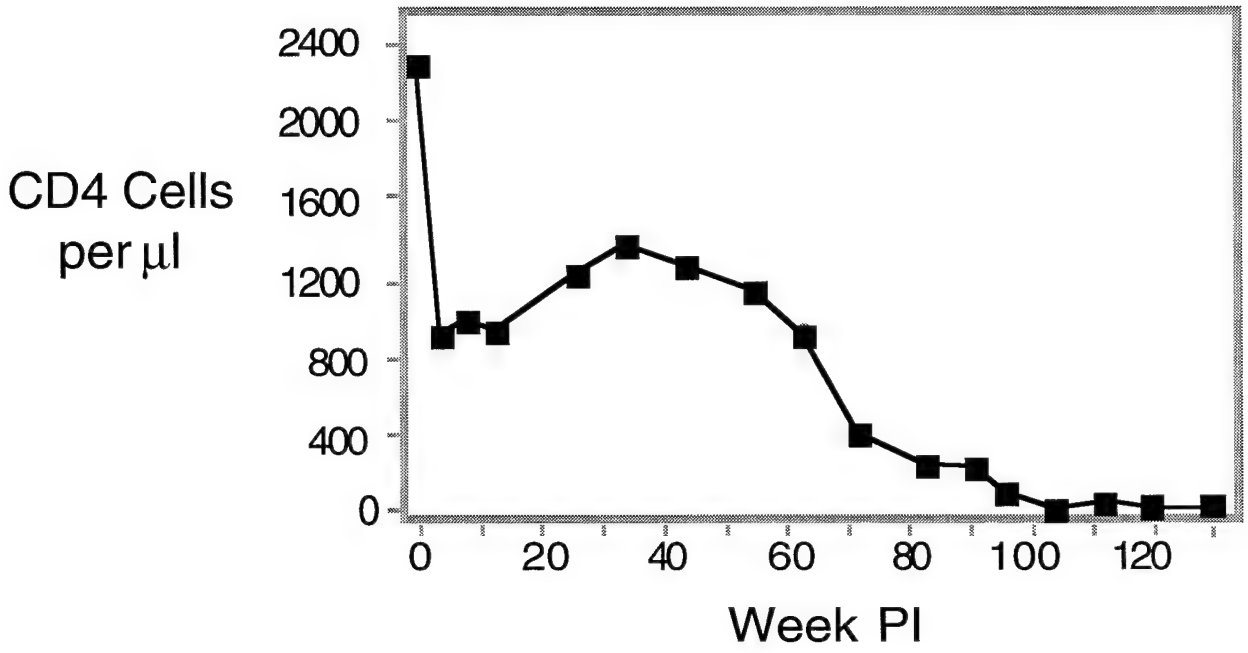

## Figure 2. Disease symptoms in macaque 25814.

- lymphopenia
  - ➡ fewer than 50 CD4 T-cells per ul
  - ➡ CD4/CD8 ratio less than 0.1
- weight loss greater than 25%
- widespread lymphoid hyperplasia with evidence of depletion
- interstitial lymphocytic pneumonia (P. carinii)
- GI tract - diffuse lymphocytic enteritis throughout with extensive bacterial colonization

Figure 3. Sequence changes in the env gene of SHIV-SF33 *in vivo.*

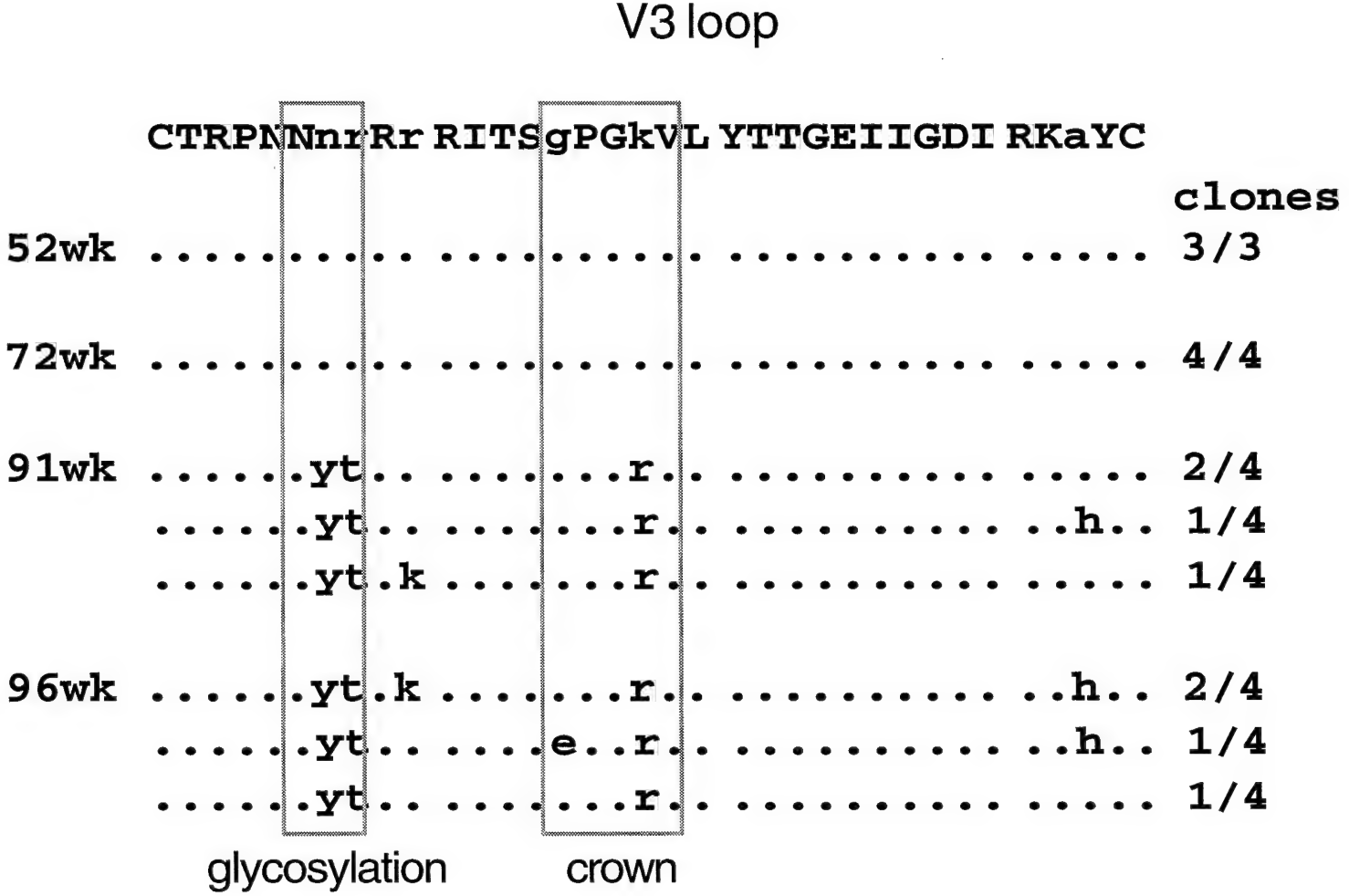

Figure 4. CD4 lymphocyte numbers after serial passage of SHIV-33 in juvenile macaques.

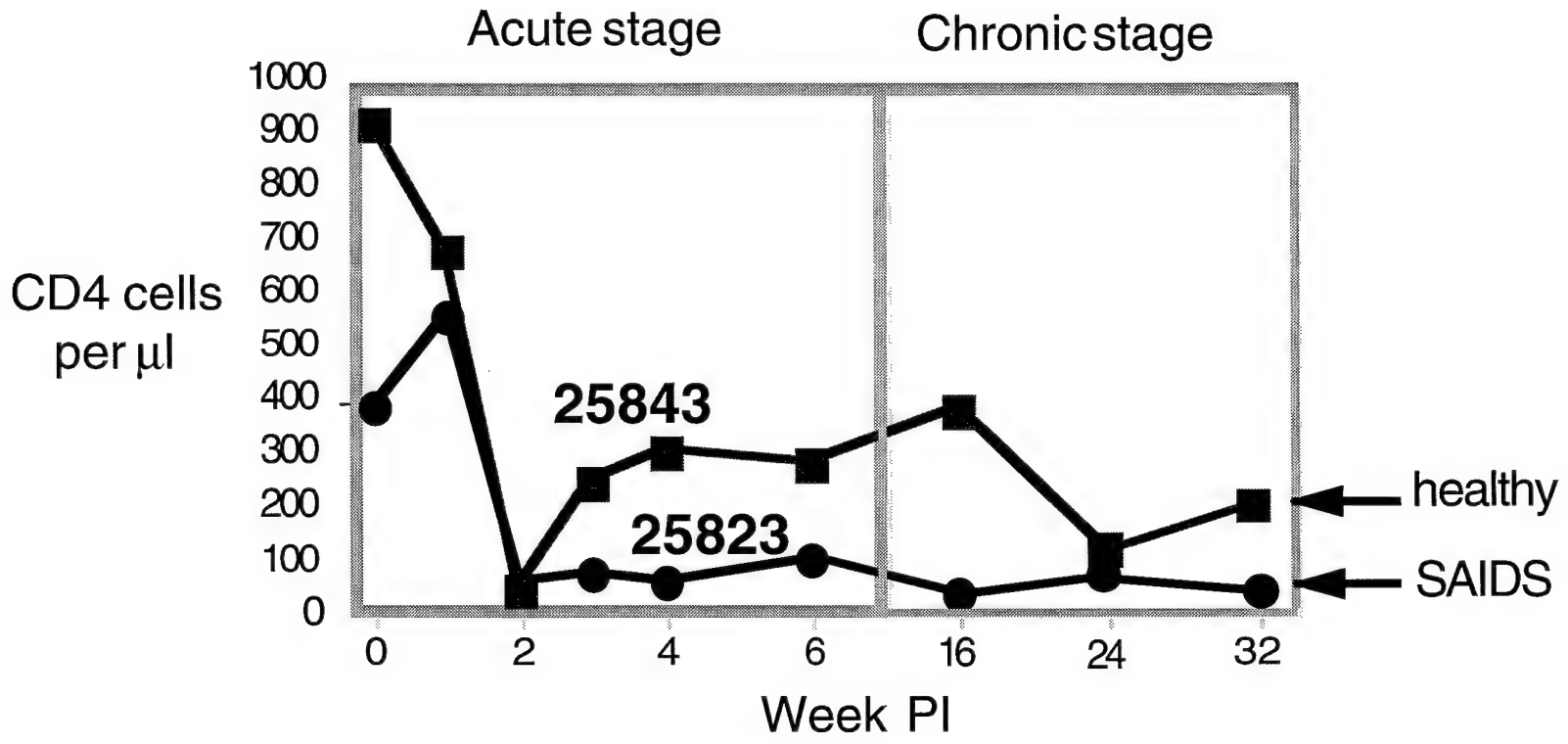

Figure 5. $CD4^+$ Lymphocyte number in newborn macaques inoculated with SHIV-SF33A.

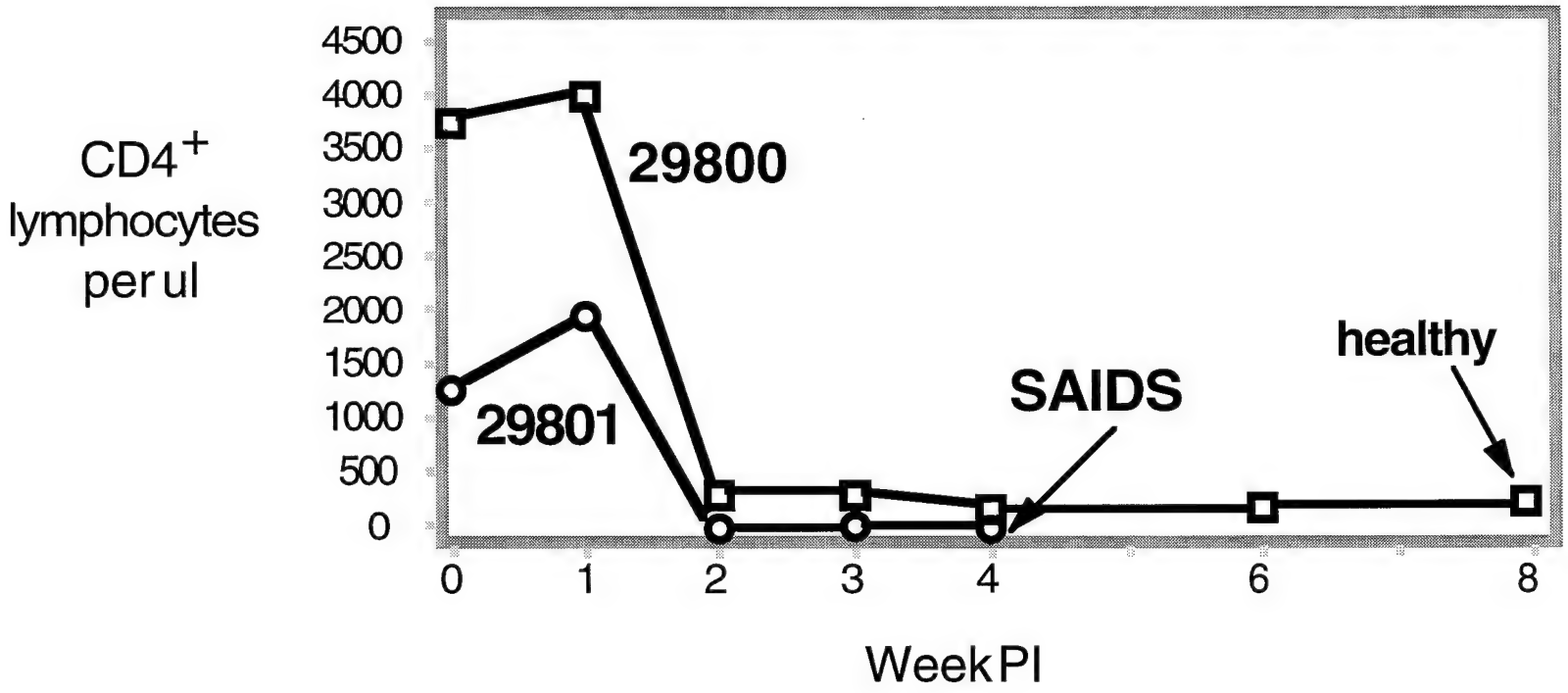

Mucosal Immune Responses Associated with Polynucleotide Vaccination, Dr. Robert Malone

Summary: Mucosal immune responses are functionally distinct from systemic immune responses, and are stimulated by antigen presentation within specialized mucosal-associated inductor tissues. The majority of HIV transmission worldwide occurs via infection at mucosal surfaces. We hypothesize that mucosal genetic vaccines will require gene transfer methods which target mucosal-associated inductor tissues such as the oropharyngeal Waldeyer's ring or intestinal Peyer's patches. We have tested this hypothesis by expressing a test antigen using a replication-defective recombinant Semliki Forest virus (SFV) preparation. Mice treated with recombinant SFV via an intravascular or intratracheal route generated systemic immune responses against the test antigen. In contrast, intranasal inoculation resulted in the production of IgA within pulmonary fluids, one hallmark of a mucosal immune response. These results indicate that transfection of mucosal effector tissues may not be sufficient for the generation of a universal mucosal immune response. We suggest that these results support the inclusion of limited studies involving the stimulation of mucosal anti-SIV immune responses using the macaque model. Such studies may be performed using both cationic lipid-mediated transfection of the SIV envelope plasmids documented in this project, and may also be performed using recombinant defective SFV vectors which express the same modified envelope-encoding sequences. The mucosal antibody responses to such vaccination would be determined using both lung and vaginal lavage specimens, cytotoxic T lymphocyte responses would be determined as recently published [23] and vaccinated macaques would be challenged using the mucosal challenge model developed at UC Davis [44].

Results: Recombinant Semliki Forest virus (SFV) particles which express the ß-galactosidase test antigen (Helper2/SFV-LacZ) were administered via intranasal and intratracheal inoculation. As a positive control, the same particles were administered intravascularly to yield a systemic immune response [45]. To control for nonspecific effects, a similar recombinant SFV preparation incorporating the influenza NP cDNA (Helper 2/SFV-NP). Groups of five female SPF Balb-C mice were pre-bled and then inoculated with $10^6$ helper-free recombinant viral particles. Serum samples were harvested 14 and 28 days after inoculation, and lung lavage fluid was obtained at 28 days upon termination of the experiment. ELISA analysis of anti-ß-galactosidase IgG response confirmed that none of the animals had detectable titers to the test antigen. All mice transduced with SFV-LacZ developed serum antibody to the test antigen by day 14 (Figure 1), consistent with previous studies which have demonstrated a rapid and robust immune response to vaccination with recombinant SFV. Serum IgG persisted in all cases to the termination of the experiment, although titers dropped by 28 days, consistent with the self-limited nature of ß-galactosidase expression, which is similar to that observed in transient acute viremia.

Serum IgA responses to the test antigen were quite different from the pattern of IgG titers. Anti-ß-galactosidase IgA titers were generally lower at 14 days than 28 days, and animals inoculated intranasally responded with low or undetectable serum titers, whereas animals inoculated via intravascular or intratracheal routes generally responded to the treatment with a variable serum IgA titer (Figure 2).

Surprisingly, lung lavage fluid from all animals which were inoculated via the nares contained significant titers of anti-ß-galactosidase IgA and IgG (Figure 3). This response was particularly striking, given the relative absence of IgA in the serum of these mice. Lavage fluid obtained from intratracheally treated animal T4 also included detectable levels of IgG and IgA,

and the systemically vaccinated animal V5 yielded significant levels of IgG in lavage fluid. As the lung lavage procedure is susceptible to contamination of lavage fluid by vascular fluid (eg: hemorrhage or rupture of alveolar wall), detection of significant levels of immunoglobulin in lavage fluid obtained from animals with significant serum immunoglobulin must be interpreted with caution. Given that little or no IgA was detected in the serum of mice treated via nares, it is particularly striking that significant levels of anti-ß-galactosidase IgA ELISA reactivity were detected in all specimens from this treatment group.

We conclude from these observations that the development of effective genetic or recombinant viral vaccines will be greatly facilitated by incorporating treatment modalities or targeting functionality which will result in antigen expression either within mucosal inductor tissues or epithelial cells overlying such tissues, where antigens can be sampled, processed and delivered by dendritic cells to responsive T and B cells. We also infer that administration of gene expression vectors to nonspecific mucosal effector tissues may result in responses which include anergy and/or local but not generalized mucosal immunity, and that such non-targeted patterns of mucosal transduction or transfection may result in systemic but not mucosal immunity.

Proposed studies: Having demonstrated a mucosal immune response in mice after expression of a test antigen, we propose to extend these findings by completing three studies: 1) Intranasally vaccinate mice (n= 5) with SIV env expression plasmids (DNA) delivered to nares using cationic lipids, and characterize resulting mucosal and systemic responses. Control groups will include intramuscular plasmid DNA injections and SFV particles which express HIV gp120 (Helper2/SFV-Env, currently available). 2) Intranasally vaccinate "rental" macaques with Helper2/SFV-LacZ particles and analyse humoral (lung lavage, vaginal wash) and cellular (biopsy, vaginal mucosal lymphocytes) mucosal immune responses. 3) Intranasally vaccinate macaques (n = 3) with the optimized SIV envelope expression plasmid identified via the ongoing murine comparison studies, and complexed with cationic lipids. Control animals will include macaques treated with a similar plasmid which does not express the SIV envelope (pND2 lux, n = 3) as well the as macaques vaccinated using direct DNA injection. Resulting mucosal immune responses will be characterized as described in 2), and vaginal challenge will be performed as previously described [44].

**Figure 1: ELISA analysis of serum titers of IgG obtained at 14 and 28 days from mice immunized with recombinant SFV particles**. Groups of five female SPF Balb-C mice were immunized with either a control expression vector (Helper 2/SFV-NP) via intratracheal administration (C1-C5), or via intratracheal (T1-T5), intravenous (V1-V5) or intranasal (N1-N5) administration of SFV particles which confer expression of the test antigen ß-galatosidase (Helper2/SFV-LacZ). Titer was defined as the most dilute serum sample which reacted to produce a $OD_{405}$ of 2.5 times above the average signal obtained with control serum (see attached manuscript, apendix).

**Figure 2: ELISA analysis of serum titers of IgA obtained at 14 and 28 days from mice immunized with recombinant SFV particles**. Groups of five female SPF Balb-C mice were immunized with either a control expression vector (Helper 2/SFV-NP) via intratracheal administration (C1-C5), or via intratracheal (T1-T5), intravenous (V1-V5) or intranasal (N1-N5) administration of SFV particles which confer expression of the test antigen ß-galatosidase (Helper2/SFV-LacZ). Titer was defined as the most dilute serum sample which reacted to produce a $OD_{405}$ of 2.5 times above the average signal obtained with control serum (see attached manuscript, apendix).

**Figure 3: ELISA analysis of IgG and IgA present in lung lavage fluid obtained at 28 days from mice immunized with recombinant SFV particles.** Groups of five female SPF Balb-C mice were immunized with either a control expression vector (Helper 2/SFV-NP) via intratracheal administration (C1-C5), or via intratracheal (T1-T5), intravenous (V1-V5) or intranasal (N1-N5) administration of SFV particles which confer expression of the test antigen ß-galatosidase (Helper2/SFV-LacZ). Data reflect lavage fluid diluted 1:2, and positive response was defined as 2.5 times the average signal obtained with control lavage fluid. Variable yield of lavage fluid introduced significant variation in dilution factor, and hence the data is plotted as the yield of reaction product ($OD_{405}$) rather than titer (see attached manuscript, apendix).

Figure 1

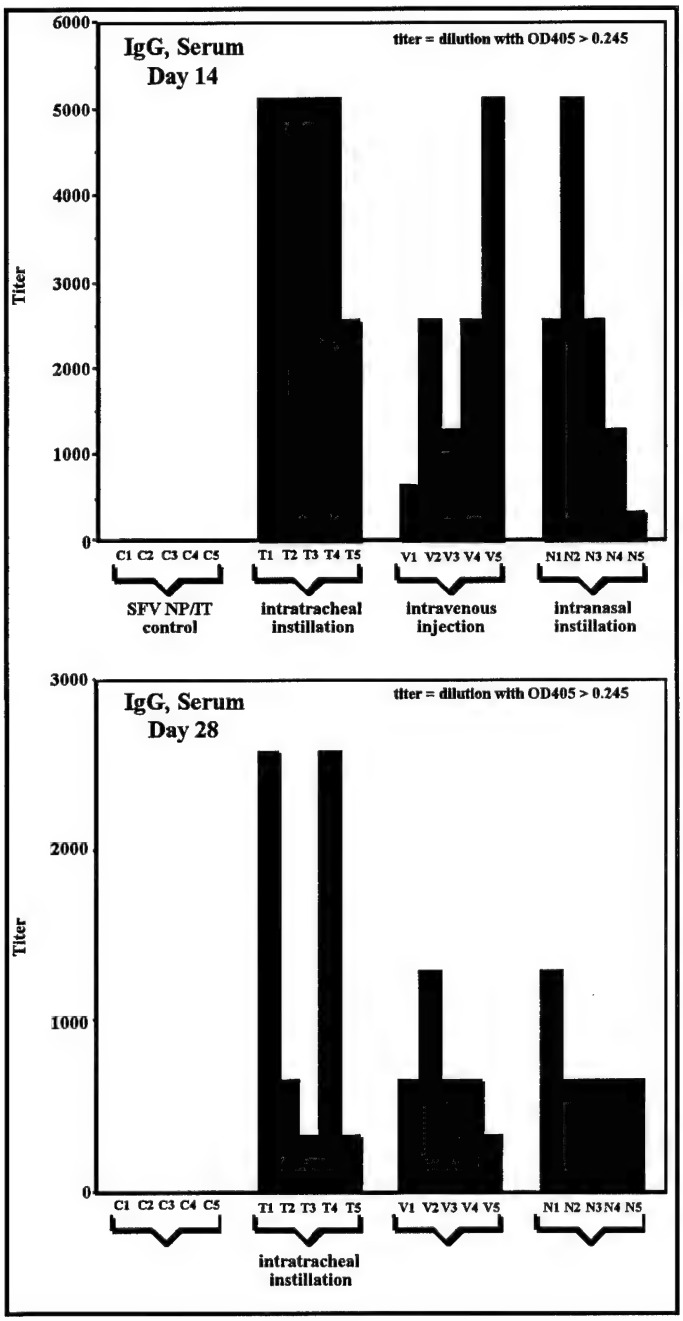
IgG, Serum
Day 14
titer = dilution with OD405 > 0.245
Titer
6000
5000
4000
3000
2000
1000
0
C1 C2 C3 C4 C5
T1 T2 T3 T4 T5
V1 V2 V3 V4 V5
N1 N2 N3 N4 N5
SFV NP/IT control
intratracheal instillation
intravenous injection
intranasal instillation
IgG, Serum
Day 28
titer = dilution with OD405 > 0.245
Titer
3000
2000
1000
0
C1 C2 C3 C4 C5
T1 T2 T3 T4 T5
V1 V2 V3 V4 V5
N1 N2 N3 N4 N5
intratracheal instillation

Figure 2

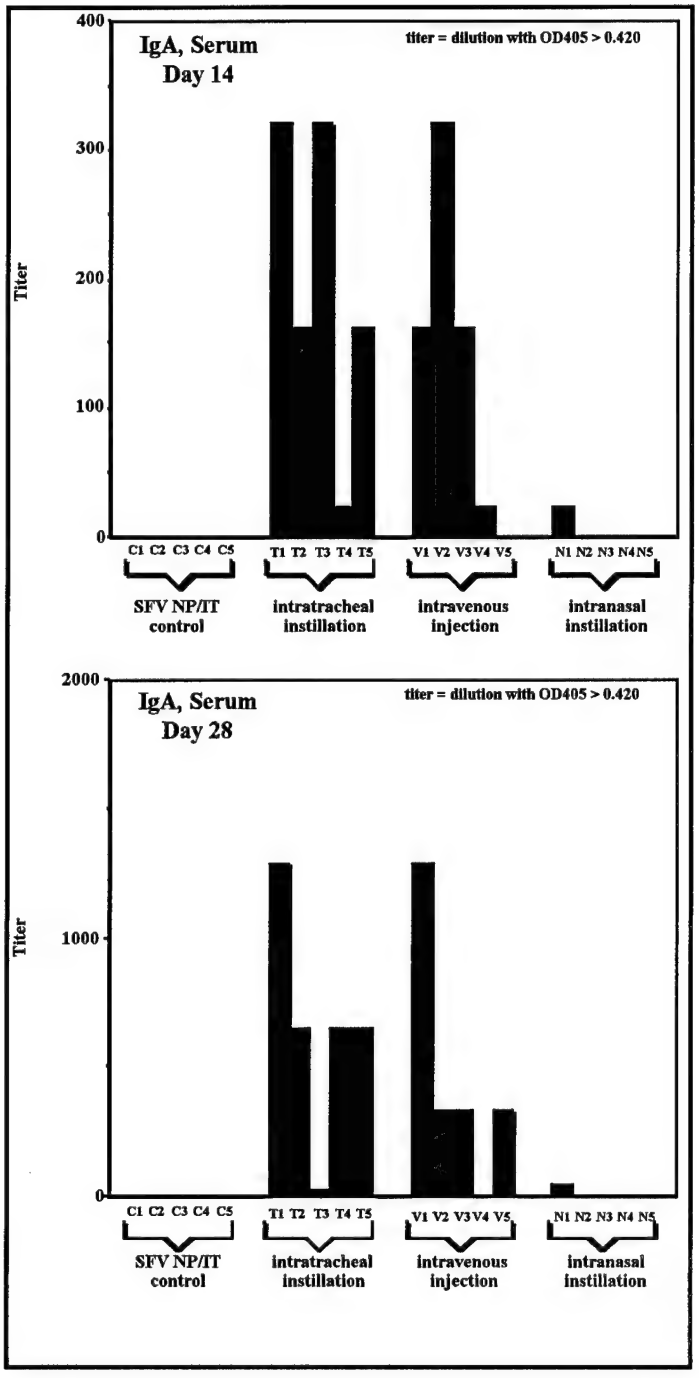
IgA, Serum
Day 14
titer = dilution with OD405 > 0.420
Titer
400
300
200
100
0
C1 C2 C3 C4 C5
T1 T2 T3 T4 T5
V1 V2 V3 V4 V5
N1 N2 N3 N4 N5
SFV NP/IT control
intratracheal instillation
intravenous injection
intranasal instillation
IgA, Serum
Day 28
titer = dilution with OD405 > 0.420
Titer
2000
1000
0
C1 C2 C3 C4 C5
T1 T2 T3 T4 T5
V1 V2 V3 V4 V5
N1 N2 N3 N4 N5
SFV NP/IT control
intratracheal instillation
intravenous injection
intranasal instillation

Figure 3

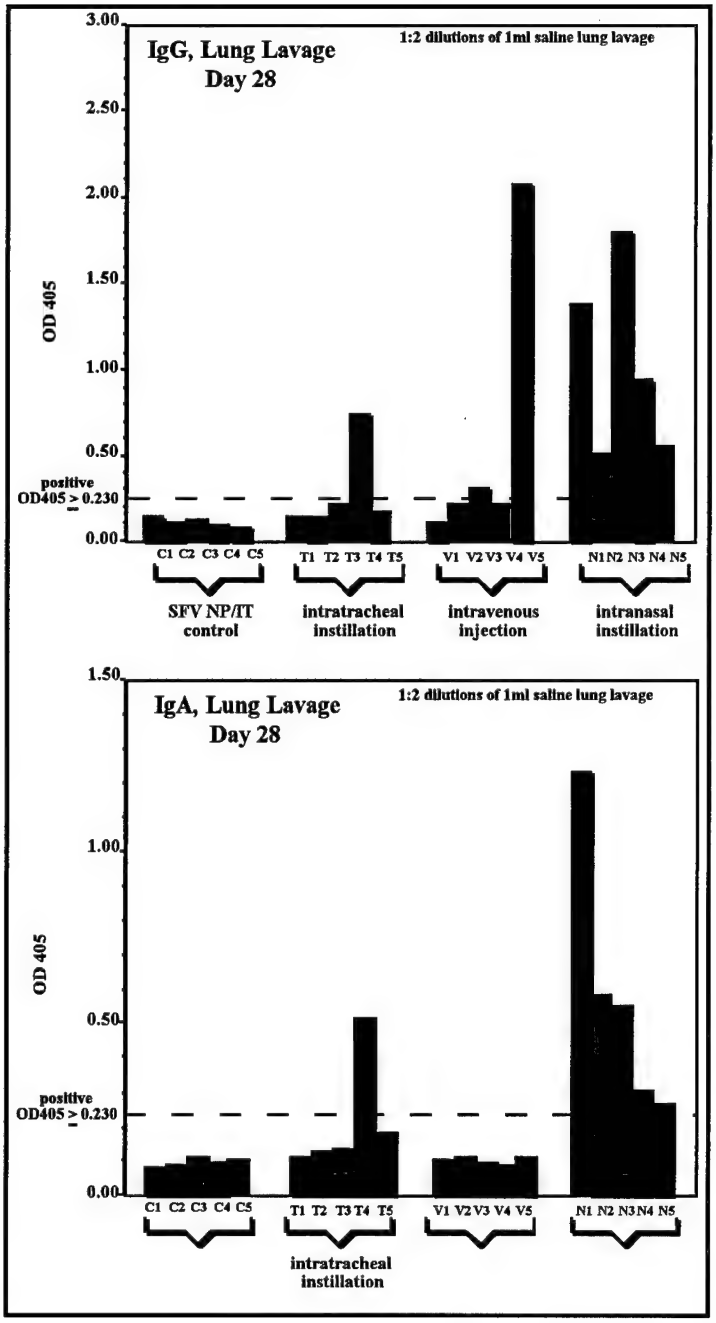
IgG, Lung Lavage
Day 28
1:2 dilutions of 1ml saline lung lavage
OD 405
3.00
2.50
2.00
1.50
1.00
0.50
positive
OD405 ≥ 0.230
0.00
C1 C2 C3 C4 C5
T1 T2 T3 T4 T5
V1 V2 V3 V4 V5
N1 N2 N3 N4 N5
SFV NP/IT
control
intratracheal
instillation
intravenous
injection
intranasal
instillation
IgA, Lung Lavage
Day 28
1:2 dilutions of 1ml saline lung lavage
OD 405
1.50
1.00
0.50
positive
OD405 ≥ 0.230
0.00
C1 C2 C3 C4 C5
T1 T2 T3 T4 T5
V1 V2 V3 V4 V5
N1 N2 N3 N4 N5
intratracheal
instillation

Conclusions and Future Directions

Expression assays for primate lymphokines have been developed, the induction of mucosal immunity by gene transfer to mucosal effector tissue has been demonstrated in the mouse, challenge systems using pathogenic SHIV virus have been developed which will allow HIV vaccine candidates to be tested in animals and a method has been developed to enhance immune responses induced by nucleic acid vaccination by coexpression of the antigen and T cell coreceptor genes. These finding lay the groundwork for development of enhanced SIV (and HIV) vaccines. Overall progress on the SIV vaccination project has been slower than anticipated this past year because of unforeseen difficulties with the plasmid expression vectors. These problems have now been solved for 3 of the 4 planned plasmids and progress has been made on the fourth.

1. All planned expression vector constructs have been made and verified. Three of the four have been grown in large quantities. A defective recombinant plasmid containing most of the SIV genome, and which produces non-infectious viral particles, has also been constructed and tested for expression *in vitro* and for induction of anti-viral antibodies in genetically immunized rabbits. Experiments to optimize nucleic acid vaccination in rhesus macaques have been started.

2. Cytokine and chemokine assays for both RNA and protein are now in place and have been tested on SIV infected macaques. These animals showed increases in TNFa expression in both lymph nodes and PBL. In addition, many macaque cytokine, chemokine and coreceptor molecules have been cloned and are available for uses to augment immune responses (see 5 below).

3. A recombinant SHIV virus has been made which is pathogenic in rhesus macaques. Such constructs will permit HIVenv vaccines to be tested in animals for their ability to prevent either infection or pathogenesis. Importantly, this model will allow studies for investigating means in which immunity can be broadened to protect from other strains of virus both from within the same clade and from other clades.

4. The induction of mucosal immune responses by transfer of antigen genes to effector tissue in the nares has been demonstrated in mice. We consider these results sufficiently novel and important that we propose testing the same system in macaques using a reporter antigen gene. These experiments will consist of inoculation of a recombinant vector into the nasal tissue and assay for IgA vaginal antibodies to the antigen. If these studies are successful, we will consider adding a mucosal challenge group in the study on macaques.

5. In mouse model studies, immunity induced by genetic vaccination has been shown to be augmented by the inclusion of the T cell coreceptor gene, B7, in the transfected cells. These findings, when coupled with the cloning of the corresponding, macaque genes (see 2 above), should lead to enhanced nucleic acid vaccines.

1. McDonnell WM, Askari FK: Molecular medicine. DNA vaccines. The New England Journal of Medicine 334(1):42-45, 1996

2. Lin R, Tarr PE, Jones TC: Present status of the use of cytokines as adjuvants with vaccines to protect against infectious diseases. Clinical Infectious Diseases 21:1439-1449, 1995

3. Raz E, Watanabe A, Baird SF, et al: Systemic immunological effects of cytokine genes injected into skeletal muscle. Proc Natl Acad Sci USA 90:4523-4527, 1993

4. Raz E, Carson DA, Parker SE, et al: Intradermal gene immunization: The possible role of DNA uptake in the induction of cellular immunity to viruses. Proc Natl Acad Sci USA 91:9519-9523, 1994

5. Haynes JR, Fuller DH, Eisenbraun MD, et al: Accell particle-mediated DNA immunization elicits humoral, cytotoxic, and protective immune responses. AIDS Research and Human Retroviruses 10:S43-S45, 1994

6. Ulmer JB, Donnelly JJ, Parker SE, et al: Heterologous protection against influenza by injection of DNA encoding a viral protein. Science 259:1745-1749, 1993

7. Robinson HL, Hunt LA, Webster RG: Protection against a lethal influenza virus challenge by immunization with a haemagglutinin-expressing plasmid DNA. Vaccine 11:957-960, 1993

8. Manickan E, Rouse RJD, Yu Z, et al: Genetic immunization against herpes simplex virus. Journal of Immunology 155:259-265, 1995

9. Xiang ZQ, Spitalnik S, Tran M, et al: Vaccination with a plasmid vector carrying the rabies virus glycoprotein gene induces protective immunity against rabies virus. Virology 199:132-140, 1994

10. Fuller DH, Haynes JR: A qualitative progression in HIV type 1 glycoprotein 120-specific cytotoxic cellular and humoral immune responses in mice receiving a DNA-based glycoprotein 120 vaccine. AIDS Research and Human Retroviruses 10:1433-1441, 1994

11. Lu S, Santoro JC, Fuller DH, et al: Use of DNAs expressing HIV-1 env and noninfectious HIV-1 particles to raise antibody responses in mice. Virology 209:147-154, 1995

12. Wang B, Ugen KE, Srikantan V, et al: Gene inoculation generates immune responses against human immunodeficiency virus type 1. Proc Natl Acad Sci USA 90:4156-4160, 1993

13. Hanke, T, Gotch and McMichael, A. Development of a DNA/MVA-based AIDS vaccine. 14th Annual Symposium on Nonhuman Primate Models for AIDS, Abstract #105, p. 201, October, 1996.

14. Mossman, SP, Pierce CE, Robertson M, Klaniecki JE, Morton WR, Benveniste RE, Hu S-L, and Haigwood NL. DNA immmunization against SIVmne in macaques using multiple viral antigens. 14th Annual Symposium on Nonhuman Primate Models for AIDS, Abstract #107, p. 203, October, 1996.

15. Wang B, Boyer JD, Ugen KE, et al: Nucleic acid-based immunization against HIV-1: induction of protective *in vivo* immune responses. AIDS 9:S159-S170, 1995

16. Murphey-Corb M, Simpson L, Montelaro R, Stefano Cole K, Clements J, Panicali D, and Haynes J. SIV challenge of rhesus macaques following a prime-boost vaccination regimen with gene gun-based DNA immunization alone or in combination with recombinant vaccinia vectors. 14th Annual Symposium on Nonhuman Primate Models for AIDS, Abstract #106, p. 202, October, 1996.

17. Letvin NL. DNA vaccine-elicited HIV-1 envelope-specific T cell immunity in rhesus macaques. 14th Annual Symposium on Nonhuman Primate Models for AIDS, Portland, OR, October 23-26, 1996.

18. Arthos SL, Montefiori DC, Yasutomi Y, et al: Simian immunodeficiency virus DNA vaccine trial in macaques. Journal of Virology 70:3978-3991, 1996

19. Malone JG, Bergland PJ, Liljestrom P, et al: Mucosal immune responses associated with polynucleotide vaccination. submitted 1996

20. Lohman BL, Miller CJ, McChesney MB: Antiviral cytotoxic T lymphocytes in vaginal mucosa of simian immunodeficiency virus-infected rhesus macaques. The Journal of Immunology 155:5855-5860, 1995

21. Stefano Cole K, Jagerski BA, Murphey-Corb M, Clements JE, Robinson, J, Wyand MS, Desrosiers RC, and Montelaro RC. Serological analysis of envelope-specific antibody responses to experimental SIV infection and immunization reveals a combination determinants that may serve as immune correlates of protection. 14th Annual Symposium on Nonhuman Primate Models for AIDS, Abstract #33, October, 1996.

22. Miller CJ, Alexander NJ, Sutjipto S, et al: Genital mucosal transmission of simian immunodeficiency virus: animal model for heterosexual transmission of human immunodeficiency virus. Journal of Virology 63:4277-4284, 1989

23. Miller CJ, Marthas M, Torten J, et al: Intravaginal inoculation of rhesus macaques with cell-free simian immunodeficiency virus results in persistent or transient viremia. Journal of Virology 68:6391-6400, 1994

24. Miller CJ, McGhee JR, Gardner MB: Mucosal immunity, HIV transmission and AIDS. Lab Investigation 68:129-145, 1993

25. Kraiselburd EN, Torres JV: Properties of virus-like particles produced by SIV-chronically infected human cell clones. Cellular and Molecular Biology 41(S1):S41-S52, 1995

26. Luciw PA, Pratt-Lowe E, Shaw KE, et al: Persistent infection of rhesus macaques with T-cell-line-tropic and macrophage-tropic clones of simian/human immunodeficiency viruses (SHIV). Proc Natl Acad Sci USA 92:7490-7494, 1996

27. Luciw PA, Mandell CP, Cheng-Mayer C: SHIV infection and fatal immunodeficiency in rhesus macaques: an animal model to analyze env gene functions. (submitted) 1996

28. Himathongkham S, Klinger J, Barnett S, et al: Chimeric SHIV with HIV-1 subtype-E envelope gene is restricted at an early step for replication in macaque lymphocytes. submitted 1996

29. Luciw PA, Low T, Mandell C, et al: Pathogenesis by replication-competent simian immunodeficiency virus (SIV) vector expressing the interleukin-2 gene. Abstract #27 13th Annual Symposium of Nonhuman Primate Models for AIDS November 5-8, 1995:Monterey, CA 1995 (Abstract)

30. Clayette P, Le Grand R, Noack O, et al: Tumor necrosis factor-alpha in serum of macaques during $SIV_{mac251}$ acute infection. Journal of Medical Primatology 24:94-100, 1995

31. Benveniste O, Vaslin B, Le Grand R, et al: Comparative interleukin (IL)-2/interferon (IFN)-gamma and IL-4/IL-10 responses during acute infection of macaques inoculated with attenuated *nef*-truncated or pathogenic SIVmac251 virus. Proc Natl Acad Sci USA 93:3658-3663, 1996

32. Cheret A, Le Grand R, Caufour P, et al: Cytokine mRNA expression in mononuclear cells from different tissues during acute SIVmac251 infection of macaques. AIDS Research and Human Retroviruses 12(13):1263-1272, 1996

33. Villinger F, Hunt D, Mayne A, Vuchetich M, Findley H, and Ansari AA. Standardization of functional, EIA, and molecular assays for cytokines in rhesus macaques and mangabeys. Cyktokine 5:469-479, 1993.

34. Ansari AA, Mayne A, Hunt D, Sundstrom JB, and Villinger F. TH1/TH2 subset analysis. I Establishment of criteria for subset identification in PBMC samples from nonhuman primates. Am. J. Primatol. 23:102-107, 1994.

35. Villinger F, Brar S, Mayne A, Chikkala N, and Ansari AA. Comparative analysis of cytokine genes from nonhuman primates. J. Immunol. 155:3945-3954, 1995.

36. Horspool JH, Perrin PJ, Woodcock JB, et al: Costimulatory requirements of humoral and cytotoxic T cell immune responses following nucleic acid vaccination. Journal of Immunology (submitted):1996

37. U Schauer, T Jung, N Krug and A Frew. Measurement of intracellular cytokines. Immunol. Today 17:305-306, 1996.

38. T Jung, U Schauer, C Heusser, C Neumann and C Rieger. Detection of intracellular cytokines by flow cytometry. J. Immunol. Meth. 159:197-207, 1993.

39. LH Elson, TB Nutman, DD Metcalfe and C Prussin. Flow cytometric analysis for cytokine production identifies Th1, Th2 and Th0 cells within human CD4+CD27- lymphocyte subpopulation. J. Immunol. 154:4294-4301, 1995.

40. PH Van der Meide, RJ Groenestein, MCDC de Labie, J Heeney, P Pala and M Slaoui. Enumeration of lymphokine-secreting cells as a quantitative measure for cellular immune responses in rhesus macaques. J. Med. Primatol. 24:723-732, 1995.

41. Rhodes GH, Dwarki VJ, Abai AA, Felgner J, Felgner PL, Gromkowski SH, and Parker SE. Injection of expression vectors containing viral genes produces cellular, humoral and protective immunity. Vaccines HS Gomsberg, F Brown, RM Chanock, and RA Lerner, eds. Cold Spring Harbor Laboratory Press, 1993.

42. Sattentaw QJ and Moore JP. Human immunodeficiency virus type 1 neutralization is determined by epitope exposure on the gp120 dimer. Journal of Experimental Medicine 182:185-196, 1995.

43. Bray M, Prasad S, Dubay JW, Hunter E, Jeang KT, Rekosh D, an Hammarskjold ML. A small element from the Mason-Pfizer monkey virus genome makes human immunodeficiency virus type 1 expression and replication Rev-independent. Proceedings of the National Academy of Sciences of the United States of America. 91:1256-1260, 1994.

44. Miller CJ, Marthas M, Torten J, Alexander NJ, Moore JP, Doncel GF, and Hendrickx AG. Intravaginal inoculation of rhesus macaques with cell-free simian immunodeficiency virus results in persistent or transient viremia. J. Virol. 68(10):6391-400, 1994.

45. Zhou X, Berglund P, Rhodes G, Parker SE, Jondal M, and Liljestrom P. Self-replicating Semliki Forest virus RNA as recombinant vaccine. Vaccine 12(16):1510-1514, 1994.

# APPENDIX 1

## Mucosal Immune Responses Associated with Polynucleotide Vaccination

**Mucosal Immune Responses Associated with Polynucleotide Vaccination.**

Running title: Mucosal Response to Polynucleotide Vaccination

Jill G. Malone[1], Peter J. Bergland[2], Peter Liljestrom[2], Gary H. Rhodes[1], and Robert W. Malone[1]

[1] Gene Therapy program, Medical Pathology, MS-1A, University of California, Davis, Davis, CA 95616 and [2] Department of Molecular Biology, Karolinska Institute, S-141 57 Huddinge, Sweden

Key Words: Genetic vaccination, Semliki Forest Virus, immune responses, IgA, IgG, pulmonary transfection, mucosal antigen presentation, β-galactosidase.

**Summary:**

A variety of gene delivery technologies can be used to express antigens within somatic tissues, resulting in systemic humoral and cellular immune responses. This observation has led to the development of polynucleotide vaccine preparations for stimulation of systemic immunity. Mucosal immune responses are functionally distinct from systemic immune responses, and are stimulated by antigen presentation within specialized mucosal-associated inductor tissues. We hypothesize that mucosal genetic vaccines will require gene transfer methods which target mucosal-associated inductor tissues such as the oropharyngeal Waldeyer's ring or intestinal Peyer's patches. We have tested this

hypothesis by expressing a test antigen using a replication-defective recombinant Semliki Forest virus (SFV) preparation. Mice treated with recombinant SFV via an intravascular or intratracheal route generated systemic immune responses against the test antigen. In contrast, intranasal inoculation resulted in the production of IgA within pulmonary fluids, one hallmark of a mucosal immune response. These results indicate that transfection of mucosal effector tissues may not be sufficient for the generation of a universal mucosal immune response. Furthermore, the results predict that techniques which target transfection or transduction to mucosal inductor tissues will enable the development of a new class of polynucleotide vaccines which exploit current concepts in mucosal immunology.

**Introduction:**

Current polynucleotide vaccination methods have been associated with systemic immune responses, but such treatments have not resulted in the production of secreted IgA, a hallmark of mucosal immune responses (Fynan, Webster et al. 1993; Livingston, Lu et al. 1995). Expression of test antigens after intranasal inoculation with recombinant viral vectors has been associated with pulmonary IgA production (Van Ginkel, Liu et al. 1995), and the basis for this difference is unresolved. There may be adjuvant effects associated with plasmid DNA or viral vectors, level and/or duration of antigen expression may be important, different test antigens may be processed and presented in a different manner, and the targeting of different cell and/or tissue types may be important.

Inductor and effector tissues associated with mucosal immune responses are anatomically and functionally distinct from systemic immune system analogs. Induction of a mucosal immune response appears to require antigen presentation within specialized

mucosal-associated lymphoid structures, classically Peyer's patches, BALT, tonsils and Waldeyer's ring (Brandtzaeg and Halstensen 1992; Kuper, Koornstra et al. 1992) After induction, mucosal lymphoid effector cells circulate and then accumulate within all mucosal tissue compartments (to varying degrees), giving rise to a common mucosal immune response (McDermott and Bienenstock 1979). Therefore, current models predict that stimulation of mucosal effector pathways by delivering antigen-encoding polynucleotides will require the transfection of cells associated with mucosal inductor sites.

Like the systemic immune compartment, the common mucosal immune system requires mechanisms for selective switching between the expansion of effector cells and the induction of tolerance. Inappropriate induction of mucosal immune responses can result in clinical syndromes including food and respiratory allergies (Holt and McMenamin 1989; Brandtzaeg, Halstensen et al. 1993) The mechanism(s) involved in switching between induction or suppression of mucosal immune responses remain to be resolved, but may involve antigen sampling and presentation by either specialized inductor tissues (stimulation) or MHC Class $II^+$ mucosal epithelial cells (tolerance in gut (Brandtzaeg, Halstensen et al. 1989), hypersensitivity or tolerance in lung (Kalb, Chuang et al. 1991)). These studies illustrate the complex nature of mucosal immune response regulation, and support the hypothesis that selection of different tissues for transfection or transduction with a mucosal polynucleotide vaccine may result in profound differences in the resulting pattern of immune response.

A variety of virally-derived gene transduction vectors have been developed for use in mammalian cells, and can be used to provoke an immune response to foreign antigens. In a sense, attenuated viral vaccines may be seen as an early example of this methodology. Examples include recombinant retroviral (Cone and Mulligan 1984; St. Louis and Verma 1988) polyomaviral (Okayama and Berg 1983), papillomaviral (Sarver, Gruss et al. 1981),

picornaviral (Burke, Evans et al. 1989), poxviral (Smith, Murphy et al. 1983), adenoviral (Van Doren, Hanahan et al. 1984; McDermott, Graham et al. 1989) and adeno-associated virus vectors (Hermonat and Muzyczka 1984). The history of direct gene transfer using free DNA and mRNA is also quite extensive (for review, see (Wolff and Lederberg 1994), and this simple methodology has recently become quite popular for the production of systemic immune responses.

More recently, a new family of viral vectors based on Sindbis (Xiong, Levis et al. 1989) and Semliki Forest (Liljestrom and Garoff 1991) alphaviruses have been introduced. Alphaviruses are positive strand RNA viruses, and hence the RNA genomes of these agents produce infectious particles upon transfection (Zhou, Berglund et al. 1994) The Semliki Forest virus (SFV) has been engineered to yield a vector system based on a genomic SFV cDNA inserted into an SP6 RNA promoter plasmid. The resulting plasmid has been modified by deletion of the SFV structural genes to allow insertion of a heterologous cDNA as part of the SFV replicon. After incorporation of the cDNA of interest, *in vitro* SP6 transcription of plasmid DNA results in mRNA preparations which encode both the recombinant protein as well as the SFV replicase. This positive-stranded mRNA can then be directly administered to cells (transfection), or assembled into viral particles and used to infect cells (transduction). Consequently, upon transfection or transduction of the recombinant mRNA into cells, expression of the polymerase results in cytoplasmic replication of the transfected recombinant mRNA, and the multiple copies of mRNA direct efficient production of the protein of interest. Typically, the polymerase and recombinant protein become a major fraction of total cellular protein (Liljestrom and Garoff 1991) and this may contribute to the cytotoxicity which typically limits expression to four to seven days, culminating in cell death.

One potential complication of all virally-derived gene transfer systems is the development of replication-competent helper virus. In alphavirus-derived systems, this occurs via polymerase strand crossover between the mRNA which encodes the protein of interest, and a trans helper mRNA which provides packaging proteins used to produce defective particles for transduction. By modifying the viral spike protein encoded by SFV, conditionally infectious particles which require activation by chymotrypsin can be produced, and this modification has reduced the production of replication-competent helper particles to undetectable levels (Berglund, Sjoberg et al. 1993). Recombinant SFV mRNA and defective particles have been shown to stimulate a strong systemic immune response to a recombinant protein after genetic vaccination (Zhou, Berglund et al. 1994; Zhou, Berglund et al. 1995)

We have exploited the efficient transduction and expression activity of recombinant SFV particles to test the hypothesis that mucosal genetic vaccines will require gene transfer methods which target mucosal-associated inductor tissues such as the oropharyngeal Waldeyer's ring or intestinal Peyer's patches. Mice were treated intravascularly, intratracheally or intranasally with identical doses of recombinant defective virus which expresses the test antigen β-galactosidase. Previous studies have demonstrated that genetic vaccination with β-galactosidase can elicit strong cytotoxic and humoral immune responses (Raz, Carson et al. 1994). After a single treatment, systemic immune responses were monitored by ELISA analyses of serum samples over a four week period, and lung lavage fluid was obtained from vaccinated mice for detection of mucosal responses upon termination of the experiment.

## Materials and Methods:

### SFV particle preparation and activation:

A recombinant alphavirus vector system which expresses the lac Z gene (ß-galactosidase) was prepared as previously described (Liljestrom and Garoff 1991; Liljestrom 1994), and defective alphavirus particles (Helper2/SFV-LacZ $10^7$/ml or Helper 2/SFV NP $10^7$/ml as control (Zhou, Berglund et al. 1994)) were activated and titered as previously described (Berglund, Sjoberg et al. 1993). Briefly, one volume of virus stock was diluted into 1/20 volume of Chymotrypsin (10 mg/ml in PBS with Ca/Mg) and 1/50 volume of $CaCl_2$ (50 mM). This was allowed to incubate at room temperature for thirty minutes, 1/2 volume of 2 mg/ml Aprotinin was added, and the mixture was cooled to 4°C. The preparation was kept on ice and used within one hour.

**Treatment Groups and inoculation procedures:**

Groups of 5 Balb-C mice (specific pathogen free (SPF) female, 6 week, Charles River) were bled via the retro-orbital venous plexus, and then each mouse was inoculated with $10^6$ ß -galactosidase-encoding virion particles (Helper2/SFV-LacZ) *via* intratracheal (T1-T5), intranasal (N1-N5) or intravenous (V1-V5) routes. Control animals were treated via intratracheal instillation using the same dose of a SFV influenza NP protein expression vector (Helper 2/SFV-NP, C1-C5). All animals were anesthetized using a cocktail of ketamine (22 mg/kg), xylazine (2.5 mg/kg) and acepromazine (0.75 mg/kg) prior to inoculation and during subsequent sampling of serum.

Intratracheal inoculations were performed by making a small medial cut through the skin of the ventral neck. Salivary glands were teased apart using blunt dissection to expose the trachea. With the trachea visualized, a 1/2" 30 gauge needle with a 1 cc tuberculin syringe attached was placed through the rings of the trachea toward the bronchi. 100 µl of the above virion particles were injected into the lung. Intranasal installation was performed by placing 50 µl of virion particles onto one the nares. Once this was taken into the nasal

passages by inhalation, the other side was inoculated in the same manner. Intravenous inoculation was performed using a 1/2" 30 gauge needle with 100 µl of the above virion particles inserted into the tail vein.

**Specimen Collection:**

Blood was collected from the retro-orbital venous plexus at day 0, 14, and 28, using a microcapillary tube. The blood was allowed to sit at room temperature for 2-4 hours to clot, and then spun in a IEC Centra MP4R centrifuge at 6,000 RPM for six minutes. The supernatant (serum) was then removed and stored at -20 until ELISA assays were run.

Lung lavages were performed at week 4 as follows: Mice were killed by carbon dioxide asphyxiation, and a tissue block consisting of heart, lung and trachea was removed using an incision immediately inferior to the larynx. One ml of BBS (89 mM boric acid, 90 mM NaCL: pH.=8.3 [NaOH]) was used to gently lavage the lungs using a 1 ml tuberculin syringe attached to a gavage needle. The solution was then clarified by centrifugation. Recovered volumes are normally in the range 0.85 to 0.95 ml. The resulting lavage fluid was stored at -20 C until analyzed by ELISA.

**Enzyme-linked immunosorbent assay (ELISA)**

ELISA assays were performed on samples using 96 well microtiter plates coated with 50 µl of 5 mg/ml ß-galactosidase protein (Calbiochem) in BBS (89 mM boric acid, 90 mM NaCL: pH.=8.3 [NaOH]). Prior to use, the ß-galactosidase protein was re-suspended to a concentration of 1 mg/ml using 5 mg/ml bovine serum albumin in PBS (United States Biochemical). The coated plates were incubated overnight at 4°C, and then dried and blocked for two hours at room temperature using 150 µl 1% bovine serum albumin (BSA) in BBS/well. Experimental serum was diluted using eight two-fold serial dilutions in BB (serum IgG and IgA- 1:10 to 1:5120, lavage IgG and IgA- 1:1 to 1:128), and was then aliquoted into the microtiter plates (50 µl per well) and incubated overnight at 4C. Plates

were washed 5-6 times with 0.05% tween in BBS and dried in room air. 50 µl of either alkaline phosphatase conjugated goat anti-mouse IgG (Jackson Labs, 1:2000 dilution in 1% BSA/BBS) or goat anti-mouse IgA (Zymed, 1:1000 dilution in 1% BSA/BBS) were then added to each well. Plates were then incubated with the second antibody for two hours at room temperature and washed and dried as described. A substrate buffer consisting of 1 mg/ml p-nitrophenol phosphate, 50 mM Na-bicarbonate buffer, pH.=9.8, 1 mM $MgCl_2$ was then added with incubation (1h, room temperature). The resulting reaction product was quantitated using a Dynotech MR5000 ELISA plate reader at 405 nm ($OD_{405}$). Background signal was defined using control serum, with positive titer identified at >2.5x background. For lavage samples, $OD_{405}$ was reported using the 1:2 dilution, with positive signal defined as 2.5x background.

**Results:**

To test the hypothesis that the response of mucosal tissues to genetic vaccination is affected by the route of administration and hence the site of antigen expression, recombinant Semliki Forest virus (SFV) particles which express the β-galactosidase test antigen (Helper2/SFV-LacZ) were administered *via* intranasal and intratracheal inoculation. As a positive control, the same particles were administered intravascularly to yield a systemic immune response (Zhou, Berglund et al. 1994). To control for nonspecific effects, a similar recombinant SFV preparation incorporating the influenza NP cDNA (Helper 2/SFV-NP). Groups of five female SPF Balb-C mice were pre-bled and then inoculated with $10^6$ helper-free recombinant viral particles. Serum samples were harvested 14 and 28 days after inoculation, and lung lavage fluid was obtained at 28 days upon termination of the experiment. ELISA analysis of anti-β-galactosidase IgG response confirmed that none of the animals had detectable titers to the test antigen. All mice transduced with SFV-LacZ developed serum antibody to the test antigen by day 14 (Figure 1), consistent with previous studies which have demonstrated a rapid and robust immune response to vaccination with recombinant SFV. Serum IgG persisted in all cases to the termination of the experiment, although titers dropped by 28 days, consistent with the self-limited nature of β-galactosidase expression, which is similar to that observed in transient acute viremia.

Serum IgA responses to the test antigen were quite different from the pattern of IgG titers. Anti-β-galactosidase IgA titers were generally lower at 14 days than 28 days, and animals inoculated intranasally responded with low or undetectable serum titers, whereas animals inoculated via intravascular or intratracheal routes generally responded to the treatment with a variable serum IgA titer (Figure 2).

Surprisingly, lung lavage fluid from all animals which were inoculated *via* the nares contained significant titers of anti-β-galactosidase IgA and IgG (Figure 3). This response was particularly striking, given the relative absence of IgA in the serum of these mice. Lavage fluid obtained from intratracheally treated animal T4 also included detectable levels of IgG and IgA, and the systemically vaccinated animal V5 yielded significant levels of IgG in lavage fluid. As the lung lavage procedure is susceptible to contamination of lavage fluid by vascular fluid (eg: hemorrhage or rupture of alveolar wall), detection of significant levels of immunoglobulin in lavage fluid obtained from animals with significant serum immunoglobulin must be interpreted with caution. Given that little or no IgA was detected in the serum of mice treated *via* nares, it is particularly striking that significant levels of anti-β-galactosidase IgA ELISA reactivity were detected in all specimens from this treatment group.

**Discussion:**

Gene delivery with antigen expression in skin, muscle, or the respiratory tissues of fowl can elicit robust, protective systemic immunity which is mediated by both humoral and cellular effectors (Fynan, Webster et al. 1993; Ulmer, Donnelly et al. 1993; Zhou, Berglund et al. 1994). This systemic immunity is similar to that observed after recovery from infection, but lacks the secretory IgA responses which are typically observed after infection *via* mucosal surfaces, and which are a hallmark of mucosal immunity.

Pulmonary gene delivery technology might be adapted to enable mucosal polynucleotide vaccines. A variety of methods for the transfection of lung tissues have been developed, including administration of free DNA, cationic amphiphile-facilitated transfection, or viral vectors (typically adenovirus). Using free plasmid DNA or cationic lipid:DNA complexes, we have been able to verify antigen expression in lung after intratracheal administration (Balasubramaniam, Bennett et al. 1996), but have not observed

antigen-specific IgA in lung lavage fluid. The pathways by which mucosal immune responses can be elicited have not been fully characterized. Mucosal antigen presentation can be associated with either immunologic stimulation or induction of tolerance(Takahashi, Nakagawa et al. 1995; Brandtzaeg 1996), and hence there are multiple hypotheses for the absence of IgA in lung lavage samples after mucosal expression of an antigenic protein via DNA vaccination. As with any negative result, the possible explanations for this finding range from the trivial to the profound. Lacking a positive control, we have not been able to validate techniques for detecting test antigen-specific IgA in murine lung lavage samples. Duration or quantity of test antigen expression might be insufficient. The gene delivery methods and reagents may interfere with subsequent immune response by any number of pathways. Alternatively, the location or type of transfected cells may be inappropriate for inducing a mucosal response to the test antigen. To discriminate between these possibilities, we have employed a helper-free recombinant viral vector system (Zhou, Berglund et al. 1994) to transiently express high levels of a test antigen after intratracheal, intranasal, or intravascular inoculation.

Many studies support the hypothesis that the generation of widespread mucosal immune responses involve an inductive limb and subsequent effector cell function, and that these two categories are associated with different anatomical structures (for reviews, see (McGhee and Kiyono 1994; Brandtzaeg 1996)). Classically, inductor tissues for mucosal immune response include Peyer's patches, BALT, tonsils and Waldeyer's ring. In the adult mouse, the analog of the tonsils and Waldeyer's ring are present in the mucosa of the lateral walls of the nasal cavity at the entrance of the pharyngeal duct (van der Ven and Sminia 1993).

We have tested the hypothesis that expression of a test antigen in different mucosal tissue sites will result in different patterns of immunologic response. As a simple and

rapid indicator of mucosal immune response, lung lavage fluid was assayed for the presence of IgA. Fecal pellet analysis might also be used, but this technique is compromised by the ability of rodent liver to assemble and secrete polymeric IgA in bile (McGhee and Kiyono 1993). Figure 3 summarizes mucosal immune responses associated with intravascular, intratracheal and intranasal transduction and expression of a test antigen, and Figures 1 and 2 summarize data on corresponding levels of serum immnoglobulins. This data demonstrates the different patterns of immune response predicted by current theory, and supports the hypothesis that antigen expression and/or presentation within mucosal inductor tissues results in a more effective and broad-based mucosal immune response than that associated with expression or presentation within mucosal effector tissues. These results are particularly intriguing in light of studies which demonstrate that mucosal and systemic immune responses can be differentially regulated, so that antigen presented at mucosa can elicit a response in one compartment and anergy in the other (Fujihashi, McGhee et al. 1996). We conclude from these observations that the development of effective genetic or recombinant viral vaccines will be greatly facilitated by incorporating treatment modalities or targeting functionality which will result in antigen expression either within mucosal inductor tissues or epithelial cells overlying such tissues, where antigens can be sampled, processed and delivered by dendritic cells to responsive T and B cells. We also infer that administration of gene expression vectors to nonspecific mucosal effector tissues may result in responses which include anergy and/or local but not generalized mucosal immunity, and that such non-targeted patterns of mucosal transduction or transfection may result in systemic but not mucosal immunity.

**Acknowledgements:**

This work was supported by a grant from the US army (DAMD17-94-J4436). We also wish to thank Dr. B.-U. Von Specht and the conference organizers for providing an opportunity to participate in this conference program and associated publication.

**Figure 1: ELISA analysis of serum titers of IgG obtained at 14 and 28 days from mice immunized with recombinant SFV particles.** Groups of five female SPF Balb-C mice were immunized with either a control expression vector (Helper 2/SFV-NP) via intratracheal administration (C1-C5), or *via* intratracheal (T1-T5), intravenous (V1-V5) or intranasal (N1-N5) administration of SFV particles which confer expression of the test antigen β-galatosidase (Helper2/SFV-LacZ). Titer was defined as the most dilute serum sample which reacted to produce a $OD_{405}$ of 2.5 times above the average signal obtained with control serum.

**Figure 2: ELISA analysis of serum titers of IgA obtained at 14 and 28 days from mice immunized with recombinant SFV particles.** Groups of five female SPF Balb-C mice were immunized with either a control expression vector (Helper 2/SFV-NP) via intratracheal administration (C1-C5), or *via* intratracheal (T1-T5), intravenous (V1-V5) or intranasal (N1-N5) administration of SFV particles which confer expression of the test antigen β-galatosidase (Helper2/SFV-LacZ). Titer was defined as the most dilute serum sample which reacted to produce a $OD_{405}$ of 2.5 times above the average signal obtained with control serum.

**Figure 3: ELISA analysis of IgG and IgA present in lung lavage fluid obtained at 28 days from mice immunized with recombinant SFV particles.** Groups of five female SPF Balb-C mice were immunized with either a control expression vector (Helper 2/SFV-NP) via intratracheal administration (C1-C5), or *via* intratracheal (T1-T5), intravenous (V1-V5) or intranasal (N1-N5) administration of SFV particles which confer expression of the test antigen β-galatosidase (Helper2/SFV-LacZ). Data reflect lavage fluid diluted 1:2, and positive response was defined as 2.5 times the average signal obtained with control lavage fluid. Variable yield of lavage fluid introduced significant variation in

dilution factor, and hence the data is plotted as the yield of reaction product ($OD_{405}$) rather than titer.

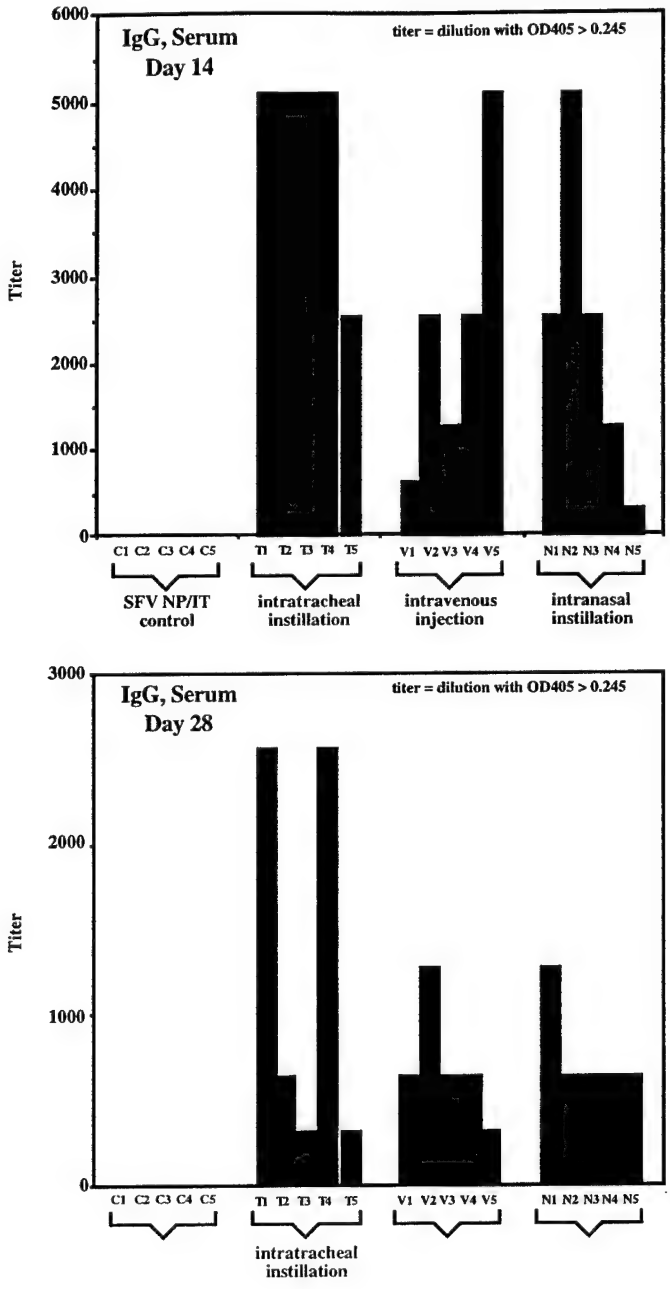
IgG, Serum
Day 14
titer = dilution with OD405 > 0.245
Titer
6000
5000
4000
3000
2000
1000
0
C1 C2 C3 C4 C5
T1 T2 T3 T4 T5
V1 V2 V3 V4 V5
N1 N2 N3 N4 N5
SFV NP/IT control
intratracheal instillation
intravenous injection
intranasal instillation
IgG, Serum
Day 28
titer = dilution with OD405 > 0.245
Titer
3000
2000
1000
0
C1 C2 C3 C4 C5
T1 T2 T3 T4 T5
V1 V2 V3 V4 V5
N1 N2 N3 N4 N5
intratracheal instillation

Figure 1

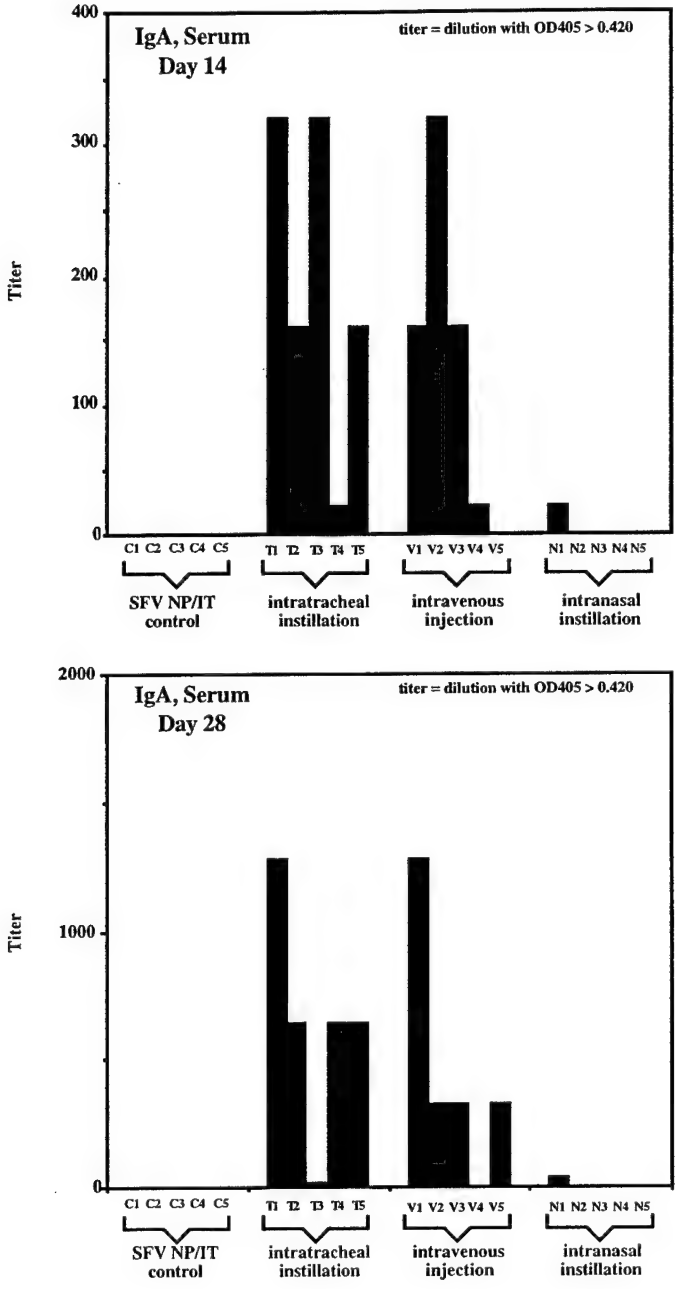
IgA, Serum
Day 14
titer = dilution with OD405 > 0.420
Titer
400
300
200
100
0
C1 C2 C3 C4 C5
T1 T2 T3 T4 T5
V1 V2 V3 V4 V5
N1 N2 N3 N4 N5
SFV NP/IT control
intratracheal instillation
intravenous injection
intranasal instillation
IgA, Serum
Day 28
titer = dilution with OD405 > 0.420
Titer
2000
1000
0
C1 C2 C3 C4 C5
T1 T2 T3 T4 T5
V1 V2 V3 V4 V5
N1 N2 N3 N4 N5
SFV NP/IT control
intratracheal instillation
intravenous injection
intranasal instillation

Figure 2

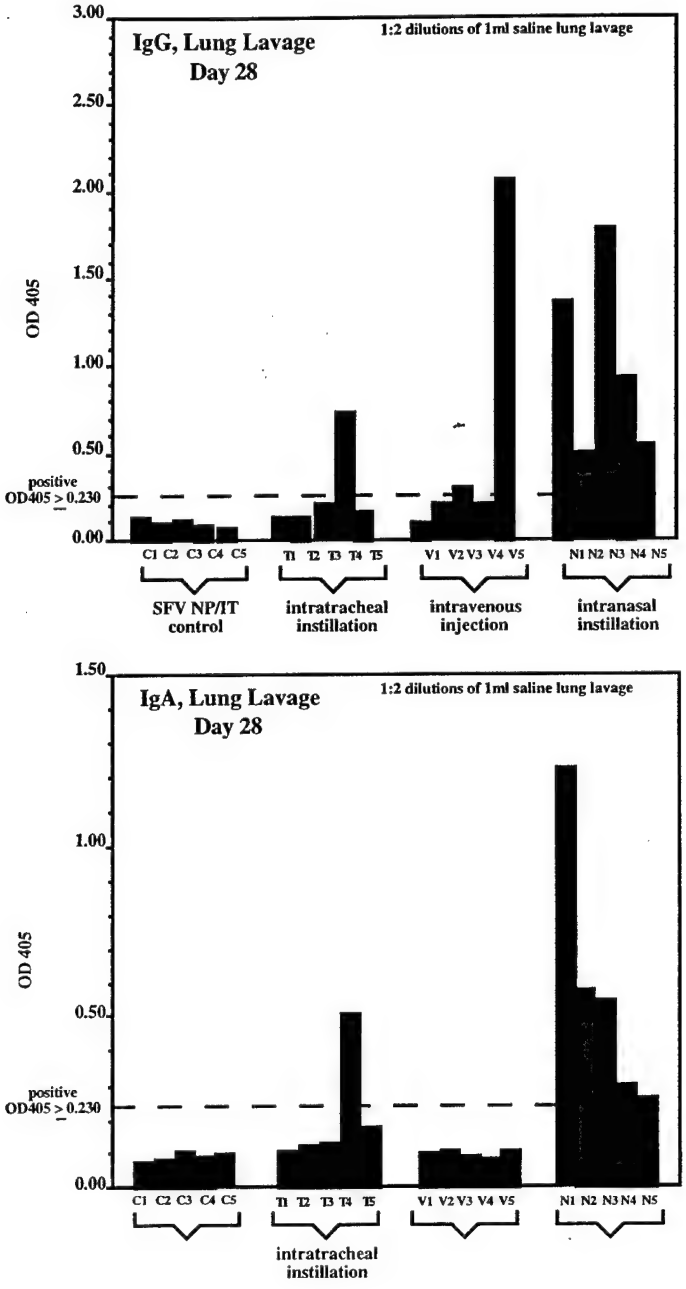
IgG, Lung Lavage
Day 28
1:2 dilutions of 1ml saline lung lavage
OD 405
3.00
2.50
2.00
1.50
1.00
0.50
positive
OD405 ≥ 0.230
0.00
C1 C2 C3 C4 C5
T1 T2 T3 T4 T5
V1 V2 V3 V4 V5
N1 N2 N3 N4 N5
SFV NP/IT control
intratracheal instillation
intravenous injection
intranasal instillation
IgA, Lung Lavage
Day 28
1:2 dilutions of 1ml saline lung lavage
OD 405
1.50
1.00
0.50
positive
OD405 ≥ 0.230
0.00
C1 C2 C3 C4 C5
T1 T2 T3 T4 T5
V1 V2 V3 V4 V5
N1 N2 N3 N4 N5
intratracheal instillation

Figure 3

**References:**

Balasubramaniam, R. P., M. J. Bennett, A. M. Aberle, J. G. Malone, M. H. Nantz and R. W. Malone (1996). "Structural and functional analysis of cationic transfection lipids: the hydrophobic domain." Gene Therapy 3(2): 163-172.

Berglund, P., M. Sjoberg, H. Garoff, G. J. Atkins, B. J. Sheahan and P. Liljestrom (1993). "Semliki Forest virus expression system: production of conditionally infectious recombinant particles." Biotechnology (N Y) 11(8): 916-20.

Brandtzaeg, P. (1996). "History of oral tolerance and mucosal immunity." Ann N Y Acad Sci 778: 1-27.

Brandtzaeg, P. and T. S. Halstensen (1992). "Immunology and immunopathology of tonsils." Adv Otorhinolaryngol 47: 64-75.

Brandtzaeg, P., T. S. Halstensen, M. Hvatum, D. Kvale and H. Scott (1993). The serologic and mucosal immunologic basis of celiac disease. Immunophysiology of the Gut. Bristol-Meyers squibb/Mead Johnson Nutrition Symposia Eds. W. A. Walker, P. R. Harmatz and B. K. Wershil. London., Academic press. 295-333.

Brandtzaeg, P., T. S. Halstensen, K. Kett, P. Krajci, D. Kvale, T. O. Rognum, H. Scott and L. M. Sollid (1989). "Immunobiology and immunopathology of human gut mucosa: humoral immunity and intraepithelial lymphocytes." Gastroenterology 97(6): 1562-84.

Burke, K. L., D. J. Evans, O. Jenkins, J. Meredith, E. D. D'Souza and J. W. Almond (1989). "A cassette vector for the construction of antigen chimaeras of poliovirus." J Gen Virol 70(Pt 9)): 2475-9.

Cone, R. D. and R. C. Mulligan (1984). "High-efficiency gene transfer into mammalian cells: generation of helper-free recombinant retrovirus with broad mammalian host range." Proc Natl Acad Sci U S A 81(20): 6349-53.

Fujihashi, K., J. R. McGhee, M. Yamamoto, T. Hiroi and H. Kiyono (1996). "Role of gamma delta T cells in the regulation of mucosal IgA response and oral tolerance." Ann N Y Acad Sci 778: 55-63.

Fynan, E. F., R. G. Webster, D. H. Fuller, J. R. Haynes, J. C. Santoro and H. L. Robinson (1993). "DNA vaccines: protective immunizations by parenteral, mucosal, and gene-gun inoculations." Proc Natl Acad Sci U S A 90(24): 11478-82.

Hermonat, P. L. and N. Muzyczka (1984). "Use of adeno-associated virus as a mammalian DNA cloning vector: transduction of neomycin resistance into mammalian tissue culture cells." Proc Natl Acad Sci U S A 81(20): 6466-70.

Holt, P. G. and C. McMenamin (1989). "Defence against allergic sensitization in the healthy lung: the role of inhalation tolerance." Clin Exp Allergy 19(3): 255-62.

Kalb, T. H., M. T. Chuang, Z. Marom and L. Mayer (1991). "Evidence for accessory cell function by class II MHC antigen-expressing airway epithelial cells." Am J Respir Cell Mol Biol 4(4): 320-9.

Kuper, C. F., P. J. Koornstra, D. M. Hameleers, J. Biewenga, B. J. Spit, A. M. Duijvestijn, P. J. van Breda Vriesman and T. Sminia (1992). "The role of nasopharyngeal lymphoid tissue [see comments]." Immunol Today 13(6): 219-24.

Liljestrom, P. (1994). "Alphavirus expression systems." Curr Opin Biotechnol 5(5): 495-500.

Liljestrom, P. and H. Garoff (1991). "A new generation of animal cell expression vectors based on the Semliki Forest virus replicon." Biotechnology (N Y) 9(12): 1356-61.

Livingston, J. B., S. Lu, H. L. Robinson and D. J. Anderson (1995). "The induction of mucosal immunity in the female genital tract using gene-gun technology. Part 1: Antigen expression." Ann N Y Acad Sci 772: 265-7.

McDermott, M. R. and J. Bienenstock (1979). "Evidence for a common mucosal immunologic system. I. Migration of B immunoblasts into intestinal, respiratory, and genital tissues." J Immunol 122(5): 1892-8.

McDermott, M. R., F. L. Graham, T. Hanke and D. C. Johnson (1989). "Protection of mice against lethal challenge with herpes simplex virus by vaccination with an adenovirus vector expressing HSV glycoprotein B." Virology 169(1): 244-7.

McGhee, J. R. and H. Kiyono (1993). "New perspectives in vaccine development: mucosal immunity to infections." Infect Agents Dis 2(2): 55-73.

McGhee, J. R. and H. Kiyono (1994). "Effective mucosal immunity. Current concepts for vaccine delivery and immune response analysis." Int J Technol Assess Health Care 10(1): 93-106.

Okayama, H. and P. Berg (1983). "A cDNA cloning vector that permits expression of cDNA inserts in mammalian cells." Mol Cell Biol 3(2): 280-9.

Raz, E., D. A. Carson, S. E. Parker, T. B. Parr, A. M. Abai, G. Aichinger, S. H. Gromkowski, M. Singh, D. Lew, M. A. Yankauckas and et al. (1994). "Intradermal gene immunization: the possible role of DNA uptake in the induction of cellular immunity to viruses." Proc Natl Acad Sci U S A 91(20): 9519-23.

Sarver, N., P. Gruss, M. F. Law, G. Khoury and P. M. Howley (1981). "Bovine papilloma virus deoxyribonucleic acid: a novel eucaryotic cloning vector." Mol Cell Biol 1(6): 486-96.

Smith, G. L., B. R. Murphy and B. Moss (1983). "Construction and characterization of an infectious vaccinia virus recombinant that expresses the influenza hemagglutinin gene and induces resistance to influenza virus infection in hamsters." Proc Natl Acad Sci U S A 80(23): 7155-9.

St. Louis, D. and I. M. Verma (1988). "An alternative approach to somatic cell gene therapy." Proc Natl Acad Sci U S A 85(9): 3150-4.

Takahashi, I., I. Nakagawa, H. Kiyono, J. R. McGhee, J. D. Clements and S. Hamada (1995). "Mucosal T cells induce systemic anergy for oral tolerance." Biochem Biophys Res Commun 206(1): 414-20.

Ulmer, J. B., J. J. Donnelly, S. E. Parker, G. H. Rhodes, P. L. Felgner, V. J. Dwarki, S. H. Gromkowski, R. R. Deck, C. M. DeWitt, A. Friedman and et al. (1993). "Heterologous protection against influenza by injection of DNA encoding a viral protein [see comments]." Science 259(5102): 1745-9.

van der Ven, I. and T. Sminia (1993). "The development and structure of mouse nasal-associated lymphoid tissue: an immuno- and enzyme-histochemical study." Reg Immunol 5(2): 69-75.

Van Doren, K., D. Hanahan and Y. Gluzman (1984). "Infection of eucaryotic cells by helper-independent recombinant adenoviruses: early region 1 is not obligatory for integration of viral DNA." J Virol 50(2): 606-14.

Van Ginkel, F. W., C. Liu, J. W. Simecka, J. Y. Dong, T. Greenway, R. A. Frizzell, H. Kiyono, J. R. McGhee and D. W. Pascual (1995). "Intratracheal gene delivery with

adenoviral vector induces elevated systemic IgG and mucosal IgA antibodies to adenovirus and beta-galactosidase." Hum Gene Ther 6(7): 895-903.

Wolff, J. A. and J. Lederberg (1994). "An early history of gene transfer and therapy." Hum Gene Ther 5(4): 469-80.

Xiong, C., R. Levis, P. Shen, S. Schlesinger, C. M. Rice and H. V. Huang (1989). "Sindbis virus: an efficient, broad host range vector for gene expression in animal cells." Science 243(4895): 1188-91.

Zhou, X., P. Berglund, G. Rhodes, S. E. Parker, M. Jondal and P. Liljestrom (1994). "Self-replicating Semliki Forest virus RNA as recombinant vaccine." Vaccine 12(16): 1510-4.

Zhou, X., P. Berglund, H. Zhao, P. Liljestrom and M. Jondal (1995). "Generation of cytotoxic and humoral immune responses by nonreplicative recombinant Semliki Forest virus." Proc Natl Acad Sci U S A 92(7): 3009-13.

# APPENDIX 2

# Costimulatory Requirements of Humoral and Cytotoxic T Cell Immune Responses Following Nucleic Acid Vaccination

# Costimulatory requirements of humoral and cytotoxic T cell immune responses following nucleic acid vaccination[1]

James H. Horspool*, Peter J. Perrin*, Juliana B. Woodcock*, Josephine H. Cox[§], Christopher L. King[§], Carl H. June*[,¶], Daniel C. St. Louis[‖] and Kelvin P. Lee*[,‡,2]

*Immune Cell Biology Program, Naval Medical Research Institute, Bethesda, MD

[‡]SRA Technologies, Rockville, MD

[§]Division of Tropical Medicine, Department of Medicine, Case Western Reserve University, Cleveland, OH.

[¶]Department of Medicine, Uniformed Services University of the Health Sciences, Bethesda, MD

[‖]Military Medical Consortium for Applied Retroviral Research, Rockville, MD

Running title: Costimulatory requirements of nucleic acid vaccination

Keywords: Vaccination, CTL, antibodies, co-stimulatory molecules

**Abstract**

Although nucleic acid vaccination (NAV) elicits robust humoral and cell-mediated immune responses, relatively little is known about the mechanisms involved. We have examined the costimulatory requirements of NAV. Blockade of the CD28 receptor abrogated sustained antibody responses following immunization with plasmids encoding β-galactosidase (pCIA/βgal). In contrast to the reported enhancement of cell-mediated responses, anti-CTLA4 mAb almost completely suppressed the humoral response to pCIA/βgal. Consistent with these findings, blockade of B7-1 and B7-2 also suppressed antibody responses to NAV. CD28 knockout mice did not mount antibody nor CTL responses to NAV. Conversely, enhancement of costimulation by coinjecting B7-expressing plasmids with pCIA/βgal augmented both antibody and CTL responses. These findings suggest that nucleic acid vaccination involves the same costimulatory pathways as protein immunization and can be manipulated through its costimulatory components. Furthermore, we have revealed a potential new role for CTLA4 activation.

## Introduction

Robust immune responses can be generated by vaccines comprised only of eukaryotic expression plasmids encoding an "antigen" gene (nucleic acid vaccination (NAV)[3] or "naked DNA" vaccination). Seminal studies have demonstrated these plasmids can be delivered intramuscularly (1), intradermally (2), intravenously or mucosally (3). Long-lived cellular and humoral immune responses against a variety of antigens have been generated in a wide range of hosts, resulting in protection against subsequent disease challenge (reviewed in 4,5). One of the most powerful aspects of nucleic acid vaccines is the technical ability to completely design and build the actual immunizing molecule. DNA vaccines that directly manipulate the immune response (6) and express the entire genome of a pathogen (7) have already been constructed. All these aspects give NAV the potential to significantly change immunization for infectious diseases, tumors and autoimmune syndromes.

The mechanisms involved in the immune response to NAV are poorly understood despite the interest in its' utility (8). With intramuscular injection, myocytes take up plasmid and express the encoded gene (9). What cell subsequently processes the expressed protein antigen and presents it to the immune system is not clear. Myocytes could be the actual antigen presenting cell (APC) as they express MHC class I, class II (induced by IFNγ) and can stimulate antigen-specific T cell proliferation (reviewed in 10). However, they do not express costimulatory ligands (11). Bone marrow-derived APCs appear to be involved in generating the CTL response (12,13). It has been proposed that myocytes produce the antigen and pass it on to professional APCs as

secreted extracellular protein (4), intracellularly through an undefined cell to cell process (13) or following myocyte destruction by antigen-specific T cells (4,12). Finally, some authors have proposed there is no actual myocyte involvement, that resident dendritic cells take up the plasmid, express and present the antigen (6). How the immune system responds so readily to a vanishingly small amount of antigen (1) and maintains persistent immune memory is also unknown.

It is therefore not surprising that the T cell costimulatory requirements in NAV are also undefined. T-dependent responses to protein immunization require both a primary signal through the TCR (via MHC/peptide binding) and costimulation through the CD28 receptor, activated upon binding to its ligand(s), B7-1 (CD80) and B7-2 (CD86) (reviewed in 14). Blockade of CD28 activation by the B7-binding protein CTLA4Ig suppressed antibody responses to keyhole limpet hemocyanin and sheep red blood cells (15). Mice genetically lacking the CD28 gene ("knockout mice") also had diminished antibody responses to vesicular stomatitis virus infection (16). Other studies have demonstrated a central role of CD28 in cytotoxic T cell activation (17,18). Activation of the second CD28 family member, CTLA4, appeared to inhibit T cell responses in most (19-27) but not all (28,29) studies. CTLA4 binds to the same B7 ligands as CD28, although with different avidities (30). Although CTLA4 is expressed on activated human B cells (31), its' role in humoral responses has not been described.

In this study we examined whether NAV requires the same costimulatory signals as protein immunization. In addition, we sought to determine if enhancing costimulation augments the subsequent response to NAV. We found that antibody blockade of CD28, B7-1, or B7-2 suppressed the humoral response to NAV. Treatment with anti-CTLA4

mAb previously reported to be blocking almost completely abrogated the antibody response following NAV. CD28 knockout mice also did not mount antibody responses to NAV, nor did they generate antigen-specific CTLs. Conversely, coimmunization with B7-expressing plasmids enhanced both antibody and CTL responses. These findings suggest that immune responses to both protein and nucleic acid vaccines involve similar mechanisms and reveal a potential new role for CTLA4 activation in antibody production. Furthermore, these results predict impaired responses to NAV will occur in states of CD28 down-regulation (such as HIV infection) and that enhancing costimulation may have general utility for adjuvanting a wide variety of DNA vaccines.

## Material and Methods

### Plasmids

The bacterial gene encoding β-galactosidase (βgal) was excised from the pADβ plasmid (Clontech, Palo Alto, CA) with NotI and subcloned into the eukaryotic expression plasmid pCIA (derived from pcDNAI and pcDNA/amp (Invitrogen, San Diego, CA, CMV promoter). Expression of βgal was confirmed by transient transfection into COS7 cells and staining for β-galactosidase activity (32,33). The murine B7 coexpression plasmids pCIA/mB7-1 and pCIA/mB7-2 were derived by subcloning the full length murine B7-1 or B7-2 cDNA (gift of Dr. G. Gray, Genetics Institute, Cambridge, MA) into the expression vector pRSV (Invitrogen, San Diego, CA). The RSV promoter-B7 cDNA-SV40 intron-poly A cassette was excised with AccI and subcloned into the ClaI site of pCIA, 880 bp 3' of the pCIA CMV promoter. pCIA/mB7-1 and pCIA/mB7-2 can simultaneously express the immunizing gene cloned into the multiple cloning site (CMV promoter) and B7 (RSV promoter). Expression of B7-1 and B7-2 was confirmed by transient transfection into COS7 cells, monoclonal antibody staining and flow cytometric analysis (34).

### DNA purification

Plasmids were transformed into *E. coli* strain JM109, expanded in large scale cultures and purified by alkaline lysis and two sequential high speed centrifugations over cesium chloride gradients (35). Endotoxin was removed using the Detoxigel kit (Pierce, Rockford, IL) per manufacturer's instructions and the DNA resuspended at 1 mg/mL in

sterile normal saline. Endotoxin levels in these preparations were less than 0.03 pg/μg DNA.

Antibodies

Antibodies used in this study were: Anti-murine B7-1 mAb 16-10A1 (gift of Dr. H. Reiser, Dana Farber Cancer Institute, Boston, MA), anti-murine B7-2 mAb GL-1 (gift of Dr. R. Hodes, National Institute of Aging, NIH, Bethesda, MD), anti-mouse CTLA-4 mAb UC10-4F10-11 (gift of Dr. J. Bluestone, University of Chicago, Chicago, IL), and anti-murine CD28 mAb PV-1 (36). Hamster IgG was used as a control for 16-10A1, PV1.1 and UC10-4F10. A rat IgG2a antibody was used as a control for GL-1. Fab fragments of anti-B7-1, anti-B7-2, PV1.1 and control antibodies were made and tested as previously described (37). In blocking studies 50 μg of antibody was injected i.p. 1 hr before and 48 hrs after immunization.

Immunizations

Five-10 week old female Balb/cByJ mice (The Jackson Laboratory, Bar Harbor, ME), CD28 knockout mice and littermate controls ($H2^d$, (16)) were utilized in accordance with the Guide for the Care and Use of Laboratory Animals, NIH Publication 85-23 (1985). Groups of 3-4 mice were injected intramuscularly in the right tibialis anterior with 100 μg of DNA in 100 μL normal saline with a 30g needle. Because of age-dependent variability in the primary antibody response, mice in the blocking studies were immunized on day 0 and again at day 42 if no response was seen in the control group by

that time. For the CD28 knockout and B7 augmentation studies, mice were immunized on day 0 and boosted biweekly for a total of 3 doses (38). Mice assayed for CTL activity were boosted with 100 μg DNA 2 weeks prior to performance of the assay.

ELISA

Serum from individual mice was collected at times indicated and analyzed for anti-β-galactosidase antibody titers by standard ELISA methodology (39). Purified β-galactosidase protein (Sigma Chemicals, St. Louis, MO) was used to assay 2 fold serial dilutions (starting at 1:20) of test sera or control anti-β-galactosidase monoclonal antibody (Sigma Chemicals, St. Louis, MO). The concentration of βgal -specific antibody was calculated from the control mAb standard curve and expressed as μg/mL. Vaccination specific titers were obtained by subtracting out the vector alone titer. Data is represented as the geometric mean of the titers from individual mice within each group.

CTL assay

CTL assays were performed as previously described (40). Splenic mononuclear cells were stimulated for 5 days with the synthetic peptide TPHPARIGL (Peptide Technologies, Washington, D.C.) representing the naturally processed H-2 $L^d$ restricted epitope spanning 876-884 of βgal. $^{51}$Cr-labelled P815 cells pulsed with 1 μg/mL βgal peptide or no peptide were used as targets at E:T ratios of 100:1, 30:1, 10:1 and 3:1. % specific lysis = [(experimental cpm-spontanous cpm)/(maximal cpm- spontanous cpm)] x 100. βgal specific CTL activity was calculated by subtracting the % specific lysis of

P815 pulsed with no peptide from % specific lysis of the βgal peptide-pulsed P815 target cells. The % specific lysis of P815 pulsed with no peptide was always <10%. Experimental values represent the mean of triplicate cpm values.

**Results**

CD28 and CTLA4 pathways are involved in humoral reponse to NAV

We initially assessed the role of CD28 in NAV by injecting anti-CD28 Fab on day 0 and 2 following a single immunization with plasmid encoding β-galactosidase (pCIA/βgal). βgal immunized mice injected with control hamster immunoglobulin generated a sustained antibody response (figure 1A). In contrast, βgal immunized mice injected with anti-CD28 Fab fragments developed a comparable early response (0-4 weeks) but were unable to sustain antibody titers beyond 4 weeks. Mice immunized with vector alone (no βgal) did not develop anti-βgal titers.

Previous studies have shown that *in vivo* blockade of CTLA4 with anti-CTLA4 mAb (including UC-4F10 used in this study) resulted in enhancement of cellular immune responses. Unexpectedly, injection of anti-CTLA4 mAb almost completely suppressed the antibody response to a single immunization with pCIA/βgal (figure 1B). Anti-CTLA4 mAb also suppressed antibody responses to immunization with β-galactosidase protein (in complete Freund's adjuvant) but to a less marked extent (data not shown).

Consistent with the above findings, antibody responses were also suppressed by either anti-B7-1 Fab or anti-B7-2 Fab injection (figure 2). Blockade of B7-1 was more effective than B7-2, as was the case with βgal protein immunization (data not shown).

To confirm the antibody blocking studies, mice genetically lacking the CD28 gene (CD28 knockout) and wild type littermate controls were immunized and boosted (0, 2, 4 wks) with pCIA/βgal (figure 3A). In contrast to the wild type controls, the CD28

knockout mice failed to mount an antibody response. Furthermore, the CD28 knockout mice also failed to develop βgal-specific CTL responses (figure 3B).

Coimmunization with B7 cDNA enhances antibody and CTL responses to NAV.

The requirement for CD28 (and possibly CTLA4) activation via B7-1/B7-2 binding suggested that coimmunization with B7-expressing cDNAs would enhance the immune response to nucleic acid vaccination. To evaluate this hypothesis, mice were immunized on day 0, 14 and 21 with 100 μg of pCIA/βgal, or 100 μg of pCIA/βgal mixed with 100 μg pCIA/mB7-1 or mB7-2 (figure 4A). Neither B7-1 nor B7-2 coinjection affected the primary antibody response. Rather, they substantially enhanced titers at later time points. There was no significant difference in βgal-specific antibody isotypes in the B7-coinjected mice vs. βgal alone (data not shown). B7 coinjection also augmented βgal specific CTL responses (figure 4B), with B7-2 more potently than B7-1.

**Discussion**

The range of responses elicited by NAV is rapidly becoming defined. In contrast, the process from "naked DNA" to immune response is only beginning to be understood. The two signal model of T cell activation by protein antigens has been well established, as has the central role of CD28 in delivering the requisite costimulatory signal (41). We have examined costimulatory requirements as a means to compare the components of nucleic acid "antigen" versus protein antigen-mediated T cell activation. Sustained antibody responses to NAV were suppressed by anti-CD28 Fab, consistent with the observation that CD28 is required to maintain antigen-specific responses (42). Antibody responses were also blocked by anti-B7-1 Fab, and to a lesser extent by anti-B7-2 Fab. The greater efficacy of B7-1 blockade may reflect differing kinetics of B7-1 vs. B7-2 expression (43) or biological roles/receptors (CD28 vs. CTLA4) of these ligands. The interpretation that B7 blockade is preventing costimulation through CD28 must be tempered by the observation that the other B7 binding receptor, CTLA4, appears to play a role in the antibody response to NAV.

CTLA4 is the other member of the CD28 gene family (44,45) and binds to the same B7 ligands as CD28 (30). *In vitro* studies have shown that antibody-mediated crosslinking of the CTLA4 receptor inhibits CD28-dependent T cell activation, IL-2 accumulation and cell cycle progression (19-23). *In vivo* studies with anti-CTLA4 mAb have demonstrated enhanced cell mediated immune responses, presumably by blocking ligand binding to CTLA4 (24-26). In contrast, we found that anti-CTLA mAb injection almost completely suppressed the antibody response to NAV. As it has been speculated that NAV can activate negative regulatory T cells (46), CTLA4 blockade may derepress

these cells leading to skewing away from or suppression of humoral responses. It is also possible that UC10-4F10 can activate CTLA4 *in vivo* (as has been reported *in vitro* (21)) resulting in suppression of T cell help and antibody production. Finally, it is possible that anti-CTLA4 mAb acts directly on B cells, which express CTLA4 upon T-cell-mediated activation (31). It has been speculated that the differences in antibody profile between the CD28 knockout mice and CTLA4-Hγ1 transgenic mice is due to a direct agonistic effect of CTLA4 activation on B cells (31,47). Further studies examining the mechanisms and kinetics of CTLA4's role in the humoral reponse to NAV are underway.

DNA vaccination of CD28 knockout mice allowed for the direct assessment of CD28's role without the variables of antibody administration and crossbinding ligands. Consistent with anti-CD28 Fab results, the knockout mice did not mount an antibody response to pCIA/βgal plasmid immunization. The less complete abrogation in the anti-CD28 Fab treated vs. knockout mice was likely due to incomplete antibody blockade, which was also seen in protein immunized mice (data not shown). This finding suggests that CD28 costimulation is not only necessary to sustain an immune response but also to initiate/amplify one, particularly against small amounts of antigen that may otherwise result in low zone tolerance (reviewed in 48). The CD28 knockout mice were also unable to generate CTL responses to NAV, which differs from the reported normal CTL responses to lymphocytic choriomeningitis virus infection (16) and may reflect differences in costimulatory requirements of viral infection vs. NAV (48).

The requirement for CD28 in NAV suggested that augmenting costimulation with B7 coexpression would enhance humoral and cellular immune responses, as has been

shown *in vivo* for B7-expressing tumors (49,50) and B7-1 coexpressing adenoviral vectors (51). Long term antibody responses were enhanced by coinjection of pCIA/mB7-1 or pCIA/mB7-2 with pCIA/βgal, consistent with a role for CD28 in maintaining immune responses. Coinjection of B7-2 (and to a lesser extent B7-1) also enhanced CTL responses. These findings are best explained by persistent *cis* expression of βgal and B7 by myocytes (dendritic cells already express high levels of B7 that would unlikely be increased by plasmid transfection), resulting in augmented costimulation and activation of trafficking T cells. The propensity of a single cell to take up two unlinked plasmids is well established *in vitro* (52) and explains the augmentation by coimmunization with separate GM-CSF cDNA and rabies G protein plasmids (6). We have obtained similar results with constructs that express βgal and B7-2 on the same plasmid, where *cis* expression is more assured (data not shown). We propose in NAV that bone marrow-derived APCs serve to activate naïve T cells (after acquiring the antigen from transfected myocytes), and that subsequent antigen "presentation" by myocytes is directly involved in amplifying and sustaining this response. CD28 may play an important role in both the initial T cell activation and subsequent amplification, potentially by enhancing effector function and development of memory. Our findings also suggest there is long term survival of βgal/B7-expressing myocytes, that these cells are not completely eliminated by the resulting cellular immune response.

Nucleic acid vaccination holds tremendous potential for the treatment of a wide range of diseases. The power of recombinant DNA technology affords unprecedented possibilities in vaccine design, construction and production. Understanding how NAV

works will not only allow for the design of more effective vaccines but may also reveal novel aspects of the immune system.

**Acknowledgements**

We would like to thank Dr. Kari Irvine (National Cancer Institute, NIH, Bethesda, MD) for originally providing the βgal peptide and CTL protocol. We would also like to thank Mr. Alfred Black, Antibody Core, Immune Cell Biology Program (Naval Medical Research Institute, Bethesda, MD) for producing many of the antibody reagents used in this study.

**References**


1. **Donnelly, J. J., S. E. Parker, G. H. Rhodes, P. L. Felgner, V. J. Dwarki, S. H. Gromkowski, R. R. Deck, C. M. DeWitt, A. Friedman, L. A. Hawe, K. R. Leander, D. Martinez, H. C. Perry, J. W. Shiver, D. L. Montgomery, and M. A. Liu**. 1993. *Science 259*:1745.

2. **Tang, D. C., M. DeVit, and S. A. Johnston**. 1992. *Nature 356*:152.

3. **Fynan, E. F., R. G. Webster, D. H. Fuller, J. R. Haynes, J. C. Santoro, and H. L. Robinson**. 1993. *Proc. Natl. Acad. Sci. U. S. A. 90*:11478.

4. **Whalen, R. G. and H. L. Davis**. 1995. *Clin. Immunol. Immunopathol. 75*:1.

5. **Liu, M. A.** 1995. *Ann. N. Y. Acad. Sci. 772:15-20*:15.

6. **Xiang, Z. and H. C. Ertl**. 1995. *Immunity. 2*:129.

7. **Barry, M. A., W. C. Lai, and S. A. Johnston**. 1995. *Nature 377*:632.

8. **Pardoll, D. M. and A. M. Beckerleg**. 1995. *Immunity. 3*:165.

9. **Wolff, J. A., R. W. Malone, P. Williams, W. Chong, G. Acsadi, A. Jani, and P. L. Felgner**. 1990. *Science 247*:1465.

10. **Hohlfeld, R. and A. G. Engel**. 1994. *Immunol. Today 15*:269.

11. **Warrens, A. N., J. Y. Zhang, S. Sidhu, D. J. Watt, G. Lombardi, C. A. Sewry, and R. I. Lechler**. 1994. *Int. Immunol. 6*:847.

12. **Doe, B., M. Selby, S. Barnett, J. Baenziger, and C. M. Walker**. 1996. *Proc. Natl. Acad. Sci., USA 93*:8578.

13. **Ulmer, J. B., R. R. Deck, C. M. DeWitt, J. J. Donnelly, and M. A. Liu**. 1996. *Immunology 89*:59.

14. **June, C. H., P. Vandenberghe, and C. B. Thompson**. 1994. *Chem. Immunol. 59:62-90*:62.

15. **Linsley, P. S., P. M. Wallace, J. Johnson, M. G. Gibson, J. L. Greene, J. A. Ledbetter, C. Singh, and M. A. Tepper**. 1992. *Science 257*:792.

16. **Shahinian, A., K. Pfeffer, K. P. Lee, T. M. Kundig, K. Kishihara, A. Wakeham, K. Kawai, P. S. Ohashi, C. B. Thompson, and T. W. Mak**. 1993. *Science 261*:609.

17. **Azuma, M., M. Cayabyab, J. H. Phillips, and L. L. Lanier**. 1993. *J. Immunol. 150*:2091.

18. **Guerder, S., S. R. Carding, and R. A. Flavell**. 1995. *J. Immunol. 155*:5167.

19. **Gribben, J. G., G. J. Freeman, V. A. Boussiotis, P. Rennert, C. L. Jellis, E. Greenfield, M. Barber, V. A. Restivo,Jr., X. Ke, G. S. Gray, and L. M. Nadler**. 1995. *Proc. Natl. Acad. Sci. U. S. A. 92*:811.

20. **Walunas, T. L., D. J. Lenschow, C. Y. Bakker, P. S. Linsley, G. J. Freeman, J. M. Green, C. B. Thompson, and J. A. Bluestone**. 1994. *Immunity. 1*:405.

21. **Walunas, T. L., C. Y. Bakker, and J. A. Bluestone**. 1996. *J. Exp. Med. 183*:2541.

22. **Krummel, M. F. and J. P. Allison**. 1995. *J. Exp. Med. 182*:459.

23. **Krummel, M. F. and J. P. Allison**. 1996. *J. Exp. Med. 183*:2533.

24. **Leach, D. R., M. F. Krummel, and J. P. Allison**. 1996. *Science 271*:1734.

25. **Perrin, P. J., J. H. Maldonado, T. A. Davis, C. H. June, and M. K. Racke**. 1996. *J. Immunol. 157*:1333.

26. **Karandikar, N. J., C. L. Vanderlugt, T. L. Walunas, S. D. Miller, and J. A. Bluestone**. 1996. *J. Exp. Med. 184*:783.

27. **Waterhouse, P., J. M. Penninger, E. Timms, A. Wakeham, A. Shahinian, K. P. Lee, C. B. Thompson, H. Griesser, and T. W. Mak**. 1995. *Science 270*:985.

28. **Linsley, P. S., J. L. Greene, P. Tan, J. Bradshaw, J. A. Ledbetter, C. Anasetti, and N. K. Damle**. 1992. *J. Exp. Med. 176*:1595.

29. **Damle, N. K., K. Klussman, G. Leytze, S. Myrdal, A. Aruffo, J. A. Ledbetter, and P. S. Linsley**. 1994. *J. Immunol. 152*:2686.

30. **Linsley, P. S., W. Brady, M. Urnes, L. S. Grosmaire, N. K. Damle, and J. A. Ledbetter**. 1991. *J. Exp. Med. 174*:561.

31. **Kuiper, H. M., M. Brouwer, P. S. Linsley, and R. A. van Lier**. 1995. *J. Immunol. 155*:1776.

32. **Kukowska-Latallo, J. F., R. D. Larsen, R. P. Nair, and J. B. Lowe**. 1990. *Genes Dev. 4*:1288.

33. **Cepko, C.** 1995. Introduction of DNA into mammalian cells. In *Current Protocols in Molecular Biology*. F.M. Ausubel, R. Brent, R.E. Kingston, D.D. Moore, J.G. Seidman, J.A. Smith and K. Struhl, eds. John Wiley and Sons, Inc. p. 9.11.9.

34. **Masteller, E. L., R. D. Larsen, L. M. Carlson, J. M. Pickel, B. Nickoloff, J. Lowe, C. B. Thompson, and K. P. Lee**. 1995. *Development 121*:1657.

35. **Helig, J. S., K. Lech, and R. Brent**. 1995. *Escherichia coli*, plasmids, and bacteriophage. In *Current Protocols in Molecular Biology*. F.M. Ausubel, R. Brent, R.E. Kingston, D.D. Moore, J.G. Seidman, J.A. Smith and K. Struhl, eds. John Wiley and Sons, Inc. p. 1.7.1.

36. **Abe, R., P. Vandenberghe, N. Craighead, D. S. Smoot, K. P. Lee, and C. H. June**. 1995. *J. Immunol. 154*:984.

37. **Racke, M. K., D. E. Scott, L. Quigley, G. S. Gray, R. Abe, C. H. June, and P. J. Perrin**. 1995. *J. Clin. Invest. 96*:2195.

38. **Wang, B., K. E. Ugen, V. Srikantan, M. G. Agadjanyan, K. Dang, Y. Refaeli, A. I. Sato, J. Boyer, W. V. Williams, and D. B. Weiner**. 1993. *Proc. Natl. Acad. Sci. U. S. A. 90*:4156.

39. **Harlow, E. and D. Lane**. 1988. Immunoassay. In *Antibodies: A laboratory manual*. AnonymousCold Spring Harbor Laboratory, p. 561.

40. **Irvine, K. R., J. B. Rao, S. A. Rosenberg, and N. P. Restifo**. 1996. *J. Immunol. 156*:238.

41. **June, C. H., J. A. Bluestone, L. M. Nadler, and C. B. Thompson**. 1994. *Immunol. Today 15*:321.

42. **Lucas, P. J., I. Negishi, K. Nakayama, L. E. Fields, and D. Y. Loh**. 1995. *J. Immunol. 154*:5757.

43. **Boussiotis, V. A., G. J. Freeman, J. G. Gribben, J. Daley, G. Gray, and L. M. Nadler**. 1993. *Proc. Natl. Acad. Sci. U. S. A. 90*:11059.

44. **Brunet, J. F., F. Denizot, M. F. Luciani, M. Roux-Dosseto, M. Suzan, M. G. Mattei, and P. Golstein**. 1987. *Nature 328*:267.

45. **Harper, K., C. Balzano, E. Rouvier, M. G. Mattei, M. F. Luciani, and P. Golstein**. 1991. *J. Immunol. 147*:1037.

46. **Waisman, A., P. J. Ruiz, D. L. Hirschberg, A. Gelman, J. R. Oskenberg, S. Brocke, F. Mor, I. R. Cohen, and L. Steinman**. 1996. *Nature Medicine 2*:899.

47. **Lane, P., C. Burdet, S. Hubele, D. Scheidegger, U. Muller, F. McConnell, and M. Kosco Vilbois**. 1994. *J. Exp. Med. 179*:819.

48. **Matzinger, P.** 1994. *Annu. Rev. Immunol. 12:991-1045*:991.

49. **Townsend, S. E. and J. P. Allison**. 1993. *Science 259*:368.

50. **Chen, L., S. Ashe, W. A. Brady, I. Hellstrom, K. E. Hellstrom, J. A. Ledbetter, P. McGowan, and P. S. Linsley**. 1992. *Cell 71*:1093.

51. **He, X. S., H. S. Chen, K. Chu, M. Rivkina, and W. S. Robinson**. 1996. *Proc. Natl. Acad. Sci. U. S. A. 93*:7274.

52. **Wigler, M., R. Sweet, Sim.G.K., B. Wold, A. Pellicer, E. Lacy, T. Maniatis, S. Silverstein, and R. Axel**. 1979. *Cell 16*:777.

**Footnotes**

[1]This work was supported by the Naval Medical Research and Development Command, Research Task No. 61305D.B998.ABH29.1H.1281. Views presented in this paper are those of the authors; no endorsement by the Department of Navy, Department of the Army or the Department of Defense has been given or should be inferred.

[2]Corresponding author
Immune Cell Biology Program, Stem Cell Biology Branch
Bldg. 18, Room 230, Naval Medical Research Institute
8901 Wisconsin Avenue Bethesda, MD 20889-5067.
Tel: 301-295-1261 Fax: 301-295-0376
email: rin0kxl@bumed30.med.navy.mil.

[3]Abbreviations used in this paper: NAV - nucleic acid vaccination, βgal - β-galactosidase

**Figure legends**

**Figure 1.** Effect of anti-CD28 or CTLA4 mAb on the antibody response to NAV. **A).** CD28 blockade. Four BALB/c female mice/group were immunized with pCIA/βgal plasmid (in saline) i.m. in the tibialis anterior muscle at time 0 (arrow), and given 50 μg of anti-murine CD28 Fab (PV1.1) (▽) or control hamster Ig (■) i.p. at time -1 and 48 hr. One group was immunized with 100 μg/100 μL pCIA alone as vector controls (●). Anti-β-galactosidase antibody titers were assayed as per *Material and Methods*. The concentration of βgal -specific antibody was calculated from the control mAb standard curve and expressed as μg/mL. Data is represented as the geometric mean of the titers from individual mice within each group. **B).** CTLA4 treatment. Four BALB/c female mice/group were immunized with pCIA/βgal plasmid (in saline) i.m. at time 0 (arrow), and given 50 μg of anti-murine CTLA mAb (UC10-4F10) (▽) or control hamster Ig (■) i.p. at time -1 hr and 48 hr. One group was immunized with 100 μg/100 μL pCIA as vector controls (●). Anti-β-galactosidase antibody titers were assayed, calculated and represented as above in **A).** This data is representative of two independent experiments.

**Figure 2.** Effect of B7-1 or B7-2 blockade on the antibody response to NAV. Four BALB/c female mice/group were immunized with 100 μg pCIA/βgal plasmid (in saline) i.m. at time 0 and 6 weeks (arrows) and given 50 μg of anti-murine B7-1 Fab (16-10A1) (▽), anti-murine B7-2 Fab (GL-1) (◆) or control hamster Ig (■) i.p. at time -1 hr and 48 hr after each immunization. One group was immunized with 100 μg/100 μL pCIA as

vector controls (●). Anti-β-galactosidase antibody titers were assayed and calculated as per *Material and Methods*. Data is represented as the geometric mean of the titers from individual mice within each group.

**Figure 3.** Absent antibody and CTL responses of CD28 knockout (KO) mice to NAV. **A).** Antibody response. CD28 KO mice or wild type (WT) littermate controls (3 per group) were immunized i.m at time 0, 2 and 4 weeks (arrows) with 100 μg pCIA (vector control, WT (●), CD28KO (▼)) or 100 μg pCIA/βgal plasmid (WT (□), CD28KO (▽)).Anti-β-galactosidase antibody titers were assayed and as per *Material and Methods*. Data is represented as the geometric mean of the titers from individual mice within each group. **B).** CTL response. CD28 KO mice or wild type (WT) littermate controls were immunized i.m. at time 0, 2, 4 and 15 weeks with 100 μg pCIA (WT (●), CD28KO (▼)) or 100 μg pCIA/βgal plasmid (WT (□), CD28KO (▽)) and sacrificed at 17 weeks. CTL assays utilizing P815 target cells pulsed with β-galactosidase peptide were performed as per *Material and Methods*. Data is represented as the % specific lysis of individual mice at E:T ratios indicated.

**Figure 4.** B7 augmentation of antibody and CTL responses to NAV. **A).** Antibody responses. BALB/c female mice (3 per group) were immunized i.m. at time 0, 2 and 4 weeks (arrows) with 100 μg pCIA (vector control (●)), 100 μg pCIA/βgal (▽), 100 μg pCIA/βgal coinjected with 100 μg pCIA/mB7-1 (in 100 μl total volume) (■), or 100 μg

pCIA/βgal coinjected with 100 μg pCIA/mB7-2 (in 100 μl total volume) (♦) plasmid. Anti-β-galactosidase antibody titers were assayed as per *Material and Methods*. Data is represented as the geometric mean of the titers from individual mice within each group. **B).** CTL responses. BALB/c female mice were immunized i.m. at time 0, 2, 4 and 32 weeks with 100 μg pCIA (vector control (●)), 100 μg pCIA/βgal (▽), 100 μg pCIA/βgal coinjected with 100 μg pCIA/mB7-1 (in 100 μl total volume) (■), or 100 μg pCIA/βgal coinjected with 100 μg pCIA/mB7-2 (in 100 μl total volume) (♦) plasmid and sacrificed for CTL assays at week 34. CTL assays utilizing P815 target cells pulsed with β-galactosidase peptide were performed as per *Material and Methods*. Data represents 2 experiments and is shown as the % specific lysis of individual mice at E:T ratios indicated.

FIGURE 1

A.

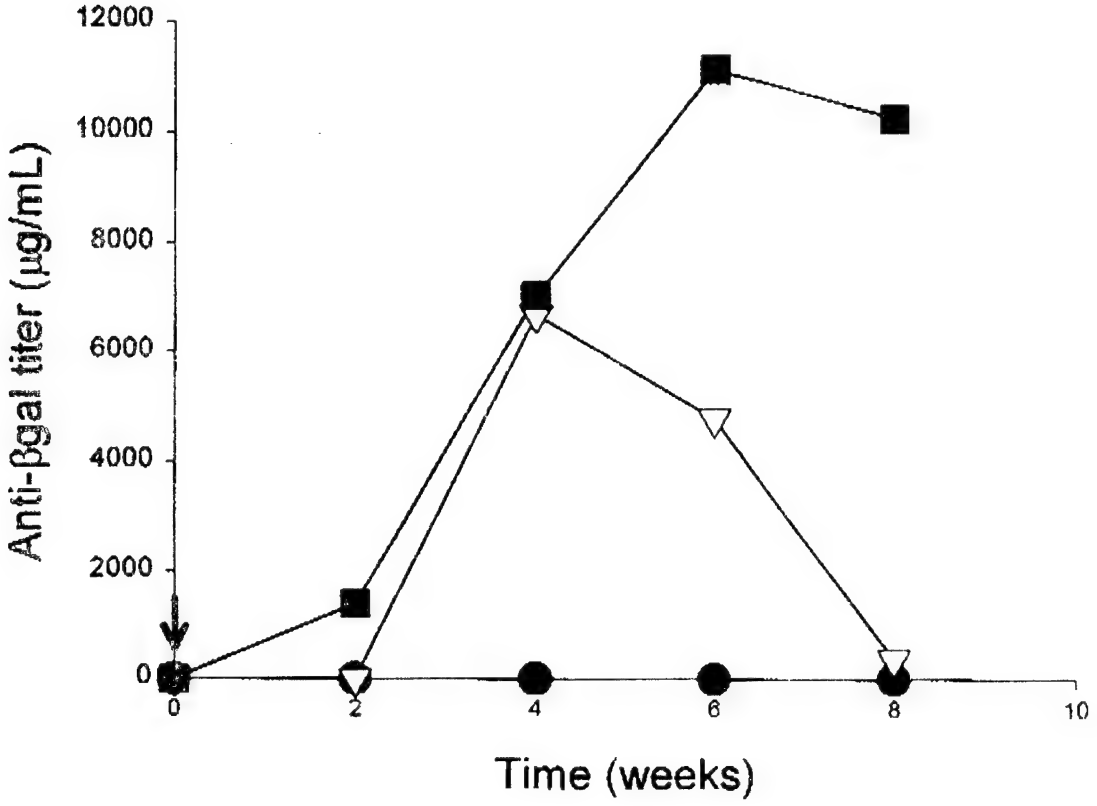
12000
10000
8000
6000
4000
2000
0
Anti-βgal titer (μg/mL)
0
2
4
6
8
10
Time (weeks)

B.

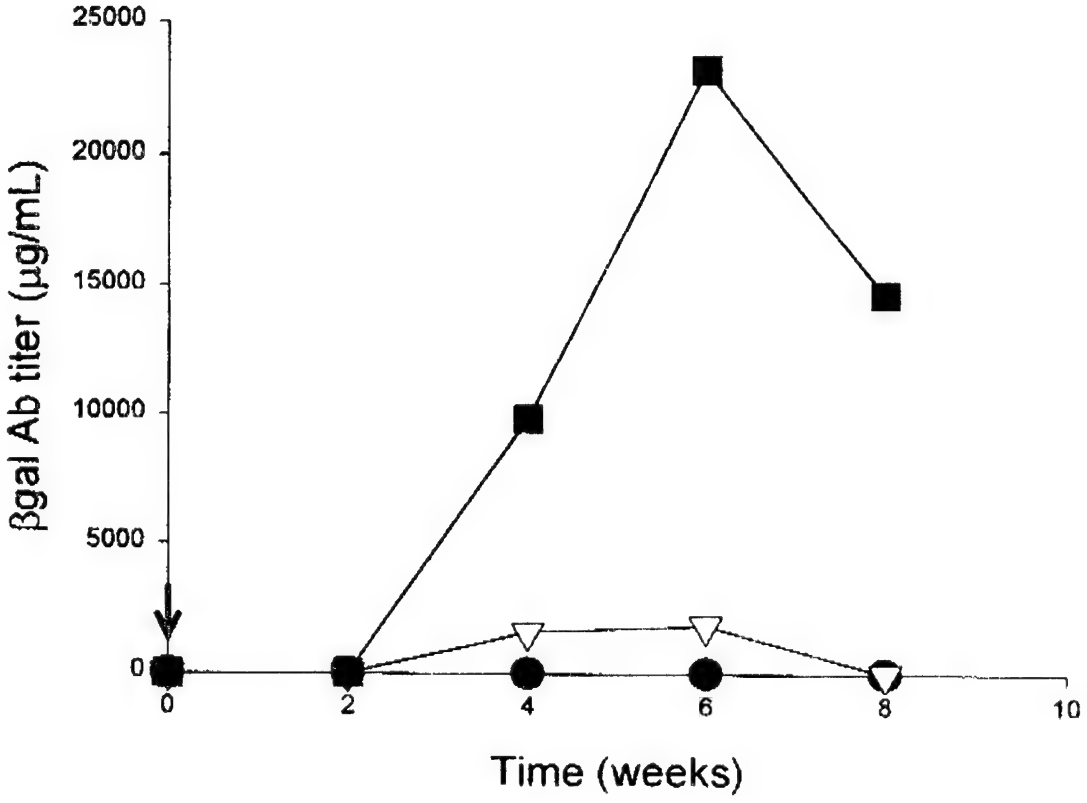
25000
20000
15000
10000
5000
0
βgal Ab titer (μg/mL)
0
2
4
6
8
10
Time (weeks)

FIGURE 2

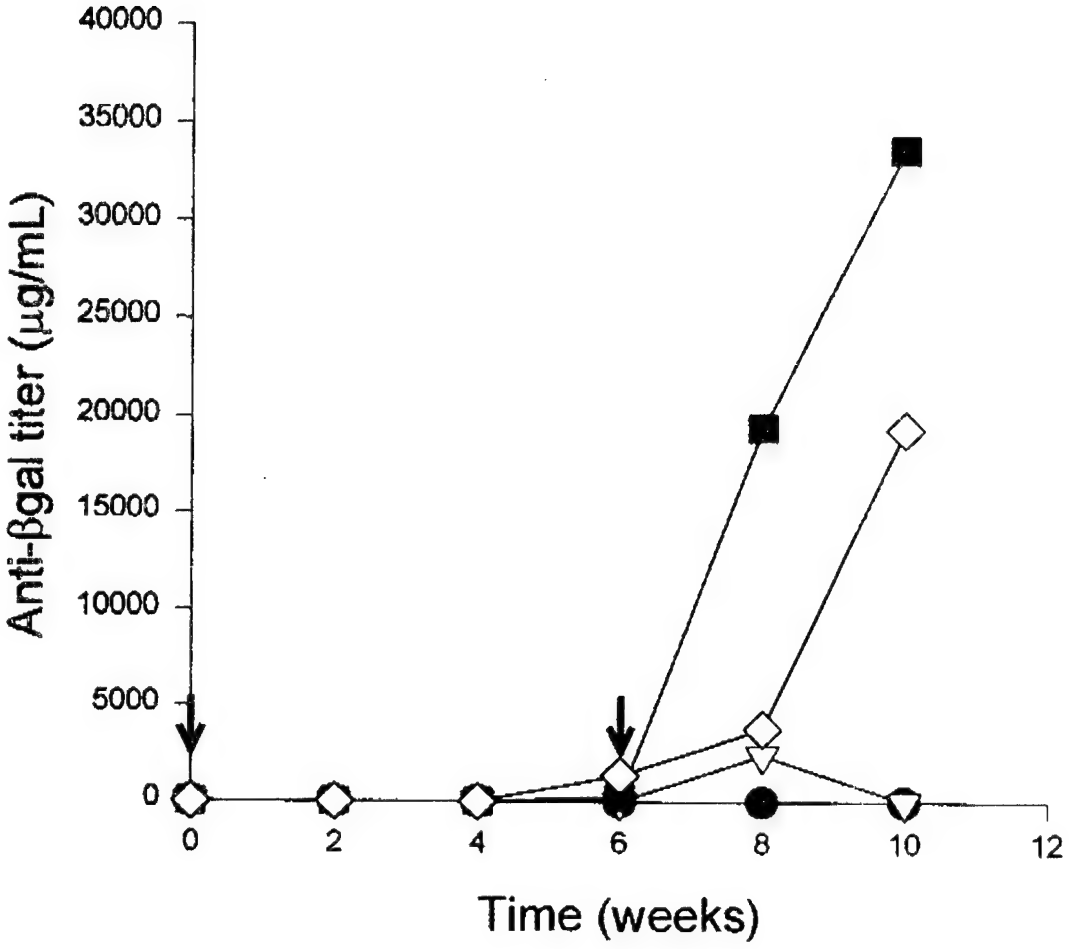
40000
35000
30000
25000
20000
15000
10000
5000
0
Anti-βgal titer (μg/mL)
0
2
4
6
8
10
12
Time (weeks)

FIGURE 3

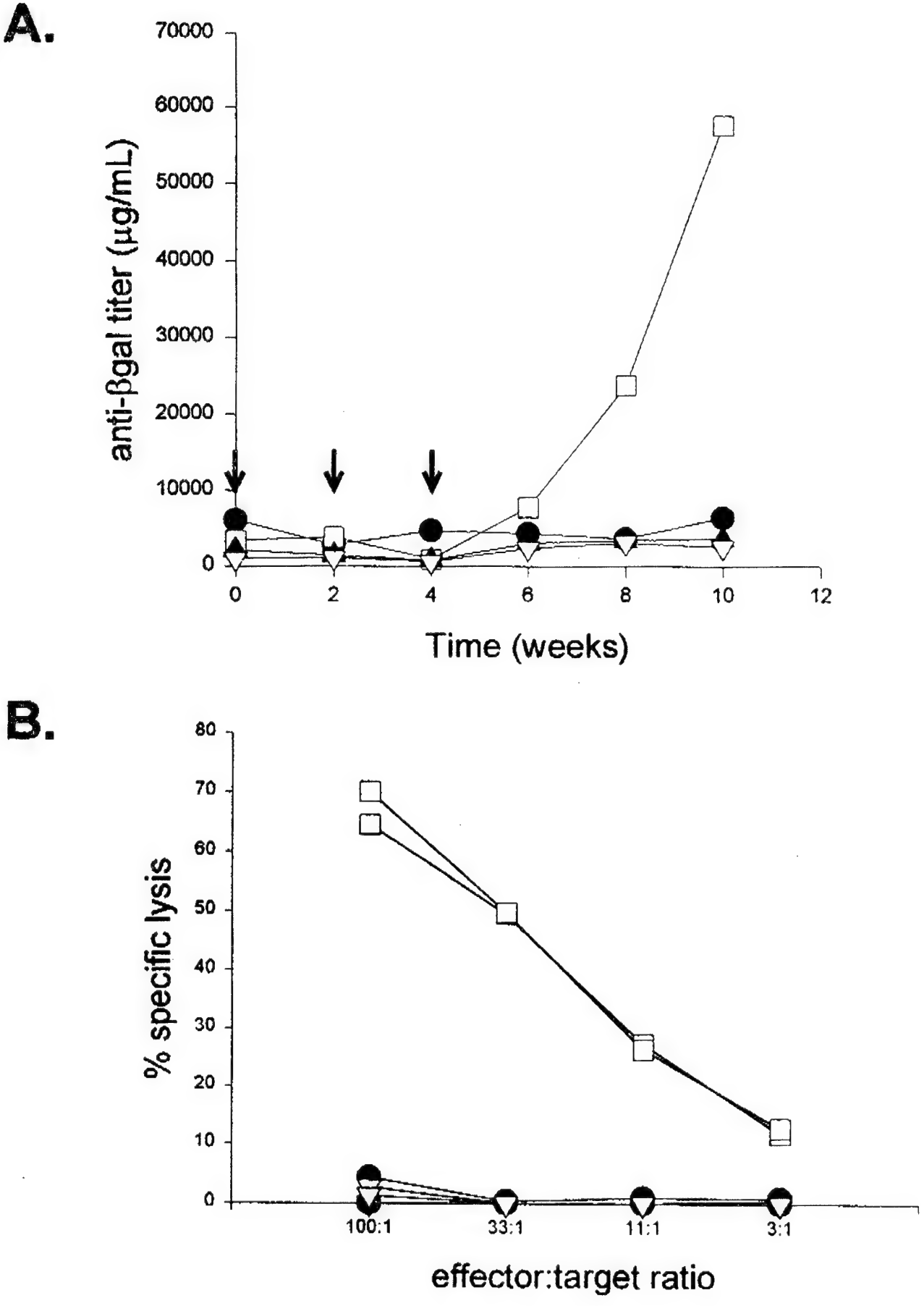
A.
70000
60000
50000
40000
30000
20000
10000
0
anti-βgal titer (μg/mL)
0
2
4
6
8
10
12
Time (weeks)
B.
80
70
60
50
40
30
20
10
0
% specific lysis
100:1
33:1
11:1
3:1
effector:target ratio

FIGURE 4

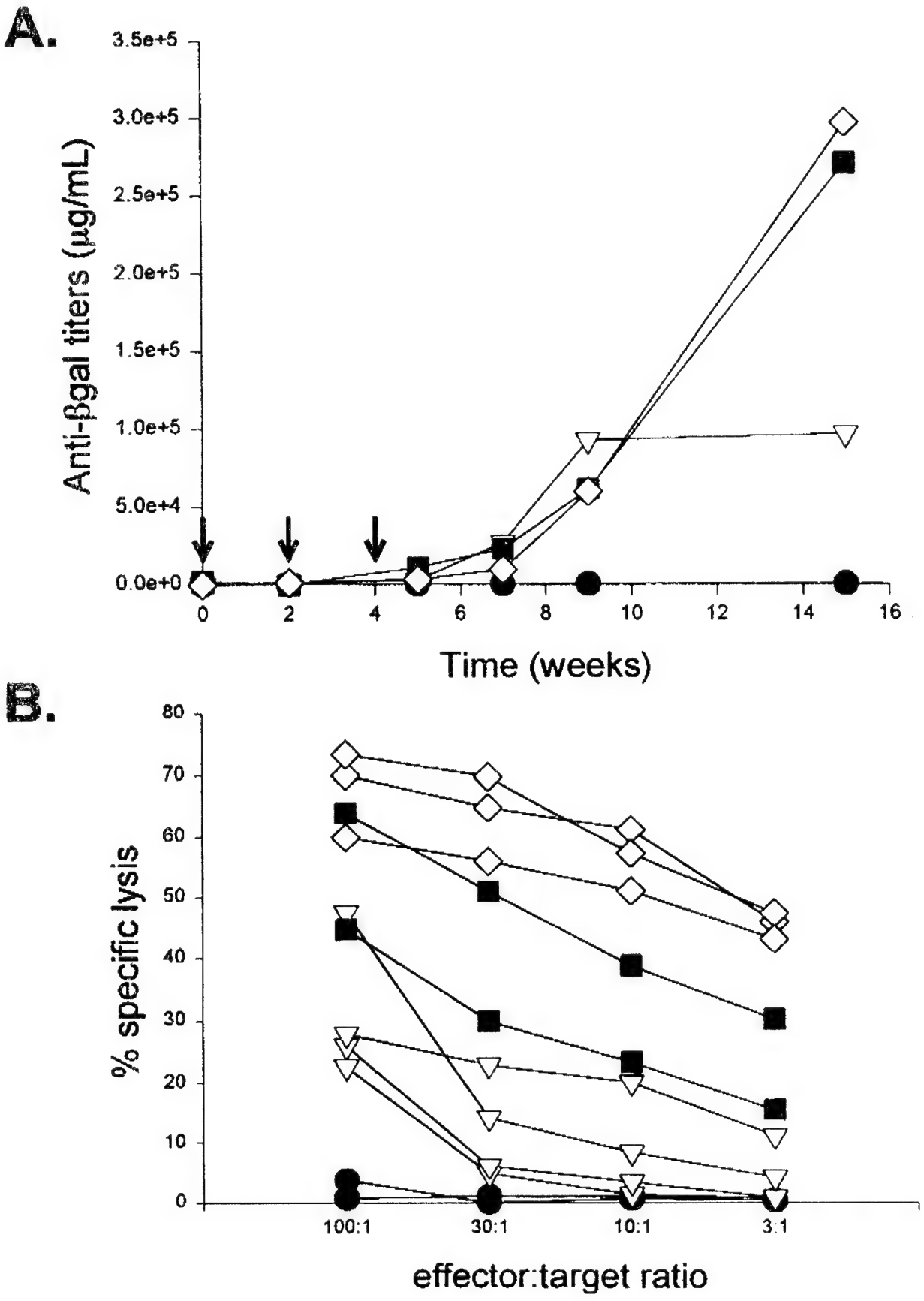
A.
3.5e+5
3.0e+5
2.5e+5
2.0e+5
1.5e+5
1.0e+5
5.0e+4
0.0e+0
Anti-βgal titers (µg/mL)
0
2
4
6
8
10
12
14
16
Time (weeks)
B.
80
70
60
50
40
30
20
10
0
% specific lysis
100:1
30:1
10:1
3:1
effector:target ratio

This activation was blunted to 12% of cells in CD40L$^{-/-}$ mice (Fig. 3C); activation of CD40 with antibody in the CD40L$^{-/-}$ mice increased B7.2 expression to 32% (Fig. 3D).

We studied the functional importance of B7-mediated costimulation of T cells to vector in wild-type C57BL/6 mice by injecting blocking antibodies to B7.1 and B7.2 at the time of vector administration. T cells from these animals failed to secrete $T_H1$- and $T_H2$-specific cytokines in response to antigen in vitro (Fig. 1A), and CTL activity to viral-infected targets was markedly diminished (Fig. 1B). This response was associated with the stabilization of transgene expression, with 82% of hepatocytes expressing *lacZ* at day 24 (Table 1). T cell–dependent B cell responses were also blunted, with diminished formation of germinal centers [20.4 ± 1.5 per section without anti-B7 and 2.5 ± 0.7 per section with anti-B7 (*11*)], less antiviral neutralizing antibody (Table 1), and a notable absence of class switching from IgM to IgG1 and IgG2a (Fig. 2). Another inhibitor of this pathway, CTLA4-Ig, has a similar effect on the cellular responses to vector in liver (*7*).

The well-characterized T and B cell responses to adenoviral vectors were useful in defining the biology of CD40L in T cell activation (*5*). Full immune competence was achieved in the absence of CD40L by activating CD40, thereby ruling out a direct effect of CD40L on the T cell. We show that CD40 signals an up-regulation of B7.2 on the APC that is necessary for T cell activation, presumably through its interaction with CD28. The interdependence of the CD40 and CD28 pathways in this system differs from the situation in models of allograft rejection where redundancies appear to exist (*4*). Our studies suggest that pharmacologic subversion of the CD40 pathway may be effective in abrogating problematic host responses to vectors, a concept that has been recently validated in murine models of liver and lung gene transfer (*8*).

## REFERENCES AND NOTES


1. R. Allen *et al.*, *Science* **259**, 990 (1993); A. Aruffo *et al.*, *Cell* **72**, 291 (1993); J. Disanto, J. Bonnefoy, J. Gauchel, A. Fischer, G. deSainte Basile, *Nature* **361**, 541 (1993); U. Korthauer *et al.*, *ibid.*, p. 539; B. Renshaw *et al.*, *J. Exp. Med.* **180**, 1889 (1994); J. Xu *et al.*, *Immunity* **1**, 423 (1994).
2. I. Grewal, J. Xu, R. Flavell, *Nature* **378**, 617 (1995); D. van Essen, H. Kikutani, D. Gray, *ibid.*, p. 620.
3. K. Campbell *et al.*, *Immunity* **4**, 283 (1996); M. Kamanaka *et al.*, *ibid.*, p. 275; L. Soong *et al.*, *ibid.*, p. 263.
4. C. P. Larsen *et al.*, *Nature* **381**, 434 (1996).
5. Y. Dai *et al.*, *Proc. Natl. Acad. Sci. U.S.A.* **92**, 1401 (1995); Y. Yang, H. C. J. Ertl, J. M. Wilson, *Immunity* **1**, 433 (1994); Q. Li, M. A. Kay, M. Finegold, L. D. Stratford-Perricaudet, S. L. C. Woo, *Hum. Gene Ther.* **4**, 403 (1993); M. A. Rosenfeld *et al.*, *Cell* **68**, 143 (1992); Y. Yang, Q. Li, H. Ertl, J. Wilson, *J. Virol.* **69**, 2004 (1995); Z. Zsengeller *et al.*, *Hum. Gene Ther.* **6**, 457 (1995).
6. Y. Yang, G. Trinchieri, J. M. Wilson, *Nature Med.* **1**, 890 (1995).
7. M. A. Kay *et al.*, *Nature Genet.* **11**, 191 (1995).
8. Y. Yang *et al.*, *J. Virol.* **70**, 6370 (1996).
9. CD40L-deficient (CD40L$^{-/-}$) mice and their control litter mates (CD40L$^{+/+}$) were obtained from Jackson Laboratory (Bar Harbor, ME). Mice (female, 7 to 8 week old) were immunized with the recombinant adenovirus H5.010CMV*lacZ* [2 × $10^9$ plaque-forming units (pfu)] through the tail vein and killed 3, 10, and 24 days later. This replication-defective vector is deleted of the early genes *E1a* and *E1b* and expresses *lacZ* from a cytomegalovirus (CMV) promoter. Liver tissues were harvested for morphological analysis, and spleens and blood samples were saved for immunological assays. Some CD40L$^{-/-}$ mice were also treated with a monoclonal antibody to CD40 (anti-CD40) (100 μg/day, Pharmingen, San Diego, CA) for 7 days after immunization, and C57BL/6 mice were treated with monoclonal antibodies to B7.1 and B7.2 (100 μg/day; Pharmingen, San Diego, CA) every 3 days after immunization for the duration of the experiment.
10. Splenocytes harvested from day 10 mice were cultured either for 2 days for analysis of T cell proliferation to antigen or for 5 days in preparation for CTL assays. The cells (6 × $10^6$ cells per well) were cultured in 1.6 ml of Dulbecco's minimum essential medium supplemented with 5% fetal bovine serum and 50 μM 2-mercaptoethanol in the presence of *lacZ* virus at a multiplicity of infection of one in 24-well Costar plates. After the 48-hour incubation with antigen, supernatants were analyzed for IL-2, IL-4, IL-10, and IFN-γ by cytokine-specific enzyme-linked immunosorbent assays (ELISAs). A standard 6-hour $^{51}$Cr release assay was performed subsequently with different ratios of effector to target cells (C57SV, H-$2^b$). These target cells were mock-infected or infected with *lacZ* virus for 18 hours and labeled with $^{51}$Cr. After incubation for 6 hours, 100-μl samples of supernatant were removed for counting in a gamma counter. The percentage of specific $^{51}$Cr release was calculated as follows: [(cpm of sample − cpm of spontaneous release)/(cpm of maximal release − cpm of spontaneous release)] × 100. Spontaneous release was determined by culturing target cells in medium, and maximal release was established by culturing target cells in a 1% solution of SDS. The percentage of specific lysis is expressed as a function of different effector-to-target ratios (6:1, 12:1, 25:1, and 50:1).
11. Spleens from C57BL/6, CD40L$^{-/-}$, and CD40L$^{-/-}$ mice treated with anti-CD40 and C57BL/6 mice treated with anti-B7.1 and anti-B7.2 were harvested 10 days after infusion of H5.010CMV*lacZ* virus, and the frozen sections were analyzed for germinal center formation. Frozen sections were fixed with methanol for 10 min at −20°C, air-dried, and rehydrated with phosphate-buffered saline (PBS). After blocking with 10% goat serum for 20 min, sections were incubated with peanut agglutinin conjugated to fluorescein isothiocyanate (FITC) (Sigma; 20 μg/ml) for 1 hour at room temperature. Sections were washed and mounted with Citiflour (Canterbury, UK). Four spleen sections from two mice (*2*) were stained for the presence of germinal centers (GCs) and analyzed. Data are represented as the number of GCs per section (mean ± SD).
12. Y. Wu, *Curr. Biol.* **5**, 1303 (1995).
13. J. Hasbold, C. Johnson-Leger, C. Atkins, E. Clark, G. Klaus, *Eur. J. Immunol.* **24**, 1835 (1994).
14. J. Allison and M. Krummel, *Science* **270**, 932 (1995).
15. Antiviral antibodies were evaluated with an ELISA assay in which microtiter plates were coated with 200 ng of viral antigen in 100 μl of PBS per well overnight at 4°C, washed three times in PBS, and blocked with 1% bovine serum albumin (BSA) in PBS for 1 hour at 37°C. Serum samples diluted 1:200 were added to antigen-coated plates and incubated for 4 hours at 37°C. Plates were washed three times with 0.05% Tween-20 in PBS and incubated with biotin-labeled goat antibody to mouse IgG1, IgG2a, or IgM (Pharmingen, San Diego, CA) at 1:1000 dilution overnight at 4°C. Plates were washed as above and anti–biotin phosphatase (Sigma) was added to each well at 1:30,000 dilution for 1 hour at 37°C. Wells were washed again as above and *p*-nitrophenyl phosphate substrate was added.


16. We thank the Vector Core and Clinical Pathology and Animal Service Units of the Institute for Human Gene Therapy for technical help. Supported by the National Institute of Diabetes and Digestive and Kidney Diseases of NIH, the Cystic Fibrosis Foundation, and Genovo, Inc., a company that J.M.W. founded and holds equity in.

13 May 1996; accepted 19 July 1996


# Requirement for CD40 Ligand in Costimulation Induction, T Cell Activation, and Experimental Allergic Encephalomyelitis


Iqbal S. Grewal, Harald G. Foellmer, Kate D. Grewal, Jianchao Xu, Fridrika Hardardottir, Jody L. Baron, Charles A. Janeway Jr., Richard A. Flavell*



The mechanism of CD40 ligand (CD40L)–mediated in vivo activation of CD4$^+$ T cells was examined by investigation of the development of experimental allergic encephalomyelitis (EAE) in CD40L-deficient mice that carried a transgenic T cell receptor specific for myelin basic protein. These mice failed to develop EAE after priming with antigen, and CD4$^+$ T cells remained quiescent and produced no interferon-γ (IFN-γ). T cells were primed to make IFN-γ and induce EAE by providing these mice with B7.1$^+$ antigen-presenting cells (APCs). Thus, CD40L is required to induce costimulatory activity on APCs for in vivo activation of CD4$^+$ T cells to produce IFN-γ and to evoke autoimmunity.


CD40 ligand is preferentially expressed on the surface of activated CD4$^+$ T cells and is critical for effective humoral immunity (*1*). The receptor for CD40L, CD40, is expressed on various APCs, such as B cells, dendritic cells, and macrophages, and in vitro experimental evidence has shown that CD40-CD40L interaction induces up-regulation of major histocompatibility complex class II, B7, and other molecules that po-


*To wh
Howard
ology, Y.
CT 0651

City Sch. of Medicine, Children's Mercy Hospital—B. Wicklund, A. Mehrhof. **MHCS investigators**: M. E. Eyster, Milton S. Hershey Medical Ctr., Hershey; M. Hilgartner, Cornell Medical Ctr.; A. Cohen, Children's Hospital of Philadelphia; B. Konkle, Thomas Jefferson Univ. Hospital; G. Bray, Children's Hospital National Medical Ctr., Washington, DC; L. Aledort, Mount Sinai Medical Ctr., New York City; C. Kessler, George Washington Univ. Medical Ctr.; C. Leissinger, Tulane Medical Sch.; G. White, Univ. of North Carolina; M. Lederman, Case Western Reserve Medical School, Cleveland; P. Blatt, Christiana Hospital; M. Manco-Johnson, Univ. of Colorado.

53. We are indebted to the children, adolescents, adults, and parents who have volunteered to participate in this study, and to the members of the Hemophilia Treatment Centers. We thank D. Lomb, S. Edelstein, M. Malasky, T. Kissner, D. Marti, B. Gerrard, A. Hutchinson, M. Weedon, X. Wu, P. Lloyd, E. Wendel, M. McNally, R. Boaze, L. Kenefic, M. Konsavich, C. Stewart, and S. Cevario for technical assistance, and B. Weir, M. Clegg, R. Adamson, and R. Gallo for helpful discussions. Computing resources were provided by the Frederick Biomedical Supercomputing Center. Supported by the Bureau of Maternal and Child Health and Resources Development (MCJ-060570), the National Institute of Child Health and Human Development (NO1-HD-4-3200), the Centers for Disease Control and Prevention, the National Institute of Mental Health, and the National Institute of Drug Abuse (DA04334). Additional support has been provided by grants from the National Center for Research Resources (General Clinical Research Centers) of NIH to the New York Hospital–Cornell Medical Center Clinical Research Center (MO1-RR06020), the Mount Sinai General Clinical Research Center, New York (MO1-RR00071), the University of Iowa Clinical Research Center (MO1-RR00059), and the University of Texas Health Science Center, Houston (MO1-RR02558). The content of this publication does not necessarily reflect the views or policies of the Department of Health and Human Services, nor does mention of trade names, commercial products, or organizations imply endorsement by the U.S. Government.

7 August 1996; accepted 3 September 1996

# CD40 Ligand-Dependent T Cell Activation: Requirement of B7-CD28 Signaling Through CD40

Yiping Yang and James M. Wilson*

The role of CD40 ligand (CD40L) in the primary activation of T cells is not clear. The cellular and humoral immune responses to adenoviral vectors in a murine model of liver-directed gene transfer were studied to define the mechanisms responsible for CD40L-dependent T cell priming. CD40L-deficient mice did not develop effective cytotoxic T cells to transduced hepatocytes, and T cell–dependent B cell responses were absent. Full reconstitution of cellular and humoral immunity was achieved in CD40L-deficient mice by administration of an activating antibody to CD40 that increased expression of B7.2 on spleen cells. Wild-type mice could be made nonresponsive to vector by administration of antibodies to B7. Thus, CD40L-dependent activation of T cells occurs through signaling of CD40 in the antigen-presenting cell to enhance requisite costimulatory pathways that include B7.

The role of CD40L in humoral immunity is illustrated by the multiple defects in B cell activation that characterize its genetic deficiency in mice and humans, including a failure to form germinal centers, activate memory B cells, and class switch (*1*). Experiments in knockout mice have implicated CD40L in the antigen-specific priming of T cells, although the precise mechanism by which this occurs is unclear (*2*). Enhanced susceptibility of CD40L-deficient ($CD40L^{-/-}$) mice to leishmania infection is consistent with an important role of this molecule in cellular immunity (*3*). The relation between CD40L and other T cell costimulatory pathways such as B7-CD28 is unclear; in models of allograft rejection, these signaling pathways appear uncoupled (*4*).

Y. Yang, Institute for Human Gene Therapy and Department of Molecular and Cellular Engineering, University of Pennsylvania Medical Center, Philadelphia, PA 19104, USA.

J. M. Wilson, Institute for Human Gene Therapy and Department of Molecular and Cellular Engineering, University of Pennsylvania Medical Center, and the Wistar Institute, Philadelphia, PA 19104, USA.

*To whom correspondence should be addressed at Institute for Human Gene Therapy, Wistar Institute, Room 204, 3601 Spruce Street, Philadelphia, PA 19104–4268, USA.

Adenoviral vectors are being tested as a possible approach to gene therapy, but the cytotoxic T lymphocyte (CTL) and B cell responses to the viral proteins and transgene products make this strategy less tenable (*5*). Activation of $CD4^+$ T cells to input viral capsid proteins, which requires stimulation through the CD40L-CD40 and B7-CD28 pathways, is necessary for both the $CD8^+$ T cell (that is, CTL) and B cell (that is, neutralizing antibody) effects (*6*– *8*). If one could minimize the immune response, the adenovirus becomes a viable option. We have used this well-studied immune response to further elucidate the mechanisms of CD40L-dependent activation of T cells (*9*).

Infusion of adenovirus missing the early (E1) genes and containing the *lacZ* gene into C57BL/6 mice led to transgene expression in 93% of hepatocytes in liver harvested 3 days later that diminished to undetectable levels by day 24 (Table 1). Analysis of $CD4^+$ lymphocytes in vitro demonstrated activation of T helper ($T_H$) cells to viral antigens of both the $T_H1$ [that is, secretion of interferon-γ (IFN-γ) and interleukin-2 (IL-2)] and $T_H2$ (that is, secretion of IL-4 and IL-10) subsets (Fig. 1A) (*10*). Chromium release assays showed the presence of CTLs to viral-infected targets in splenocytes harvested 10 days after gene transfer (Fig. 1B) (*10*). Infusion of vector stimulated the development of germinal centers [20.4 ± 1.5 per section (*11*)] and the formation of antiviral antibodies of immunoglobulin M (IgM), IgG1, and IgG2 isotypes (Fig. 2) that are neutralizing (Table 1).

Similar studies performed in mice genetically deficient in CD40L demonstrated the requirement of CD40L-CD40 interactions in the full spectrum of cellular and humoral immune responses to adenoviral vectors in mouse liver; transgene expression was stable for 24 days in $CD40L^{-/-}$ mice (82% of hepatocytes still express *lacZ*, Table 1), and activation of CTLs to viral-infected cells was markedly blunted (*8*) (Fig. 1B). $CD4^+$ T cells harvested 10 days after gene transfer failed to respond to viral antigens; however, the basal secretion of cytokines was increased as compared with that observed in C57BL/6 mice (Fig. 1A). $CD40L^{-/-}$ mice failed to develop germinal centers [that is, no germinal centers were detected in four sections from two mice (*11*)] or neutralizing antibodies (Table 1). Antiviral IgM was formed, but class switch to IgG1 or IgG2a was virtually absent (Fig. 2).

Several models have been suggested to explain the dependent role of CD40L on T cell priming. A critical question is whether CD40L directly transduces an activating signal to the T cell at the time of engagement with its receptor CD40, or whether the role of CD40L is indirect, effecting T cell activation through CD40-mediated signaling in the antigen-presenting cell (APC) that leads to enhanced costimulation of downstream pathways. Previous in vivo studies in the $CD40L^{-/-}$ mouse documented a primary defect in T cell priming to soluble antigens without clarification of the mechanisms (*2*), although in vitro studies have shown that wild-type but not CD40L-deficient T cells activate costimulatory activity in B cells (*12*). Activation of CD40L with soluble CD40 in the $CD40L^{-/-}$ mice partially reconstituted formation of germinal centers, although isotype switching was not observed (*2*); thus,

# APPENDIX 3

# Antiviral Cytotoxic T Lymphocytes in Vaginal Mucosa of Simian Immunodeficiency Virus-Infected Rhesus Macaques

# Antiviral Cytotoxic T Lymphocytes in Vaginal Mucosa of Simian Immunodeficiency Virus-Infected Rhesus Macaques[1]

Barbara L. Lohman,[2]* Christopher J. Miller,† and Michael B. McChesney[3]‡

**The mucosal immune system of the female reproductive tract is of central importance for protection against sexually transmitted diseases, including HIV; however, this arm of the immune system remains poorly understood. Antiviral CTL responses never have been documented in the genital tract and the role of CTL in this anatomic site is unknown. In this study, $CD8^+$ intraepithelial lymphocytes (IEL) in the vaginas of six simian immunodeficiency virus (SIV)-infected female rhesus macaques were identified by immunohistochemistry to be $CD2^+$ and TCR $\beta$-chain$^+$. In addition, the majority of $CD8^+$ IEL contained TIA-$1^+$ cytoplasmic granules that are associated with CTL activity. $CD8^+$ T cells were isolated from the vaginal epithelium and submucosa and amplified by limiting dilution in the presence of feeder cells. SIV $p55^{gag}$ and/or $gp160^{env}$-specific lysis was detected in cultures of vaginal epithelial but not submucosal $CD8^+$ T lymphocytes. Estimated SIV-specific precursor CTL frequencies were higher in the vaginal $CD8^+$ IEL population of chronically infected monkeys than in the same cells from acutely infected monkeys or a naive control monkey. These results provide the first demonstration that antiviral CTL are present in the vaginal epithelium, and suggest that a vaccine may be able to generate anti-HIV CTL in the genital mucosa.** ***The Journal of Immunology,*** **1995, 155: 5855–5860.**

In female rhesus macaques and women, the tissues of vagina and cervix contain a full complement of immune cells including APCs and effector lymphocytes (1–3). The female reproductive tract has the capacity to mount an Ab response to a variety of pathogens and Ags, including HIV and simian immunodeficiency virus (SIV)[4] (4–8). But the role of local antiviral CTL in this anatomic site is unknown. $CD8^+$ MHC class I-restricted CTL have been identified in the blood and organs of HIV-infected people and SIV-infected monkeys (9–11), but there have been no reports of HIV- or SIV-specific CTL in the genital tract. In fact, antiviral CTL responses have never been documented in the genital mucosa of any species. Because HIV and SIV can be transmitted sexually (12–14), any vaccine should attempt to limit the spread of HIV from the reproductive tract to the systemic lymphoid tissues. Thus, it is essential to characterize the local immune response to vaginal pathogens.

There are numerous $CD8^+$ T cells in the epithelium and superficial submucosa of the vagina and cervix in both rhesus macaques and humans (1–3). At other mucosal surfaces that have been examined, namely gut and respiratory mucosa, the $CD8^+$ intraepithelial lymphocyte (IEL) population, at least in mice, contains about 50% TCR $\alpha\beta^+$ T cells and 50% $\gamma\delta$ T cells (15). In this study, we show that the $CD8^+$ vaginal IEL in the rhesus monkey are $CD2^+$ and TCR $\beta$-chain$^+$, consistent with a primary population of $\alpha\beta^+$ T lymphocytes in this compartment. Furthermore, most of these cells contain TIA-$1^+$ cytoplasmic granules that have been associated with classical $CD8^+$ CTL activity (16, 17). We therefore sought to determine whether SIV-specific CTLs are present in the vaginal mucosa of SIV-infected rhesus macaques.

## Materials and Methods

### *Animals and SIV infection*

Colony-bred adult female rhesus macaques (*Macaca mulatta*), seronegative for simian type D retroviruses, simian T cell leukemia virus, and SIV, were housed in accordance with the American Association for Accreditation of Laboratory Animal Care. The investigators adhered to the guidelines of the Committee on Care and Use of Laboratory Animals, National Resources Council. Two acutely infected monkeys (2 wk) and four chronically infected monkeys (6 to 10 mo) had been inoculated intravaginally with SIVmac251, an uncloned biologic isolate propagated in PBMC. Two virus stocks were used that had been titrated by intravaginal inoculation of female rhesus macaques to establish a persistent infection (13). The virus used to prepare these stocks was provided by R. C. Desrosiers, New England Regional Primate Research Center (Southborough, MA). The presence of SIV in the PBMC of rhesus macaques was detected by coculture of 5 to 10 $\times$ $10^6$ PBMC with $10^6$ CEM $\times$ 174 cells, as previously described (18). Cultures were maintained for 8 wk before terminating as negative. Beginning at 2 wk postinfection, SIVp27 Ag was consistently detected in PBMC coculture supernatants from the four monkeys with chronic SIV infection. SIV was isolated from PBMC and peripheral lymph nodes of the monkeys killed at 2 wk postinfection. All the animals were clinically healthy at the time they were killed by i.v. injection of pentobarbital. One uninfected adult female macaque was killed as a mock control for the histologic and immunologic assays described below.

### *Histology and immunohistochemistry*

At necropsy, inguinal, axillary, and genital (iliac or obturator) lymph nodes, spleen, and vagina were obtained and divided three ways. One portion of each tissue sample was collected in sterile medium for lymphocyte

*California Regional Primate Research Center; †Department of Pathology, Microbiology and Immunology, School of Veterinary Medicine; and ‡Department of Pathology, School of Medicine; University of California-Davis, Davis, CA 95616

Received for publication June 26, 1995. Accepted for publication September 25, 1995.

The costs of publication of this article were defrayed in part by the payment of page charges. This article must therefore be hereby marked *advertisement* in accordance with 18 U.S.C. Section 1734 solely to indicate this fact.

[1] This work was supported by the Contraceptive Research and Development Program (CONRAD, DPE-3044-A-00–6063–00), National Institutes of Health Grants AI-35545 and RR-00169, and Pediatric AIDS Foundation Grant 50440–15-PG. M.B.M. is supported by a Scholar Award from the American Foundation for AIDS Research. The views expressed by the authors do not necessarily reflect the views of CONRAD.

[2] Present address: Department of Pathology, University of Massachusetts Medical Center, Worcester, MA 01655.

[3] Address correspondence and reprint requests to Dr. M. B. McChesney, California Regional Primate Research Center, University of California Davis, Davis, CA 95616–8542.

[4] Abbreviations used in this paper: SIV, simian immunodeficiency virus; CTLp, cytotoxic T lymphocyte precursor; IEL, intraepithelial lymphocyte.



0022-1767/95/$02.00

isolation, one portion was fixed in formalin for routine histologic examination, and the remaining portion was embedded in O.C.T. compound (Tissue-Tek, Wiles Inc., Elkhart, IN) snap-frozen in liquid nitrogen-cooled Freon, and stored at −70°C. Frozen sections of vagina were examined for specific cell populations using previously described immunohistochemical techniques (19). The following mouse anti-human mAbs were used: anti-CD2 mAb (T11; Coulter Immunology, Hialeah, FL), anti-CD8 mAb (T8; Dako Corp., Carpenteria CA), TIA-1 mAb (Coulter Immunology), and anti-TCR β-chain mAb (bF1; T Cell Diagnostics, Cambridge, MA). Briefly, cryostat sections of approximately 6 μm in thickness were mounted on silane-coated slides and fixed in methanol. Sections from all animals were examined with all mAbs using single-label indirect immunoflourescence. In the single-labeled sections, the binding of the mAb was detected with a FITC-conjugated horse anti-mouse IgG (Vector Labs., San Francisco, CA) polyclonal sera. Immunofluorescence triple staining of $CD2^+/CD8^+/TIA\text{-}1^+$ T cells in the vaginal epithelium (Fig. 2) utilized a TIA-1/Aminomethylcoumarin(AMCA)-conjugated horse anti-mouse (Vector Labs.) combination followed by a biotinylated-T8/streptavidin-Texas Red (Vector Labs.) combination and a FITC-conjugated anti-CD2 mAb. Immunofluorescence double staining of TCR $\beta$-chain$^+/CD8^+$ cells in the vaginal epithelium (Fig. 3) utilized the anti-β-chain Ab/FITC-conjugated horse anti-mouse IgG combination followed by the biotinylated-T8/streptavidin-Texas Red combination. Between each staining step, the slides were extensively washed in PBS. As a negative control, an irrelevant mouse mAb was substituted for the primary Ab. The stained slides were examined by epifluorescence microscopy using a Zeiss Axiophot microscope with appropriate filters (Carl Zeiss, Inc. Thornwood, NY). To view double-labeled slides, a combination FITC/Texas Red filter was used (Zeiss) and to photograph the triple-labeled slides, a double exposure of the slide using the FITC/Texas Red filter and the AMCA filter was made.

### *Isolation of lymphocytes from vaginal mucosa*

The vaginal epithelium was manually separated from the submucosa after incubation for 1 h in Dispase II, 1.2 U/ml (Boehringer Mannheim, Indianapolis, IN) at 37°C. The epithelium was disassociated into a cell suspension by incubation in 0.25% trypsin for 1 h followed by repeated pipetting. $CD8^+$ cells were positively selected from the cell suspension using two rounds of immunomagnetic bead isolation (M450 anti-CD8 Dynabeads; Dynal, Great Neck, NY). The anti-$CD8^+$ beads were removed from the cells using Detach-a-Bead (Dynal) according to the manufacturer's directions. The $CD8^+$ vaginal epithelial cells were washed once in PBS and resuspended in RPMI 1640 medium.

Lymphocytes were isolated from the vaginal submucosa following enzymatic digestion (20). The vaginal submucosa was diced into 1 $cm^3$ pieces and incubated overnight on an orbital shaker at 37°C in RPMI 1640 containing 10% FCS, 25 mM HEPES buffer (Life Technologies, Gaithersburg, MD), 100 U/ml penicillin, 100 μg/ml streptomycin (Life Technologies, Inc.), 2.5 μg/ml amphotericin B (Life Technologies, Inc.), $10^{-5}$ M β-mercaptoethanol (Kodak, Rochester, NY), 0.01% collagenase (Boehringer Mannheim), 0.01% deoxyribonuclease (Sigma Chemical Co., St. Louis, MO), and 0.01% soybean trypsin inhibitor (Sigma Chemical Co.). After digestion, the cells were isolated by low speed centrifugation and the cell pellet resuspended in 20 ml complete medium. The cell suspension was overlayed on a 25% isotonic Percol (Pharmacia Biotech, Inc. Pisataway, NJ) gradient and centrifuged at 2000 rpm for 20 min. The cell pellet was recovered and $CD8^+$ lymphocytes were positively selected as described above.

### *Detection of SIV-specific CTL*

The details of the bulk CTL assay have been previously reported (21). Briefly, lymphocytes were stimulated with Con A, 10 μg/ml, (Sigma Chemical Co.) and cultured for 14 days in RPMI 1640 medium supplemented with 10% FCS, antibiotics, and 5% human lymphocyte-conditioned medium (human IL-2; Schiaparelli Biosystems, Columbia, MD) and 20 U/ml recombinant human IL-2 (donated by Cetus Corp., Emeryville, CA). Autologous B lymphocytes were transformed by *Herpes papio* (594S × 1055 producer cell line, provided by M. Sharp, Southwest Foundation for Biomedical Research, San Antonio, TX) and infected overnight with wild-type vaccinia virus (vvWR) or recombinant vaccinia viruses expressing the SIV major core protein, $p55^{gag}$, (vvgag) or envelope glycoprotein, $gp160^{env}$ (vvenv) of SIVmac239 (provided by L. Giavedoni and T. Yilma, University of California, Davis, CA) and then labeled with 50 μCi of $^{51}$chromium ($Na_2CrO_4$; Amersham, Arlington Heights, IL) per $10^6$ cells. Effector and target cells were added together at multiple E/T ratios in a 4-h chromium-release assay, and percent specific lysis was calculated from supernatant chromium measured in a liquid scintillation counter (Microbeta 1450, Wallac Biosystems, Gaithersburg, MD). Specific lysis was considered positive if it was greater than twofold (three SDs) above the lysis of vvWR targets, and if it was at least 10%.

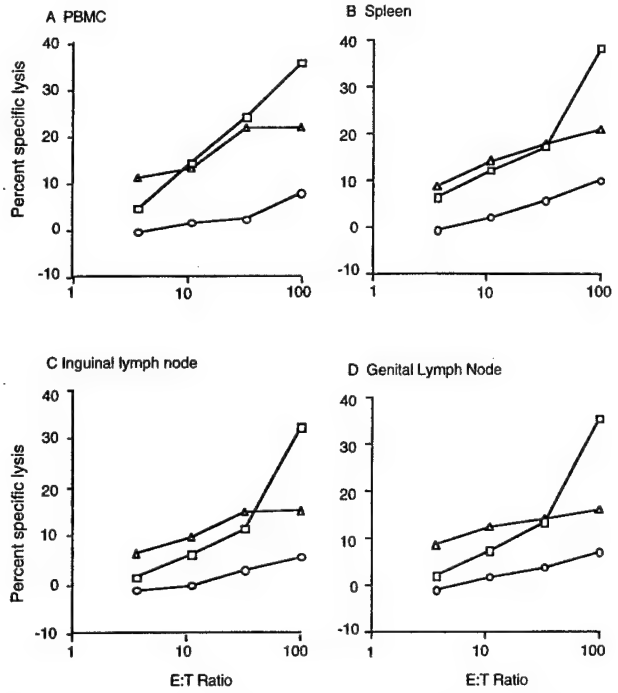


**FIGURE 1.** SIV-specific cytolytic activity in lymphoid tissues of chronically infected Monkey 23024. *A*, PBMC; *B*, spleen; *C*, inguinal lymph node; *D*, genital lymph node. Lymphocytes were stimulated for 14 days, and then cytotoxic activity was measured against autologous lymphoblastoid cells infected with wild-type vaccinia virus (open circles), recombinant vaccinia virus expressing SIVgag (squares) or recombinant vaccinia virus expressing SIVenv (triangles).

Lymphocytes isolated from the vaginal epithelium and submucosa were cultured in a limiting dilution format due to the low number of recovered cells. The relative frequencies of SIV *gag* and *env*-specific cytotoxic T lymphocyte precursor (CTLp) were determined using standard methods (22). Isolated $CD8^+$ lymphocytes were diluted threefold serially for three dilutions in complete medium with replicates of 28 to 30 wells per dilution in 96-well round-bottom plates (Fisher Scientific, Santa Clara, CA). The cells were stimulated with Con A (10 μg/ml, Sigma Chemical Co.) and supplemented with human irradiated PBMC as feeder cells at a concentration of $1 \times 10^5$/well and 5% human IL-2 (Schiaparelli). On day 7 of culture, 20 U/ml recombinant human IL-2 (provided by Cetus, Inc.) was added. Cytotoxicity was measured on day 14. Individual wells were split three ways and assayed for cytolytic function in a 5-h chromium-release assay against autologous target cells infected with vvWR, vvgag, or vvenv as described above. Positive wells had at least 15% specific lysis based on a bimodal distribution of chromium release (23) and greater than twofold specific lysis above the vvWR target. CTLp frequencies were calculated by $\chi^2$ goodness of fit analysis using the method of maximum likelihood (24).

## Results

### *CTL activity in peripheral lymphoid tissues of monkeys after intravaginal inoculation of SIVmac*

The four animals that were infected with SIV for 9 to 10 mo were seropositive for SIV Ags by whole-virus ELISA (data not shown) and were clinically healthy at the time they were killed. Before selection for use in this study, all the animals chronically infected with SIV had CTL activity in PBMC directed against the SIV major core protein, $p55^{gag}$, and envelope glycoprotein, $gp160^{env}$. The effector activity was associated with a $CD8^+$, MHC-restricted lymphocyte population (data not shown). At the time of necropsy, CTL activity against both SIV *gag* and *env* Ags was detected in PBMC and lymphocytes isolated from spleen, genital, and inguinal or axillary lymph nodes of three of four chronically infected monkeys. There was no difference in the strength of the CTL response

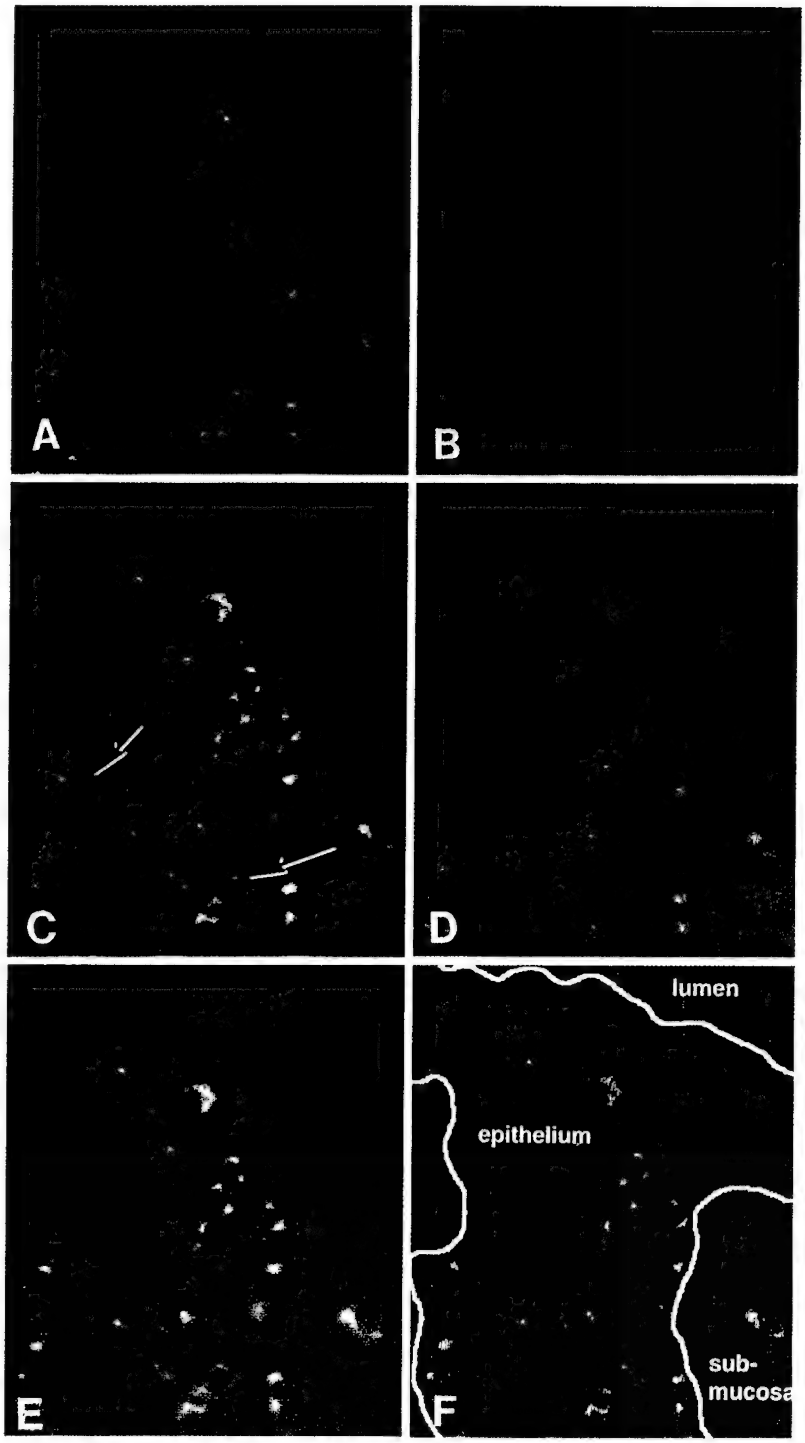


**FIGURE 2.** A single, representative frozen section of vaginal mucosa from a chronically SIV-infected monkey was stained with three mAbs. *A*, $CD2^+$ T cells (green) in vaginal epithelium. *B*, $CD8^+$ cells (red) in same tissue section. *C*, Immunofluorescence double staining of $CD2^+/CD8^+$ cells in same section of vaginal epithelium. Note that all $CD2^+$ T cells in vaginal epithelium are $CD8^+$. Double-labeled cells are yellow, some cells (arrows) have variably distinct areas of red (CD8 expression) and yellow (colocalization of CD2 and CD8) staining or green (CD2 expression) and yellow (colocalization of CD2 and CD8) staining. *D*, TIA-$1^+$ cytoplasmic granules (blue) in $CD8^+$ T cells in same section of vaginal epithelium. *E*, Immunofluorescence triple staining of $CD2^+/CD8^+$/TIA-$1^+$ T cells in vaginal epithelium. This figure demonstrates that all $CD2^+$,$CD8^+$ T cells in vaginal epithelium are TIA-$1^+$. *F*, A computer-labeled image to clarify anatomic components in *A–E*. Original magnification: ×630.

detected in the genital lymph nodes, inguinal nodes, blood, or spleen (Fig. 1). The fourth animal had low level *env*-specific lysis in all the tissues. CTL activity against SIV *gag* was not detected in this animal (data not shown). Of the two acutely infected monkeys, one had low level *env*-specific CTL activity but no detectable *gag*-specific CTL activity in the genital lymph nodes, PBMC, and systemic lymphoid tissues. The other acutely infected monkey had both *gag*- and *env*-specific CTL activity in the PBMC and spleen and low level env-specific activity in lymph nodes. Thus, in most of the acutely and chronically infected monkeys, CTL activity could be detected in the genital lymph nodes and systemic lymphoid tissues. The uninfected monkey had very low *env*-specific CTL activity and no detectable *gag*-specific activity in peripheral blood (data not shown).

### *$CD8^+$ lymphocytes in vaginal epithelium express αβ TCR and have cytotoxic granules*

As reported previously for normal multiparous female rhesus macaques and women (1–3), immunohistochemical staining demonstrated significant numbers of $CD2^+$,$CD8^+$ T cells in the vaginal epithelium and superficial submucosa of all animals, including the control monkey (Fig. 2, *A–C*). The single-labeled sections demonstrated cells positively labeled for CD8, CD2, and TIA-1 Ags in

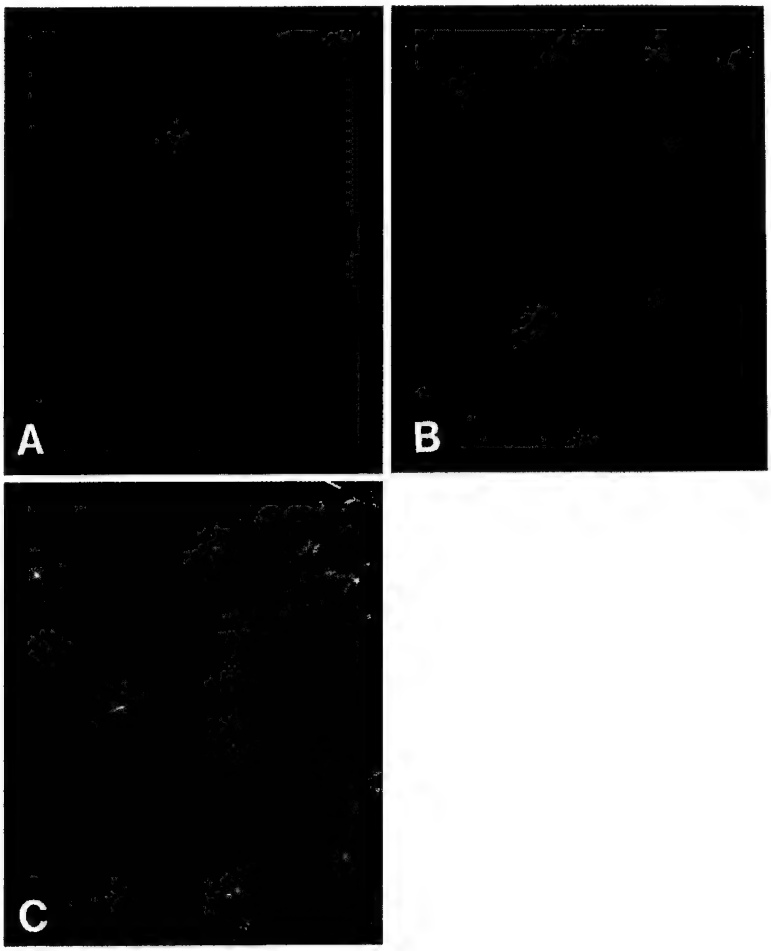


**FIGURE 3.** A frozen section of vagina (serial section of slide in Fig. 2). *A–C,* Photographs of a single representative cryostat section stained with two mAbs. *A,* Cells expressing TCR β-chain (green) in vaginal mucosa. *B,* $CD8^+$ cells (red) in same section of vaginal mucosa. *C,* Coexpression of CD8 and TCR β-chain in vaginal epithelial T cells. Double-labeled cells are yellow. This figure demonstrates expression of TCR β-chain by all $CD8^+$ T cells in vaginal epithelium. Original magnification: ×630.

all sections of vaginal mucosa examined, and these markers seemed to localize to the same population of cells. The majority of $CD8^+$ IEL contained cytoplasmic TIA-$1^+$ granules (Fig. 2*D*). The triple-labeled sections confirmed that the CD8, CD2, and TIA-1 Ags were coexpressed by a single population of cells (Fig. 2*E*). The expression of TIA-1 by $CD8^+$ lymphocytes is associated with cytotoxic activity (16, 17, 25). Compared with the control animal and previously published reports (3), the number of $CD8^+$ T cells in the vaginal mucosa of both the acutely and chronically infected monkeys was increased slightly. In addition, in the SIV-infected animals, the $CD8^+$ cells extended into the superficial layers of the stratified squamous vaginal epithelium. These changes were present despite the fact that no significant histopathologic changes in the epithelium were recognized. All of the $CD8^+$ T cells in the vaginal epithelium of SIV-infected animals and the control animal expressed the β-chain of the TCR as determined by immunohistochemistry (Fig. 3, *A–C*). Thus, these $CD8^+$,TIA-$1^+$ vaginal IEL belong to the subset of T cells expressing the αβ-TCR. We were unable to identify mAbs capable of detecting γδ $TCR^+$ T cells in cryostat sections of rhesus macaques, and we cannot state categorically that γδ T cells do not exist in the vaginal mucosa. However, we were able to demonstrate that all $CD8^+$ cells in the vaginal mucosa express the TCR β-chain (Fig. 2). Thus, by exclusion, it is unlikely that $CD8^+$ γδ T cells are present in the vaginal mucosa of rhesus macaques. As previously reported (3), $CD4^+$ T cells were seen only rarely in the vaginal epithelium, although significant numbers were seen in the submucosa.

*Vaginal IEL of SIV-infected monkeys contain antiviral CTL*

In this study, all rhesus macaques intravaginally inoculated with SIV had detectable SIV-specific CTLp in the vaginal epithelium (Table I). In contrast, SIV-specific lysis could not be detected in the $CD8^+$ lymphocytes isolated from the vaginal submucosa of these four animals. The estimated frequencies of CTLp in the vaginal IEL population varied among the animals, but there tended to be higher CTLp frequencies in the chronically infected monkeys compared with the monkeys infected for 2 wk, as shown in Figure 4. SIV *gag*-specific CTL activity was detected in the $CD8^+$ vaginal IEL of all four animals chronically infected with SIV. In the vaginal epithelium of Monkey 24877, CTLp were relatively common with an estimated frequency of 1 in 2425 $CD8^+$ lymphocytes. This was the only chronically infected animal that had detectable env-specific CTL activity in the vaginal epithelium, with a CTLp frequency of 1 in 8566 $CD8^+$ lymphocytes. Monkey 23024 had the lowest level of *gag*-specific CTLp in the vaginal epithelium: 1 in 11,097 $CD8^+$ lymphocytes.

CTLp frequencies were also estimated in the vaginal $CD8^+$ IELs isolated from the monkeys infected with SIV for 2 wk. Monkey 24803 had a *gag*-specific CTLp frequency of 1 in 26,686 $CD8^+$ lymphocytes and an env-specific frequency of 1 in 19,654 $CD8^+$ lymphocytes. The second monkey, 25597, had no detectable precursor frequency for *gag* and 1 in 18,664 $CD8^+$ lymphocytes were positive for env-specific lysis. Under identical limiting dilution conditions, we could not establish an estimate for anti-SIV

Table I. *SIV-specific cytotoxic T cells in the vaginal epithelium of rhesus macaques*

| Monkey # | Duration of Infection | Reciprocal of SIV *gag* and *env* CTLp Frequencies | |
|---|---|---|---|
| | | vv-*gag* targets | vv-*env* targets |
| 20035 | Chronic | 4,306 (2,589–12,777)[a] | >60,000 |
| 22429 | Chronic | 5,114 (3,697–8,288) | >182,000 |
| 23024 | Chronic | 11,097 (6,180–54,279) | >64,400 |
| 24877 | Chronic | 2,425 (1,685–4,321) | 8,566 (5,286-22,560) |
| 24803 | Acute | 26,686 (13,307–4,999,507) | 19,654 (9,951-790,556) |
| 25597 | Acute | >294,000 | 18,664 (13,027-32,901) |
| 16947 | Naive | >70,000 | >70,000 |

[a] 95% confidence intervals.

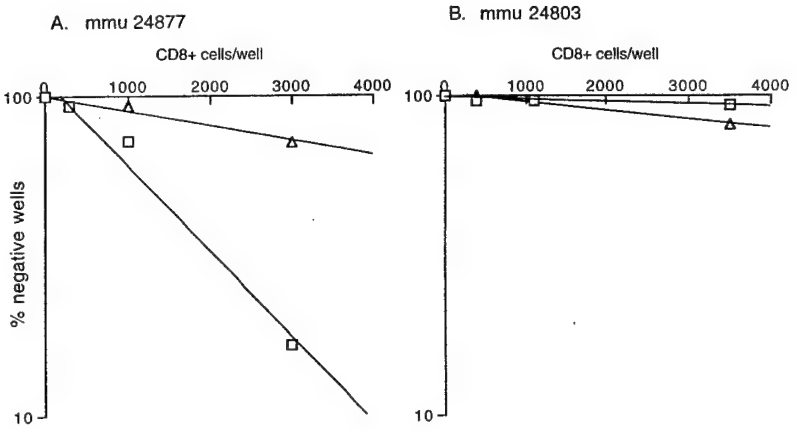


**FIGURE 4.** Comparison of SIV-specific pCTL frequencies in vaginal epithelium from a chronically SIV-infected rhesus macaque (*A*), and an acutely SIV-infected rhesus macaque (*B*). Vaginal epithelial $CD8^+$ lymphocytes were stimulated in culture for 14 days and then analyzed for cytotoxic activity against autologous lymphoblastoid cells infected with vvWR, vvgag (squares), and vvenv (triangles). Percentage of negative wells is plotted against number of $CD8^+$ T cells per well, and frequency is extrapolated from *x* intercept of regression line with 37%.

CTLp frequencies in axillary lymph node lymphocyte or vaginal $CD8^+$ IELs from the naive monkey (Table I).

Flow cytometric analysis of the cell populations derived from the epithelial lymphocyte cultures demonstrated that 98% of the cells were $CD8^+$ (data not shown). In some experiments, after the limiting dilution wells were harvested for cytotoxicity assays, selected positive wells were restimulated at 100 cells/well with fresh feeder cells and mitogen. When retested after 14 days, most wells that were initially positive or negative for SIV-specific lysis remained so. Individual wells were subsequently expanded, but we were unable to maintain lytic activity after several months of growth.

## Discussion

These results demonstrate that SIV-specific CTL activity is present in the $CD8^+$ T cell population in the vaginal epithelium of SIV-infected animals. Monkeys with a chronic infection had a higher CTLp frequency than the monkeys infected for 2 wk. The frequency estimates of SIV *gag*-specific CTL in the vaginal lymphocytes were consistent with the previously reported range of CTLp present in PBMC of SIV-infected rhesus macaques, a range of 1 in 7,180 to 1 in 12,490 PBMC (26). In previous reports, we (21) and others (27) have shown that the effector cells from SIV-infected monkeys, generated by secondary in vitro stimulation with Con A, are $CD8^-$ and MHC restricted. The present immunohistochemical results confirm that $CD8^+$ vaginal IEL are also $CD2^+$ and TCR $\beta$-$chain^-$. Although we were unable to directly label TCR $\gamma\delta$ cells, we were able to indirectly demonstrate that such cells are not present or are very rare in the vaginal mucosa of rhesus macaques. Thus, it is unlikely that the $CD8^+$ vaginal IEL mediating SIV-specific target cell lysis are $\gamma\delta$ T cells. But we cannot completely exclude the possibility that the isolated $CD8^+$ vaginal IEL populations contained a few $\gamma\delta$ T cells.

CTL have been shown to be the major means by which an immune response eliminates many systemic viral infections (28–32). The generation of antiviral CTL activity in vaginal IEL appears to be part of the normal immune response to intravaginal inoculation of SIV. SIV-infected cells have been detected in the vaginal epithelium of chronically infected rhesus macaques (19), and the CTL in the vaginal epithelium may be recognizing these cells. In fact, $CD8^+$ CTL have been found in the skin rash that occurs in SIV-infected macaques (11), and the $CD8^-$ T cells in the lesion were in contact with degenerating $CD4^+$ Langerhans cells (33), suggesting that the CTL may have been responding to viral Ag in these cells. It is also possible that these SIV-specific $CD8^+$ CTL are homing to the vaginal epithelium as part of a normal pattern of lymphocyte recirculation unrelated to the presence of virus-infected cells. The immune cell population in the ectocervical and vaginal epithelia are immunophenotypically similar (3), and it is likely that similar CTL activity is present in the $CD8^+$ T cells in the ectocervical squamous epithelium.

The route of infection may be important for the generation of mucosal CTL. All the monkeys used in this study were infected by vaginal inoculation of SIV. It will be informative to determine whether i.v. inoculated animals have similar anti-SIV CTL activity in the genital immune system. Virus-specific CTLs can be induced in the gut-associated lymphoid tissues as well as in other mucosa-associated tissues by mucosal viral infections or mucosal contact with viral Ags (34–36). Following intravaginal immunization with live-attenuated HSV type 2, mice are protected against genital transmission of virulent HSV type 2 (37). Protection is transferred to naive, syngeneic mice by adoptive transfer of genital lymph node lymphocytes, and these HSV-stimulated lymphocytes migrate preferentially to the genital tract of challenged mice (38). This result suggests that virus-specific CTL generated in the genital lymph nodes participate in

effective genital immune responses against a sexually transmitted viral pathogen.

The induction of an effective CTL response to a virus is usually advantageous to the host. Mucosal immune responses, secreted Ab, and CTL, capable of preventing or eliminating virus infection, comprise the first line of immune defense to prevent viral dissemination and subsequent systemic infection. The success of a vaccine capable of preventing the heterosexual transmission of HIV may rely on the ability of the vaccine to generate specific immune responses in genital tissues and draining lymph nodes. The results reported in this study provide the first direct demonstration that antiviral CTL are present in the vaginal epithelium, and suggest that an appropriate immunization regimen may be able to generate anti-HIV CTL in the mucosal immune system of the genital tract.

## Acknowledgments

This work was made possible by the excellent technical support of Jennifer Collins, Steven Joye, Ellen McGowan, Carol Oxford, and Judy Torten. We thank Dr. J. R. McGhee for critical review of the manuscript.

## References

1. Edwards, J. N. T., and H. B. Morris. 1985. Langerhans cells and lymphocyte subsets in the female genital tract. *Br. J. Obstet. Gynecol. 92:974.*
2. Roncalli, M., M. Sideri, P. Gie, and E. Servida. 1988. Immunophenotypic analysis of the transformation zone of human cervix. *Lab. Invest. 58:141.*
3. Miller, C. J., M. McChesney, and P. F. Moore. 1992. Langerhans cells, macrophages and lymphocyte subsets in the cervix and vagina of rhesus macaques. *Lab. Invest. 67:628.*
4. Ogra, P., and S. Ogra. 1973. Local antibody response to polio vaccine in the human female genital tract. *J. Immunol. 110:1307.*
5. Merriman, H., S. Woods, C. Winter, A. Fahnlander, and L. Corey. 1984. Secretory IgA antibody in cervicovaginal secretions from women with genital infection due to herpes simplex virus. *J. Infect. Dis. 149:505.*
6. Belec, L., A. Georges, G. Steenman, and P. Martin. 1989. Antibodies to human immunodeficiency virus in vaginal secretions of heterosexual women. *J. Infect. Dis. 160:385.*
7. Miller, C., D. Kang, M. Marthas, Z. Moldoveanu, H. Kiyono, P. Marx, J. Eldridge, J. Mestecky, and J. McGhee. 1992. Genital secretory immune response to chronic SIV infection: a comparison between intravenously and genitally inoculated rhesus macaques. *Clin. Exp. Immunol. 88:520.*
8. Lu, X. S., L. Belec, and J. Pillot. 1993. Anti-gp 160 IgG and IgA antibodies associated with a large increase in total IgG in cervicovaginal secretions from human immunodeficiency virus type 1-infected women. *J. Infect. Dis. 167:1189.*
9. Autran, B., F. Plata, and P. Debre. 1991. MHC-restricted cytotoxicity against HIV. *J. Acquired Immune Defic. Syndr. 4:361.*
10. Reimann, K. A., K. Tenner-Racz, P. Racz, D. C. Montefiori, Y. Yasutomi, W. Lin, B. J. Ransil, and N. L. Letvin. 1994. Immunopathogenic events in acute infection of rhesus monkeys with simian immunodeficiency virus of macaques. *J. Virol. 68:2362.*
11. Yamamoto, H., D. J. Ringler, M. D. Miller, Y. Yasutomi, T. Hasunuma, and N. L. Letvin. 1992. Simian immunodeficiency virus-specific cytotoxic T lymphocytes are present in the AIDS-associated skin rash in rhesus monkeys. *J. Immunol. 149:728.*
12. Miller, C. J., N. J. Alexander, S. Sutjipto, A. A. Lackner, A. G. Hendrickx, A. Gettie, L. J. Lowenstine, M. Jennings, and P. A. Marx. 1989. Genital mucosal transmission of simian immunodeficiency virus: animal model for heterosexual transmission of human immunodeficiency virus. *J. Virol. 63:4277.*-4284
13. Miller, C. J., M. Marthas, J. Torten, N. J. Alexander, J. P. Moore, G. F. Doncel, and A. G. Hendrickx. 1994. Intravaginal inoculation of rhesus macaques with cell-free simian immunodeficiency virus results in persistent or transient viremia. *J. Virol. 68:6391.*- 6400
14. Miller, C. J., J. R. McGhee, and M. B. Gardner. 1993. Mucosal immunity, HIV transmission and AIDS. *Lab. Invest. 68:129.*-145
15. Lefrancois, L., and L. Puddington. 1995. Extrathymic intestinal T cell development: virtual reality? *Immunol. Today 16:16.*
16. Tian, Q., M. Streuli, H. Saito, S. F. Schlossman, and P. J. Anderson. 1991. A polyadenylate binding protein localized to the granules of cytolytic lymphocytes induces DNA fragmentation in cells. *Cell 67:629.*
17. Tenner-Racz, K., P. Racz, C. Thome, C. G. Meyer, P. J. Anderson, S. F. Schlossman, and N. L. Letvin. 1993. Cytotoxic effector granules recognized by the monoclonal antibody TIA-1 are present in the $CD8^+$ lymphocytes in lymph nodes of human immunodeficiency virus-1-infected patients. *Am. J. Pathol. 142:1750.*
18. Lohman, B., J. Higgins, M. Marthas, P. Marx, and N. Pedersen. 1991. Development of simian immunodeficiency virus isolation, titration, and neutralization assays which use whole blood from rhesus monkeys and an antigen capture enzyme-linked immunosorbent assay. *J. Clin. Microbiol. 29:2187.*
19. Miller, C. J., P. Vogel, N. J. Alexander, S. Sutjipto, A. G. Hendrickx, and P. A. Marx. 1992. Localization of SIV in the genital tract of chronically infected female rhesus macaques. *Am. J. Pathol. 141:655.*
20. James, S., and A. Graeff. 1985. Spontaneous and lymphokine-induced cytotoxic activity of monkey intestinal mucosal lymphocytes. *Cell. Immunol. 93:387.*
21. Lohman, B. L., M. B. McChesney, C. J. Miller, E. McGowan, S. M. Joye, K. K. A. Van Rompay, E. Reay, L. Antipa, N. C. Pedersen, and M. L. Marthas. 1994. A partially attenuated simian immunodeficiency virus induces host immunity that correlates with resistance to pathogenic virus challenge. *J. Virol. 68:7021.*
22. Lefkovits, I., and H. Waldman. 1979. *Limiting Dilution Analysis of Cells in the Immune System.* Cambridge University Press, Cambridge, UK.
23. Carmichael, A., X. Jin, P. Sissons, and L. Borysiewicz. 1993. Quantitative analysis of human immunodeficiency virus type 1 (HIV-1)-specific cytotoxic T lymphocyte (CTL) response at different stages of HIV-1 infection: differential CTL response to HIV-1 and Epstein Barr virus in late disease. *J. Exp. Med. 177:249.*
24. Taswell, C. 1981. Limiting dilution assays for the determination of immunocompetent cell frequencies. I. Data analysis. *J. Immunol. 126:1614.*
25. Anderson, P. J., C. Nagler-Anderson, C. O'Brien, H. Levine, S. Watkons, H. S. Slayter, M. L. Blue, and S. F. Schlossman. 1990. A monoclonal antibody reactive with a 15 kDa cytoplasmic granule associated protein defines a subpopulation of $CD8^+$ lymphocytes. *J. Immunol. 144:574.*
26. Venet, A., I. Bourgault, A.-M. Aubertin, M.-P. Kieny, and J.-P. Levy. 1992. Cytotoxic T lymphocyte response against multiple simian immunodeficiency virus (SIV) proteins in SIV-infected macaques. *J. Immunol. 148:2899.*
27. Miller, M. D., C. I. Lord, V. Stallard, G. P. Mazzara, and N. L. Letvin. 1990. The *gag*-specific cytotoxic T lymphocytes in rhesus monkeys infected with the simian immunodeficiency virus of macaques. *J. Immunol. 144:122.*
28. Yap, K. L., G. L. Ada, and I. F. C. McKenzie. 1978. Transfer of specific cytotoxic T lymphocytes protects mice inoculated with influenza virus. *Nature 273:238.*
29. Quinnan, G. V. J., N. Kirmani, A. H. Rook, J. F. Manischewitz, L. Jackson, G. Moreschi, G. W. Santos, R. Saral, and W. Burns. 1982. Cytotoxic T cells in cytomegalovirus infection: HLA-restricted T-lymphocyte and non-T-lymphocyte cytotoxic responses correlate with recovery from cytomegalovirus infection in bone marrow transplant recipients. *N. Engl. J. Med. 307:7.*
30. Byrne, J. A., and M. B. A. Oldstone. 1984. Biology of cloned cytotoxic T lymphocytes specific for lymphocytic choriomeningitis virus: clearance of virus in vivo. *J. Virol. 51:682.*
31. Lukacher, A. E., V. L. Braciale, and T. J. Braciale. 1984. In vivo effector function of influenza virus-specific cytotoxic T lymphocyte clones is highly specific. *J. Exp. Med. 160:814.*
32. Cannon, M. J., P. J. M. Openshaw, and B. A. Askonas. 1988. Cytotoxic T cells clear virus but augment lung pathology in mice infected with respiratory syncitial virus. *J. Exp. Med. 168:1163.*
33. Ringler, D. J., W. W. Hancock, N. W. King, N. L. Letvin, M. D. Daniel, R. C. Desrosiers, and G. F. Murphy. 1987. Immunophenotypic characterization of the cutaneous exanthem of SIV-infected rhesus monkeys: apposition of degenerative Langerhans cells and cytotoxic lymphocytes during the development of acquired immunodeficiency syndrome. *Am. J. Pathol. 126:199.*
34. Issekutz, T. B. 1984. The response of gut-associated T lymphocytes to intestinal viral immunization. *J. Immunol. 133:2955.*
35. London, S. D., D. H. Rubin, and J. J. Cebra. 1987. Gut mucosal immunization with reovirus serotype 1/L stimulates virus-specific cytotoxic T cell precursors as well as IgA memory cells in Peyer's patches. *J. Exp. Med. 165:830.*
36. Offit, P. A., and K. I. Dudzik. 1989. Rotavirus-specific cytotoxic T lymphocytes appear at the intestinal mucosal surface after rotavirus infection. *J. Virol. 63:3507.*
37. McDermott, M. R., J. R. Smiley, P. Leslie, J. Brais, H. E. Rudzroga, and J. Bienenstock. 1984. Immunity in the female genital tract after intravaginal vaccination of mice with an attenuated strain of herpes simplex virus type 2. *J. Virol. 51:747.*
38. McDermott, M. R., C. H. Goldsmith, K. L. Rosenthal, and L. J. Brais. 1989. T lymphocytes in genital lymph nodes protect mice from intravaginal infection with herpes simplex virus type 2. *J. Infect. Dis. 159:460.*

# APPENDIX 4

## Chimeric SHIV with HIV-1 Subtype-E Envelope Gene is Restricted at an Early Step for Replication in Macaque Lymphocytes

# Chimeric SHIV with HIV-1 Subtype-E Envelope Gene is Restricted at an Early Step for Replication in Macaque Lymphocytes

**Sunee Himathongkham[1], Julie Klinger[2], Susan Barnett[2], and Paul A. Luciw[1*]**

1 Department of Medical Pathology
University of California
Davis, CA 95616

2 Chiron Corporation
Emeryville, CA 94608

* Corresponding author
tel: 916-752-3430
fax: 916-752-4548
Email: PALuciw@UCDavis.edu

## ABSTRACT

Studies on HIV-1 have been conducted largely on subtype-B viral strains prevalent in North America and Europe. The envelope glycoprotein (*env* gp) of subtype-B isolates is known to be an important determinant of several viral properties (e.g., cell tropism, cytopathicity) and the target of anti-viral immune responses. Accordingly, studies are needed to examine such biological and immunological properties of other viral subtypes. We have focused on subtype-E strains of HIV-1 that are prevalent in Thailand. With the aim of analyzing HIV-1 genes in a non-human primate model for lentivirus infection and AIDS, we have constructed SIV/HIV-1 recombinants in which the *env* gene of the pathogenic clone $SIV_{mac239}$ is replaced with the counterpart region of HIV-1 clones. For the present study, such a SHIV clone has been constructed to contain the *env* gp160 of $HIV\text{-}1_{9466}$ which is a subtype-E isolate from an AIDS patient in Thailand. This clone, designated $SHIV_{9466E}$, does not produce infectious virus after transfection of human lymphoid cells. Subsequently, we constructed a second SHIV by recombining the $HIV\text{-}1_{9466}$ subtype-E *env* gene with the $HIV\text{-}1_{SF33}$ subtype B *env* gene and then inserting the recombinant *env* gene into the $SIV_{mac239}$ clone. This latter SHIV, designated $SHIV_{9466E/B}$, contains the gp120 surface domain and the ectodomain of the gp41 transmembrane subunit from $HIV\text{-}1_{9466}$; the intracellular portion of the gp41 subunit is derived from $HIV\text{-}1_{SF33}$. $SHIV_{9466E/B}$ replicated efficiently in human lymphoid cells (including primary lymphocytes); however, this chimeric virus was restricted for replication in rhesus macaque lymphocytes. PCR analysis revealed that this restriction was at a step before viral DNA synthesis, presumably during the process of virion entry into cells. In contrast, several SHIVs containing the subtype-B *env* gp160 gene replicated efficiently in

macaque lymphocytes. Current efforts are aimed at constructing additional SHIV subtype-E clones for analysis in macaque cells with the aim of defining the precise step(s) that blocks SHIV$_{9466E/B}$ replication and SHIV$_{9466E}$ infectivity. Additionally, such studies on recombinant SHIV may have significance for analyzing patterns of recombination between/among different HIV-1 subtypes in humans.

## INTRODUCTION

Genetic variability is the hallmark of human immunodeficiency virus (HIV-1). Diverse HIV-1 genotypes have been identified in the worldwide epidemic, and these viruses have been classified into subtypes A through I (major group, M) as well as the highly divergent group O (outlier) by comparison of amino acid sequences in *env* or *gag* regions (Myers, 1995). The *env* glycoprotein of HIV-1 governs several viral properties (i. e. cell tropism, cytopathology) and is the major target for anti-viral immune responses. Thus, the high degree of sequence variability of HIV-1 *env* presents a significant challenge for vaccine development.

HIV-1 subtype-E, identified as a unique subtype by genetic sequences in *env*, was first discovered in Thailand (Ou et al., 1992; McCutchan et al., 1992). In the last 8 years, HIV-1 infection has spread extensively throughout the country, predominately in the heterosexual population (Nelson et al., 1993; Sittitrai and Brown, 1994; Brown and Sittitrai, 1994; Wasi et al., 1995; Kalish et al., 1995; Kunanusont et al., 1995; reviewed in Quinn, 1996). At present, subtype-E viruses are the most prevalent strains in Thailand and neighboring nations in southeast Asia (Weniger et al., 1991, 1994; Menu et al., 1996) and have been found in Africa (Myers, 1995). Recently, subtype-E viruses have

begun to enter western countries (Artenstein et al., 1995, 1996; Brodine et al., 1995).

Interpatient variation in the *env* region of subtype-E viruses from Asia was less than that in such viruses in Africa (McCutchan et al., 1996; Murphy et al., 1993). Epidemiology studies and sequence analysis suggest that subtype-E viruses in Thailand might have originated from Africa and that the relative homogeneity of subtype-E viruses in Thailand is due to a "founder effect" (Weniger et al., 1994; Murphy et al., 1993; Myers et al., 1995). Accordingly, heterogeneity of subtype-E viruses in Thailand is predicted to increase as the AIDS epidemic continues. Interpatient isolates from late-stage of infection with subtype-E viruses show more diversity in *env* sequences than those in the early-stage of infection (McCutchan et al., 1996).

Intersubtype recombinant viruses have been recently identified in HIV-1 infected individuals (Myers et al., 1995; Gao et al., 1996). Recombination between/among different viral subtypes has been inferred from comparisons of (i) sequences of full-length proviral genomes or (ii) sequences representing two or more regions of individual viral isolates. HIV-1 subtype-E isolates from Thailand, originally classified by sequences in the gp120 subunit of *env*, exhibit subtype-A sequences in *gag* and the 3' terminus of the transmembrane subunit (gp41) of *env* (Louwagie et al., 1993; Myers et al., 1995). Thus, it has been suggested that "subtype-E" viruses are A/E intersubtype recombinants (Sharp et al., 1995; Gao et al., 1996).

A small number of studies have examined phenotypic properties of subtype-E viruses. Analysis of a region of gp120 from HIV-1 isolates from individuals in northern Thailand revealed that emergence of SI (syncytium-inducing) phenotype of subtype-E virus was associated with the development of AIDS, whereas almost all NSI (non-syncytium-inducing) isolates were from non-

symptomatic patients in the early stage of infection (Yu et al., 1995; Ichimura et al., 1994). Differences in biological properties (e. g., Langerhans cell tropism) of subtype-E viruses might account for the ability of these viruses to be transmitted through heterosexual practices (i. e., *via* mucosal membranes) in greater efficiency than other subtypes (Soto-Ramirez et al., 1996).

The lack of an animal model for HIV-1 infection and fatal immunodeficiency has hindered the elucidation of determinants of transmission and pathogenesis of different viral subtypes (Gardner and Luciw, 1996). To address issues related to functions of HIV-1 genes *in vivo*, several investigators have constructed replication-competent recombinant viruses by substituting genes of the pathogenic clone $SIV_{mac239}$ with various genes from HIV-1 subtype-B clones (Li et al., 1992, 1995; Shibata et al., 1992; Igarashi et al., 1994; Kuwata et al., 1995; Luciw et al., 1995; Reimann et al., 1996a). These recombinants, or chimeras, are designated simian-human immunodeficiency viruses (SHIV). For the present study, we focused on the $HIV\text{-}1_{9466}$ isolate, a syncytium-inducing strain of subtype-E virus, which was recovered from an AIDS patient in the northern part of Thailand (Ichimura et al., 1994). Cloned DNA from this virus was used to construct SHIV clones and the restriction of HIV-1 subtype-E replication in macaque cells was analyzed. These studies were conducted to determine the viral gene(s) responsible for restricted replication and the step(s) in replication that is blocked in macaque cells. Analysis of SHIV clones with Thai subtype-E env genes *in vitro* and in non-human primates could also provide insight on intertypic HIV-1 recombination that now appears to be occurring in some parts of the world.

## MATERIALS AND METHODS

### Construction of SHIV Chimeric Clones

To study the restriction of HIV-1 (subtype-E) in non-human primates, we constructed two SHIV chimeric clones, SHIV$_{9466E}$ and SHIV$_{9466E/B}$, and tested these viral clones for replication in rhesus macaque PBMC, human PBMC, and CEMX174 cells. The structures and cloning strategies for these chimeric clones are shown in Figures 1, 2, and 3. SHIV$_{9466E}$ is a clone containing env, tat, rev, and vpu of the HIV-1$_{9466}$ (subtype-E) isolate from the pathogenic clone SIVmac239 (Kestler et al., 1990) (Fig. 1B and Fig. 2). Both SHIV clones containing the HIV-1 subtype-E sequences were provided by Chiron Vaccines (Emeryville, CA) for this study. The cloning strategy for SHIV$_{9466E}$ is similar to that of SHIV$_{SF33env}$ described elsewhere (Luciw, 1995). This clone did not produce any infectious virus after transfection into either CEMX174 cells or rhabdosarcoma cells followed by cocultivation with human PBMC. The second construct, SHIV$_{9466E/B}$, contains subtype-E sequences encompassing the env surface domain (gp120) and the amino-terminal half of the env transmembrane subunit (gp41); the 3' end of the subtype-E env DNA fragment in this clone is the AflII site located in the membrane spanning domain of gp41 (Fig. 1C and Fig. 3). The carboxy-terminal half of gp41 in SHIV$_{9466E/B}$ is from the subtype-B virus HIV-1$_{SF33}$. This latter chimeric virus produced infectious virus after transfection of rhabdosarcoma cells which were subsequently cocultured with human PBMC. Both SHIV clones containing the HIV-1 subtype-E sequences were provided by Chiron Vaccines (Emeryville, CA) for this study.

## Replication Kinetics of the Chimeric Viruses

Culture medium for PBMC was RPMI 1640 supplemented with 10% fetal bovine serum, 100 units/ml penicillin, 100 µg/ml streptomycin and 1mM L-glutamine. Human PBMC from a healthy, HIV seronegative donor were prepared by Ficoll-Hypaque density centrifugation of heparinized blood resuspended in the culture medium described above, and stimulated with 5 µg/ml of phytohemagglutinin for 3 days. PBMC from rhesus macaques were also prepared by the same procedure except these cells were stimulated with 0.5 µg/ml of *Staphylococcus* enterotoxin A (Toxin Technology, Inc., Sarasota, FL). CD8-depleted PBMC were prepared by using magnetic beads coated with anti-CD8 monoclonal antibody (Dynal, Oslo, Norway). After the three-day stimulation period, cultures of PBMC and CD8-depleted PBMC were inoculated with SHIV$_{9466E/B}$ (0.1 pg of viral p27 core antigen per cell) and maintained in culture medium supplemented with 100 units per ml human recombinant interleukin-2 (AIDS Research and Reference Reagent Program, NIH). Macaque PBMC were also exposed to the control viruses SHIV$_{SF33}$ and SIV$_{mac239}$. Culture supernatants were collected at 0, 3, 7, 10, and 14 days after infection and analyzed for virus production by measuring p27 SIV core protein (Coulter, Hialeah, FL).

## PCR Analysis of Viral DNA

PCR analysis was accessed to determine SHIV$_{9466E/B}$ DNA in rhesus macaque PBMC and CEMX174 cells. The PCR primer pair specific for the LTR/gag region of SIV$_{mac239}$, S265 and S267, was used to detect a late reverse transcription product (475 bp). Sequences for these primers are in the publication by Zou and Luciw (1996). Stimulated rhesus macaque PBMC and CEMX174 cells in the absence or presence of 10 µM AZT were exposed to

SHIV9466E/B and SHIVSF33 at a 0.1 pg per cell and incubated at 37°C for 1.5 hour. After adsorption, cells were washed three times and maintained in culture medium supplemented with recombinant IL-2. Cell samples were collected at 0, 6, 12, and 24 hours after infection and cell pellets were lysed in buffer containing 10mM Tris (pH 8.3), 0.45% NP-40, 0.45% Tween-20, and 100 mg proteinase K. To control for the amount of infected cell DNA substrate for PCR amplification, a primer pair specific for the human ß-globin gene, PC03 and PC04, was included in all reactions (Saiki et al., 1988). For detection of PCR amplification products, one primer from each pair of primers was end-labeled with $^{32}$P-ATP by T4-polynucleotide kinase. Buffer for PCR amplification contained 1.5 mM $MgCl_2$, 50 mM KCl, 100 mM Tris pH. 8.3 was mixed to 0.2 mM dNTP per nucleotide, 2 units of *Taq* polymerase (Perkin-Elmer Cetus, USA), and 20 pmol of the appropriate primers in a total volume of 50 µl. The PCR mixtures were subjected to 30 cycles of amplification by Thermal Cycler (Perkin-Elmer Cetus, USA) at 94°C for 1.5 min and 72°C for 3 min, and extension at 72°C for 7 min. After the PCR amplification, DNA products were analyzed by electrophoresis on polyacrylamide gels and visualized by autoradiography of dried gels.

## RESULTS

Replication properties of SHIV9466E/B were analyzed in human and macaque cell cultures. To ensure that these cultures could support virus growth, SHIVSF33 and SIVmac239 were also tested (Fig. 4). Although SHIV9466E/B replicated and caused cytopathology in human PBMC and CD8-depleted human PBMC, this virus did not replicate in macaque PBMC, CD8-

depleted macaque PBMC, and CEMX174 cells (Fig. 4A). In control experiments, macaque PBMC were permissive for growth of SHIV$_{SF33}$ and SIV$_{mac239}$ (Fig. 4B) (also see Himathongkham and Luciw, 1996). Taken together, these results indicate that gp120 and/or the ectodomain of gp41 of the HIV-1$_{9466}$ (subtype-E) isolate play a critical role in restricting SHIV$_{9466E/B}$ replication in macaque cells.

To determine the step that accounts for the block of SHIV$_{9466E/B}$ infection in macaque lymphocytes and CEMX174 cells, levels of viral DNA were measured by a semiquantitative PCR assay in cell cultures at 0, 6, 12, and 24 hours after infection with this virus. Complete or nearly complete proviral DNA was monitored by measuring the amount of the 475 bp DNA produced by PCR amplification with primers specific for SIV sequences (Fig. 5A). After infection with SHIV$_{9466E/B}$, viral DNA was barely detected in macaque PBMC (Fig. 5B), but was clearly evident in CEMX174 cells (Fig. 5C). SHIV$_{SF33}$ infected macaque PBMC and CEMX174 cells served as positive controls for detection of newly synthesized viral DNA (Fig. 5B and 5C). Analysis of viral DNA synthesis in cultures treated with the reverse transcriptase inhibitor azidothymidine (AZT) was performed to ensure that viral DNA detected in these studies was newly synthesized and not carried over in virions (Fig. 5B and 5C). Taken together, these results demonstrated that the block to SHIV$_{9466E/B}$ replication in rhesus macaque PBMC was at the early phase of viral infection, involving a step(s) at/or prior to reverse transcription. Because viral DNA was detected in CEMX174 cells infected with SHIV$_{9466E/B}$, the block in these cells involves a step viral life cycle after reverse transcription.

## DISCUSSION

Studies on several HIV-1 subtype-B isolates have shown that the envelope glycoprotein of HIV-1 plays a major role in virion entry of $CD4^+$ lymphocytes and influences cell tropism (reviewed in Weiss, 1993; Luciw, 1996). HIV-1 subtype-B virus does not productively infect rhesus macaque PBMC; the restriction is at the entry step of replication, before or/at reverse transcription but after virion attachment (Himathongkham and Luciw, 1996). Chimeric SHIV containing the subtype-B *env* gene replicate efficiently *in vitro* in macaque cell cultures and establish either transient or persistent infection in macaques (Li et al., 1992, 1995; Shibata et al., 1992; Sakuragi et al., 1992; Luciw et al., 1995; Reimann et al.; 1996a). Recently, SHIV clones producing an AIDS-like disease in these animals have been described (Joag et al., 1996; Reimannn et al. 1996b; P. Luciw and C. Cheng-Mayer, unpublished results). Thus, the *env* glycoprotein of subtype-B isolates from North America and Europe does not appear to be responsible for the block to viral infection in macaque cells. Here, we demonstrate that in contrast to subtype-B viruses, the *env* gene of an HIV-1 subtype-E isolate from Thailand is a major factor that restricts replication of this virus in macaque cells. Studies with a SHIV recombinant revealed that the viral determinant for restriction resides within the region of HIV-1 subtype-E env encompassing gp120 and/or the ectodomain of gp41. Additionally, biochemical analysis reveals that an early step(s) in replication of this SHIV, containing gp120 and ectodomain of gp41 of HIV-1 subtype-E, is blocked in macaque cells.

**SHIV-19466E/B**

Consideration of the properties of the gp120 subunit and the ectodomain of the gp41 subunit provides a basis for speculating on the mechanism of restriction of HIV-1 subtype-E in macaque cells. Sequence analysis of *env* of the majority of subtype-E isolates from Thailand shows an extra cysteine pair in the V4 region of gp120 compared to subtype-E from Africa (McCutchan et al., 1996) or subtype-B isolates from North America and Europe (Myers et al., 1995). The *env* sequence of HIV-19466 (subtype-E), which is the virus used in this study, also contains the extra cysteine pair in the V4 region, whereas V4 of HIV-1SF33 gp120 (subtype-B) does not. Because all cysteine residues in gp120 subunits of subtype-B viruses are believed to form disulfide bonds (Leonard et al., 1990), it is possible that the extra cysteine pair in subtype-E virus *env* glycoprotein might significantly affect tertiary structure and thereby alter biological function(s) such as species tropism. Because the extra cysteine pair in the V4 region is located immediately adjacent to the CD4 binding domain of gp120, attachment of virions to the CD4 receptor on macaque cell membranes might be disturbed by this conformational change and thus lead to lack of infection. The potential role of the V4 region in restricted replication of SHIV9466E/B in macaque cells needs to be investigated by additional genetic and biochemical studies with subtype-SHIV clones containing subtype-E *env* genes lacking the extra cysteine pair in the V4 region (e. g., the subtype-E HIV-1 90CR402.1 isolate from Africa; B. Hahn, unpublished results) as well as SHIV clones with site-specific mutations in the subtype-E *env* gene.

Analysis of biological characteristics of chimeric viruses in tissue culture cells revealed differences between SHIV with subtype-E and subtype-B *env* genes (Table 1). Although SHIV9466E/B replicated efficiently in human primary lymphocytes, this virus was blocked at a step after viral DNA synthesis in the

hybrid human T/B cell line CEMX174. However, this cell line was permissive for infection with SIVmac and also with HIV-1 subtype-B viruses. The parental subtype-E HIV-19466, a NSI, T-lymphotropic virus, replicated in human PBMC and certain T-cell lines (Ichimura et al., 1994), but did not replicate in CEMX174 cells. Thus, the restriction of HIV-19466 replication in CEMX174 cells is controlled by a determinant in the gp120 subunit and/or the ectodomain of the gp41 subunit of *env*. Studies with additional SHIV clones, constructed by producing hybrid *env* genes from subtype-E and subtype-B viruses, will be necessary to identify the region within the *env* glycoprotein responsible for the block of HIV-1 subtype-E in macaque cells and in the CEMX174 cell line.

**SHIV-19466E**

The basis for lack of infectivity of SHIV9466E, a chimeric clone containing the entire *env* gp160 gene from the HIV-19466 subtype-E isolate, is not resolved. HIV-1 isolates from Thailand have a unique gp120 sequence that distinguishes these viruses as members of subtype-E; however, sequences in the *gag* gene and cytoplasmic tail of gp41 of these viruses are related to subtype-A viruses (Myers et al., 1995). Incorporation of env glycoprotein oligomers into virion membranes during particle assembly depends on a specific interaction between the cytoplasmic tail of gp41 glycoproteins with the matrix (MA) domain in the Gag polyprotein precursors (Freed and Martin, 1995; Yu et al., 1993). Thus, the lack of infectivity of SHIV9466E could be due to lack of interaction between the cytoplasmic tail of the subtype-A gp41 subunit with the MA domain in SIV Gag. Another possibility is that Tat of SHIV9466E may not be functionally compatible with SIV Tat responsive element (TAR) in the long terminal repeat (LTR). Thus, Tat-mediated transactivation may be blocked in

SHIV9644E. The genetic basis for lack of infectivity of SHIV9466E can be resolved by studies with additional novel SHIV constructs involving exchanges between subtype-A, B, and E *env* genes as well as *tat* genes.

### Recombination between Viral Subtypes

The evidence that HIV-1 subtype-E isolates from Thailand are intertypic recombinants, containing hybrid subtype-E and subtype-A *env* genes (Fig. 1, Chapter 1), requires further investigation. Some individuals in Thailand were found to harbor both subtype-E and subtype-B viruses (Kalish et al., 1995; Wasi et al., 1995); this suggests that superinfection (or coinfection) by different HIV-1 subtypes, followed by recombination, can occur. HIV-1 variants produced by recombination, may potentially possess novel immunochemical and biological properties (e.g., cell tropism, pathogenicity) (Robertson et al., 1995a,b). Thus, studies of SHIV clones may have significance for analyzing patterns of recombination between/among different HIV-1 subtypes in humans. Such recombination could have impact on the future global spread of HIV infection and AIDS. Additionally, efforts at vaccine development to achieve protective immunity need to consider the role of viral subtypes and recombination events. These efforts will be facilitated by studies in non-human primates infected with SHIV clones containing subtype-E *env* genes, as well as *env* genes from other subtypes and intertypic recombinants.

## ACKNOWLEDGEMENTS

We thank Murray Gardner for many helpful discussions. The research in this paper was supported by funds from the National Institutes of Health

(AI34772), the University of California AIDS Research Program (R96-D-166), and the Department of Defense (DAMD 17-94-J-4436).

## FIGURE LEGENDS

Fig.1 Structures of the SHIV9466E and SHIV9466E/B contructs. The SHIVSF33 chimera (Luciw *et al.*, 1995) is shown at the top. Shaded boxes represent sequences derived from the HIV-1SF33 (subtype-B) clone. Boxes with diagonal lines represent sequences derived from the HIV-19466 (subtype-E) isolate. The surface (SU) gp120 and transmembrane (TM) gp41 regions of the envelope glycoproteins are shown.

Fig. 2 Cloning strategies of SHIV9466E chimeric virus. (A) pKJNnefR, plasmid vector contains the 3' portion of SIVmac239 from the SphI restriction site at nucleotide 6706 through the 3' LTR; this plasmid contains a full-length open reading frame of the *nef* gene. The *tat*, *rev*, *vpu*, and *env* genes of HIV-9466E were cloned in the SphI-XhoI restriction sites of this vector as shown in (B) The 5' junction and (C) The 3' junction of SHIV9466E.

Fig. 3 Cloning strategy for the SHIV9466E/B chimeric virus. (A) The SHIV9466E/B clone contains env gp120 and the ectodomain of gp41 of HIV-19466 (subtype-E); *tat*, *rev*, and the intracytoplasmic region of gp41 are from HIV-1SF33 (subtype-B). These portions of the two HIV-1 clones were used to replace counterpart regions in the pathogenic clone SIVmac239 ($nef^+$). The HIV-19466 portion was cloned in the (B) BbsI at the 5' junction and (C) AflII at the 3' junction of SHIV9466E/B.

Fig. 4 SHIV9466E/B replication *in vitro* in human and macaque cells. (A) SHIV9466E/B viral production, measured by ELISA for SIV p27 antigen, was analyzed in human PBMC, CD8-depleted human PBMC, CEMX174 cells,

macaque PBMC, and CD8-depleted macaque PBMC. (B) Replication of SHIV$_{9466E/B}$, SHIV$_{SF33}$ and SIV$_{mac239}$ in macaque PBMC was also measured by the same ELISA.

Fig. 5 PCR analysis of SHIV$_{9466E/B}$ DNA in rhesus macaque PBMC and CEMX174 cells. (A) The PCR primer pair ($^{32}$-P labeled) specific for the LTR/*gag* region of SIV$_{mac239}$, S265 and S267, detects a late reverse transcription product (475 bp). (B) Stimulated rhesus macaque PBMC and (C) CEMX174 cells in the absence or presence of 10 μM AZT were exposed to SHIV$_{9466E/B}$ and SHIV$_{SF33}$ and measured for viral DNA at 0, 6, 12, and 24 hours after infection. A primer pair specific for the human ß-globin was included in all reactions to serve as control. After PCR amplification, DNA products were analyzed by electrophoresis on polyacrylamide gels and visualized by autoradiography of dried gels.

## REFERENCES

Artenstein, A. W., J. Coppola, A. E. Brown, J. K. Carr, E. Sanders-Buell, E. Galbarini, J. R. Mascola, T. C. VanCott, P. Schonbrood, and F. E. McCutchan. 1995. Multiple introductions of HIV-1 subtype E into the western hemisphere. **Lancet** 346:1197-8.

Brodine, S. K., J. R. Mascola, P. J. Weiss, S. I. Ito, K. R. Porter, A. W. Artenstein, F. C. Garland, F. E. McCutchan, and D. S. Burke. 1995. Detection of diverse HIV-1 genetic subtypes in the USA. **Lancet** 346:1198-9.

Brown, T., W. Sittitrai, S. Vanichseni, and U. Thisyakorn. 1994. The recent epidemiology of HIV and AIDS in Thailand. **AIDS** 8:S131-41.

Gao, F., S. G. Morrison, D. L. Robertson, C.L. Thornton, S. Craig; G. Karlsson, J. Sodroski, M. Morgado, B. Galvao-Castro, H. von Briesen*et al.* 1996. Molecular cloning and analysis of functional envelope genes from human immunodeficiency virus type 1 sequence subtypes A through G. The WHO and NIAID Networks for HIV Isolation and Characterization. **J Virol** 70:1651-7.

Gardner, M. B., and P. A. Luciw. 1996. Simian retroviruses. In: Wormser, G ed. **AIDS and Other Manifestations of HIV Infection**. New York: Raven Press, Ltd.

Himathongkham, S., and P. A. Luciw. 1996. Restriction of HIV-1 (subtype B) replication at the entry step in rhesus macaque cells. **Virology** 219:485-8.

Ichimura, H., S. C. Kliks, S. Visrutaratna, C. Y. Ou, M. L. Kalish, and J. A. Levy. 1994. Biological, serological, and genetic characterization of HIV-1 subtype E isolates from northern Thailand. **AIDS Res Hum Retroviruses** 10:263-9.

Igarashi, T., R. Shibata, F. Hasebe, Y. Ami, K. Shinohara, T. Komatsu, C. Stahl-Hennig, H. Petry, G. Hunsmann, and T. Kuwata 1994. Persistent infection with SIVmac chimeric virus having *tat*, *rev*, *vpu*, *env* and *nef* of HIV type 1 in macaque monkeys. **AIDS Res Hum Retroviruses** 10:1021-9.

Joag, S. V., Z. Li, L. Foresman, E. B. Stephens, L. J. Zhao, I. Adany, D. M. Pinson, H. M. McClure, and O. Narayan. 1996. Chimeric simian/human immunodeficiency virus that causes progressive loss of CD4+ T cells and AIDS in pig-tailed macaques. **J Virol** 70:3189-97.

Kalish, M. L., A. Baldwin, S. Raktham, C. Wasi, C. C. Luo, G. Schochetman, T. D. Mastro, N. Young, S. Vanichseni, H. Rubsamen-Waigmann, *et al.* 1995. The evolving molecular epidemiology of HIV-1 envelope subtypes in injecting drug users in Bangkok, Thailand: implications for HIV vaccine trials. **AIDS** 9:851-7.

Kestler, H., T. Kodama, D. Ringler, M. Marthas, N. Pedersen, A. Lackner, D. Regier, P. Sehgal, M. Daniel, N. King, *et al.* 1990a. Induction of AIDS in rhesus monkeys by molecularly cloned simian immunodeficiency virus. **Science** 248:1109-12.

Kunanusont, C., H. M. Foy, J. K. Kreiss, S. Rerks-Ngarm, P. Phanuphak, S. Raktham, C. P. Pau, and N. L. Young. 1995. HIV-1 subtypes and male-to-female transmission in Thailand. **Lancet** 345:1078-83.

Kuwata, T., T. Igarashi, E. Ido, M. Jin, A. Mizuno, J. Chen, and M. Hayami. 1995. Construction of human immunodeficiency virus 1/simian immunodeficiency virus strain mac chimeric viruses having *vpr* and/or *nef* of different parental origins and their *in vitro* and in vivo replication. **J Gen Virol** 76:2181-91.

Leonard, C. K., M. W. Spellman, L. Riddle, R. J. Harris, J. N. Thomas, and T. J. Gregory. 1990. Assignment of intrachain disulfide bonds and characterization of potential glycosylation sites of the type 1 recombinant human immunodeficiency virus envelope glycoprotein (gp120) expressed in Chinese hamster ovary cells. **J Biol Chem** 265:10373-82.

Li, J., C. I. Lord, W. Haseltine, N. L. Letvin, and J. Sodroski. 1992. Infection of cynomolgus monkeys with a chimeric HIV-1/SIVmac virus that expresses the HIV-1 envelope glycoproteins. **J Acquir Immune Defic Syndr** 5:639-46.

Li, J. T., M. Halloran, C. I. Lord, A. Watson, J. Ranchalis, M. Fung, N. L. Letvin, and J. G. Sodroski. 1995. Persistent infection of macaques with simian-human immunodeficiency viruses. **J Virol** 69:7061-7.

Louwagie, J., F. E. McCutchan, M. Peeters, T. P. Brennan, E. Sanders-Buell, G. A. Eddy, G. van der Groen, K. Fransen, G. M. Gershy-Damet, R. Deleys, *et al.* 1993. Phylogenetic analysis of gag genes from 70 international HIV-1 isolates provides evidence for multiple genotypes. **AIDS** 7:769-80.

Luciw, P. A., E. Pratt-Lowe, K. E. Shaw, J. A. Levy, and C. Cheng-Mayer. 1995. Persistent infection of rhesus macaques with T-cell-line-tropic and macrophage-tropic clones of simian/human immunodeficiency viruses (SHIV). **Proc Natl Acad Sci USA** 92:7490-4.

Luciw, P. A. Human immunodeficiency viruses and their replication. In: Fields BN, Knipe DM, Howley PM ed. **Fundamental Virology**. New York: Raven Press, Ltd., pp 845-916.

McCutchan, F. E., P. A. Hegerich, T. P. Brennan, P. Phanuphak, P. Singharaj, A. Jugsudee, P. W. Berman, A. M. Gray, A. K. Fowler, and D. S. Burke. 1992. Genetic variants of HIV-1 in Thailand. **AIDS Res Hum Retroviruses** 8:1887-95.

McCutchan, F. E., A. W. Artenstein, E. Sanders-Buell, M. O. Salminen, J. K. Carr, J. R. Mascola, X. F. Yu, K. E. Nelson, C. Khamboonruang, D. Schmitt, M. P. Kieny, J. G. McNeil, and D. S. Burke. 1996. Diversity of the envelope glycoprotein among human immunodeficiency virus type 1 isolates of clade E from Asia and Africa. **J Virol** 70:3331-8.

Menu, E., T. T. X. Lien, M. Lafon, N. T. H. Lan, M. C. Muller-Trutwin, *et al.* 1996. HIV type 1 Thai subtype E is predominant in South Vietnam. **AIDS Res Hum Retroviruses** 12:629-633.

Murphy, E., B. Korber, M. C. Georges-Courbot, B. You, A. Pinter, D. Cook, M. P. Kieny, A. Georges, C. Mathiot, and F. Barre-Sinoussi 1993. Diversity of V3 region sequences of human immunodeficiency viruses type 1 from the central African Republic. **AIDS Res Hum Retroviruses** 9:997-1006.

Myers, G., B. H. Hahn, J. W. Mellors, L. E. Henderson, B. Korber, K. Jeang, F. E. McCutchan, and J. N. Pavlakis. **Human Retroviruses and AIDS**. Los Alamos, NM: Los Alamos National Laboratory, 1995

Nelson, K. E., D. D. Celentano, S. Suprasert, N. Wright, S. Eiumtrakul, S. Tulvatana, A. Matanasarawoot, P. Akarasewi, S. Kuntolbutra, S. Romyen, *et al.* 1993. Risk factors for HIV infection among young adult men in northern Thailand. **JAMA** 270:955-60.

Ou, C. Y., Y. Takebe, C. C. Luo, M. Kalish, W. Auwanit, C. Bandea, N. de la Torre, J. L. Moore, G. Schochetman, S. Yamazaki, *et al.* 1992. Wide distribution of two subtypes of HIV-1 in Thailand. **AIDS Res Hum Retroviruses** 8:1471-2.

Quinn, T. C. 1996. Global burden of the HIV pandemic. **Lancet** 348:99-106.

Reimann, K. A., J. T. Li, G. Voss, C. Lekutis, K. Tenner-Racz, P. Racz, W. Lin, D. C. Montefiori, D. E. Lee-Parritz, Y. Lu, R. G. Collman, J. Sodroski, and N. L. Letvin. 1996a. An *env* gene derived from a primary human immunodeficiency virus type 1 isolate confers high *in vivo* replicative capacity to a chimeric simian/human immunodeficiency virus in rhesus monkeys. **J Virol** 70:3198-206.

Reimann, K. A., J. T. Li, R. Veazy, M. Halloran, I-W. Park, G.B. Karlsson, J. Sodroski, and N. L. Letvin. 1996b. A chimeric simian/human immunodeficiency virus expressing a primary patient human immunodeficiency viurs type 1 isolate env causes an AIDS-like disease after in vivo passage in rhesus monkeys. **J Virol** 70:6922-6928.

Robertson, D. L., P. M. Sharp, F. E. McCutchan, and B. H. Hahn. 1995a. Recombination in HIV-1. **Nature** 374:124-6.

Robertson, D. L., B. H. Hahn, and P. M. Sharp. 1995b. Recombination in AIDS viruses. **J Mol Evol** 40:249-59.

Saiki, R. K., D. H. Gelfand, S. Stoffel, S. J. Scharf, R. Higuchi, G. T. Horn, K. B. Mullis, and H. A. Erlich. 1988. Primer-directed enzymatic amplification of DNA with a thermostable DNA polymerase. **Science** 239:487-91.

Sakuragi, S., R. Shibata, R. Mukai, T. Komatsu, M. Fukasawa, H. Sakai, J. Sakuragi, M. Kawamura, K. Ibuki, and M. Hayami. 1992. Infection of macaque monkeys with a chimeric human and simian immunodeficiency virus. **J Gen Virol** 73:2983-7.

Sharp, P. M., D. L. Robertson, F. Gao, and B. H. Hahn. 1994. Origins and diversity of human immunodeficiency viruses. **AIDS** 8 (suppl. 1):S27-S42.

Shibata, R., M. Kawamura, H. Sakai, M. Hayami, A. Ishimoto, and A. Adachi. 1991. Generation of a chimeric human and simian immunodeficiency virus infectious to monkey peripheral blood mononuclear cells. **J Virol** 65:3514-20.

Shibata, R., H. Sakai, M. Kawamura, K. Tokunaga, and A. Adachi. 1995. Early replication block of human immunodeficiency virus type 1 in monkey cells. **J Gen Virol** 76:2723-30.

Sittitrai, W., and T. Brown. 1994. Risk factors for HIV infection in Thailand. **AIDS** 8:S143-53.

Soto-Ramirez, L. E., B. Renjifo, M. F. McLane, R. Marlink, C. O'Hara, R. Sutthent, C. Wasi, P. Vithayasai, V. Vithayasai, C. Apichartpiyakul *et al.* 1996. HIV-1 Langerhans' cell tropism associated with heterosexual transmission of HIV. **Science** 271:1291-3.

Wasi, C., B. Herring, S. Raktham, S. Vanichseni, T. D. Mastro, N. L. Young, H. Rubsamen-Waigmann, H. von Briesen, M. L. Kalish, C. C. Luo, *et al.* 1995. Determination of HIV-1 subtypes in injecting drug users in Bangkok, Thailand, using peptide-binding enzyme immunoassay and heteroduplex mobility assay: evidence of increasing infection with HIV-1 subtype E. **AIDS** 9:843-9.

Weiss, R. A. Cellular receptors and viral glycoproteins involved in retrovirus entry. In: Levy JA ed. **The Retroviridae**. New York: Plenum Press. 1993: 1-108.

Weniger, B. G., Y. Takebe, C. Y. Ou, and S. Yamazaki. 1994. The molecular epidemiology of HIV in Asia. **AIDS** 8:S13-28.

Yu, X. F., Z. Wang, C. Beyrer, D. D. Celentano, C. Khamboonruang, E. Allen, and K. Nelson. 1995. Phenotypic and genotypic characteristics of human immunodeficiency virus type 1 from patients with AIDS in northern Thailand. **J Virol** 69:4649-55.

Zou, J. X., and P. A. Luciw. 1996. The requirement for Vif of SIVmac is cell-type dependent. **J Gen Virol** 77:427-34.

Table 1. Biologic properties of SHIV chimeric viruses containing HIV-1 subtype-B and E *env* genes

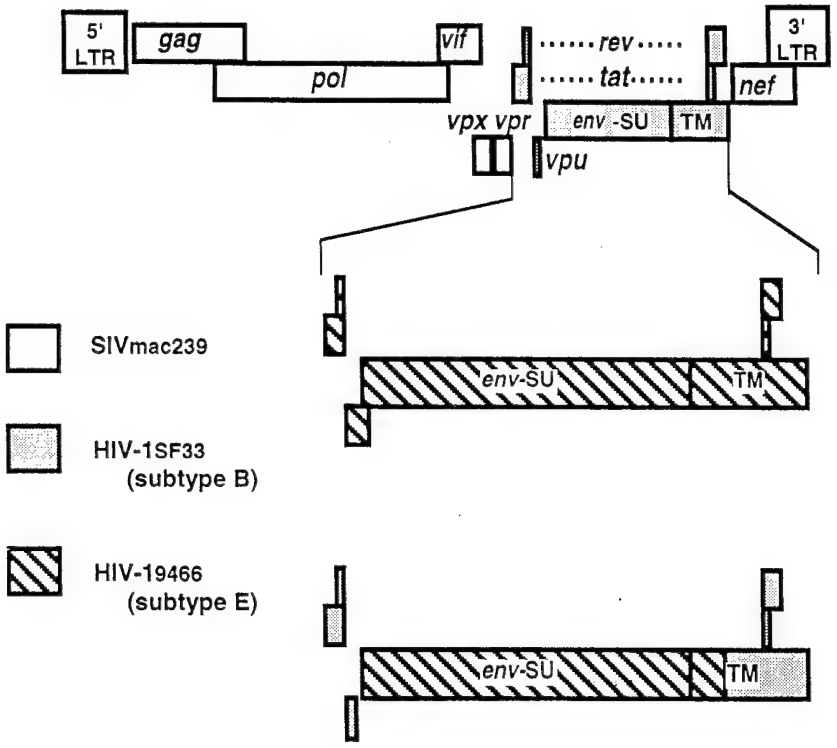


| | env subtype | Replication in: CEMX174 cells | human PBMC | macaque PBMC |
|---|---|---|---|---|
| SHIVSF33 | B | + | + | + |
| SHIV9466E | E (E/A) | – | – | ND |
| SHIV9466E/B | E/B | – | + | – |

**Figure 1: Structures of the $SHIV_{9466E}$ and $SHIV_{9466E/B}$ constructs.**

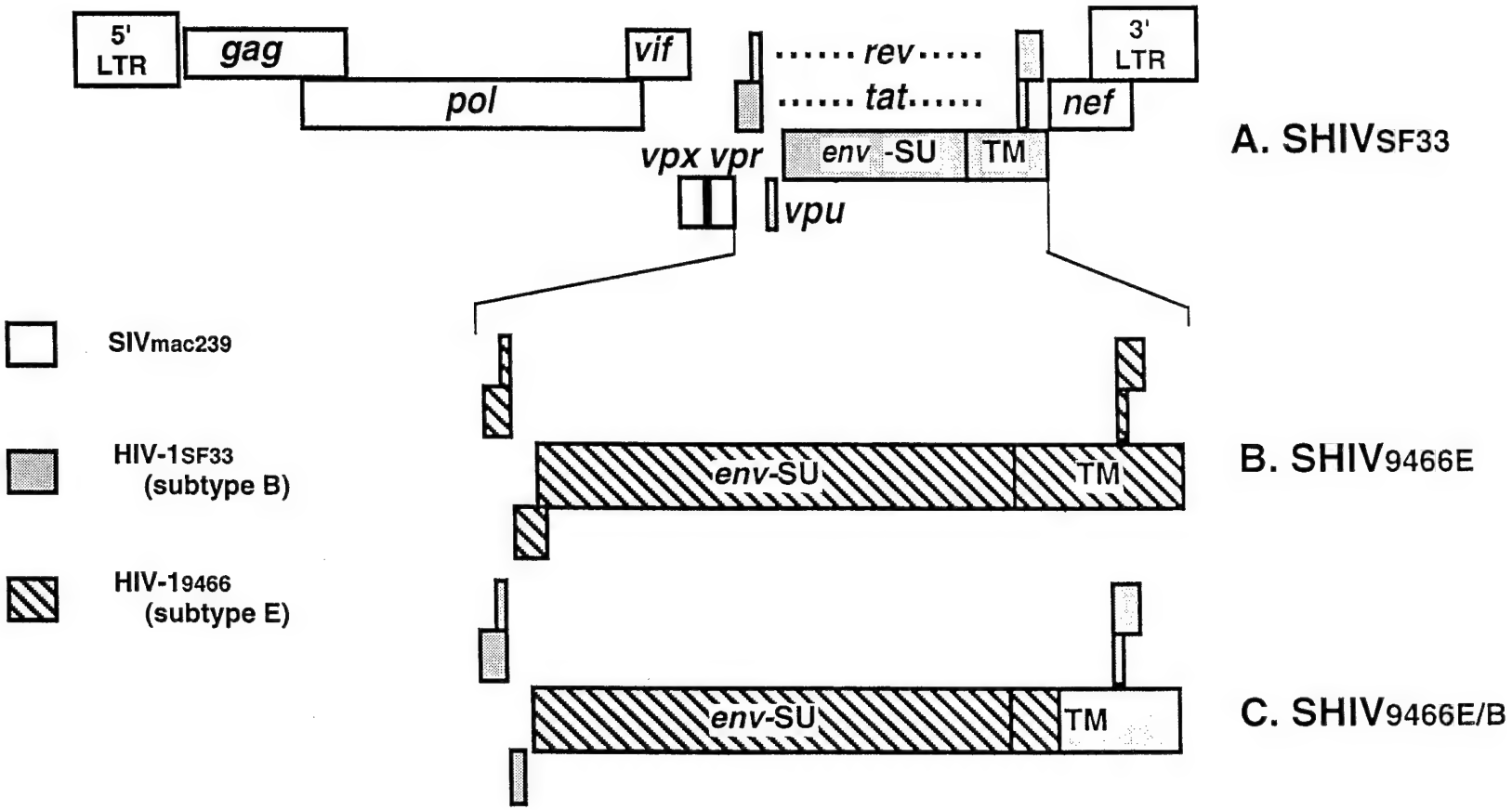

## Figure 2: Cloning strategies of $SHIV_{9466E}$ chimeric virus.

### A. Plasmid vector for SHIV (nef open and 3' LTR of $SIV_{mac239}$)

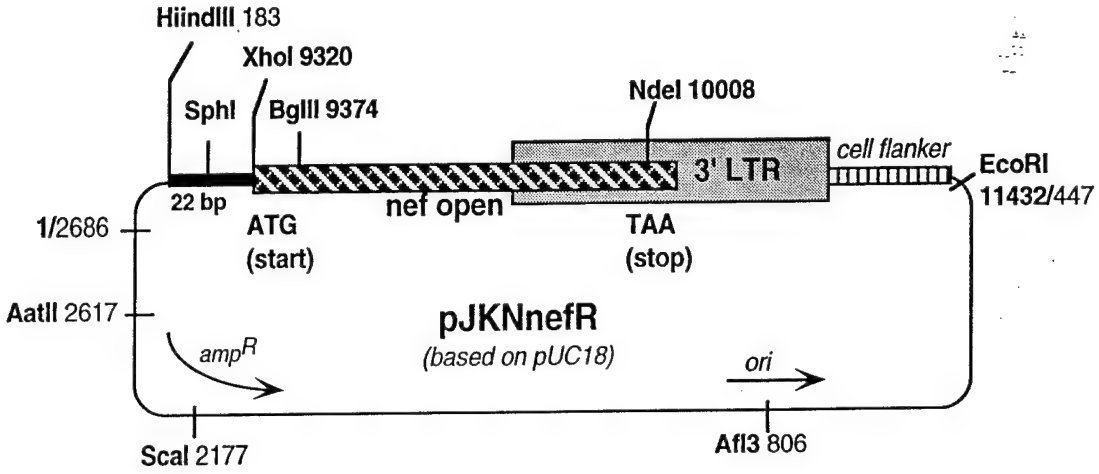


### B. 5' junction of $SHIV_{9466E}$

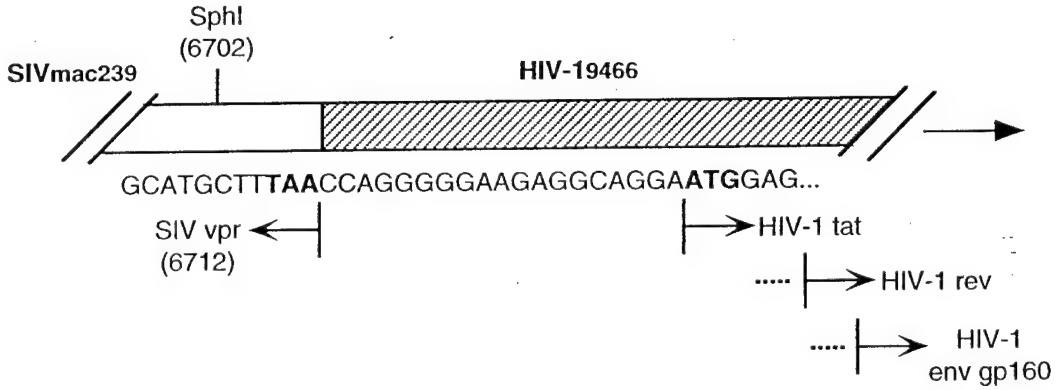


### C. 3' junction of $SHIV_{9466E}$

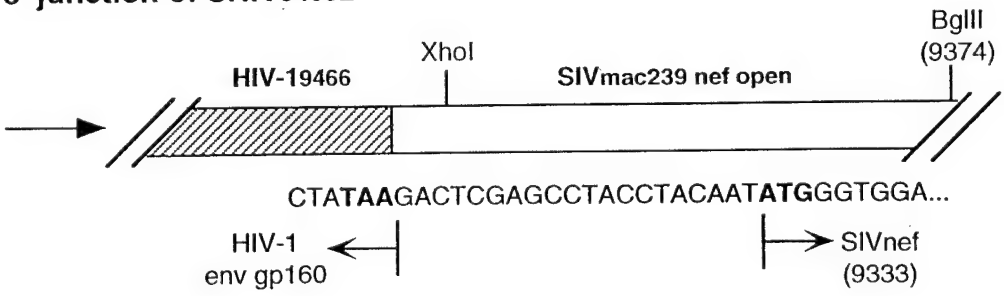

## Figure 3: Cloning strategies of SHIV9466E/B chimeric virus.

### A. Structure of SHIV9466E/B

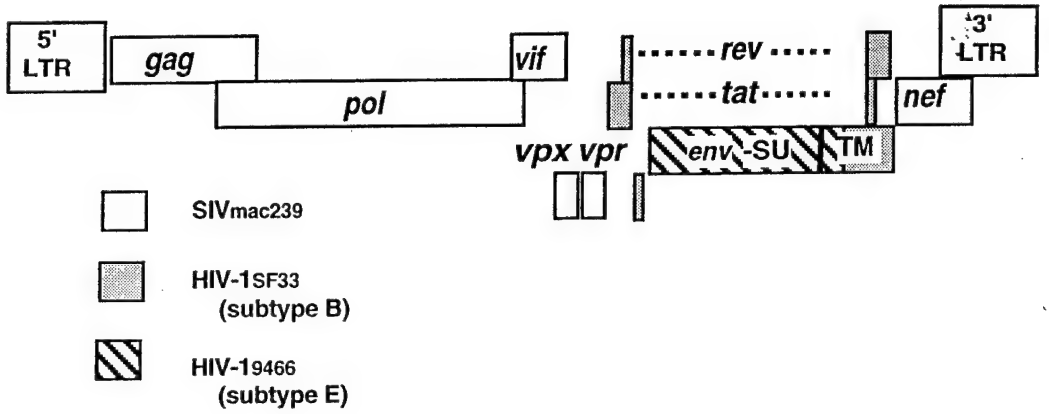


### B. 5' junction of SHIV9466E/B

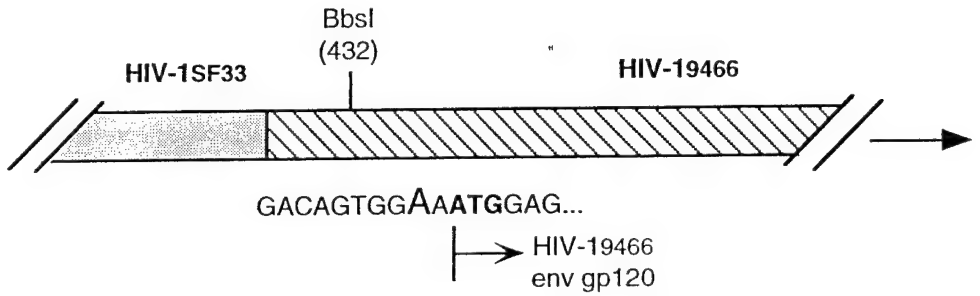


### C. 3' junction of SHIV9466E/B

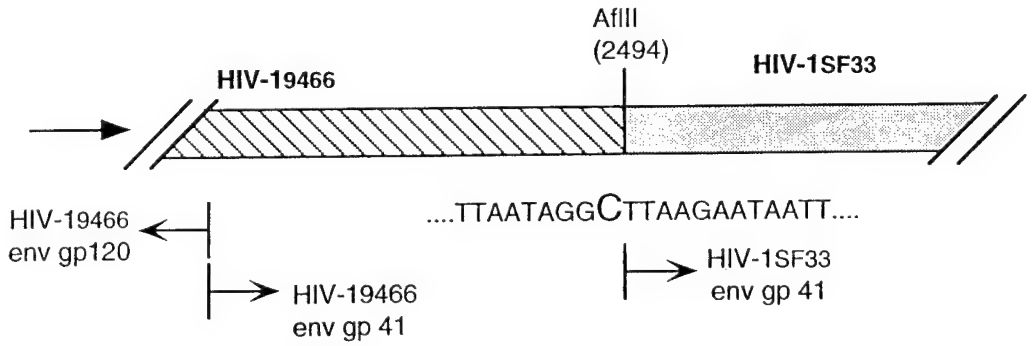

**Figure 4. SHIV9466E/B replication in vitro in human and macaque cells.**

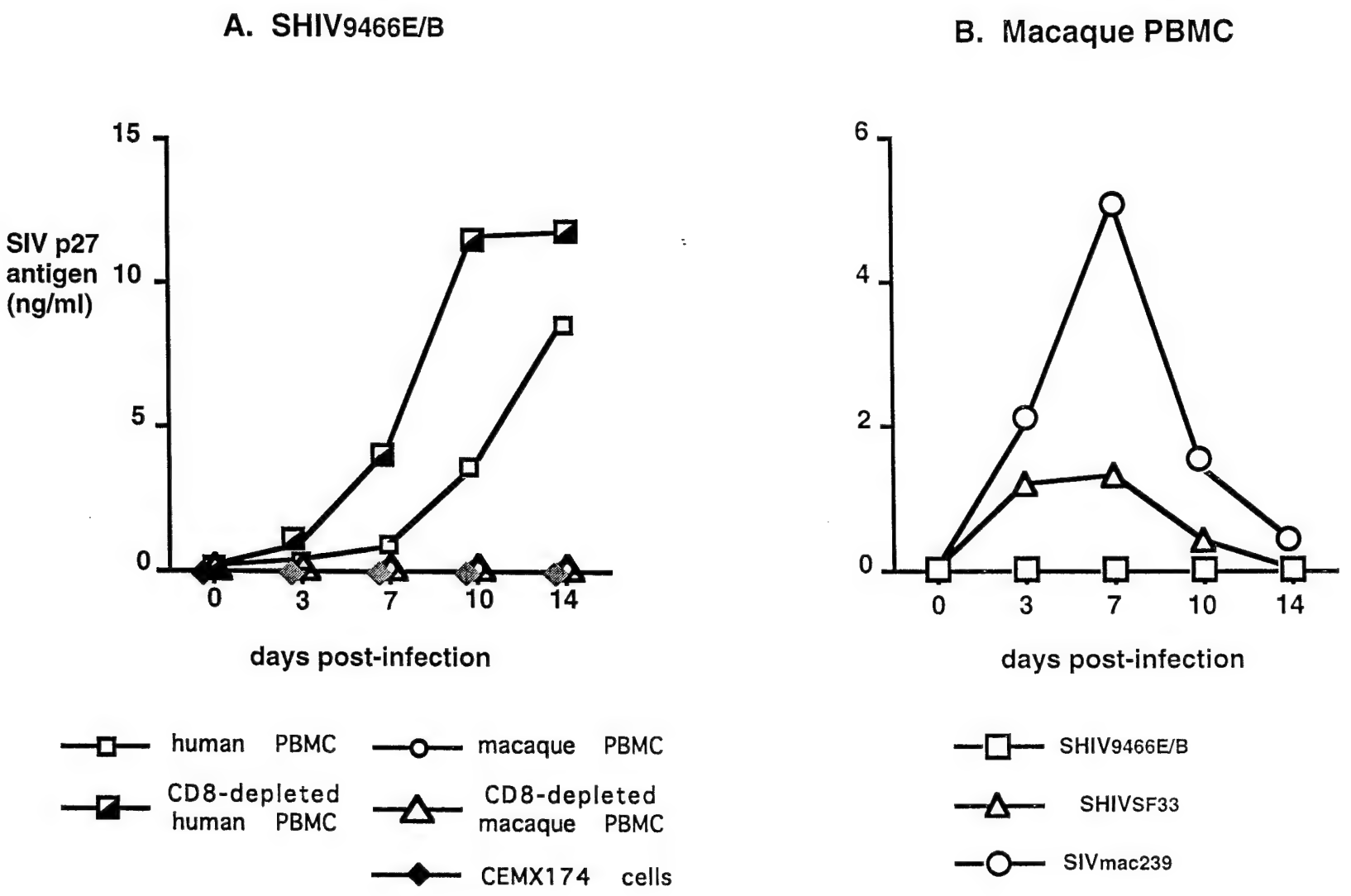

FIGURE 5

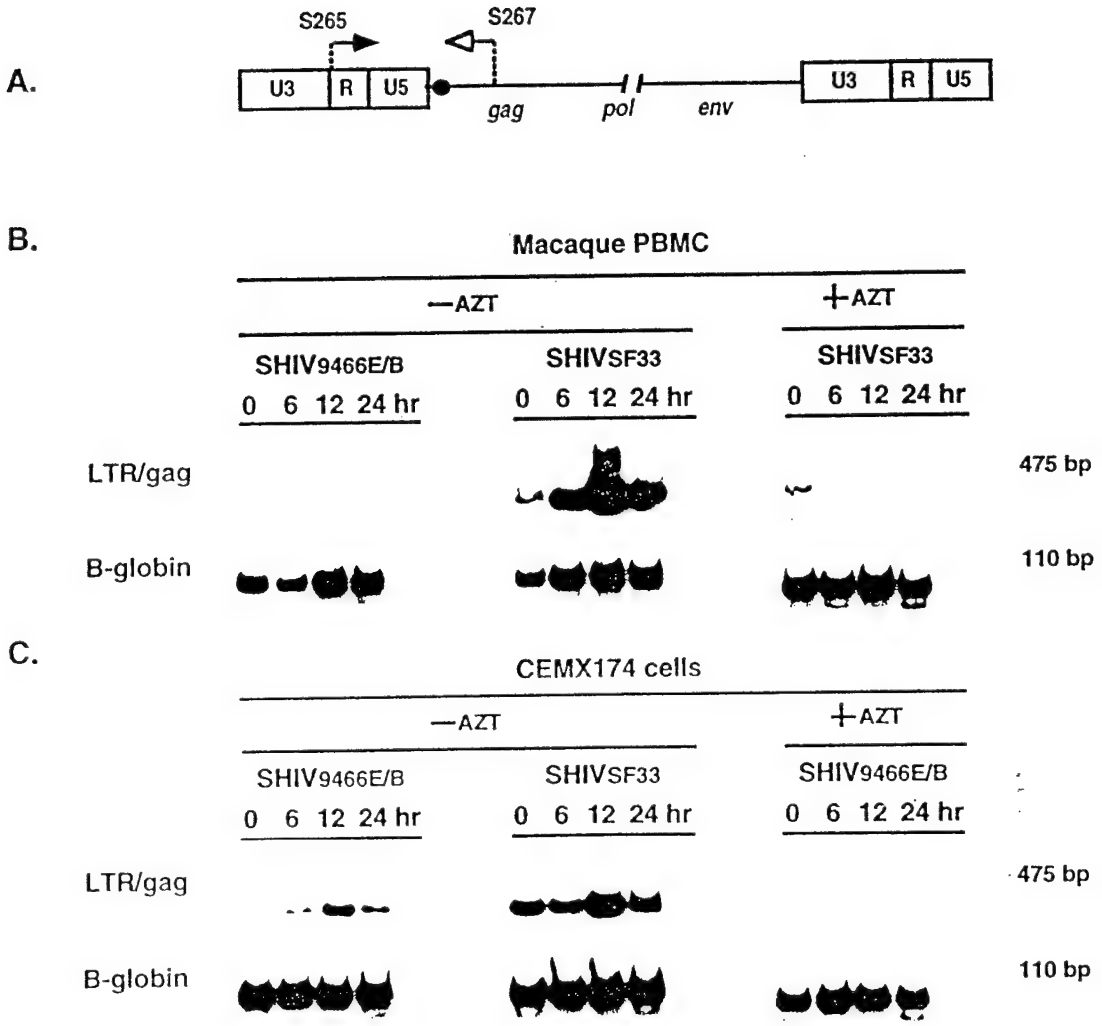
A.
S265
S267
U3
R
U5
gag
pol
env
U3
R
U5
B.
Macaque PBMC
—AZT
+AZT
SHIV9466E/B
SHIVSF33
SHIVSF33
0 6 12 24 hr
0 6 12 24 hr
0 6 12 24 hr
LTR/gag
475 bp
B-globin
110 bp
C.
CEMX174 cells
—AZT
+AZT
SHIV9466E/B
SHIVSF33
SHIV9466E/B
0 6 12 24 hr
0 6 12 24 hr
0 6 12 24 hr
LTR/gag
475 bp
B-globin
110 bp

# APPENDIX 5

# Activation of PAK by HIV and SIV Nef: Importance for AIDS in Rhesus Macaques

# Activation of PAK by HIV and SIV Nef: importance for AIDS in rhesus macaques

Earl T. Sawai*, Imran H. Khan*, Phillip M. Montbriand*, Cecilia Cheng-Mayer† and Paul A. Luciw*

**Background:** The primate lentiviruses, human immunodeficiency virus types 1 and 2 (HIV-1 and HIV-2) and simian immunodeficiency virus (SIV), encode a conserved accessory gene product, Nef. *In vivo*, Nef is important for the maintenance of high virus loads and progression to AIDS in SIV-infected adult rhesus macaques. In tissue culture cells expressing Nef, this viral protein interacts with a cellular serine kinase, designated Nef-associated kinase.

**Results:** This study identifies the Nef-associated kinase as a member of the p21-associated kinase (PAK) family of kinases and investigates the role of this Nef-associated kinase *in vivo*. Mutants of Nef that do not associate with the cellular kinase are unable to activate the PAK-related kinase in infected cells. To determine the role of cellular kinase association in viral pathogenesis, macaques were infected with SIV containing point-mutations in Nef that block PAK activation. Virus recovered at early time points after inoculation with mutant virus was shown to revert to prototype Nef function and sequence. Reversion of the kinase-negative mutant to a kinase-positive genotype in macaques infected with the mutant virus preceded the induction of high virus loads and disease progression.

**Conclusions:** Nef associates with and activates a PAK-related kinase in lymphocytes infected *in vitro*. These findings reveal that there is a strong selective pressure *in vivo* for the interaction between Nef and the PAK-related kinase. Moreover, the Nef-mediated activation of a PAK-related kinase correlates with the induction of high virus loads and the development of AIDS in the infected host.

Addresses: *Department of Medical Pathology, University of California, Davis, California 95616, USA. †Aaron Diamond AIDS Research Center, 455 1st Ave, 7th floor, New York, New York 10016, USA.

Correspondence to: Earl T. Sawai
E-mail: etsawai@ucdavis.edu **(Author: is it OK to use your E-mail address? If so, is this the correct one?)**

Received: **27 August 1996**
Revised: **17 September 1996**
Accepted: **20 September 1996**

**Current Biology 1996, Vol 6 No 11:000–000**



## Introduction

The *nef* gene of human immunodeficiency virus types 1 and 2 (HIV-1 and HIV-2) and simian immunodeficiency virus (SIV) encodes a 27–34 kDa myristylated and phosphorylated protein that is expressed in the early stage of the viral replication cycle (reviewed in [1–3]). Although Nef is dispensable for productive infection in T-cell lines, this viral accessory protein plays an important role in the induction of acquired immune deficiency syndrome (AIDS) in SIV-infected rhesus macaques [4]. Studies addressing Nef function in tissue culture cells [5–7], transgenic mice [8] and SIV-infected macaques [9] suggest that this viral protein alters a cell signalling pathway(s). In T-cell cultures, Nef decreases the levels of the CD4 antigen on the cell surface [10–12] and increases virion infectivity [13–15] (reviewed in [1–3]). In transgenic mice expressing HIV-1 Nef, thymocytes display altered cell activation responses [8]. Rhesus macaques infected with SIVmac239nefYE, a clone containing two point mutations that generate a novel SH2-like domain near the amino terminus of Nef, exhibit an acute, fatal, gastrointestinal tract disease accompanied by T-cell proliferation in several lymphoid organs [9]. This mutant *nef* also transforms murine NIH3T3 cells *in vitro* [9]. Taken together, these observations implicate a role for Nef in perturbing a cell-activation pathway(s) which is presumed to influence the level of viral replication in the host and/or cause dysfunction of cells in the immune system.

An important approach to study Nef function(s) has been to identify and characterize cellular proteins that interact with this viral protein. Accordingly, Nef has been reported to bind CD4 [7,16], Lck [7,17], p53, mitogen-activated protein (MAP) kinase [7], the SH3 domains of Hck and Lyn [18,19], c-src [9] and β-COP [20]. However, most of these reports lack experiments that demonstrate that Nef and these various cellular proteins form complexes in permissive cells infected with virus, they also lack genetic analysis using viruses bearing mutations in *nef* that would establish the significance of such protein–protein interactions **(****Author: OK? (We cannot use numbering of points)****)**. To address these limitations, we have previously shown that Nef expressed in HIV-1-infected lymphocytes associates with a cellular serine kinase

(Nef-associated kinase) which phosphorylates two cellular proteins, p62 and p72, that co-immunoprecipitate with Nef [21]. Additionally, mutation analysis demonstrated that amino-terminal myristylation and the central conserved domain of Nef were important for the Nef-associated kinase activity [22].

## Results

### Characterization of the Nef-associated kinase

To identify the cellular kinase activity that associates with Nef, we screened numerous commercially available antibodies to known signal transduction molecules for their ability to recognize two cellular proteins, p62 and p72, that coimmunoprecipitate with Nef from lymphoid cells infected with HIV-1 or SIV. During this screening process, an antibody directed against a p21-associated kinase (PAK) was found to immunoprecipitate proteins of 62 and 72 kDa in an *in vitro* kinase assay. The PAKs are highly conserved ubiquitous serine kinases important for the transduction of external signals to the nucleus [23–28]. These kinases, ranging in size from 62 to 70 kDa, become activated and autophosphorylate after they bind the p21 Rho-like GTP-binding proteins, Rac-1 and Cdc42Hs [23–31].

A polyclonal antiserum specific for the amino-terminal 20 amino acids of PAK-1 from rat brain was used to immunoprecipitate PAK from uninfected CEMx174 cells and cells

**Figure 1**

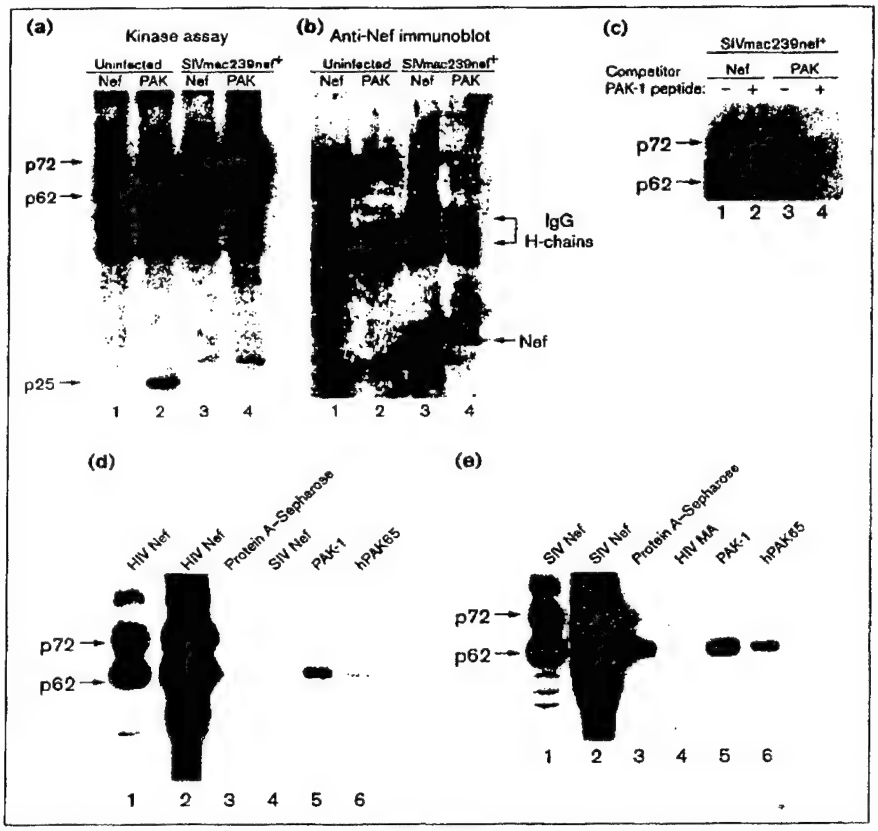


Association between Nef and a PAK-related kinase. **(a)** An *in vitro* kinase assay was performed on anti-SIV Nef (lanes 1 and 3) and anti-PAK (lanes 2 and 4) immunoprecipitates from uninfected (lanes 1 and 2) and SIVmac239nef+-infected (lanes 3 and 4) CEMx174 extracts as described [21] **(Author: OK?)**. Nef was immunoprecipitated with a monoclonal anti-SIV Nef antibody (17.2) and PAK was immunoprecipitated with a polyclonal serum directed against the amino-terminal 20 amino acids of rat PAK-1. Proteins were separated by SDS–PAGE on a 12 % gel and transferred to PVDF membranes. Radiolabeled proteins were visualized by autoradiography. The positions of p62, p72 and p25 are indicated by arrows on the left. Phosphorylated bands in the 46 kDa range were non-specific in these immunoprecipitations. **(b)** Immunological detection of Nef in anti-PAK immunoprecipitates. The PVDF filter from (a) was probed with the anti-Nef monoclonal antibody (17.2) as described in Materials and methods. The positions of Nef and immunoglobulin G (IgG) heavy chains are indicated on the right. **(c)** Specificity of the anti-PAK antibody. Kinase assays were performed on anti-Nef (lanes 1 and 2) and anti-PAK (lanes 3 and 4) immunoprecipitates that had been preincubated with (+, lanes 2 and 4) or without (–, lanes 1 and 3) a competitor peptide corresponding to the amino terminus of PAK-1 that is recognized by the anti-PAK antiserum. **(d)** Re-immunoprecipitation of PAK from HIV-1 Nef immunoprecipitates. A kinase assay was performed on a Nef immunoprecipitate from HUT78 cells chronically infected with the HIV-$1_{SF11114}$ strain; lanes 1 and 2) **(****Author: OK? If not, please clarify****)**. Proteins associated with Nef were released from the Nef immunoprecipitates with kinase extraction buffer [21] containing 0.1 % SDS. The supernatant was subjected to two successive incubations with protein A–Sepharose; lane 3 represents the pellet from the second protein A–Sepharose clearance. The supernatant was split three ways and immunoprecipitated with anti-SIV Nef control (lane 4) antibodies, anti-PAK-1 (lane 5) antibodies or anti-human PAK65 (hPAK65, lane 6) antibodies. Lanes 2–6 represent a 5 day autoradiographic exposure; lane 1 represents an overnight exposure of lane 2. **(e)** Re-immunoprecipitation of PAK from SIV Nef immunoprecipitates. A PAK re-immunoprecipitation analysis was performed on a SIV Nef immunoprecipitate from CEMx174 cells chronically infected with SIVmac239nef+ as described in (d): lanes 1 and 2, SIV Nef immunoprecipitates; lane 3, second protein A–Sepharose clearance; lane 4, anti-HIV-1 matrix protein (MA) control; lane 5, anti-PAK-1; lane 6, anti-human PAK65 (hPAK65). Lanes 2–6 represent a 5 day autoradiographic exposure; lane 1 represents an overnight exposure of lane 2.

**Figure 2**

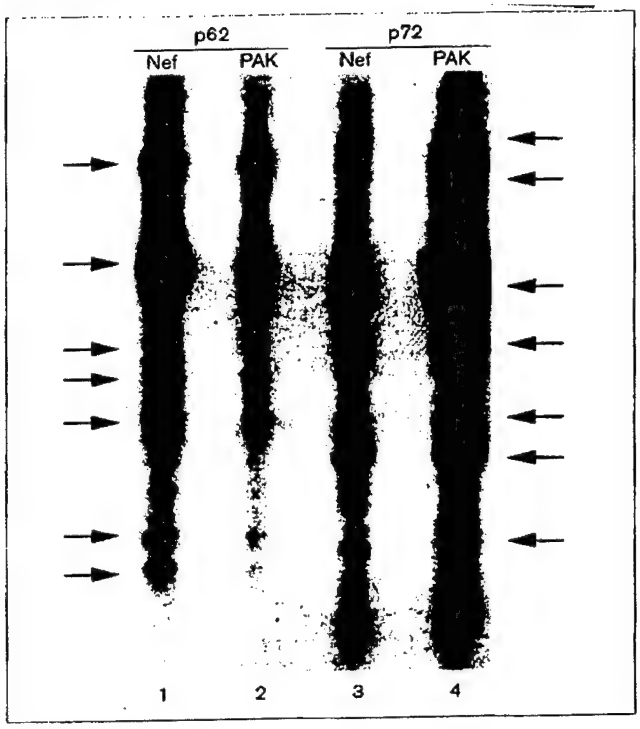


Phosphopeptide maps of p62 and p72. Partial chymotryptic digestion was performed on bands corresponding to p62 (lanes 1 and 2) and p72 (lanes 3 and 4) from SIV Nef (lanes 1 and 2) and PAK (lanes 2 and 4) immunoprecipitates. The arrows indicate the positions of the major partial peptide cleavage products for p62 (right side) and p72 (left side) respectively.

chronically infected with SIVmac239nef$^+$ (an SIV clone containing a wild-type *nef* gene) **(Author: OK?)**. *In vitro* kinase assays performed on these immunoprecipitates from infected cells revealed two phosphorylated proteins of 62 and 72 kDa (Fig. 1a, lane 4) which are hyperphosphorylated forms of the 62 and 72 kDa proteins observed in PAK immunoprecipitates from uninfected cell lines (Fig. 1a, lane 2). Interestingly, these phosphorylated proteins were similar in size to the two proteins (p62 and p72) that co-immunoprecipitated with Nef (Fig. 1a, lane 3). In the anti-Nef immunoprecipitate, p62 and p72 were the major and minor phosphorylated species, respectively (Fig. 1a, lane 3); whereas p72 was the major and p62 was the minor phosphorylated species in the anti-PAK-1 immunoprecipitate (Fig. 1a, lane 4). In uninfected CEMx174 cells, a phosphorylated protein (designated PAK) migrating slightly faster than p62, and a phosphorylated protein of 25 kDa (p25) were detected in the anti-PAK-1 immunoprecipitate (Fig. 1a, lane 2). Neither PAK nor p25 was found in immunoprecipitates from infected cells (Fig. 1a, lane 4). The identity and significance of p25 for Nef-mediated PAK activation remain to be elucidated.

To determine whether the hyperphosphorylation of p72 in SIV-infected lymphocytes was PAK-specific, kinase assays were performed on Nef and PAK immunoprecipitates using antibodies that were preincubated with a PAK-1 competitor peptide (Fig. 1c). This peptide represents the epitope recognized by the anti-PAK-1 antibody. Because p72 was not phosphorylated after anti-PAK sera was preincubated with the PAK-1 competitor peptide, the hyperphosphorylation of p72 in SIV-infected cells was indeed PAK-specific.

### Identification of the Nef-associated kinase as a PAK-related kinase

To determine whether Nef and PAK associate in infected cells, an immunoblot analysis (Fig. 1b) using a Nef-specific antibody probe was performed on immunoprecipitates produced with anti-Nef and anti-PAK-1 antibodies (Fig. 1a). Nef was detected in both the anti-Nef and anti-PAK-1 immunoprecipitates from cells infected with SIVmac239nef$^+$ (Fig. 1b, lanes 3 and 4). Nef was not detected in uninfected CEMx174 cells (Fig. 1b, lanes 1 and 2). Using the PAK-1-specific antibody to probe the anti-Nef and anti-PAK-1 immunoprecipitates described above, we detected p62 in the anti-PAK-1 immunoprecipitates from uninfected and infected cells (data not shown). However, it was difficult to demonstrate the presence of p62 in the anti-Nef immunoprecipitate of cells infected with SIVmac239nef$^+$ (data not shown); this could result from the small proportion of PAK-1 (or a PAK-related protein) that is associated with Nef in infected cells. These results indicate that Nef forms a complex with PAK-1 (or a PAK-related protein) in infected lymphoid cells.

To confirm that Nef associates with a PAK-related kinase, a re-immunoprecipitation analysis was performed on a HIV-1 Nef immunoprecipitate (Fig. 1d). Anti-PAK antibodies recognized p62, which was released from the HIV-1 Nef immunoprecipitates (Fig. 1d). Similar results were obtained with SIV Nef immunoprecipitates (Fig. 1e). Note that p62 was not observed in the lane containing the non-specific antibody control (Fig. 1d,e; lane 4). These results confirm data from a recent study [32] showing that a HIV-1 Nef fusion protein expressed by a retroviral vector in T lymphocytes associates with a member of the PAK family of proteins. Taken together, these studies show that Nef associates with a PAK-related protein in cells infected with HIV-1 or SIV.

### Comparison of p62 and p72 by analysis of phosphopeptide maps

The relationship between p62 and p72 from anti-Nef and anti-PAK-1 immunoprecipitates was investigated by phosphopeptide mapping. Immunoprecipitated radiolabelled proteins were subjected to SDS–PAGE and $^{32}$P-labeled bands corresponding to p62 and p72 were isolated and

**Figure 3**

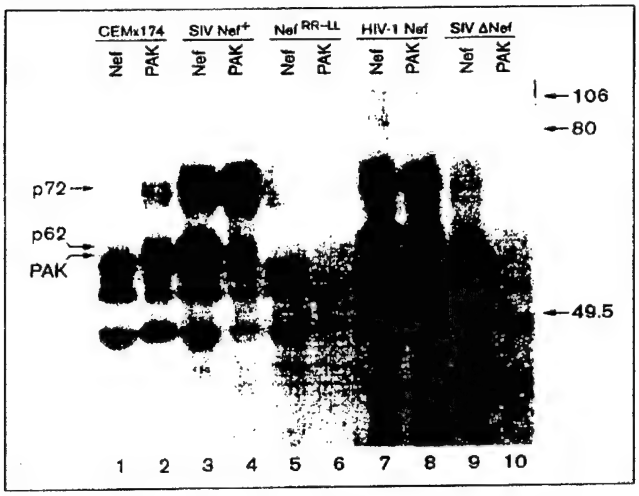


Analysis of HIV and SIV Nef mutants for activation of PAK. Kinase assays were performed on anti-SIVmac239 Nef (N, lanes 1,3,5 and 9), anti-HIV-$1_{SF2}$ Nef (lane 7) and anti-rat PAK-1 (P, lanes 2,4,6,8 and 10) immunoprecipitates from uninfected CEMx174 cells (lanes 1 and 2), CEMx174 cells chronically infected with SIVmac239nef+ (lanes 3 and 4), SIVmac239nef$^{RR-LL}$ (RR–LL, lanes 5 and 6)or SIVmac239Δnef (ΔNef, lanes 9 and 10) or HUT78 cells chronically infected with HIV-$1_{SF2}$ (lanes 7 and 8). The positions of migration of PAK from uninfected cells, and of p62 and p72 are indicated on the left.

**Figure 4**

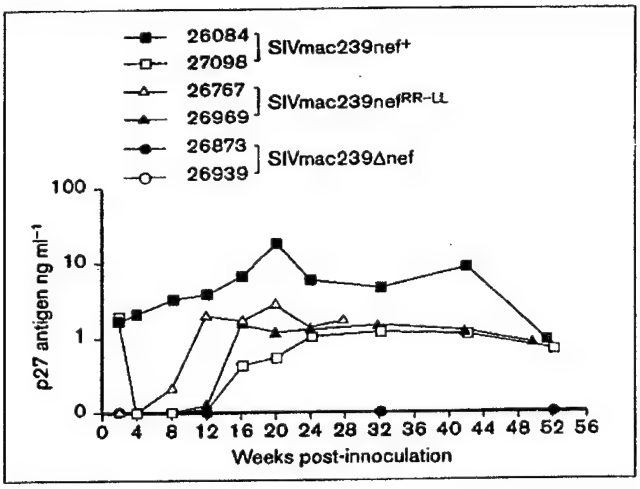


Viral loads in SIV-infected rhesus macaques. SIV p27gag antigenemia was measured by enzyme-linked immunosorbent assay (ELISA) from the plasma of monkeys infected with SIVmac239nef+ (26084 and 27098), SIVmac239nef$^{RR-LL}$ (26767 and 26969) or SIVmac239Δnef (26873 and 26939) at the indicated weeks post-inoculation **(Author: is antigenemia OK? or should I rephrase to say "The levels of SIV p27gag were measured...."?).**

subjected to partial protease cleavage with chymotrypsin **(Author: OK? If not, please clarify)**. The phosphopeptide maps of p62 from anti-SIV Nef and anti-PAK-1 immunoprecipitates were similar, indicating that p62 associated with SIV Nef and PAK-1 was highly related (Fig. 2, lanes 1 and 2). Additionally, the phosphopeptide maps of p72 from anti-SIV Nef and anti-PAK-1 immunoprecipitates were also similar (Fig. 2, lanes 3 and 4). However, it is important to note that the partial proteolytic cleavage maps for p62 and p72 are distinct (Fig. 2). Similar results were obtained when phosphopeptide maps of p62 and p72 from cells infected with SIV or HIV-1 were compared after partial proteolysis with staphylococcal V8 protease (data not shown). Taken together, these results indicate that p62 and p72 are different molecules.

### Mutants of Nef defective for kinase association do not activate PAK

Previously, we have shown that mutation of two highly conserved arginine residues at positions 137 and 138 of Nef from SIVmac239 abrogates association with the Nef-associated kinase in transient expression assays [22]. These point mutations and a large deletion of *nef* [4] were introduced into the molecular clone of SIVmac239nef+ to produce the two clones SIVmac239nef$^{RR-LL}$ (in which the arginine residues are replaced by lysines) and SIVmac239Δnef, respectively **(Author: OK?)**. The synthesis and stability of the $R^{137}R^{138}$–LL mutant Nef in cells infected with SIVmac239nef$^{RR-LL}$ were indistinguishable from those of the prototype Nef in cells infected with SIVmac239nef+ (data not shown), but the ability of the mutant Nef to associate with and activate PAK was abrogated (Fig. 3, compare lanes 3 and 4 with 5 and 6). The cellular proteins p62 and p72 were phosphorylated by the Nef-associated kinase in cells chronically infected with SIVmac239nef+ (Fig. 3, lanes 3 and 4) but not in cells infected with SIVmac239nef$^{RR-LL}$ (Fig. 3, lanes 5 and 6) or SIVmac239Δnef (Fig. 3, lanes 9 and 10). Nef was not detected by immunoblot analysis of PAK immunoprecipitates from cells infected with SIVmac239nef$^{RR-LL}$ or SIVmac239Δnef (data not shown) **(Author: OK?)**. Interestingly, infection of CEMx174 cells with Nef mutants results in hypophosphorylation of p72 and a loss of basal PAK activity (compare lanes 6 and 10 with lane 4). The mechanism by which this loss of PAK activation occurs during virus infection has not been elucidated. Nevertheless, the hyperphosphorylation of p72 is a marker for the Nef-mediated activation of the PAK-related kinase. These data, based on a combination of genetic and biochemical experiments, demonstrate that the ability of Nef to activate the PAK-related kinase in productively infected lymphoid cells is linked to its ability to bind the PAK-related kinase.

Because Nef from T-cell lines infected with HIV-1 strain SF2 (HIV-$1_{SF2}$) interacts with the Nef-associated kinase

[21], we examined the activation of the PAK-related kinase by HIV-1 infection (Fig. 3, lanes 7 and 8) **(Author: OK? If not, please define HIV-$1_{SF2}$).** *In vitro* kinase assays revealed that the PAK-related kinase was activated in the T-cell line HUT78 chronically infected with HIV-$1_{SF2}$. Thus, the property of Nef-mediated activation of the PAK-related kinase in lymphoid cells is shared between HIV-1 and SIV.

### *In vivo* analysis of SIV Nef mutants

To examine the role of the association between Nef and the PAK-related kinase in viral pathogenesis, we compared virus load and disease potential of SIVmac239nef$^{RR-LL}$ with those of the non-pathogenic clone SIVmac239Δnef and the pathogenic clone SIVmac239nef$^{+}$ in juvenile rhesus macaques. Figure 4 shows that plasma virus load in macaques infected with SIVmac239nef$^{RR-LL}$ (macaques 26767 and 26969) or the non-pathogenic clone SIVmac239Δnef (macaques 26873 and 26939) was below the level of detection in the first 4 weeks after infection, whereas viral antigen was readily detected in this acute stage of infection in plasma from macaques inoculated with SIVmac239nef$^{+}$ (macaques 26084 and 27098). After 4 weeks, there was an increase in the level of viral antigen in plasma from macaques inoculated with SIVmac239nef$^{RR-LL}$. However, in macaques infected with SIVmac239Δnef, plasma antigen remained below the level of detection (Fig. 4).

**Figure 5**

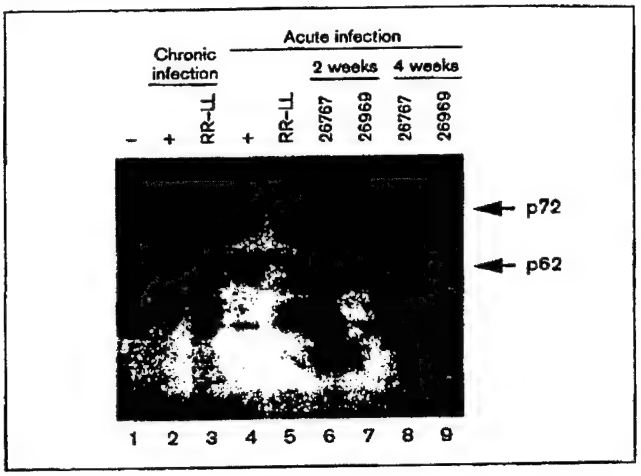


Functional and genetic changes in Nef from macaques infected with SIVmac239nef$^{RR-LL}$. Phenotypic reversion. A polyclonal anti-SIV Nef antibody was used to immunoprecipitate cellular extracts from uninfected CEMx174 cells (–, lane 1), or from CEMx174 cells chronically infected (lanes 2 and 3) or acutely infected (lane 4 and 5) with SIVmac239nef$^{+}$ (+, lanes 2 and 4), SIVmac239nef$^{RR-LL}$ (RR–LL, lanes 3 and 5) or virus recovered 2 or 4 weeks after inoculation from the PBMCs of macaques 26767 (lanes 6 and 8) or 26969 (lanes 7 and 9). *In vitro* kinase assays were performed on all of the immunoprecipitates.

The increase in plasma virus load in the two macaques after 4 weeks of infection with SIVmac239nef$^{RR-LL}$ suggested that the mutation in *nef* may have reverted. At 2 and 4 weeks after inoculation, Nef was analyzed from virus isolated from the peripheral blood mononuclear cells (PBMCs) of both of these animals **(Author: OK?)**. Immunoprecipitation studies revealed a low level of Nef-associated kinase activity from virus recovered at 2 weeks (Fig. 5a, lanes 6 and 7). A striking enhancement in the ability of Nef to associate with the kinase was observed from virus collected at 4 weeks (Fig. 5a, lanes 8 and 9). Thus, the ability of Nef to associate with the kinase had been restored during the acute stage of infection in the two animals inoculated with SIVmac239nef$^{RR-LL}$. Furthermore, both animals exhibited a progressive increase in virus load (Fig. 4) and developed clinical signs of disease (Table 1). To determine the nature of the genetic changes in the viruses showing this phenotypic reversion, DNA was isolated from PBMCs collected from the two SIVmac239nef$^{RR-LL}$-infected macaques at 2 and 4 weeks after inoculation, and the *nef* gene was amplified by the polymerase chain reaction (PCR) and sequenced. All *nef* clones from the 2 week samples had the mutant leucine codons at positions 137 and 138. In contrast, the leucine (mutant) codon at position 138 had been replaced with a codon for arginine in the majority (19/20 PCR clones) of *nef* sequences from both animals at 4 weeks (Table 2) **(Author: OK? Figure 5b is now Table 2)**. Moreover, both

**Table 1**

**Clinical summary**

| Monkey | Virus | Time of death | Number of CD4$^{+}$ cells | Pathological findings |
|---|---|---|---|---|
| 26767 | SIVmac239nef$^{RR-LL}$ | 28 weeks | Decreased | Multiple malignant abdominal and spinal lymphonas. Lymphadenopathy and pneumonia (*Pneumococcus carinii*) |
| 26969 | SIVmac239nef$^{RR-LL}$ | 50 weeks | Decreased | Wasting, diarrhea, lymphadenopathy, splenic lymphoid hyperplasia and multiple opportunistic infections (*Trichonomas, Giardia, Blastocystis hominis* and *Entamoeba coli*) |
| 26084 | SIVmac239nef$^{+}$ | 51 weeks | Decreased | Wasting, diarrhea, lymphadenopathy and pneumonia |
| 27098 | SIVmac239nef$^{+}$ | 87 weeks | Decreased | Wasting, diarrhea and lymphadenopathy |

**Table 2**

**Analysis of viral DNA sequences in macaque PBMCs**

| | Macaque 26969 | | Macaque 26767 | |
|---|---|---|---|---|
| Time after innoculation | Number of clones | Sequence | Number of clones | Sequence |
| 2 weeks | 8 | CTA CTA = L,L | 8 | CTA CTA = L,L |
| 4 weeks | 8 | CTA CGA = L,R | 4 | CTA CGA = L,R |
| | 1 | CTA CTA = L,L | 6 | CGA CGA = R,R |
| | | | 1 | CCA CGA = P,R |
| 8 weeks | 7 | AGA AGA = R,R | 1 | CGA CGA = R,R |
| | 1 | CTA CTA = L,L | 7 | AGA AGA = R,R |

*nef* genes from macaques (26767 and 26969) infected with SIVmac239nef$^{RR-LL}$ were sequenced from DNA isolated from PBMCs collected at 2, 4 and 8 weeks post-inoculation. The codons for amino-acid residues 137 and 138 are shown, and the amino acids they encode are indicated in single-letter code. Numbers indicate the number of nef clones with the respective sequence. The input virus, which was negative for cellular kinase association had the sequence CTA CTA, which encodes leucine (L) residues, at positions 137 and 138, whereas the corresponding sequence of the SIVmac239nef$^{+}$ prototype virus was AGA AGA, which encodes arginine (R) residues.

leucine (mutant) codons were replaced by arginine codons at positions 137 and 138 in several (6/11) of the *nef* clones from macaque 26767. By 8 weeks, almost all (15/16) of the *nef* sequences had the prototype Nef amino acids, with arginines at positions 137 and 138. Interestingly, the reversion of leucine at position 138 to arginine occurred before the leucine-to-arginine reversion at position 137 (Table 2). This pattern of genetic change suggested that the arginine at position 138 in the di-arginine motif is more important for Nef function. This finding is consistent with previous mapping studies with HIV-$1_{SF2}$ Nef, in which the second arginine of the di-arginine motif (positions 109 and 110) was shown to be critical for the association between Nef and the cellular kinase [22]. Although the first arginine residue of the di-arginine motif was not critical for the Nef–kinase association (see macaque 26969 at the 4 week time point in Fig. 5a and Table 2), this residue may be important for maintaining an optimal structure for kinase association.

Clinical signs of disease were monitored to assess the pathogenic potential of these viruses. Macaques 26767 and 26969, which were inoculated with SIVmac239nef$^{RR-LL}$, and macaques 26084 and 27098, which received the prototype virus SIVmac239nef$^{+}$, developed simian AIDS and were euthanized at 28, 50, 51, and 87 weeks after infection, respectively (Table 1). Analysis of the cell-associated virus load in PBMCs and lymph nodes and measurements of cell-free virus in plasma revealed that all four animals contained high amounts of infectious virus in the period immediately prior to and at the time of necropsy (data not shown). Pathological and histopathological examination of several organs collected at necropsy confirmed that these macaques had signs of simian AIDS, including lymphadenopathy and infection with one or more opportunistic pathogens (Table 1). Control macaques inoculated with SIVmac239Δnef had low viral loads and no clinical abnormalities for an observation period of over one year (see also [4]). Taken together, the above results demonstrate that there is strong selective pressure for restoring the ability of Nef to activate PAK *in vivo*, and that activation of a PAK-related kinase correlates with the induction and maintenance of high viral loads and disease progression.

## Discussion

### Nef activates a PAK-related kinase

In this study, Nef from lymphoid cells infected with HIV-1 or SIV was shown to associate with and activate a cellular serine kinase in the PAK family. Nef forms a complex with a PAK or PAK-related protein in infected lymphoid cells as demonstrated by the co-immunoprecipitation of Nef with PAK in PAK immunoprecipitates (Fig. 1b), the re-immunoprecipitation of PAK released from Nef immunoprecipitates (Fig. 1d), and the proteolytic mapping studies of p62 and p72 from Nef and PAK immunoprecipitates (Fig. 2). Furthermore, these findings are supported by genetic studies using a transdominant mutant of PAK65 that blocked Nef-mediated PAK activation in a transient expression assay (data not shown). Recently, a highly conserved motif in the amino-terminus of PAK65 has been shown to be responsible for interacting with the Rac1/Cdc42 GTPases; this regulatory domain is found in a number of cellular kinases [33]. Thus, it is possible that the Nef-associated kinase is either a known PAK, or a kinase that shares the amino terminus of PAK-1. Further studies are required to determine the exact relationship of p62 and p72 with the PAK family of serine kinases.

### Nef-associated kinase and viral pathogenesis

This study demonstrates that a mutation in Nef, which abrogates the association with and activation of a PAK-related kinase, rapidly reverts to a PAK activation-positive phenotype and genotype *in vivo* (Fig. 5). Importantly, this reversion correlates with the induction of high viral loads (Fig. 4) and progression of infected macaques to disease (Table 1). Although a previous study demonstrated that reversion of a premature stop codon in the SIV Nef translation frame correlated with increased virus load and development of disease [4], our report links a specific biochemical function — the ability of Nef to associate with and activate a PAK — to induction of high viremia and pathogenesis. The precise relationship between virus load and the rate of disease progression in macaques infected with molecular clones of SIVmac is not clear. In a previous study, macaques infected with SIVmac239/nef-stop, a clone with a premature translational termination codon in nef, showed a similar range of times until death as macaques infected with SIVmac239nef$^{+}$ [4,34]. Complex

host factors (such as the genetics of the host's immune responses) as well as potential cofactors (such as opportunistic pathogens) can influence virus load and disease progression.

### Activation and Nef functions

Perturbation of a key cell-activation pathway(s) could explain the seemingly disparate roles attributed to Nef, such as downregulation of cell-surface CD4 and enhancement of virion infectivity (reviewed in [1–3]). The effects of Nef on cellular activation may influence the levels of CD4 surface expression and/or transcription of lymphoid cell genes; such changes mediated by Nef may lead to dysfunction of T-helper lymphocytes and subsequent immunodeficiency. The effects of Nef on infectivity may be a consequence of changes in phosphorylation of a viral structural protein(s) during particle assembly, which is a process presumed to involve components of intracellular architecture. For example, Nef activation of PAK may influence, either directly or indirectly, phosphorylation of the matrix protein (MA) in the viral core during virion morphogenesis. Modification of MA by phosphorylation is important for viral infectivity [35–37]. Additionally, the enhancement of virion infectivity and transcriptional activation of the provirus are expected to produce high virus load, which is associated with the depletion of CD4 cells and disease progression [38].

### Nef structure and function

The di-arginine motif, which reverts *in vivo*, is located within the conserved central domain of Nef that is important for kinase association. The importance of the conserved central region of Nef for viral pathogenesis has also been highlighted by the finding that SIVmac clone 8, which encodes a Nef protein with a 4 amino-acid deletion, reverts from an attenuated to a pathogenic phenotype by the duplication of sequences flanking the deletion [39] **(Author: OK?)**. Another intriguing report, which focuses attention on the conserved central region of Nef, describes a group of long-term nonprogressors infected with a strain of HIV-1 that contains a deletion in this region ([40], see also [41]). Further studies are required to precisely define the domain of Nef responsible for PAK activation in the context of the structural model recently deduced by nuclear magnetic resonance spectroscopy [42] and X-ray crystalography [43]. It is intriguing to note that the X-ray crystallographic structure of Nef [43] suggests the importance of the second arginine in the central di-arginine pair of the conserved domain for both HIV-1 [22] and SIVmac239 (this study). Accordingly, knowledge of the structure and function(s) of the PAK(s) interacting with Nef will not only help to elucidate the key intracellular signalling events in the mechanism of viral pathogenesis, but also may be used to design novel drugs that inhibit virus replication and block progression to AIDS.

## Conclusions

This study demonstrates that both HIV-1 and SIV Nef associate with and activate a PAK-related kinase in productively infected lymphocytes. Furthermore, mutations of Nef that abrogate cellular kinase association do not activate PAK. Using the SIV/rhesus macaque model for AIDS pathogenesis, we found that there is a strong selective pressure for the ability of Nef to associate with the PAK-related kinase. Moreover, the reversion of Nef from an PAK activation-defective to a PAK activation-positive phenotype correlates with the induction of high virus loads and disease progression in infected macaques. These results should facilitate the development of novel therapeutic approaches to inhibit HIV replication and prevent AIDS progression.

## Materials and methods

### *Cells, virus and antibodies*

CEMx174, a T-/B-hybrid human lymphoid cell line, permissive for replication of SIVmac clones, was obtained from J. Hoxie. CEMx174 cells chronically infected with SIVmac clones and HUT 78 cell cultures chronically infected with HIV-$1_{SF2}$ were derived as outgrowths of acute infection with the respective virus and were cultured as described previously [21]. Human rhabdomyosarcoma cells (RD-4), obtained from the ATCC, were maintained in Dulbecco's minimal essential medium containing 10% fetal bovine serum (FBS), 1% glutamine, and 1% penicillin–streptomycin (complete DMEM). HIV-$1_{SF11114}$, a primary isolate from a patient classified as a rapid progressor, was kindly provided by J.A. Levy. Polyclonal antisera directed against SIVmac239 Nef was prepared in rabbits (Babco) using recombinant Nef protein produced in *Escherichia coli* (a generous gift from C. Morrow). A monoclonal antibody directed against SIV Nef (17.2) was generously provided by K. Krohn. The rabbit anti-HIV-$1_{SF2}$ Nef antibody was described previously [21]. The anti-rat PAK-1 (PAK) polyclonal antibody, recognizing the amino-terminal 20 amino acids, and the corresponding amino-terminal PAK-1 competitor peptide was purchased from Santa Cruz Biotechnology. The polyclonal antisera to human PAK65 (hPAK65) was generously provided by A. Abo [24]. A monoclonal antibody directed against HIV-1 MA, was obtained from the ATCC.

### Construction of SIVmac239 proviral clones containing mutations in Nef

The $R_{138}R_{139}$–LL mutation, which substitutes arginine codons at positions 137 and 138 of Nef from SIVmac239 for leucine codons [22], and the Δnef mutation [4] were subcloned into the 3′ half of the SIVmac239 provirus. Recombinant SIVmac239nef$^{RR-LL}$ was produced by cotransfecting the 5′ and 3′ proviral halves of SIVmac239 into RD-4 cells and co-cultivating them with CEMx174 lymphoid cells as previously described [44]. Virus released into the culture supernatant was recovered after 7 days and titered by p27gag ELISA (Coulter).

### *Kinase assay, phosphopeptide mapping and immunoblot analysis*

Cell extraction, immunoprecipitation, SDS–PAGE and the *in vitro* kinase assay were performed as described previously [21]. Procedures for partial proteolytic cleavage and phosphopeptide mapping have been described previously [45]. Chymotryptic digestions were performed on $^{32}$P-labeled bands corresponding to p62 and p72 from Nef and PAK immunoprecipitates. For the immunoblot analyses, PVDF filters were washed four times with blocking buffer (Tris-buffered saline containing 0.1% NP40, 0.1% Tween 20 and 0.25% gelatin) and

probed with the anti-SIV Nef monoclonal antibody (17.2). After four washes with blocking buffer, the membranes were incubated with a secondary goat antimouse antibody conjugated with alkaline phosphatase (Southern Biotechnology Associates), washed four times with blocking buffer, and twice with 100 mM Tris–HCl (pH 9.5). A BCIP/NBT detection kit (Vector Laboratories) was used for detection.

*PAK Re-immunoprecipitation analysis*

An *in vitro* kinase assay was performed on HIV-1 Nef immunoprecipitates from HUT78 cells chronically infected with HIV-$1_{SF11114}$ or on SIV Nef immunoprecipitates from CEMx174 cells chronically infected with SIVmac239nef$^+$. The immune complexes were incubated with kinase extraction buffer (KEB, [21]) containing 0.1 % SDS for 1 h. The pellet was washed three times with KEB and resuspended in SDS gel loading buffer (DB). To clear the supernatant of released IgG, the supernatant was incubated twice with protein A–Sepharose. The pellet from the second protein A–Sepharose clearance was washed twice with KEB and resuspended in DB. The supernatant from the second protein A–Sepharose clearance was divided equally into three tubes and incubated with either anti-SIV Nef (control), anti-PAK-1 or anti-hPAK65 antibodies. Immunocomplexes were collected after PAS incubation, washed three times with KEB, and resuspended in DB.

*Infection of rhesus macaques*

All rhesus macaques (*Macaca mulatta*) in this study were housed in accordance with the American Association for Accreditation of Laboratory Animal Care Standards (A3433-01) at the California Regional Primate Research Center (CRPRC). Two colony-bred juvenile rhesus macaques free of simian type D retroviruses, SIV, and STLV were inoculated intravenously with 1000 $TCID_{50}$ ($TCID_{50}$: 50 % of the tissue culture infective dose) of either SIVmac239nef$^+$ or the mutant viruses SIVmac239Δnef or SIVmac239nef$^{RR-LL}$ (******Author: OK?******). The titer of each virus in this study was measured in CEMx174 cells by end-point dilution as previously described [46]. Animals were monitored for weight loss, lymphadenopathy, splenomegaly and opportunistic infections; complete differential blood counts included enumeration of $CD4^+$ and $CD8^+$ T lymphocytes by flow cytometry. Infected macaques that became seriously ill were humanely euthanized and necropsied. Post-mortum examination included histological analysis of all organ specimens. Detection and quantitation of plasma antigenimia (levels of p27gag measured by ELISA), viremia and cell-associated virus load were performed as described previously [46,47] (******Author: OK?******).

*Characterization of virus recovered from monkeys*

Acute infections of CEMx174 cells ($1 \times 10^6$) were performed using 1.0 ml of virus recovered from each monkey (26767 and 26969) at 2 and 4 weeks post-inoculation. After 5 days, infected cells were extracted for immunoprecipitation with an anti-SIV Nef serum and kinase assays were performed. DNA was isolated and purified from 400 µl of peripheral blood drawn from macaques 26767 and 26969 at 2, 4 and 8 weeks after infection with SIVmac239nef$^{RR-LL}$. This DNA served as a template for amplification of *nef* by PCR. In the first round (30 cycles) of PCR amplification the following 5′ and 3′ primers were used for *nef*: 5′–CCAGAGGCTCTCTGCGACCCTAC and 5′–AGAGGGCTTTAAGCAAGCAAGCGTG, respectively. For the second round (30 cycles), the 5′ primer was the same and the 3′ primer (5′–GCCTCTCCGCAGAGCGACTGAATAC) was used. PCR amplifications were carried out in a DNA Thermal Cycler (Perkin-Elmer Cetus) with *Taq* polymerase (Perkin-Elmer). A final product of 992 base-pairs that contained the full-length *nef* gene was produced. The PCR product was cloned into pCRII (Invitrogen) and the DNA was sequenced.

## Acknowledgements

We thank C.J. Weber and E. Antonio for their expert technical assistance in viral load and DNA sequence analyses, and C. Mandell, R. Tarara and D. Canfield for the pathology studies on SIV-infected macaques. J.A. Levy, M. Gardner, M. Peterlin and A. Abo are acknowledged for helpful discussions, reagents and reviewing the manuscript. This work was supported by NIH grants AI38718 (to E.T.S.), AI38532 (to P.A.L.) and AI25128 (to C.C.M.), and by US Army grant DAMD 17-94-J4436 (to P.M.M.). E.T.S. and I.H.K. were supported in part by fellowships from the Universitywide AIDS Research Program of the University of California. I.H.K. was supported in part by a NIH training grant (AI07398). Studies involving rhesus macaques required resources at the CRPRC (base grant RR00169 from the National Center for Research Resources) at the University of California, Davis.

## References

1. Cullen BR: **The role of Nef in the replication cycle of the human and simian immunodeficiency viruses.** *Virology* 1994, 205:1–6.
2. Ratner L, Niederman TMJ: **Nef.** *Cur Top Micro Immunol* 1995, 169–208.

**(****Author: please provide the volume number for this reference****)**

3. Trono D: **HIV accessory proteins: leading roles for the supporting cast.** *Cell* 1995, 82:189–192.
4. Kestler HW, Ringler DJ, Mori K, Panicali DL, Sehgal PK, Daniel MD, *et al.*: **Importance of the nef gene for maintenance of high virus loads and for the development of AIDS.** *Cell* 1991, 65:651–662.
5. Baur AS, Sawai ET, Dazin P, Fantl WJ, Cheng-Mayer C, Peterlin BM: **HIV-1 Nef leads to inhibition or activation of T cells depending on its intracellular localization.** *Immunity* 1994, 1:373–384.
6. De SK, Marsh JW: **HIV-1 Nef inhibits a common activation pathway in NIH-3T3 cells.** *J Biol Chem* 1994, 269:6656–6660.
7. Greenway A, Azad A, McPhee D: **Human immunodeficiency virus type 1 Nef protein inhibits activation pathways in peripheral blood mononuclear cells and T-cell lines.** *J Virol* 1995, 69:1842–1850.
8. Skowronski J, Parks D, Mariani R: **Altered T cell activation and development in transgenic mice expressing the HIV-1 *nef* gene.** *EMBO J* 1993, 12:703–713.
9. Du Z, Lang SM, Sasseville VG, Lackner AA, Ilynskii PO, Daniel MD, *et al.*: **Identification of a nef allele that causes lymphocyte activation and acute disease in macaque monkeys.** *Cell* 1995, 82:665–674.
10. Aiken C, Konner J, Landau NR, Lenburg ME, Trono D: **Nef induces CD4 endocytosis: requirement for a critical dileucine motif in the membrane-proximal CD4 cytoplasmic domain.** *Cell* 1994, 76: 853–864.
11. Foster JL, Anderson SJ, Frazier AL, Garcia JV: **Specific suppression of human CD4 surface expression by Nef from the pathogenic simian immunodeficiency virus SIVmac239open.** *Virology* 1994, 201:373–379.
12. Garcia JV, Miller AD: **Serine phosphorylation-independent downregulation of cell-surface CD4 by nef.** *Nature* 1991, 350:508–11.
13. Chowers MY, Spina CA, Kwoh TJ, Fitch NJ, Richman DD, Guatelli JC: **Optimal infectivity *in vitro* of human immunodeficiency virus type 1 requires an intact nef gene.** *J Virol* 1994, 68:2906–2914.
14. Miller MD, Warmerdam MT, Gaston I, Greene WC, Feinberg MB: **The human immunodeficiency virus-1 nef gene product: a positive factor for viral infection and replication in primary lymphocytes and macrophages.** *J Exp Med* 1994, 179:101–113.
15. Miller MD, Warmerdam MT, Page KA, Feinberg MB, Greene WC: **Expression of the human immunodeficiency virus type 1 (HIV-1) *nef* gene during HIV-1 production increases progeny particle infectivity independently of gp160 or viral entry.** *J Virol* 1995, 69:579–584.
16. Harris MP, Neil JC: **Myristoylation-dependent binding of HIV-1 Nef to CD4.** *J Mol Biol* 1994, 241:136–142.
17. Collette Y, Dutartre H, Benziane A, Ramos-Morales F, Olive D: **Physical and functional interaction of Nef with Lck – HIV-1 Nef-induced T-cell signaling defects.** *J Biol Chem* 1996, 271:6333–6341.
18. Lee CH, Leung B, Lemmon MA, Zheng J, Cowburn D, Kuriyan J, *et al.*: **A single amino acid in the SH3 domain of Hck determines its high affinity and specificity in binding to HIV-1 Nef protein.** *EMBO J* 1995, 14:5006–5015.
19. Saksela K, Cheng G, Baltimore D: **Proline-rich (PxxP) motifs in HIV-1 Nef bind to SH3 domains of a subset of Src kinases and are required for the enhanced growth of Nef+ viruses but not for down-regulation of CD4.** *EMBO J* 1995, 14:484–491.
20. Benichou S, Bomsel M, Bodeus M, Durand H, Doute M, Letourneur F, *et al.*: **Physical interaction of the HIV-1 Nef protein with β-COP, a**

component of non-clathrin-coated vesicles essential for membrane traffic. *J Biol Chem* 1994, **269**:30073–30076.
21. Sawai ET, Baur A, Struble H, Peterlin BM, Levy JA, Cheng-Mayer C: **Human immunodeficiency virus type 1 Nef associates with a cellular serine kinase in T lymphocytes.** *Proc Natl Acad Sci USA* 1994, **91**:1539–1543.
22. Sawai ET, Baur AS, Peterlin BM, Levy JA, Cheng-Mayer C: **A conserved domain and membrane targeting of Nef from HIV and SIV are required for association with a cellular serine kinase activity.** *J Biol Chem* 1995, **270**:15,307–15,314.
23. Manser E, Leung T, Salihuddin H, Zhao ZS, Lim L: **A brain serine/threonine protein kinase activated by Cdc42 and Rac1.** *Nature* 1994, **367**:40–46.
24. Martin GA, Bollag G, McCormick F, Abo A: **A novel serine kinase activated by rac1/CDC42Hs-dependent autophosphorylation is related to PAK65 and STE20.** *EMBO J* 1995, **14**:1970–1978.
25. Bagrodia S, Derijard B, Davis RJ, Cerione RA: **Cdc42 and PAK-mediated signaling leads to Jun kinase and p38 mitogenactivated protein kinase activation.** *J Biol Chem* 1995, **270**:27995–27998.
26. Bagrodia S, Taylor SJ, Creasy CL, Chernoff J, Cerione RA: **Identification of a mouse p21Cdc42/Rac activated kinase.** *J Biol Chem* 1995, **270**:22731–22737.
27. Brown JL, Stowers L, Baer M, Trejo J, Coughlin S, Chant J: **Human Ste20 homologue hPAK1 links GTPases to the JNK MAP kinase pathway.** *Curr Biol* 1996, **6**:598–605.
28. Zhang S, Han J, Sells MA, Chernoff J, Knaus UG, Ulevitch RJ, *et al.*: **Rho family GTPases regulate p38 mitogen-activated protein kinase through the downstream mediator Pak1.** *J Biol Chem* 1995, **270**:23934–23936.
29. Knaus UG, Morris S, Dong HJ, Chernoff J, Bokoch GM: **Regulation of human leukocyte p21-activated kinases through G protein-coupled receptors.** *Science* 1995, **269**:221–223.
30. Leung T, Manser E, Tan L, Lim L: **A novel serine/threonine kinase binding the Ras-related RhoA GTPase which translocates the kinase to peripheral membranes.** *J Biol Chem* 1995, **270**:290512904.
31. Pombo CM, Kehrl JH, Sanchez I, Katz P, Avruch J, Zon LI, *et al.*: **Activation of the SAPK pathway by the human STE20 homologue germinal centre kinase.** *Nature* 1996, **377**:750–754.
32. Nunn MF, Marsh JW: **Human immunodeficiency virus type 1 Nef associates with a member of the p21-activated kinase family.** *J Virol* 1996, **70**: 6157–6161.
33. Burbelo PD, Drechsel D, Hall A: **A conserved binding motif defines numerous candiate target proteins for both CDC42 and Rac GTPases.** *J Biol Chem* 1995, **270**:29071–29074.
34. Kestler H, Kodama T, Ringler D, Marthas M, Pedersen N, Lackner A, *et al.*: **Induction of AIDS in rhesus monkeys by molecularly cloned simian immuno deficiency virus.** *Science* 1990, 248:1109–1112.
35. Bukrinskaya AG, Ghorpade A, Heinzinger NK, Smithgall TE, Lewis RE, Stevenson M: **Phosphorylation-dependent human immunodeficiency virus type 1 infection and nuclear targeting of viral DNA.** *Proc Natl Acad Sci USA* 1996, **93**:367–371.
36. Gallay P, Swingler S, Aiken C, Trono D: **HIV-1 infection of nondividing cells: C-terminal tyrosine phosphorylation of the viral matrix protein is a key regulator.** *Cell* 1995, **80**:379–388.
37. Gallay P, Swingler S, Song J, Bushman F, Trono D: **HIV nuclear import is governed by the phosphotyrosine-mediated binding of matrix to the core domain of integrase.** *Cell* 1995, **83**:569–576.
38. Pantaleo G, Fauci AS: **New concepts in the immunopathogenesis of HIV infection.** *Ann Rev Immunol* 1995, **13**:487–512.
39. Whatmore AM, Cook N, Hall GA, Sharpe S, Rud EW, Cranage MP: **Repair and evolution of nef *in vivo* modulates simian immunodeficiency virus virulence.** *J Virol* 1995, **69**:5117–5123.
40. Deacon NJ, Tsykin A, Solomon A, Smith K, Ludford-Menting M, Hooker DJ, *et al.*: **Genomic structure of an attenuated quasi species of HIV-1 from a blood transfusion donor and recipients.** *Science* 1995, **270**:988–991.
41. Kirchhoff F, Greenough TC, Brettler DB, Sullivan JL, Desrosiers RC: **Absence of intact nef sequences in a long-term survivor with nonprogressive HIV-1 infection.** *New Eng. J Med* 1995, **332**:228–232.
42. Grzesiek G, Bax A, Clore GM, Gronenborn AM, Hu JS, Kaufman J, *et al.*: **The solution structure of HIV-1 nef reveals an unexpected fold and permits delineation of the binding surface for the SH3 domain of hck tyrosine protein kinase.** *Nature Med* 1996, **3**:340–345.
43. Lee CH, Saksela K, Mirza UA, Chait BT, Kuriyan J: **Crystal structure of the conserved core of HIV-1 nef complexed with a src family SH3 domain.** *Cell* 1996, **85**:931–942.
44. Luciw PA, Pratt-Lowe E, Shaw KE, Levy JA, Cheng-Mayer C: **Persistent infection of rhesus macaques with T-cell-line-tropic and macrophage-tropic clones of simian/human immunodeficiency viruses (SHIV).** *Proc Natl Acad Sci USA* 1995, **92**:7490–7494.
45. Sawai ET, Butel JS: **Association of a cellular heat shock protein with simian virus 40 large T antigen in transformed cells** *J Virol* 1989, **63**:3961–3973.
46. Marthas ML, Ramos RA, Lohman BL, Van Rompay K, Unger RE, Miller CJ, *et al.*: **Viral determinants of simian immunodeficiency virus (SIV) virulence in rhesus macaques assessed by using attenuated and pathogenic molecular clones of SIVmac.** *J Virol* 1993, **67**:6047–6055.
47. Unger RE, Marthas ML, Lackner AA, Pratt LE, Lohman BL, Van RK, *et al.*: **Detection of simian immunodeficiency virus DNA in macrophages from infected rhesus macaques.** *J Med Primatol* 1992, **21**:74–81.

# CURRENT BIOLOGY

## Copyright assignment/offprints order form

### a) Assignment of copyright

I hereby transfer to Current Biology Ltd all right, title, and interest to this article, its original artwork and photographs, including the right to claim copyright throughout the world, the right to grant permission to republish the work in whole or in part, and the right to republish the work in whole or in part in any format including print, electronic and transparencies. Authors must seek permission for the use of the article and its original artwork and photographs. Permission is usually granted, provided full credit is given to the original Current Biology Ltd publication.

Signed..... Date.....

### b) Order for offprints

You are entitled to *25 FREE offprints* of your paper. If you wish to order additional offprints, please complete the form below. **It is vital that offprint orders are received before the issue goes to press.** Orders received after this time will be charged at reprint prices, for which quotations will be given; reprint prices are extremely high.

Additional offprints must be ordered in multiples of 25. The cost of additional offprints for papers of up to 8 pages is £50/US$100 for the first batch of 25, and £25/US$50 for each additional batch thereafter; for papers of more than 8 pages the cost is £75/US$150 for the first batch of 25, and £50/US$100 for each additional batch. If you would like a cover on your offprints the cost is an extra £50/US$100 for the first batch of 25 and £25/US$50 for each additional batch. **Payment for offprints MUST accompany this order — ORDERS WITHOUT PAYMENT CANNOT BE FULFILLED.**

### c) Order for slides

If you would like to order colour slides from any figures in your article, the cost is £3.10/US$6.00 for the first pair of slides for each figure. Additional slides cost £1.80/US$3.50 per pair for each figure.

❒ I wish to pay for slides. **(PAYMENT MUST ACCOMPANY THIS ORDER)**

---

### ORDER FORM FOR OFFPRINTS

Name .....

Address to which offprints should be sent:

.....

.....

.....

.....

Telephone: .....

Number of offprints required .....

Number of covers required.....

Number of slides required .....

Total amount payable.....

Signature ..... Date .....

❒ Am Ex ❒ VISA ❒ MasterCard

Card no ☐☐☐☐☐☐☐☐☐☐☐☐☐☐☐☐

Exp date ☐☐☐☐

❒ Cheque/Eurocheque enclosed payable to Current Biology Ltd

£ sterling must be drawn on a UK bank, US$ on a US bank

❒ Please send a receipt

Amount payable for offprints.....

Amount payable for covers.....

Amount payable for slides.....

EC VAT No*: ☐☐☐☐☐☐☐☐☐☐☐☐☐☐☐

*EC customers may be liable to pay VAT at the applicable rate.

---

Please return this form with your corrected proof and payment for offprints to:

Editor, **CURRENT BIOLOGY**, Current Biology Ltd, 34–42 Cleveland Street, London, W1P 6LB, UK

Tel: +44 (0)171 580 8377 Fax: +44 (0)171 580 8167

Current Biology VAT No: GB 466 2477 23 Registered No: 2472262

# APPENDIX 6

# Considerations for the Design of Improved Cationic Amphiphile-Based Transfection Reagents

JOURNAL OF LIPOSOME RESEARCH, 6(3), 545–565 (1996)

# CONSIDERATIONS FOR THE DESIGN OF IMPROVED CATIONIC AMPHIPHILE-BASED TRANSFECTION REAGENTS

Michael J. Bennett[1], Alfred M. Aberle[1], Rajiv P. Balasubramaniam[1], Jill G. Malone[2], Michael H. Nantz[1], Robert W. Malone[2]
Departments of Chemistry[1] and Medical Pathology[2],
University of California, Davis
Davis, CA 95616

## ABSTRACT

Cationic amphiphiles (cytofectins) are widely used for the transfection of cultured cells, and may become useful for the development of genetic medicines. Although fundamental research focused on clarification of physicochemical structure/biologic function correlations has been limited, general principles relating to optimization of cytofectin structure are beginning to emerge. We review these general conclusions and suggest considerations which may assist in the development of improved compounds. Data which relates to formulation is also discussed. The formulation studies address the tendency of high concentration cytofectin:polynucleotide complexes to precipitate. From these observations we postulate that a thermodynamically stable product can be formed by sonication with heating of cytofectin:polynucleotide complexes, and that this process reduces the kinetically driven aggregation and precipitation which currently complicates many *in vivo* studies.

## INTRODUCTION

Strategies to introduce exogenous polynucleotides into cells have been the foundation for a variety of proposed therapeutics including gene therapies and genetic immunization. The therapeutic potential of gene transfer seems limited only by the imagination of the scientific community. Unfortunately, the potential of gene transfer-based research to improve human health will be restricted unless improved methods are developed for *in vivo* delivery of foreign genetic material into cells and tissues. Currently used viral and non-viral transfection reagents have been

compromised by one or more problems pertaining to: 1) associated health risks, 2) immunological complications, 3) inefficient *in vivo* transfection efficiency, and 4) direct cytotoxicity. The development of safe and effective polynucleotide-based medicines will require improved solutions which address these problems.

Cationic amphiphiles are currently regarded as an alternative to viral vector technology for *in vivo* polynucleotide delivery. Cationic lipid-based reagents avoid many of the health and immunological concerns associated with viral vectors. In a practical sense, cationic amphiphile-based delivery agents are relatively simple to use, and offer unparalleled flexibility in the nature of the material that can be delivered. Typically, cationic lipid complexes are prepared by mixing the cationic lipid (cytofectin) with the desired DNA (1), RNA (2), antisense oligomer (3), or protein (4) to yield active particles; in contrast to the laborious recombinant DNA and cell culture manipulations which are typically required to produce virus-derived delivery agents.

Since the original report (1) that liposomes comprised of equal amounts of the cytofectin DOTMA (N-[1-(2,3-dioleyloxy)propyl]-N,N,N-trimethylammonium chloride) and neutral lipid DOPE (dioleoyl phosphotidylethanolamine) spontaneously associate with DNA to form efficient transfection complexes, the technology has advanced incrementally. There have been few cytofectins developed which have improved upon the *in vivo* activity of the prototypic agent DOTMA. This lack of progress may reflect funding priorities which have focused on the application of cationic lipid technology to biologic problems, rather than research focusing on principles which effect cytofectin-mediated gene delivery. Specifically, studies focused on the mechanism(s) involved in cytofectin actions, barriers to cytofectin-mediated *in vivo* gene delivery, and clarification of cytofectin structure/activity relationships would facilitate the development of improved cationic lipid-based delivery reagents. While research into the mechanism responsible for cationic amphiphile-mediated gene delivery is ongoing in a number of laboratories (5,6,7), even the most basic aspects of the mechanism of action of cytofectins (the relative contributions of direct cytoplasmic membrane fusion and endocytosis) remain unresolved.

Currently, several cationic amphiphile preparations are commercially available, and new analogs have been published. However, these agents are frequently reported without comparison to existing compounds, and therefore it is difficult to derive insights into the relationship of structural motifs to polynucleotide

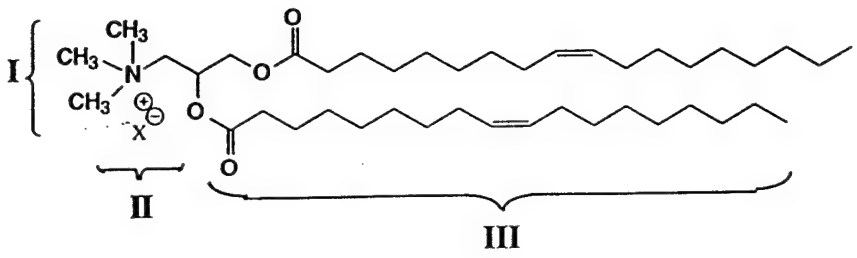


**Fig. 1 Identification of cytofectin structural domains.** Cytofectins can be divided into three structural domains: a cationic polynucleotide binding domain (**I**), a negatively charged counter-ion (**II**), and a hydrophobic domain (**III**).

transfection. This difficulty has been exacerbated by the variability in: 1) transfected cell types exploited in the initial report, 2) reporter genes used to characterize transfection, 3) methods for reporting biologic response (typically reporter protein expression) and 4) specific expression vector design. In addition, there have been few reports which describe the effects of alternative formulation methods. Paradoxically, the relative lack of such fundamental information implies that significant improvements in cytofectin-mediated gene transfer technology may be achieved by further systematic study.

The intent of this manuscript is to review and summarize data derived from studies of cationic lipid structure/activity relationships and cationic amphiphile/polynucleotide formulation. It is our hope that this information will facilitate the development of future cationic lipid-based gene delivery reagents and formulations, thereby facilitating the development of polynucleotide medicines for direct *in vivo* administration.

## CYTOFECTIN STRUCTURAL DOMAINS

Cytofectins can be defined by three principal structural motifs (Figure 1): a cationic polynucleotide binding domain (**I**), a negatively charged counter-ion (**II**), and a hydrophobic domain (**III**). The chemical nature of these domains dictates the biophysical properties exhibited by the cytofectin. Thus, structural modifications within each motif can result in significant alterations in the behavior of pharmaceuticals containing these amphiphiles. For this reason, researchers have

attempted to correlate biophysical properties, compound structure, and functional assessments of polynucleotide transfection. Such structure/activity studies have begun to establish general principals which can be applied to the design of cytofectin-based polynucleotide delivery pharmaceuticals.

## Polar Domain Structural Considerations

In general, various functionalities have been incorporated into cytofectin polar domains. Many of these functionalities are known to modulate the binding and condensation of polynucleotides. These polynucleotide binding domains, usually comprised of nitrogen-based groups, are cationic either as a consequence of their basicity in aqueous solutions, or via N-alkylation to yield quaternary amines. Researchers have prepared several cytofectins which contain a variety of nitrogen-based functionality including: tetraalkylammonium (1,8,9), polyammonium (10,11,12), monoalkylammonium (13), and amidine-based (14). Such functionality may have an influence on the efficiency with which polynucleotides interact with cationic lipid particles, the interactions between lipid/DNA complexes and biological membranes, and the mechanism(s) by which these complexes deliver polynucleotides into the cells. Therefore, studies correlating polar domain chemical structure and physical properties with transfection activity would be predicted to clarify the role of polar domain hydration and intermolecular bonding on polynucleotide delivery.

A number of investigations into polar domain structure/activity relationships have been reported. Previous studies have focused on the optimization of the alkyl chain length separating the lipidic domain and polynucleotide binding group (15,16); correlations between cationic functionality (tetraalkylammonium vs. trialkylammonium), protein kinase C activity, and transfection efficacy (16); and correlations between headgroup charge density and transfection activity (17). Subsequently, research in our laboratories has been conducted to explore the correlations between transfection activity and functional modifications of the tetraalkylammonium moiety used to bind anionic regions of DNA, RNA, and related polymers. The decision to use tetraalkylammonium-derivatized cytofectins for this study was based on unpublished observations that tertiary ammonium analogs of DOTMA-related compounds are not active transfection agents.

Evidence supporting the hypothesis that modifications in cytofectin headgroup structure (and associated physical properties) can influence transfection

activity comes from research performed by Felgner *et al.* (9) and our laboratories (18,19). These studies have shown that cytofectins which incorporate a hydroxyethyl-derivatized tetraalkylammonium group in their polar domain demonstrate enhanced transfection activity when compared to analogs which do not incorporate such groups (e.g.. DORI vs. DOTAP).

We postulate that variations in the chemical composition of the tetraalkylammonium group of cytofectins might effect transfection activity by: 1) influencing cationic liposome/polynucleotide interactions during formulation, 2) altering interactions between cationic liposome/polynucleotide complexes and cell membranes, 3) altering pathways by which these complexes enter cells, 4) altering intracellular trafficking of lipid:polynucleotide complexes, and 5) altering the disassociation of the lipid:polynucleotide complex. We hypothesize that the covalent attachment of select functional groups, like the hydroxyethyl group, to the ammonium moiety can influence both lipid surface hydration and the effective charge of ammonium group. These effects can alter the cytofectins' transfection activity by influencing one or more of the above processes.

Surface hydration may be one important property by which modifying the polar domain may alter cytofectin transfection activity. The degree of lipid surface hydration can influence intermolecular lipid interactions both prior to and following addition of polynucleotide. Such effects might occur via a variety of interactions. The addition of alkyl groups of increasing chain length to the ammonium group could weaken intermolecular lipid interactions by increasing the cross-sectional area of the headgroup (steric effects). The presence or absence of functional groups which can participate in hydrogen bond formation as either acceptors or donors will effect hydration, interaction with polynucleotide, and bonding to adjacent lipids (e.g. cytofectins, DOPE or cellular lipids). The inclusion of electron withdrawing functionality may influence the effective cationic charge of the binding domain through the inductive effect. However, these complex interactions make it difficult to identify the principal factors influencing cytofectin transfection activity. An example is the inclusion of functional groups capable of hydrogen bonding. In this example, either stronger or weaker lipid-lipid interactions might arise as a consequence of 1) intermolecular hydrogen bonding or 2) increased headgroup hydration respectively. Thus, we chose to empirically analyze the effect of such alterations on the DNA transfection activity.

In order to test hypotheses pertaining to lipid surface hydration and effective cationic charge, a panel of cationic amphiphiles (Figure 2) were prepared by simple

A.

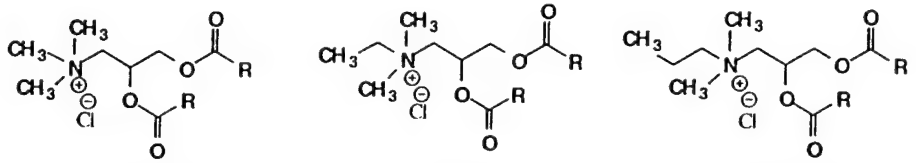

DMTAP DMEAP DMPAP

Increase in cross-sectional area of polar domain

B.

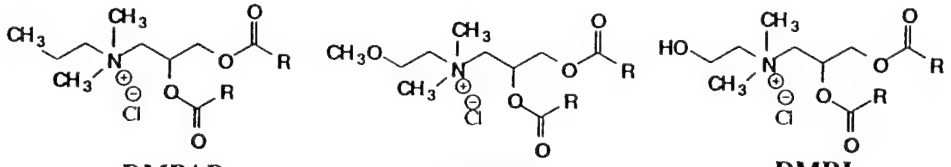

DMPAP DMMEP DMRI

Increase in available hydrogen bonding modes

C

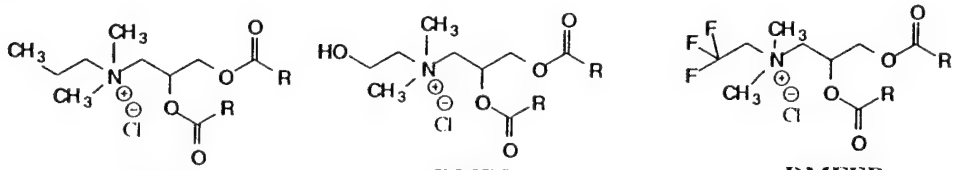

DMPAP DMRI DMFEP

Increase in inductive influence on charged center

$R = -(CH_2)_{15}CH_3$

**Fig. 2** **Experimental design for polar domain analysis.** Cytofectins are grouped so as to determine what influence polar domain cross-sectional area (**A**), hydrogen bonding (**B**), or effective positive charge (**C**) has on cytofectin transfection activity.

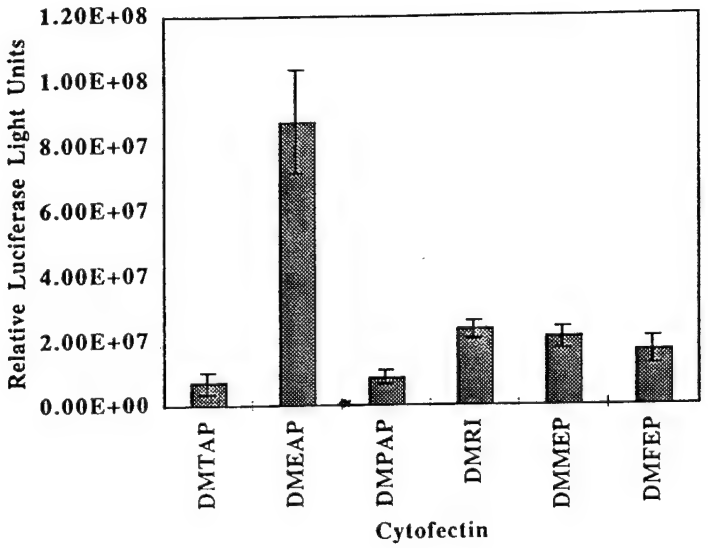


**Fig. 3 Comparison of cytofectin polar domain structure to transfection activity in NIH 3T3 cells.** Liposome formulations containing a 1:1 mole ratio of Cytofectin and DOPE were mixed with 1 µg of pNDCLUX plasmid DNA to give a 2:1 molar charge ratio (lipid charge to DNA phosphate). The resultant complex was placed directly on to the cell surface. Cell lysates obtained 48 hours after transfection were analyzed for luciferase activity. Each data point reflects the mean value of total light units derived from four transfections and the standard deviation from this mean.

N-alkylation of N,N-dimethyl-1,2-dimyristoyloxy-3-aminopropane with the corresponding alkyl halide, using a procedure analogous to that used by Felgner *et al.* (9). Lipid thin-films containing these amphiphiles and an equal molar amount of DOPE were hydrated using sterile deionized water, mixed with the plasmid DNA pNDCLUX (20), (encoding the *P. pyralis* luciferase) and the resulting complexes were used to transfect NIH 3T3 murine fibroblast cells. The experimental design is outlined in Figure 2. Based on the data obtained from this experiment (Figure 3), the following conclusions can be made: 1) Of the lipids selected to examine correlations between lipid polar domain cross sectional area and transfection activity, DMEAP had the highest levels of plasmid transfection activity. 2) Of the lipids selected to test the influences of hydrogen bonding, both the methyl ether containing lipid DMMEP and the hydroxyethyl containing lipid showed a 2-fold

enhancement over DMPAP, which has no hydrogen bonding capabilities. We observed no correlation between the number or modes of hydrogen bonding (acceptor vs. donor). Correlations between the increasing electron withdrawing nature of the functionality on the beta carbon to the ammonium group were inconclusive. Biophysical characterization of the fluidity and hydration of lipid films prepared with these compounds are in progress, as are *in vivo* activity analyses.

## Counterion Considerations

All positively charged cytofectin polar domains incorporating monoalkylammonium, polyammonium, or tetraalkylammonium-based functionality, have an associated negatively charged counterion. Monoalkylammonium and polyammonium-containing lipids typically have one or more hydroxide counterions as a consequence of ammonium salt formation resulting from the basicity of the corresponding primary, secondary, or tertiary amine in aqueous media. Tetraalkylammonium-based cytofectins acquire their negatively charged counterion when the ammonium salt is formed as a result of N-alkylation.

As a result of the association of the negatively charged counterion with the positively charged polynucleotide binding domain, we believe that the chemical nature of the counterion may effect the physicochemical properties of cytofectins. Specifically, the counterion could influence lipid surface hydration, vesicle fluidity, and lipid polymorphism. Therefore, the counterion could also influence the transfection activity of cytofectins.

In order to study possible counterion influences on cytofectin-mediated transfection activity, a panel of DOTAP (N-[1,2,3-dioleoyloxy)propyl]-N,N,N-trimethylammonium) analogs, differing only in the anionic counterion, were prepared using ion exchange chromatography (20). The series of counterions (Table 1) were selected so that direct comparisons between anion-water interactions could be made. Previous studies have shown that there is a correlation between membrane behavior in various salt solutions and the nature of the anions categorized according to the Hofmeister series (21, 22, 23), which groups ions as either kosmotropes (water structuring) or chaotropes (water destabilizing) (Table 1).

**TABLE 1**

**Summary of cytofectin counterions**

| Kosmotropes | Chaotropes |
|---|---|
| $HSO_4^{-1}$ | $I^-$ |
| $CF_3SO_3^{-1}$ | $Br^-$ |
| $H_2PO_4$ | $Cl^-$ |
| $SO_4^{-2}$ | $CH_3C(O)O^-$ |

Transfection analyses using these cytofectins were performed *in vitro* (NIH 3T3 murine fibroblasts), and *in vivo* (intratracheal instillation into mice) with excellent correlation between the *in vitro* (Figure 4) and *in vivo* data (Figure 5). One may infer that the trends observed in these screenings may be applicable to a variety of cell types. Furthermore, the data suggests that the highly delocalized polar kosmotropic oxyanions, bisulfate and trifluoromethanesulfonate (triflate), promote the highest levels of luciferase expression. Among the halogens examined, the DOTAP iodide analog was the most active. It is believed that iodide most closely associates with the alkylammonium headgroup due to electrostatic interactions, while oxyanions competitively bind water away from the lipid surface. Thermodynamic arguments have suggested that lipid:solvent interactions directly influence lipid polymorphism. Thus, there may be an exclusion of water and closer interchain packing. In conclusion, these results indicate that incorporation of anions which can facilitate dehydration of the cytofectin polar domain leads to increased cytofectin transfection activity .

## Hydrophobic Domain Structural Considerations

There are two types of hydrophobic domains which have been used in the design of cytofectins; sterol-based and di-acyl/alkyl-based domains. The hydrophobic domain, which clearly serves as a scaffold from which a lipid bilayer

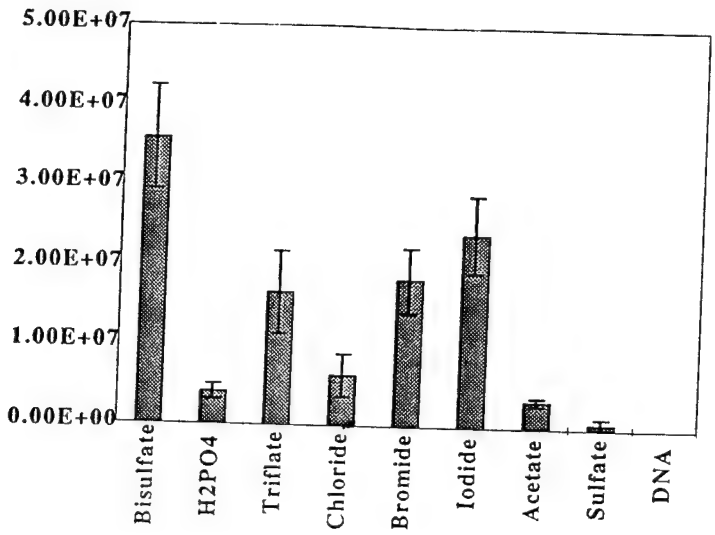


**Fig. 4 Comparison of cytofectin counterions to transfection activity in NIH 3T3 cells.** Liposome formulations containing a 1:1 mole ratio of Cytofectin and DOPE were mixed with 1 μg of pNDCLUX plasmid DNA to give a 2:1 molar charge ratio (lipid charge to DNA phosphate). The resultant complex was placed directly on to the cell surface. Cell lysates obtained 48 hours after transfection were analyzed for luciferase activity. Each data point reflects the mean value of total light units derived from four transfections and the standard deviation from this mean.

structure is built, also modulates bilayer fluidity and lipid polymorphism. Increased bilayer fluidity can lead to more efficient formation of lipid:DNA complexes and enhanced fusion of cytofectin:DNA complexes with cell or endosomal membranes, which is likely to be a key mechanistic step of the transfection process. While the contribution of sterol hydrophobic domains to bilayer fluidity is primarily dependent on the relative concentration of the sterol in the lipid particle, it is the chemical structure of the aliphatic groups contained in di-acyl/alkyl-based lipids which dictate their contribution to membrane fluidity.

It has been previously stated that there is a direct correlation between cytofectin transfection activity and transfection lipid bilayer fluidity. This hypothesis was originally forwarded by Akao *et al.* (24), and suggests that one primary requirement of an amphiphile for DNA transfection is that the $T_c$ (phase transition temperature between the gel and liquid crystalline phases) be lower than

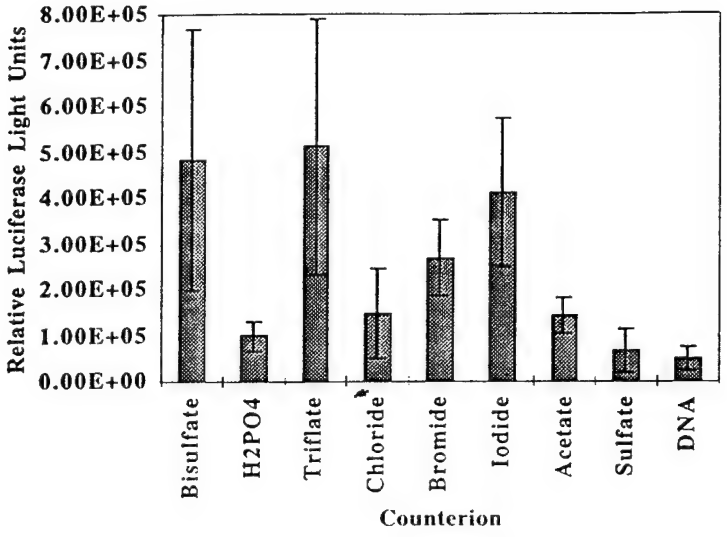


**Fig. 5 Comparison of cytofectin counterions to *in vivo* transfection activity in Balb-C lung.** Balb-C mice were transfected with lipid/DNA complexes formed from mixing pNDCLUX plasmid DNA with various cytofectins (2:1 lipid to DNA phosphate charge ratio). Intratracheal installations of cytofectin:DNA complexes were performed as described elsewhere (19). Results are summarized in bar graph form as the mean (n=4) and standard deviation of total luciferase light units obtained from trachea/lung blocks lysed 48 hours after treatment with 20 μg of DNA

37 °C, so that the transfection lipid assumes a fluid liquid crystalline state at cell culture temperatures. Research supporting this hypothesis (9, 24) has relied on analysis of a limited number of cytofectin analogs and cell lines. In interpreting such studies, we believe it is important that results be obtained using multiple cell lines or tissues before drawing general conclusions correlating hydrophobic domain structure, bilayer physical properties, and transfection activity (19). There is no evidence that the fluidity of neat cytofectin lipids predicts the fluidity of lipidic structures when bound to polynucleotide, and hence such studies will be required to resolve this issue.

The bilayer fluidity of liposomes containing di-acyl/alkyl-based cytofectins can be modified by manipulating the symmetry, chain length, and saturation of the aliphatic groups contained in these lipids. In order to understand the relationships between cytofectin hydrophobic domain structure and transfection activity, we

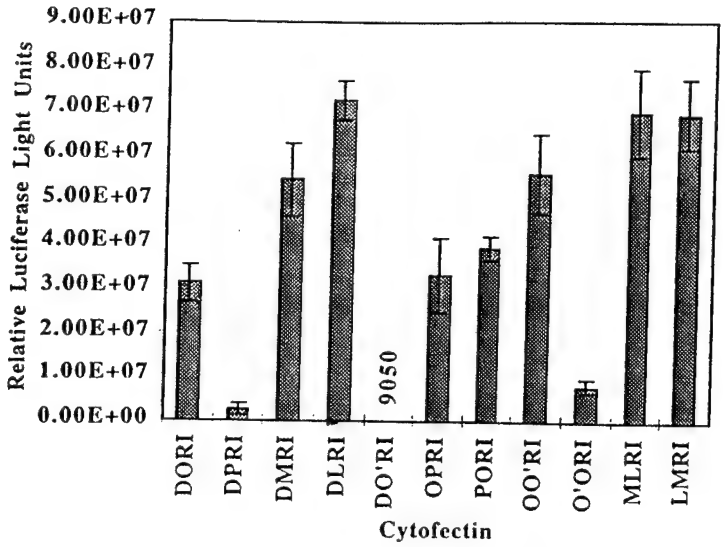


**Fig. 6** **Comparison of cytofectin hydrophobic structure to transfection activity in NIH 3T3 cells.** Liposome formulations containing a 1:1 mole ratio of Cytofectin and DOPE were mixed with 1 μg of pCMVL plasmid DNA to give a 2:1 molar charge ratio (lipid charge to DNA phosphate). The resultant complex was placed directly on to the cell surface. Cell lysates obtained 48 hours after transfection were analyzed for luciferase activity. Each data point reflects the mean value of total light units derived from four transfections and the standard deviation from this mean.

prepared a panel of cytofectins differing only in the composition of the aliphatic groups contained in the hydrophobic domain (19). Cytofectins examined in this study included compounds with both symmetric and dissymmetric hydrocarbon side chains which varied in length from C18:1 to C8:0. A previous report (9) also examined a similar series of cytofectins. However, only symmetric hydrocarbon side chains varying in length form C18:1 to C14:0 were examined using a single cell line (COS-7). This previous study indicated that the dimyristyl-containing compound DMRIE was most effective for DNA transfection of COS-7 cells. Since shorter side chains were not examined, the minimal effective acyl chain length was not defined. Cationic liposomes containing these cytofectins were formulated using 1:1 molar ratios of the cytofectin and DOPE. Transfection studies using NIH 3T3 murine fibroblast cells (Figure 6), CHO cells, and a cultured respiratory

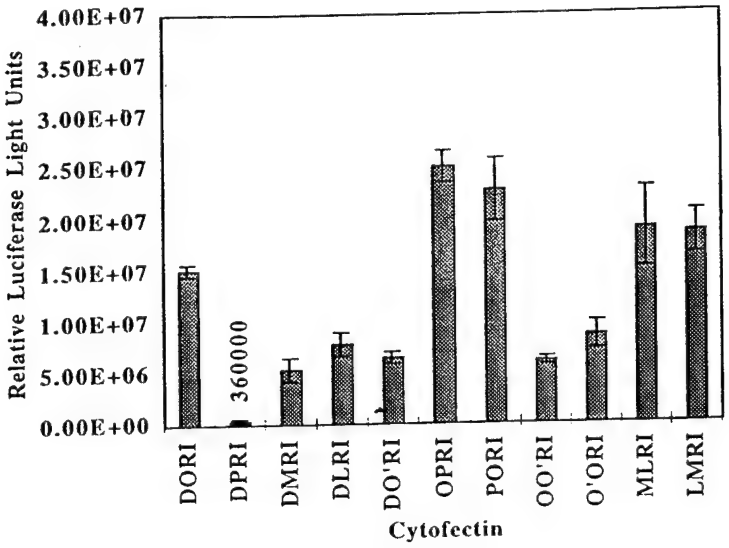


**Fig. 7 Comparison of cytofectin hydrophobic structure to transfection activity in human bronchial epithelial cells (16HBE14o-).** Liposome formulations containing a 1:1 mole ratio of Cytofectin and DOPE were mixed with 1 μg of pCMVL plasmid DNA to give a 2:1 molar charge ratio (lipid charge to DNA phosphate). The resultant complex was placed directly on to the cell surface. Cell lysates obtained 48 hours after transfection were analyzed for luciferase activity. Each data point reflects the mean value of total light units derived from four transfections and the standard deviation from this mean.

epithelial cell line (16HBE14o-) (Figure 7) revealed some intriguing observations. These are: 1) no single symmetric or dissymetric analog was most effective for DNA transfection of either cell line examined, 2) dissymmetric lipids resulted in levels of luciferase expression that were equal to or better than the most active symmetric lipid analogs, 3) dissymmetric cytofectins with shorter side chains (C12:0, C14:0) were among the most active lipids in the cell lines screened, and 4) the dioctanoyl (di C8:0) compound was generally the least active, indicating that the effective lower limit of fatty acyl chain length is defined at C(12).

## FORMULATION CONSIDERATIONS

Cytofectins spontaneously form transfection complexes with a variety of biological polymers upon mixing in aqueous solvent. The mixing or formulation

**TABLE 2**

**Summary of symmetric and dissymmetric cytofectins.**

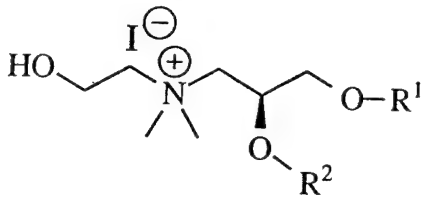


| Cytofectin | R1 | R2 |
|---|---|---|
| DORI | Oleoyl (18:1) | Oleoyl (18:1) |
| DPRI | Palmitoyl (16:0) | Palmitoyl (16:0) |
| DMRI | Myristoyl (14:0) | Myristoyl (14:0) |
| DLRI | Lauroyl (12:0) | Lauroyl (12:0) |
| DO'RI | Octanoyl (8:0) | Octanoyl (8:0) |
| OPRI | Oleoyl (18:1) | Palmitoyl (16:0) |
| PORI | Palmitoyl (16:0) | Oleoyl (18:1) |
| OO'RI | Oleoyl (18:1) | Octanoyl (8:0) |
| O'ORI | Octanoyl (8:0) | Oleoyl (18:1) |
| MLRI | Myristoyl (14:0) | Lauroyl (12:0) |
| LMRI | Lauroyl (12:0) | Myristoyl (14:0) |

protocols used to prepare active transfection complexes currently involve optimization of; 1) the ratio of cationic lipid:neutral lipid, 2) solvent type, and 3) the molar ratio of cationic charge:polynucleotide phosphate charge.

Many optimized formulations incorporate Dioleoyl phosphatidylethanolamine (DOPE) along with the cytofectin prior to mixing with DNA, although the high activity frequently observed with neat DOTAP indicates that DOPE is not always required. DOPE is known to be a strong destabilizer of lipid bilayers (25), and hence can enhance the intrinsic fusogenic properties of many cytofectins. Empirical optimization of cytofectin:DOPE molar ratio for various cell lines, tissues, and cytofectins can result in marked enhancement of transfection activity for the chosen application. In our hands, the optimized molar ratio has ranged from 9:1 to 1:2 (cytofectin:DOPE).

Cell culture experiments typically employ a formulation solvent consisting of either the media in which the cell line is cultured, or OptiMem (Gibco/BRL), a serum-free media which is enriched in factors including transferrin and various growth factors. The enhanced transfection activity which can be observed with OptiMem may reflect incorporation of the added biologically active agents into the lipid:polynucleotide complex. In such cases, binding to cell surface may be facilitated by specific ligand:receptor interactions. Complexes are typically prepared for in vivo administration using either water for injection or isotonic solvents such as physiologic saline. In contrast to cell culture results, solvent-specific enhancement has not been reported.

Molar cytofectin:polynucleotide phosphate charge ratio employed during formulation is frequently not reported, but typically ranges from 1:1 to 4:1 for cultured cells. Protocols for *in vivo* application, and particularly for pulmonary transfection, frequently employ strikingly different molar charge ratios. Yoshimura (26) first described the use of very low cytofectin:DNA charge ratios for pulmonary delivery, and performed an *in vivo* charge titration ranging from approximately 1:2.5 to 1:35. Optimal activity was obtained using the 1:35 ratio of cytofectin:DNA charge. This *in vivo* protocol also employed up to 1.4 milligram of plasmid/200 microliter injection, a 1,000 to 10,000 fold higher concentration of polynucleotide than is typically used for transfection of cultured cells. As the direct injection of free plasmid DNA into murine lung can result in significant levels of reporter gene expression (26, 27,19), it is conceivable that complexes formulated with very low cytofectin:DNA ratios are not the active principle in the observed pulmonary transfections. We hypothesize that the transfection activity observed by Yoshimura reflects the activity of unbound or minimally bound polynucleotide. In this case, the enhanced transfection activity which was observed upon adding small quantities of lipofectin to concentrated plasmid DNA may reflect partial protection from nucleases, rather than lipid-mediated transfection which occurs in cell culture. We have observed that similar charge titration experiments employing 20 micrograms of plasmid DNA/200 microliters result in optimized cytofectin:DNA charge ratios of 2:1 to 3:1, depending on cytofectin type and DOPE ratio (unpublished observations).

High concentration lipid:DNA complexes (2:1 lipid:DNA charge ratio, 0.1 mg/ml or greater) are relatively insoluble, and tend to precipitate during formulation (Table 3). We have observed that such precipitates are relatively inactive as

**TABLE 3**

**Effect of Formulation with Heating and Sonication on Cytofectin:DNA Particle Size.** Dynamic light scattering (DLS) estimates of sonicated versus unsonicated DNA-lipid complexes for increasing plasmid DNA concentrations at a fixed 2:1 lipid-DNA charge ratio. Sizing experiments were designed to mimic murine lung transfection conditions. The complex was sonicated briefly (30" to 2 minutes) using a bath sonicator (Laboratory equipment, Hicksville NY) at 56° C until visible aggregates were dispersed. DLS experiments were performed using a Brookhaven Instruments BI-90 particle sizer at 25 °C, sampled continuously for five minutes and analyzed by the methods of cumulants. No significant shift in particle size distribution was observed over time (data not shown).

| | Sonicated | | Unsonicated | |
|---|---|---|---|---|
| [DNA] mg/ml | effective diameter | polydispersity index | effective diameter | polydispersity index |
| 0.1 | 400 | 0.268 | 3900 | 1.548 |
| 0.2 | 300 | 0.019 | 2800 | 1.413 |
| 0.4 | 288 | 0.092 | 5700 | 3.682 |
| 0.8 | 334 | 0.154 | 2268 | 2.094 |
| 1.0 | 929 | 0.685 | 2110 | 1.800 |

transfection agents both in cell culture and *in vivo*. Furthermore, even apparently stable lipid:polynucleotide emulsions can precipitate when stored at room temperature for prolonged periods. Vortex mixing and heating tend to facilitate the precipitation of high concentration complexes. The precipitation of cytofectin:DNA complexes represents a significant obstacle to the development of cytofectin medicines. We hypothesize that these precipitates represent a kinetic product of lipid:DNA association rather than the thermodynamically stable product which forms upon mixing at low concentration. This hypothesis follows from the following model: 1) During initial lipid:DNA binding, DNA induces lipid reorganization (polynucleotide coating), resulting in DNA condensation and/or particle restructuring (complex maturation- formation of the thermodynamic product). There are energetic barriers to such restructuring which reflect lipid:lipid

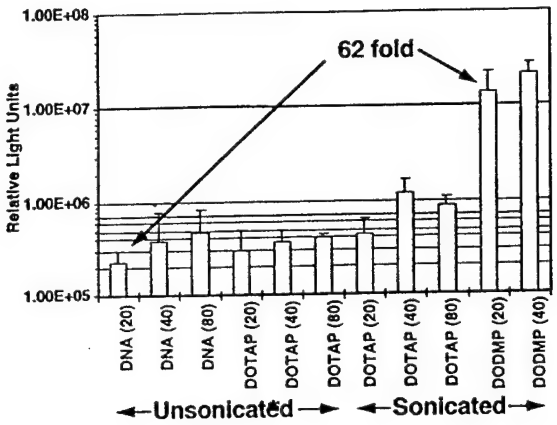


**Fig. 8 The effects of formulation conditions on luciferase expression in murine lung.** An overall increase in luciferase expression was noted for sonicated (DOTAP.$HSO_4$)-DNA complexes with increasing DNA concentrations at a fixed 2:1 charge ratio. Sonicated complexes were prepared as described previously (see Table 3). Naked DNA has been provided as a control comparison. Included are examples illustrating the effect of sonication with heating on both the active lipid DODMP·Cl as well as DOTAP·$HSO_4$, a widely used cationic transfection lipid.

interactions, displacement of the counterion during polynucleotide binding, lipid:polynucleotide binding, and alterations in polynucleotide hydration during condensation. Therefore, the rate of such reorganization will be a function of lipid structure, counterion type, polynucleotide structure, and temperature. 2) Partially reorganized complexes are subject to aggregation upon collision in solution. This aggregation (eg. cross linked proto-complexes- a kinetic product) may be mediated via binding of uncoated polynucleotide by uncomplexed cytofectin present on the surface of the colliding particle. Therefore, we predict that aggregation will be a function of concentration, system energy (temperature, vortexing), solution viscosity, and time.

Methods for overcoming the aggregation and precipitation of high concentration complexes would greatly facilitate preparation of cytofectin-based genetic medicines. Unfortunately, adding thermal energy would be predicted to both facilitate "maturation" and to increase diffusion within the system, thereby increasing collision rate and energy. We hypothesize that heating combined with

either an increase in system viscosity or use of sonication to rapidly resolve aggregates prior to restructuring and precipitation will favor formation of the thermodynamic product. As demonstrated in Table 3, the combination of heating with sonication does result in the formation of stable, smaller lipidic particles. Furthermore, this process appears to enhance the pulmonary transfection activity of a range of lipids (Figure 8), including the relatively inactive compound DOTAP. Additional experimentation will be required to test these hypotheses and inferences, and may yield additional improvements in formulation protocol.

## CONCLUSIONS

Although cytofectins may become useful for the development of polynucleotide medicines, current limited understanding of the interactions between physicochemical structure, mechanism of action, and biologic activity in cultured cells and intact tissues has limited the application of this promising technology. Research which integrates novel compound synthesis, biophysical analysis, and testing in a range of cell types and animal models can yield insights into cytofectin design and formulation, and can significantly improve cytofectin-mediated transfection. Further mechanistic and functional analyses are likely to result in continuing improvements in cytofectin efficacy for a range of applications.

## ACKNOWLEDGMENTS

This research was supported by grants from the Cystic Fibrosis Foundation (S883, S884), the California Tobacco Related Disease Research Program (4KT-0205), Promega Corporation (93K188), and DAMD (17-94-J4436). We thank Professor John Crowe and Dr. Lois Crowe (Department of Cellular and Molecular Biology, University of California, Davis) for their generosity in providing the use of the DSC, DLS, and numerous useful discussions. We would also like to thank Dr. Gary Rhodes and Phillip Montbriand for plasmid construction, Zachary Malone for his patience, and Drs. Al Fasbender, Phil Felgner, and Frank Szoka for their comments.

## REFERENCES

1. Felgner, P. L., Gadek, T. R., Holm, M., Roman, R., Chan, H. W., Wenz, M., Northrop, J. P., Ringold, G. M. and Danielsen, M. 1987. Lipofection: a highly efficient, lipid-mediated DNA-transfection procedure. Proc. Natl. Acad. Sci. U.S.A. 84(21): 7413-7.

2. Malone, R. W., Felgner, P. L. and Verma, I. M. 1989. Cationic liposome-mediated RNA transfection. Proc. Natl. Acad. Sci. U.S.A. 86: 6077-6081.

3. Chiang, M. Y., Chan, H., Zounes, M. A., Freier, S. M., Lima, W. F. and Bennett, C. F. 1991. Antisense oligonucleotides inhibit intercellular adhesion molecule 1 expression by two distinct mechanisms. J. Biol. Chem. 266(27): 18162-71.

4. Walker, C., Selby, M., Erickson, A., Cataldo, D., Valensi, J. P. and Van Nest, G. V. 1992. Cationic lipids direct a viral glycoprotein into the class I major histocompatibility complex antigen-presentation pathway. Proc. Natl. Acad. Sci. U.S.A. 89(17): 7915-8.

5. Sternberg, B., Sorgi, F. L. and Huang, L. 1994. New structures in complex formation between DNA and cationic liposomes visualized by freeze-fracture electron microscopy. FEBS. Lett. 356(2-3): 361-6.

6. Wrobel, I. and Collins, D. 1995. Fusion of cationic liposomes with mammalian cells occurs after endocytosis. Biochim. Biophys. Acta 1235(2): 296-304.

7. Zabner, J., Fasbender, A. J., Moninger, T., Poellinger, K. A. and Welsh, M. J. 1995. Cellular and molecular barriers to gene transfer by a cationic lipid. J. Biol. Chem. 270(32): 18997-9007.

8. Leventis, R. and Silvius, J. R. 1990. Interactions of mammalian cells with lipid dispersions containing novel metabolizable cationic amphiphiles. Biochim. Biophys. Acta 1023(1): 124-32.

9. Felgner, J. N., Kummar, R., Sridhar, C. N., Wheeler, C., Tsai, Y. J., Border, R., Ramsay, P., Martin, M. and Felgner, P. 1994. Enhanced gene delivery and mechanism studies with a novel series of cationic lipid formulations. J. Biol. Chem. 269(4): 2550-2561.

10. Behr, J. P., Demeneix, B., Loeffler, J. P. and Perez-Mutul, J. 1989. Efficient gene transfer into mammalian primary endocrine cells with lipopolyamine-coated DNA. Proc. Natl. Acad. Sci. U.S.A. 86(18): 6982-6.

11. Zhou, X. H., Klibanov, A. L. and Huang, L. 1991. Lipophilic polylysines mediate efficient DNA transfection in mammalian cells. Biochim. Biophys. Acta 1065(1): 8-14.

12. Puyal, C., Milhaud, P., Bienvenue, A. and Philippot, J. R. 1995. A new cationic liposome encapsulating genetic material. A potential delivery system for polynucleotides. Eur. J. Biochem. 228(3): 697-703.

13. Gao, X. A. and Huang, L. 1991. A novel cationic liposome reagent for efficient transfection of mammalian cells. Biochem. Biophys. Res. Commun. 179(1): 280-5.

14. Ruysschaert, J. M., el Ouahabi, A., Willeaume, V., Huez, G., Fuks, R., Vandenbranden, M. and Di Stefano, P. 1994. A novel cationic amphiphile

for transfection of mammalian cells. Biochem. Biophys. Res. Commun. 203(3): 1622-8.

15. Ito, A., Miyazoe, R., Mitoma, J., Akao, T., Osaki, T. and Kunitake, T. 1990. Synthetic cationic amphiphiles for liposome-mediated DNA transfection. Biochem. Int. 22(2): 235-41.

16. Farhood, H., Bottega, R., Epand, R. M. and Huang, L. 1992. Effect of cationic cholesterol derivatives on gene transfer and protein kinase C activity. Biochim. Biophys. Acta 1111(2): 239-46.

17. Remy, J. S., Sirlin, C., Vierling, P. and Behr, J. P. 1994. Gene transfer with a series of lipophilic DNA-binding molecules. Bioconjug. Chem. 5(6): 647-54.

18. Bennett, M. J., Malone, R. W. and Nantz, M. H. 1995. A flexible approach to synthetic lipid ammonium salts for polynucleotide transfection. Tetrahedron Lett. 36(1): 2207-2210.

19. Balasubramaniam, R. P., Bennett, M. J., Aberle, A. M., Malone, J. G., Nantz, M. H. and Malone, R. W. 1996. Structural and functional analysis of cationic transfection lipids: the hydrophobic domain. Gene Ther. 3(2):163-172.

20. Aberle, A. M., Bennett, M. J., Malone, R. W. and Nantz, M. H. 1996. The counterion influence of cationic lipid-mediated transfection of plasmid DNA. Biochim. Biophys. Acta 1299(3):281-283.

21. Epand, R. M. and Bryszewska, M. 1988. Modulation of the bilayer to hexagonal phase transition and solvation of phosphatidylethanolamines in aqueous salt solutions. Biochemistry 27(24): 8776-9.

22. Koynova, R. D., Tenchov, B. G. and Quinn, P. J. 1989. Sugars favour formation of hexagonal (HII) phase at the expense of lamellar liquid-crystalline phase in hydrated phosphatidylethanolamines. Biochim. Biophys. Acta 980: 377-380.

23. Collins, K. D. and Washabaugh, M. W. 1985. The Hofmeister effect and the behaviour of water at interfaces. Q. Rev. Biophys. 18(4): 323-422.

24. Akao, T., Osaki, T., Mitoma, J., Ito, A. and Kunitake, T. 1991. Correlation between Physicochemical Characteristics of Synthetic Cationic Amphiphiles and Their DNA Transfection Ability. Bull. Chem. Soc. Jpn. 64: 3677.

25. Litzinger, D and Huang, L. 1992. Phosphatidylethanolamine liposomes: drug delivery, gene transfer and immunodiagnostic applications. Biochim. Biophys. Acta 1113, 201-227.

26. Yoshimura, K., Rosenfeld, M. A., Nakamura, H., Scherer, E. M., Pavirani, A., Lecocq, J. P. and Crystal, R. G. 1992. Expression of the human cystic fibrosis transmembrane conductance regulator gene in the mouse lung after in

vivo intratracheal plasmid-mediated gene transfer. Nucleic Acids Res. 20(12): 3233-40.

27. Meyer, K.B., Thompson, M.M., Levy, M.Y., Barron, L.G. and Szoka, F.C. 1995. Intratracheal gene delivery to the mouse airway: characterization of plasmid DNA expression and pharmacokinetics Gene Ther. 2(7): 450-60.